Family symmetries and radiative corrections in multi-scalar extensions of the Standard Model

Wessén, Jonas

2018

Document Version:
Publisher's PDF, also known as Version of record

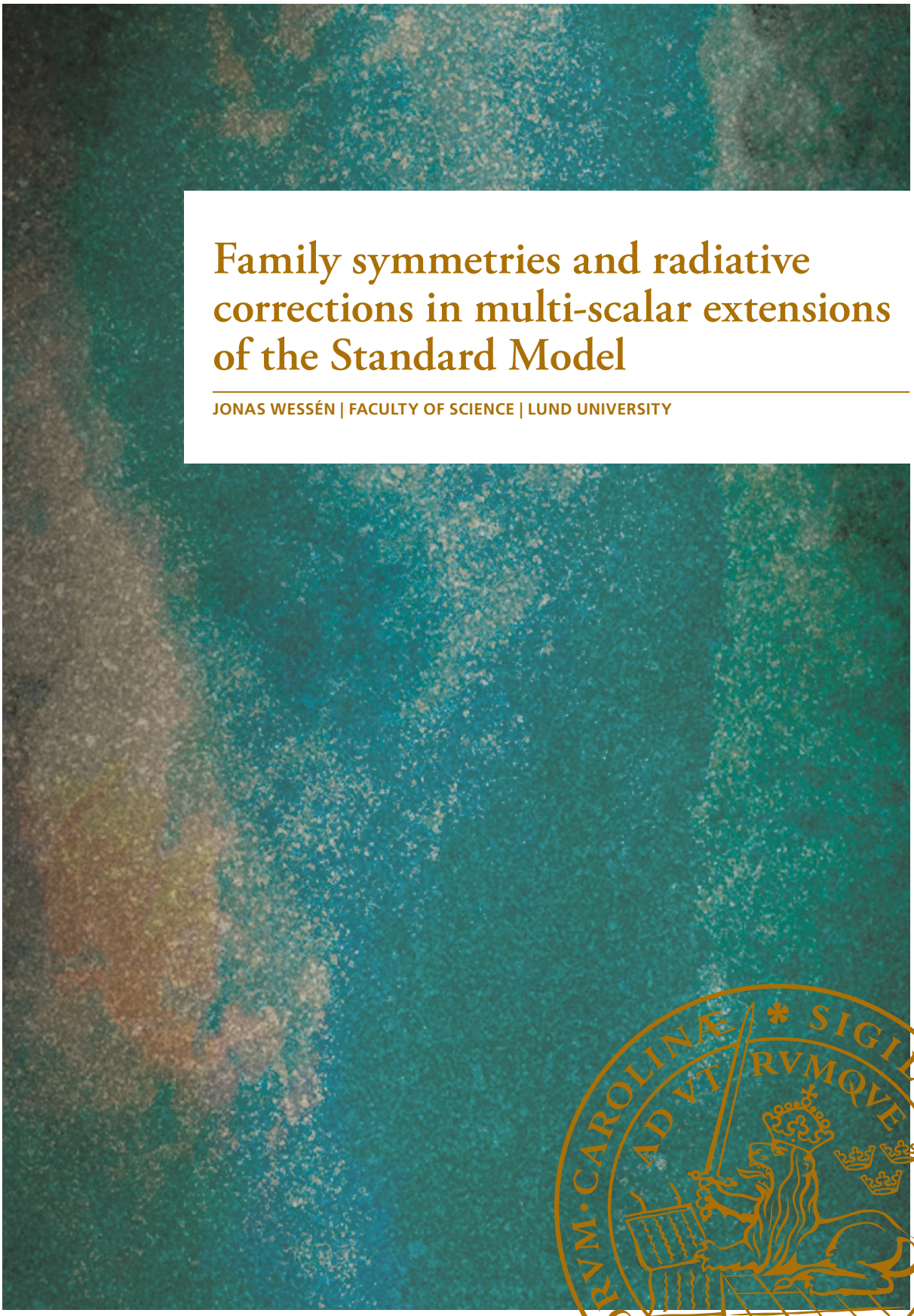

Family symmetries and radiative corrections in multi-scalar extensions of the Standard Model

JONAS WESSÉN | FACULTY OF SCIENCE | LUND UNIVERSITY

Family symmetries and radiative corrections in multi-scalar extensions of the Standard Model

Family symmetries and radiative corrections in multi-scalar extensions of the Standard Model

by Jonas Wessén

LUND
UNIVERSITY

Thesis for the degree of Doctor of Philosophy
Thesis advisor: Dr. Roman Pasechnik
Faculty opponent: Prof. Werner Porod

To be presented, with the permission of the Faculty of Science of Lund University, for public criticism in hall K404 at the Department of Astronomy and Theoretical Physics on Friday, the 18th of May 2018 at 13:00.

Organization
LUND UNIVERSITY

Department of Astronomy and Theoretical Physics
Sölvegatan 14A
SE–223 62 Lund
Sweden

Author(s)
Jonas Wessén

Document name
DOCTORAL DISSERTATION

Date of disputation
2018-05-18

Sponsoring organization

Title and subtitle
Family symmetries and radiative corrections in multi-scalar extensions of the Standard Model

Abstract
The four articles contained in this thesis all concern aspects of model building beyond the Standard Model (BSM). While Paper I mainly serves as a "tool paper" in which the results can be used to simplify certain calculations of one-loop effects from new heavy particles, Paper II–IV all deal with consequences of family symmetries in several BSM scenarios.

Paper I. We derive expressions for any number of derivatives of the Coleman-Weinberg potential in a general renormalisable four-dimensional field theory with arbitrary number of fields with spin ≤ 1. These correspond to the one-loop contributions to scalar n-point functions neglecting external momenta. The results are applied to two singlet extensions of the Standard Model, where we study the one-loop effects on the triple-Higgs coupling from the new exotic heavy states.

Paper II. In this paper we study a non-supersymmetric trinification theory where a novel $\mathrm{SU}(3)_\mathrm{F}$ family symmetry is imposed on the model. The tree-level scalar potential often has a global minimum where the trinification gauge group is broken to a Left-Right symmetric gauge group, and after integrating out all particles with masses of the order of the grand unification scale we show that the renormalisation group is able to trigger a radiative breaking down to the Standard Model gauge group with light Higgs doublets still remaining in the spectrum.

Paper III. This paper is about a supersymmetrised version of the $\mathrm{SU}(3)_\mathrm{F}$ symmetric trinification model of Paper II. The absence of an appropriate scalar potential minimum is rectified by adding novel gauge adjoint chiral superfields. The resulting superpotential allows for a breaking of the grand unification symmetry, while all subsequent symmetry breaking scales are given by soft supersymmetry breaking parameters. The tree-level mass spectrum resulting from this soft breaking of supersymmetry is discussed.

Paper IV. A three Higgs doublet model is introduced with a $\mathrm{U}(1) \times \mathrm{U}(1)$ family symmetry that simultaneously enforces a Cabibbo quark mixing under charged current interactions and forbids tree-level flavour changing neutral currents. Furthermore, a hierarchy in the vacuum expectation values of the three doublets produces a SM-like Higgs boson and hierarchical fermion masses, and also causes the exotic scalar states to couple most strongly to the second quark family. A search strategy for the lightest charged scalar boson in the model is proposed that utilises the $c\bar{s}$ fusion channel, and is shown to be capable of probing a large portion of the model's parameter space. This is formulated in a model independent manner such that it can be directly applied to any model with the same discovery channel.

Key words
Beyond the Standard Model, Trinification, Grand unification, Three Higgs doublet models, Coleman-Weinberg potential, Supersymmetry, Left-Right symmetry

Classification system and/or index terms (if any)

Supplementary bibliographical information

Language
English

ISSN and key title

ISBN
978-91-7753-671-0 (print)
978-91-7753-672-7 (pdf)

Recipient's notes

Number of pages
196

Price

Security classification

Signature  Date 2018-04-12

Family symmetries and radiative corrections in multi-scalar extensions of the Standard Model

by Jonas Wessén

LUND
UNIVERSITY

A doctoral thesis at a university in Sweden takes either the form of a single, cohesive research study (monograph) or a summary of research papers (compilation thesis), which the doctoral student has written alone or together with one or several other author(s).

In the latter case the thesis consists of two parts. An introductory text puts the research work into context and summarizes the main points of the papers. Then, the research publications themselves are reproduced, together with a description of the individual contributions of the authors. The research papers may either have been already published or are manuscripts at various stages (in press, submitted, or in draft).

Cover illustration front: Detail from the cover art of *From Beyond* (Credits: Martin Paulsson). *From Beyond* is the debut album by the band Delve in which I play the pump organ, and has been a work in progress throughout all my years as a Ph.D. student. It will be released digitally and on vinyl during 2018.

Faculty of Science, Department of Astronomy and Theoretical Physics

ISBN: 978-91-7753-671-0 (print)
ISBN: 978-91-7753-671-7 (pdf)

Printed in Sweden by Media-Tryck, Lund University, Lund 2018

Populärvetenskaplig sammanfattning

Människans vilja att förstå universums mest fundamentala byggstenar och dess naturlagar är den drivkraft som ligger till grund för elementarpartikelfysiken. Den teoretiska forskningen inom detta område vägleds idag till stor del av data från LHC-experimentet utanför Genève (LHC förkortar 'Large Hadron Collider', dvs. den Stora Hadronacceleratorn). Vid LHC accelereras protoner till extremt höga hastigheter varpå de kollideras parvis med varandra. I kollisionerna bildas nya partiklar ur protonernas rörelseenergi tack vare Einsteins berömda ekvation $E = mc^2$ som säger att massa kan konverteras till energi och vice versa, och de nya partiklarnas egenskaper, såsom massa eller elektrisk laddning, kan därefter uppmätas. Vi kan genom detta lära oss mer om redan kända partiklar, samt leta efter nya hittills oupptäckta partiklar.

På grund av den höga energin som uppnås vid LHC rör sig partiklarna med en hastighet som oftast är mycket nära ljusets, vilket betyder att Einsteins speciella relativitetsteori behövs för en korrekt beskrivning av vad som händer i dessa partikelkollisioner. Dessutom sker processer under extremt korta tidsintervall på ofantligt små avstånd vilket medför att kvantmekanik behöver tillämpas. Sammanförandet mellan den speciella relativitetsteorin och kvantmekaniken leder till den s.k. kvantfältteorin där alla partiklar av en viss sort, t.ex. elektronen, beskrivs som små vågor, eller kvantexcitationer, av ett och samma elektron*fält* vars utbredning sträcker sig över hela universum.

Den s.k. standardmodellen är en viss kvantfältteori som på ett elegant och matematiskt konsistent vis beskriver alla hittills detekterade elementarpartiklar (Higgspartikeln blev den sista partikeln i standardmodellen att få sin existens experimentellt bekräftad, vilket skedde år 2012). Med endast ett tjugotal fria parametrar kan forskare med hjälp av standardmodellen framgångsrikt förutsäga resultaten på ofantligt många experimentella mätningar, vilket gör att få idag betvivlar standardmodellens korrekthet.

Genom att bestämma de numeriska värdena på de fria parametrarna i standardmodellen utifrån experimentella mätningar, framgår dock vissa mönster som helt saknar förklaring inom standardmodellen själv. Till exempel finns det tre kopior, eller s.k. familjer, av varje fermion (t.ex. elektronen) som är helt identiska förutom i hur mycket de väger. Det finns t.ex. två tyngre, men i övrigt identiska, kopior av elektronen (myonen och tau-partikeln). Orsaken till den hierarkiska struktur som fermionmassorna uppvisar utgör idag ett av standardmodellens stora mysterier.

Standardmodellen innehåller en beskrivning av tre av naturens fyra fundamentala krafter som vi hittills känner till (alla utom gravitationen): den elektromagnetiska kraften, den svaga kraften (vilken bland annat är orsaken till en del radioaktiva sönderfall) samt den starka kraften (vilken bland annat binder samman kvarkarna till protoner och neutroner). I standardmodellen sammanförs den elektromagnetiska kraften med den svaga kraften genom den s.k. Higgs-mekanismen, vilket visar att dessa två krafter egentligen är "två sidor av samma mynt", dvs. den elektrosvaga kraften. På ett liknande sätt kan hypotetiska storföreningsteorier (eller "Grand Unified Theories") sammanföra den elektrosvaga kraften med den starka kraften till en enda fundamental kraft. Två av artiklarna i denna avhandling (artikel II och III) handlar om en viss sorts storfören-

ingsteori, dvs. den s.k. trinifieringsteorin, där vi dessutom lägger till en ny hittills outforskad symmetri mellan fermionfamiljerna. Dessa artiklar handlar om hur en del av standardmodellens egenskaper, t.ex. de hierarkiska fermionmassorna, skulle kunna förklaras av att naturen på väldigt små avstånd (mycket mindre än vad som hittills har utforskats experimentellt) beskrivs av en sådan trinifieringsmodell. Den första artikeln i avhandlingen, artikel I, handlar om ett matematiskt verktyg som kan användas för att förenkla beräkningar av kvantmekaniska effekter i utvidgningar av standardmodellen, såsom modellerna i artikel II och III, där traditionella metoder för att göra dessa beräkningar lätt kan bli onödigt krångliga på grund av det stora antal nya partiklar som ofta ingår i sådana modeller.

Den fjärde och sista artikeln i denna avhandling, artikel IV, handlar om en annan typ av utvidgning av standardmodellen, där existensen av nya Higgsfält postuleras. I standardmodellen finns nämligen bara ett Higgsfält, men i modellen i artikel IV finns tre familjer av Higgsfält, liknande de tre familjerna av fermioner. Genom att lägga till fler Higgsfält kan man också lägga till familjesymmetrier som i sin tur gör en del av standardmodellens strukturer mindre godtyckliga. I artikel IV föreslår vi också en metod som experimentalister skulle kunna använda sig av för att leta efter den lättaste av de nya elektriskt laddade Higgspartiklarna som denna modell förutsäger.

Contents

Introduction

The main body of this thesis consists of four journal articles (hereafter referred to as Paper I, Paper II, Paper III and Paper IV respectively) that all deal with various aspects of model building beyond the Standard Model of particle physics. The purpose of this introduction is to present the reader with the background theory required for understanding these articles. I have tried to write this introduction such that as much of it as possible would be accessible to perhaps an undergraduate student that has for a few years been enrolled in a standard theoretical physics program with a specialization towards particle theory. I.e. a familiarity with basic group theory, the theory of special relativity and the framework of quantum mechanics is assumed of the reader, as well as hopefully a few previous encounters with field theory.

The Standard Model (which due to overwhelming observational evidence today constitute our best understanding of all observed elementary particles and their interactions), as well as the vast majority of its speculated extensions, are all formulated in the language of quantum field theory (QFT). This is the subject of both Sec. 1 (which is devoted to non-interacting QFTs) and Sec. 2 (in which we introduce interactions). These sections are heavily based on my favourite parts of standard QFT textbooks [1, 2, 3, 4], and contain very little original material. They do however contain a few key ideas that help explaining *why* modern theories of elementary particles are the way they are; ideas that are well known in the community but perhaps not often taught in basic QFT courses (at least they were not in any of mine!) which is the reason I wanted to write about them. For example, Sec. 1.2 contains the very definition of what we today mean by a (quantum) particle (i.e. the quantum states that follow from Wigner's classification of the representations of the Poincaré group), where after it is shown in Secs. 1.3–1.5 how the standard free relativistic wave equations follow from this, depending on e.g. the spin and the mass of the corresponding particle. These wave equations, such as Maxwell's equations or the Dirac equation, are often either derived in a historically correct but not very illuminating way, or simply "pulled out of a hat". Another example (in Sec. 2.2)

is Polchinski's argument for why "things look renormalisable" when the ultra violet cut-off of the theory is far above experimentally accessible energies.

Sec. 2 also contains important material for in particular Papers I–III. The quantum effective action and the so called Coleman-Weinberg potential are introduced in Sec. 2.2, and are especially important for Paper I. In Paper I, we derive closed form analytical expressions for an arbitrary number of derivatives of the Coleman-Weinberg potential in a general four-dimensional renormalisable field theory with arbitrary numbers of fields with spin ≤ 1. These correspond to the one-loop corrections to connected and amputated n-point functions with only scalar external particles, in the approximation where external momenta are neglected in internal propagators (this is explained in Sec. 2.2). This approximation is justified when the momenta of the external particles are all much smaller than the masses of the particles running in the loops. This is indeed the typical situation when one is interested in the effects from heavy virtual particles on the effective couplings among light particles that in turn may be directly measured in experiment. Our results in Paper I can therefore serve as a tool for model builders e.g. trying to figure out the low-energy predictions of Standard Model extensions containing new heavy particles. This tool would be particularly useful in theories with many new fields, since a standard diagrammatic approach in such cases tends to be both very cumbersome and error-prone due to the large number of particles and diagrams involved. Sec. 2.5 contains a brief discussion on the concept of effective field theory which is mainly important for Paper II, but also to some extent for Paper III. These papers deal with a non-supersymmetric and a supersymmetric version, respectively, of a trinification model (the trinification model itself is described in Sec. 4.3) where a novel $\mathrm{SU}(3)_{\mathrm{F}}$ family symmetry is introduced that greatly increases the degree of unification compared to standard trinification constructions. The long term goal of these research projects is to study if the Standard Model (or something very similar) can be found as a low-energy effective field theory from such a trinification model, and in Paper II and Paper III we take a first few steps in this direction. In fact, the discussion on effective field theories in Sec. 2.5 is based on a toy model which in its structure is very similar to the model in Paper II.

Sec. 3 then follows, in which the Standard Model is introduced. Its scalar sector, gauge sector and fermion sector are all described, and in particular how they are affected in the Higgs mechanism for the electro-weak symmetry breaking. Special attention is given in Sec. 3.4 to the flavour structure of the Standard Model, such as the fermion mass hierarchies and the almost Cabibbo form of the flavour mixing under charged current interactions. This is important mainly for Paper IV, where we study a model where the Standard Model scalar sector is augmented by two additional Higgs doublets (i.e. this is a so-called 3 Higgs Doublet Model, or 3HDM for short). While there is no a priori reason for the Standard Model flavour patterns to be found within the Standard Model itself, the increased field content in 3HDMs makes it possible to impose additional symmetries that can partly enforce such structures. In Paper IV we impose a $\mathrm{U}(1) \times \mathrm{U}(1)$ family symmetry on a 3HDM, which in particular makes it so that the heaviest quark family couples exclusively to the "third" Higgs doublet H_3. The two lightest quark families couple to the other two Higgs doublets $H_{1,2}$ such that the up-type and the down-type quarks receive their masses from H_1 and H_2 respectively. This leads directly to an

exact Cabibbo quark mixing, and a hierarchy in the vacuum expectation values of the Higgs doublets, $\langle H_{1,2}\rangle \ll \langle H_3\rangle$, can be directly linked to the quark mass hierarchies[1]. Two important consequences of this hierarchy is that the scalar spectrum contains a Standard Model-like Higgs boson, and that the other exotic scalar particles couple most strongly to the second quark family, i.e. to the charm and the strange quarks. The second point is interesting because searches for new physics often focus instead on the heaviest quark family. In Paper IV we also propose a search strategy for the lightest electrically charged scalar particle in the model that utilises this fact, and show that a significant part of the model's parameter space can be probed already with current experimental data if our analysis were to be used by the experimental collaborations.

In Sec. 4 I describe a few possible ways in which the Standard Model may be extended. Sec. 4.1 contains a minimalistic review of supersymmetry that is relevant for Paper III. Sec. 4.2 then follows in which the idea of Grand Unification is described, and in particular how the non-observation of proton decay is in some tension with the simplest realisations of Grand Unification. Sec. 4.3 is then devoted to the particular Grand Unification scenario called trinification, in which the proton is naturally much more stable than in other Grand Unification models. After a quick review of previous work on trinification models, I move on to discuss a few aspects of the trinification models in Paper II and Paper III, where the trinification gauge group is augmented by a novel $\mathrm{SU}(3)_\mathrm{F}$ family symmetry.

So called natural units are employed throughout this thesis, where $\hbar = c \equiv 1$ (here, $\hbar$ is the reduced Planck constant and c is the speed of light). The basic unit of energy will be gigaelectronvolt (GeV), which in natural units corresponds to

$$1 \text{ GeV} \sim 10^{-27} \text{ kg} \sim \left(10^{-16} \text{ m}\right)^{-1} \sim \left(10^{-24} \text{ s}\right)^{-1} , \tag{1.1}$$

in standard SI units. I have used the "mostly minus" convention for the Minkowski metric, i.e. $\eta^{\mu\nu} = \mathrm{diag}(1, -1, -1, -1)$.

1 Quantum field theory: free fields

The framework of *quantum field theory* (QFT) has provided, since its gradual invention starting in the 1920's, an accurate description of physical phenomena over an astonishingly wide range of energy scales. It is used to explain observations involving energies all the way from the 10's of TeV range (i.e. in proton-proton collisions at the Large Hadron Collider) down to the MeV scale relevant for nuclear physics, and even certain precision effects in atomic physics[2]. Moreover, theorists today use the language of QFT, mostly without worry, when postulating new models whose energy range of

[1] The tuning of the *two* numbers $\langle H_{1,2}\rangle$ may be considered a slight improvement compared to the tuning of the *four* quark masses $m_{u,d,c,s}$ in the Standard Model.

[2] The energy difference between ${}^2S_{\frac{1}{2}}$ and ${}^2P_{\frac{1}{2}}$ levels in the hydrogen atom amounts to roughly a few μeV, and can be attributed to the quantum vacuum fluctuations of the electro-magnetic field. This is the so called *Lamb shift*.

validity sometimes extends up to the Grand Unification scale, which can be as large as 10^{16} GeV, i.e. *twelve orders of magnitude above* the highest energy scale that has been directly probed in experiments (such models are the topics of some of the articles included in this thesis). However, we will soon see that both the general framework of QFT, as well as the particular form of the usual Lagrangians for spin ≤ 1 fields, follow from very general (and reasonable) assumptions.

1.1 The Lorentz group and the Poincaré group

The starting point for our discussion of QFT will be the Poincaré group, which I very briefly introduce in this section. This is the group of combined space-time translations ($x^\mu \to x^\mu + a^\mu$) and Lorentz transformations (i.e. $x^\mu \to \Lambda^\mu{}_\nu\, x^\nu$ with $\Lambda^\mu{}_\rho \Lambda^\nu{}_\sigma \eta^{\rho\sigma} = \eta^{\mu\nu}$). There are 10 generators of this group in the four-dimensional space-time we live in: the temporal and the three spatial components of the four-momentum P^μ generate time and space translations respectively, while the generators of Lorentz transformations can be grouped into an anti-symmetric object $\mathcal{J}^{\mu\nu} = -\mathcal{J}^{\nu\mu}$ such that $\mathcal{J}^{ij}$ generate rotations in the $x^i x^j$ plane, while $\mathcal{J}^{0i}$ generate boosts in the x^i direction. These generators obey the Poincaré algebra,

$$\begin{aligned} [P^\mu, P^\nu] = 0\,, \quad [\mathcal{J}^{\mu\nu}, P^\rho] = \mathrm{i}\,(\eta^{\mu\rho} P^\nu - \eta^{\nu\rho} P^\mu)\ , \\ [\mathcal{J}^{\mu\nu}, \mathcal{J}^{\rho\sigma}] = \mathrm{i}\,(\eta^{\mu\rho}\mathcal{J}^{\nu\sigma} - \eta^{\nu\rho}\mathcal{J}^{\mu\sigma} + \eta^{\nu\sigma}\mathcal{J}^{\mu\rho} - \eta^{\mu\sigma}\mathcal{J}^{\nu\rho})\ . \end{aligned} \tag{1.2}$$

The last line only involves generators of the Lorentz group $\mathrm{SO}(1,3)$, i.e. the $\mathcal{J}^{\mu\nu}$ from the Lorentz algebra. If we write $\mathcal{J}^{ij} \equiv \epsilon^{ijk} J^k$ and $\mathcal{J}^{0i} \equiv K^i$, and form the combinations $J^i_\pm \equiv J^i \pm \mathrm{i} K^i$, then one can check that the Lorentz algebra is equivalent to two factorized SU(2) algebras,

$$[J^i_\pm, J^j_\pm] = \mathrm{i}\epsilon^{ijk} J^k_\pm\,, \quad [J^i_+, J^j_-] = 0\,. \tag{1.3}$$

The representations of the Lorentz group are therefore very simple if you are familiar with the representations of SU(2). The irreducible representations of SU(2) are labelled by a half-integer $s = 0, \frac{1}{2}, 1, \frac{3}{2}, \ldots$, each with dimensionality $2s+1$. Eq. (1.3) tells us that the irreducible representations of the Lorentz group can always be put in the form of $(2s+1)$ by $(2r+1)$ matrices where $s, r = 0, \frac{1}{2}, 1, \frac{3}{2}, \ldots$. We can therefore label irreducible representations of the Lorentz group by pairs of non-negative half-integers (s, r). Also, note that (s, r) and (r, s) are related both by complex conjugation (since $(J^i_\pm)^* = J^i_\mp$) and by parity (since $J^i \to J^i$ and $K^i \to -K^i$ and therefore $J^i_\pm \to J^i_\mp$ under $\vec{x} \to -\vec{x}$).

The simplest representation of the Lorentz group is the scalar $(0,0)$. Next up are the 2-component Weyl spinors $(\frac{1}{2}, 0)$ and $(0, \frac{1}{2})$, which are referred to as "left-handed" and "right-handed" respectively. I will often use the so-called "dotted/undotted" notation where indices belonging to $(0, \frac{1}{2})$ are over-set by a dot $\cdot$ to distinguish them from $(\frac{1}{2}, 0)$ indices. For example, if $\xi_\alpha \sim (\frac{1}{2}, 0)$, then $(\xi^\alpha)^\dagger \equiv \xi^{\dagger\dot{\alpha}} \sim (0, \frac{1}{2})$. Two Weyl spinors ξ^α and χ^α can combine into a Lorentz invariant through the 2-dimensional Levi-Cevita tensor as $\xi^\alpha \chi^\beta \epsilon_{\alpha\beta} \equiv \xi^\alpha \chi_\alpha \equiv \xi\chi$. Similarly, $\xi^{\dagger\dot{\beta}} \chi^{\dagger\dot{\alpha}} \epsilon_{\dot{\alpha}\dot{\beta}} \equiv \xi^\dagger_{\dot{\alpha}} \chi^{\dagger\dot{\alpha}} \equiv \xi^\dagger \chi^\dagger$ is a Lorentz invariant.

The $(\frac{1}{2},\frac{1}{2})$ representation corresponds to the Lorentz vector (or the four-vector) representation, i.e. the defining representation of the Lorentz group. Pairs of $(\frac{1}{2},0)$ and $(0,\frac{1}{2})$ indices can always be traded for a four-vector index through contractions with either $(\bar{\sigma}^\mu)^{\dot{\alpha}\alpha}$ or $(\sigma^\mu)_{\alpha\dot{\alpha}}$. Here, $\bar{\sigma}^\mu = (1,-\vec{\sigma})$ and $\sigma^\mu = (1,\vec{\sigma})$, where $\vec{\sigma}$ are the Pauli matrices, i.e. $\sigma^1 = \begin{pmatrix} 0 & 1 \\ 1 & 0 \end{pmatrix}$, $\sigma^2 = \begin{pmatrix} 0 & -\mathrm{i} \\ \mathrm{i} & 0 \end{pmatrix}$ and $\sigma^3 = \begin{pmatrix} 1 & 0 \\ 0 & -1 \end{pmatrix}$.

1.2 The Hilbert space and the free Hamiltonian

Having outlined the basics of the Poincaré group, we are now ready to start constructing quantum theories implementing this symmetry group. As with any quantum theory, the first thing we need to do is to specify which states we want to include in our theory. In the end we want to be able to handle multi-particle states, but let us first design our one-particle states which will be the irreducible representations of the Poincaré group. In particular, let first consider single particle momentum eigenstates,

$$\text{one-particle state:} \quad |p,\sigma\rangle \ . \tag{1.4}$$

Here, σ is just a generic label, but we will soon find its significance by studying how $|p,\sigma\rangle$ behaves under Lorentz transformations. By being an eigenstate of the four-momentum operator P^μ (with eigenvalue p^μ), the state in Eq. (1.4) transforms with an over-all phase under space-time translations: $|p,\sigma\rangle \to \mathrm{e}^{-\mathrm{i}P^\mu a_\mu}\,|p,\sigma\rangle = \mathrm{e}^{-\mathrm{i}p^\mu a_\mu}\,|p,\sigma\rangle$ under $x^\mu \to x^\mu + a^\mu$.

Consider a Lorentz transformation Λ that takes p^μ into some other four-momentum $p'^\mu = \Lambda^\mu{}_\nu p^\nu$. There must be a corresponding unitary operator $U(\Lambda)$ that acts on $|p,\sigma\rangle$ to produce the corresponding state with momentum $\vec{p}\,'$.

$$|p',\sigma'\rangle = U(\Lambda)\,|p,\sigma\rangle \ . \tag{1.5}$$

Note that I have allowed for $U(\Lambda)$ to also act on σ in order to not loose generality.

Given $|p,\sigma\rangle$, let us now consider the subset of Lorentz transformations λ that leave p^μ invariant, i.e. $p^\mu = \lambda^\mu{}_\nu p^\nu$. These transformations form a subgroup of the Lorentz group, often called "Wigner's Little Group", or just the "little group" for short. Such transformations merely scramble the states with different σ's but common four-momentum p^μ, i.e.

$$|p,\sigma\rangle \to |p,\sigma'\rangle = U(\lambda)\,|p,\sigma\rangle = \sum_{\sigma''} W(\lambda)_{\sigma'\sigma''}\,|p,\sigma''\rangle \ , \tag{1.6}$$

where the $W_{\sigma\sigma'}$'s are *matrix* representations of the little group. For a particle with mass $m \neq 0$, the four-momentum can always be brought to $p^\mu = (m,\vec{0})$ by a Lorentz transformation. The little group for massive particles is therefore the group of spatial rotations SO(3), since these are the Lorentz transformations that leave $(m,\vec{0})$ invariant. But the representations of SO(3) are well known: σ is simply the *spin* of the particle! That is, one-particle states of a massive particle can be arranged into representations of SO(3) that are labelled by a non-negative half-integer $s = 0, \frac{1}{2}, 1, \ldots$, where each such multiplet is composed out of $2s+1$ states that mix under Lorentz transformations.

The situation is radically different for massless particles. For a massless particle, the best we can do is e.g. to bring its four-momentum to the form $p^\mu \propto (1,0,0,1)$, i.e. with its three-momentum directed in the z-direction. This is invariant under rotations only in the xy-plane (i.e. SO(2) transformations)[3]. Therefore, σ labels the spin along the direction of motion which is the so-called *helicity*, i.e. one-particle states of massless particles are labelled by a half integer $h = 0, \pm\frac{1}{2}, \pm 1, \ldots$. States with different h do not mix under Lorentz transformations; only the momentum and the phase of the state change.

The above discussion has taught us that one-particle states are labelled by the momentum and the spin (helicity) for massive (massless) particles, and is a baby version of the classic derivation by Wigner in 1939 [5]. It is the fundamental reason for why massless particles have less degrees of freedom than massive ones!

Quite often in calculations, one has to integrate over all possible three-momenta of a particle. We can do this in a Lorentz invariant way by using the measure

$$\int \frac{\mathrm{d}^4 p}{(2\pi)^4} \cdot (2\pi)\delta(p^2 - m^2)_{p^0>0} = \int \frac{\mathrm{d}^3 p}{(2\pi)^3} \frac{1}{2E_p}\,, \tag{1.7}$$

with $E_p = \sqrt{\vec{p}^{\,2} + m^2}$. If we now choose our one-particle states to have the Lorentz invariant normalisation

$$\langle p, \sigma | q, \sigma' \rangle = 2E_p (2\pi)^3 \delta^{(3)}(\vec{p} - \vec{q}) \delta_{\sigma,\sigma'}\,, \tag{1.8}$$

the factor $1/(2E_p)$ in Eq. (1.7) will often cancel against the $2E_p$ in Eq. (1.8), making the calculations simpler to perform.

The Hilbert space (of a specific particle species) will be composed of all possible n-particle states,

$$n\text{-particle state:} \quad |p_1, \sigma_1; p_2, \sigma_2; \ldots; p_1, \sigma_n\rangle\,, \tag{1.9}$$

where we now know that σ stands for the spin (helicity) for massive (massless) particles. At this point, it becomes extremely convenient to introduce so-called creation operators $a^\dagger_{p,\sigma}$, defined as

$$|p, \sigma\rangle = \sqrt{2E_p} a^\dagger_{p,\sigma} |0\rangle\,. \tag{1.10}$$

where $|0\rangle$ is the 0-particle state. I have here explicitly taken out a factor $\sqrt{2E_p}$ to account for the normalization of the states in Eq. (1.8). The n-particle states in Eq. (1.9) can then be expressed as

$$\sqrt{2E_{p_1}} a^\dagger_{p_1,\sigma_1} \cdots \sqrt{2E_{p_n}} a^\dagger_{p_n,\sigma_n} |0\rangle\,. \tag{1.11}$$

One reason that this notation is convenient is that we can encode whether the particles obey Bose or Fermi statistics by having the $a^\dagger$'s obeying commutation or anti-commutation relations respectively,

$$\begin{aligned} a^\dagger_{p,\sigma} a^\dagger_{q,\sigma'} - a^\dagger_{q,\sigma'} a^\dagger_{p,\sigma} &= [a^\dagger_{p,\sigma}, a^\dagger_{q,\sigma'}] = 0\,, \quad \text{(bosons)}, \\ a^\dagger_{p,\sigma} a^\dagger_{q,\sigma'} + a^\dagger_{q,\sigma'} a^\dagger_{p,\sigma} &= \{a^\dagger_{p,\sigma}, a^\dagger_{q,\sigma'}\} = 0\,, \quad \text{(fermions)}. \end{aligned} \tag{1.12}$$

[3]The little group for massless particles is in fact larger than SO(2) since there are also combinations of boosts and rotations that leave $(1,0,0,1)$ invariant. However, the actual massless particles in nature are singlets under such transformations.

Similarly, we can define the annihilation operators $a_{p,\sigma}$ from

$$\langle p,\sigma| = \sqrt{2E_p}\,\langle 0|\,a_{p,\sigma}\,. \tag{1.13}$$

The annihilation operators also either commute or anti-commute for bosons and fermions respectively, and are assumed to annihilate the 0 particle state, i.e. $a_{p,\sigma}\,|0\rangle = 0$.

Furthermore, we can find commutators and anti-commutators between $a^\dagger$'s and a's from Eq. (1.8). E.g. for bosons,

$$\begin{aligned} 2E_p(2\pi)^3\delta^{(3)}(\vec{p}-\vec{q})\delta_{\sigma,\sigma'} &= \sqrt{2E_p}\sqrt{2E_q}\,\langle 0|\,a_{p,\sigma}a^\dagger_{q,\sigma'}\,|0\rangle \\ &= \sqrt{2E_p}\sqrt{2E_q}\left(\langle 0|\,[a_{p,\sigma},a^\dagger_{q,\sigma'}]\,|0\rangle + \underbrace{\langle 0|\,a^\dagger_{q,\sigma'}a_{p,\sigma}\,|0\rangle}_{=0}\right) \end{aligned} \tag{1.14}$$

such that

$$[a_{p,\sigma},a^\dagger_{q,\sigma'}] = (2\pi)^3\delta^{(3)}(\vec{p}-\vec{q})\delta_{\sigma,\sigma'}\,,\quad \text{(bosons)}\,. \tag{1.15}$$

Similarly, one can show that

$$\{a_{p,\sigma},a^\dagger_{q,\sigma'}\} = (2\pi)^3\delta^{(3)}(\vec{p}-\vec{q})\delta_{\sigma,\sigma'}\,,\quad \text{(fermions)}\,. \tag{1.16}$$

The spin-statistics theorem [6] tells us that integer (half-integer) spin particles must be bosons (fermions).

Eqs. (1.15) and (1.16) give us a simple way to express the free Hamiltonian H_0 (i.e. the Hamiltonian assuming no interaction energy between particles) in terms of the creation and annihilation operators. Using these equations, one can easily show that the operator $N_p = \sum_\sigma a^\dagger_{p,\sigma}a_{p,\sigma}$ counts the number of particles with momentum p when applied to some state. Therefore, to get H_0 we simply need to sum N_p over all possible three-momenta weighted by the energy $E_p = \sqrt{\vec{p}^{\,2}+m^2}$ that we want to associate with a single particle, i.e.

$$H_0 = \int \frac{\mathrm{d}^3p}{(2\pi)^3}E_p\sum_\sigma a^\dagger_{p,\sigma}a_{p,\sigma}\,. \tag{1.17}$$

To construct *local* interaction terms that we can add to H_0, we first need to construct functions of a's and $a^\dagger$'s that depend on position $\vec{x}$ rather than momentum (i.e. through the Fourier transform). Such functions are the *quantum fields*. I will now proceed to find the fields and their conjugate momenta for the spin 0, $\frac{1}{2}$ and 1 cases respectively. We will then express in each case the creation and annihilation operators in terms of the fields and conjugate momenta, which can then be plugged into Eq. (1.17). This will lead to the Hamiltonians for all the familiar relativistic wave equations such as the Klein-Gordon equation, the Dirac equation or Maxwell's equations.

1.3 Free fields: spin 0

Let me for now focus on the spin 0 case (where we can drop the σ index on the quantum states). I will define the real scalar field $\phi(\vec{x})$ such that it produces the Fourier

transforms of the one-particle states when acting on $|0\rangle$, i.e.

$$\phi(\vec{x})\,|0\rangle = \int \frac{\mathrm{d}^3p}{(2\pi)^3}\frac{1}{2E_p}\mathrm{e}^{-\mathrm{i}\vec{p}\cdot\vec{x}}\,|p\rangle \;\;,\;\; \langle 0|\,\phi(\vec{x}) = \int \frac{\mathrm{d}^3p}{(2\pi)^3}\frac{1}{2E_p}\mathrm{e}^{\mathrm{i}\vec{p}\cdot\vec{x}}\,\langle p| \tag{1.18}$$

This means that $\phi(\vec{x})$ can be expressed in terms of creation and annihilation operators as

$$\phi(\vec{x}) = \int \frac{\mathrm{d}^3p}{(2\pi)^3}\frac{1}{\sqrt{2E_p}}\left(a_p^\dagger \mathrm{e}^{-\mathrm{i}\vec{p}\cdot\vec{x}} + a_p \mathrm{e}^{\mathrm{i}\vec{p}\cdot\vec{x}}\right) . \tag{1.19}$$

In the Heisenberg picture, the creation and annihilation operators evolve in time according to $\frac{\mathrm{d}a^\dagger}{\mathrm{d}t} = \mathrm{i}[H, a^\dagger]$, which is solved by

$$a_p^\dagger \to \mathrm{e}^{\mathrm{i}tE_p}a_p^\dagger\,, \quad a_p \to \mathrm{e}^{-\mathrm{i}tE_p}a_p\,, \tag{1.20}$$

assuming no interactions, i.e. $H = H_0$. We can therefore write

$$\phi(x) = \int \frac{\mathrm{d}^3p}{(2\pi)^3}\frac{1}{\sqrt{2E_p}}\left(a_p^\dagger \mathrm{e}^{\mathrm{i}px} + a_p \mathrm{e}^{-\mathrm{i}px}\right) , \tag{1.21}$$

where $p^0 = E_p$ is understood.

Let us give the time-derivative of $\phi(x)$ its own name,

$$\pi(x) \equiv \frac{\partial\phi(x)}{\partial t} = \mathrm{i}\int \frac{\mathrm{d}^3p}{(2\pi)^3}\sqrt{\frac{E_p}{2}}\left(a_p^\dagger \mathrm{e}^{\mathrm{i}px} - a_p \mathrm{e}^{-\mathrm{i}px}\right) . \tag{1.22}$$

The commutation relations for the creation and annihilation operators are now equivalent to the equal-time (i.e. $x^0 = y^0$) commutators

$$\begin{aligned} [\phi(x), \phi(y)] = [\pi(x), \pi(y)] = 0 \\ [\phi(x), \pi(y)] = \mathrm{i}\delta^{(3)}(\vec{x} - \vec{y})\,. \end{aligned} \tag{1.23}$$

These canonical commutation relations suggest that we are looking at the quantum version of a classical system where $\pi(\vec{x})$ is conjugate momentum to the classical degree of freedom $\phi(\vec{x})$. A straightforward calculation shows that H_0 can be expressed in terms of $\phi(\vec{x})$ and $\pi(\vec{x})$ as

$$H_0 = \int \mathrm{d}^3x \left(\frac{1}{2}\pi^2 + \frac{1}{2}(\vec{\nabla}\phi)^2 + \frac{1}{2}m^2\phi^2\right) . \tag{1.24}$$

up to a constant. The classical equation of motion for ϕ that follows from this Hamiltonian is the Klein-Gordon equation

$$(\partial^2 + m^2)\phi(x) = 0\,. \tag{1.25}$$

We can also derive the Lagrangian for a free scalar field from Eq. (1.24), yielding

$$\mathcal{L}_0^{\mathrm{s}=0} = \frac{1}{2}(\partial_\mu\phi)(\partial^\mu\phi) - \frac{1}{2}m^2\phi^2\,. \tag{1.26}$$

1.4 Free fields: spin $\frac{1}{2}$

Previously, the σ label on the one-particle states denoted the components of the polarization vectors for a generic spin. In this section, I will instead label this by α's and β's as is customary for spin $\frac{1}{2}$ particles. Furthermore, we can isolate the polarization spinors from the creation operators $a^\dagger_{p,\alpha}$ by writing

$$a^\dagger_{p,\alpha} = \frac{1}{\sqrt{m}} \sum_s u^s(\vec{p})_\alpha b^\dagger_{p,s} \tag{1.27}$$

where $u^s(\vec{p})_\alpha$ is the polarization 2 component spinor (with components labelled by α) for spin mode s at the given momentum. The factor $\frac{1}{\sqrt{m}}$ is purely for future convenience and could be absorbed into the normalization of the polarization vector. Now, $u^s(\vec{p})$ transforms under the Lorentz group as the corresponding spin representation of the particle, while $b^\dagger_{p,s}$ is an operator that transforms as the $a^\dagger_p$ for the spin 0 particle. For a spin $\frac{1}{2}$ particle (massless or massive), the index s in Eq. (1.27) labels the "spin up" and "spin down" modes ($s = \uparrow, \downarrow$) e.g. along the $\hat{z}$ direction. In the massive case, we can pick the following basis for the polarization vectors in the rest frame:

$$u^\uparrow(\vec{0})_\alpha = \sqrt{m}\begin{pmatrix}1\\0\end{pmatrix}, \quad u^\downarrow(\vec{0})_\alpha = \sqrt{m}\begin{pmatrix}0\\1\end{pmatrix}. \tag{1.28}$$

Since $u^s(\vec{p})$ transforms as the spin $\frac{1}{2}$ representation under rotations, it must belong either to the $(\frac{1}{2},0)$ or the $(0,\frac{1}{2})$ representation of the Lorentz group (these transform identically under rotations, but oppositely under boosts). We will pick the $(\frac{1}{2},0)$ option, but this choice is arbitrary as we can always go between the two. If we boost (with rapidity η) to a general four-momentum,

$$(m,\vec{0}) \to (E_p,\vec{p}) = m(\cosh\eta, \hat{p}\sinh\eta), \tag{1.29}$$

where $\hat{p}$ is the unit vector in the direction of $\vec{p}$, we get the corresponding polarization vector in that frame as

$$u^s(\vec{p})_\alpha = \left(\mathrm{e}^{-\frac{1}{2}\eta\hat{p}\cdot\vec{\sigma}}\right)_\alpha^{\ \beta} u^s(\vec{0})_\beta = \left(\sqrt{\frac{p\cdot\sigma}{m}}\right)_\alpha^{\ \beta} u^s(\vec{0})_\beta, \tag{1.30}$$

where

$$\sqrt{p\cdot\sigma} = \frac{(E_p+m) - \vec{p}\cdot\vec{\sigma}}{\sqrt{2(E_p+m)}} \tag{1.31}$$

satisfies $\sqrt{p\cdot\sigma}\cdot\sqrt{p\cdot\sigma} = p\cdot\sigma$.

Under Lorentz transformations, we have that $|p,\alpha\rangle \sim (\frac{1}{2},0)$ meaning that $(|p,\alpha\rangle)^* \sim (0,\frac{1}{2})$ (which would appropriately be named $\langle p,\dot{\alpha}|$ using the dotted/undotted notation). If it is this kind of state that corresponds to $\langle p,\sigma|$ in Eq. (1.8), then we are in trouble because we would have defined our state normalization from $\langle p,\dot{\alpha}|q,\alpha\rangle \propto \delta_{\dot{\alpha}\alpha}$ which transforms non-trivially under Lorentz transformations. We can rectify this by instead defining

$$\langle p,\alpha| \equiv \langle p,\dot{\alpha}|\left(\frac{p\cdot\bar{\sigma}}{m}\right)^{\dot{\alpha}\alpha}. \tag{1.32}$$

Let us also define

$$v^s(\vec{p})^\alpha \equiv u^{s*}(\vec{p})_{\dot{\alpha}} \left(\frac{p\cdot\bar{\sigma}}{m}\right)^{\dot{\alpha}\alpha} . \tag{1.33}$$

If we now look at $\langle p,\alpha|q,\beta\rangle$ and assume that $\{b^\dagger_{r,q}, b_{s,p}\} = \delta_{rs}(2\pi)^3\delta^{(3)}(\vec{p}-\vec{q})$, then Eq. (1.8) holds provided that

$$\sum_s v^s(\vec{p})^\alpha u^s(\vec{p})_\beta = m\delta^\alpha_\beta. \tag{1.34}$$

This relation is easily verified in the rest frame (i.e. where $\vec{p}=\vec{0}$).

Let us now construct a field operator $\xi(\vec{x})_\alpha$ as

$$\xi(\vec{x})_\alpha \equiv \sum_s \int \frac{\mathrm{d}^3p}{(2\pi)^3}\frac{1}{\sqrt{2E_p}}\left(u^s(\vec{p})_\alpha b^\dagger_{p,s}\mathrm{e}^{-\mathrm{i}\vec{p}\cdot\vec{x}} + v^s(\vec{p})_\alpha b_{p,s}\mathrm{e}^{\mathrm{i}\vec{p}\cdot\vec{x}}\right) . \tag{1.35}$$

Like the scalar field operator $\phi(\vec{x})$, this operator satisfies

$$\xi(\vec{x})_\alpha|0\rangle = \sqrt{m}\int\frac{\mathrm{d}^3p}{(2\pi)^3}\frac{1}{2E_p}\mathrm{e}^{-\mathrm{i}\vec{p}\cdot\vec{x}}|p,\alpha\rangle , \tag{1.36}$$

and similarly when acting on $\langle 0|$.

For a real scalar field, there is one generalized coordinate degree of freedom (d.o.f.) and one corresponding conjugate momentum d.o.f. at each space point $\vec{x}$. We should have twice that number of phase space d.o.f.'s (i.e. 4 per space point) for a massive spin $\frac{1}{2}$ field. But treating the components of ξ and $\xi^\dagger$ as independent already amounts to 4 d.o.f.'s. Therefore, the conjugate momentum to ξ must somehow be built out of $\xi^\dagger$. With the benefit of hindsight, let us put in an additional factor 'i',

$$\pi(\vec{x})_{\dot{\alpha}} \equiv \mathrm{i}\xi^\dagger(\vec{x})_{\dot{\alpha}} . \tag{1.37}$$

By brute force computation one can show that

$$\begin{aligned}\{\xi(\vec{x})_\alpha, \xi(\vec{y})_\beta\} = \{\pi(\vec{x})_{\dot{\alpha}}, \pi(\vec{y})_{\dot{\beta}}\} = 0 ,\\ \{\xi(\vec{x})_\alpha, \pi(\vec{y})_{\dot{\alpha}}\} = \mathrm{i}\delta_{\alpha\dot{\alpha}}\delta^{(3)}(\vec{x}-\vec{y}) ,\end{aligned} \tag{1.38}$$

i.e. ξ_α and $\pi_{\dot{\beta}}$ obey canonical equal time anti-commutation relations. To figure out the classical dynamics of ξ_α, we need to write H_0 in Eq. (1.17) in terms of ξ_α and $\pi_{\dot{\alpha}}$ and then compute the classical equations of motion that follow from this Hamiltonian. First, one can show that $b_{p,s}$ and $b^\dagger_{p,s}$ can be expressed in terms of ξ_α and $\pi_{\dot{\alpha}}$ as[4],

$$\begin{aligned} b_{p,s} &= \frac{1}{\sqrt{2E_p}}\int \mathrm{d}^3x\,\mathrm{e}^{-\mathrm{i}\vec{x}\cdot\vec{p}}\left[v^{s\dagger}(\vec{p})_\alpha\xi(\vec{x})_\alpha - \mathrm{i}u^s(\vec{p})^{\dot{\alpha}}\pi(\vec{x})^{\dot{\alpha}}\right] ,\\ b^\dagger_{p,s} &= \frac{1}{\sqrt{2E_p}}\int \mathrm{d}^3x\,\mathrm{e}^{\mathrm{i}\vec{x}\cdot\vec{p}}\left[u^{s\dagger}(\vec{p})^\alpha\xi(\vec{x})^\alpha - \mathrm{i}v^s(\vec{p})_{\dot{\alpha}}\pi(\vec{x})_{\dot{\alpha}}\right] .\end{aligned} \tag{1.39}$$

[4] I am aware that the spinor index contractions look very strange in Eqs. (1.39). For example, a downstairs index on $v^{s\dagger}$ is contracted with the downstairs index on ξ in the first line, which is certainly not Lorentz invariant. These are not typos!

Then, we note that $H_0 = \int \frac{\mathrm{d}^3p}{(2\pi)^3} E_p \sum_s b^\dagger_{p,s} b_{p,s}$, so if we plug in the above expressions for the creation and annihilation operators, one can arrive at

$$H_0 = \int \mathrm{d}^3x \left[\mathrm{i}\pi_{\dot\alpha} (\vec\sigma \cdot \vec\nabla)^{\dot\alpha\beta} \xi_\beta + \frac{m}{2} \left(\xi^\alpha \xi_\alpha - \pi_{\dot\alpha} \pi^{\dot\alpha} \right) \right] , \tag{1.40}$$

up to a constant. The corresponding Lagrangian is

$$\mathcal{L}_0^{s=1/2} = \mathrm{i}\xi^\dagger_{\dot\alpha} (\bar\sigma^\mu)^{\dot\alpha\alpha} \partial_\mu \xi_\alpha - \frac{m}{2} (\xi^\alpha \xi_\alpha + \xi^\dagger_{\dot\alpha} \xi^{\dagger\dot\alpha}) , \tag{1.41}$$

and the classical equation of motion for ξ_α is

$$\mathrm{i}(\bar\sigma^\mu)^{\dot\alpha\alpha} \partial_\mu \xi_\alpha = -m \xi^{\dagger\dot\alpha} . \tag{1.42}$$

Consider now the theory of two free Weyl fermions ξ and χ with the same mass m,

$$\mathcal{L} = \mathrm{i}\xi^\dagger \bar\sigma^\mu \partial_\mu \xi + \mathrm{i}\chi^\dagger \bar\sigma^\mu \partial_\mu \chi - \frac{m}{2} (\xi\xi + \chi\chi + \text{c.c.}) . \tag{1.43}$$

This theory has an SO(2) symmetry,

$$\begin{pmatrix} \xi \\ \chi \end{pmatrix} \to \begin{pmatrix} \cos\theta & -\sin\theta \\ \sin\theta & \cos\theta \end{pmatrix} \begin{pmatrix} \xi \\ \chi \end{pmatrix} . \tag{1.44}$$

The eigenstates of this symmetry operation are

$$\psi_\mathrm{L} \equiv \frac{1}{\sqrt{2}} (\xi + \mathrm{i}\chi) , \quad \psi_\mathrm{R} \equiv \frac{1}{\sqrt{2}} (\xi - \mathrm{i}\chi) \tag{1.45}$$

which transform as $\psi_{\mathrm{L,R}} \to \mathrm{e}^{\pm\mathrm{i}\theta} \psi_{\mathrm{L,R}}$ respectively, under (1.44). By introducing the *Dirac spinor* $\Psi(x)$

$$\Psi \equiv \begin{pmatrix} \psi_{\mathrm{L}\alpha} \\ \psi^{\dagger\dot\alpha}_\mathrm{R} \end{pmatrix} , \tag{1.46}$$

which belongs to the $(\frac{1}{2}, 0) \oplus (0, \frac{1}{2})$ representation of the Lorentz group, we can write Eq. (1.43) in a very condensed form,

$$\mathcal{L} = \mathrm{i}\bar\Psi \gamma^\mu \partial_\mu \Psi - m \bar\Psi \Psi \tag{1.47}$$

where

$$\gamma^\mu \equiv \begin{pmatrix} 0 & \sigma^\mu \\ \bar\sigma^\mu & 0 \end{pmatrix} \quad \text{and} \quad \bar\Psi \equiv \Psi^\dagger \gamma^0 . \tag{1.48}$$

Eq. (1.47) is just the Dirac Lagrangian, from which we can see that the classical dynamics of $\Psi(x)$ is described by the Dirac equation

$$(\mathrm{i}\gamma^\mu \partial_\mu - m)\Psi = 0 . \tag{1.49}$$

1.5 Free fields: spin 1

For a massive spin 1 particle in its rest frame, we need to define $2s+1=3$ basis polarization vectors $\epsilon^s(\vec{0})$ that transform in the spin 1 representation of SO(3). Given this transformation property, and that they also necessarily belong to some representation of the Lorentz group, we conclude that the ϵ^s's must be four-vectors (meaning that the σ label on the one-particle states in this section will correspond to a Lorentz vector index μ). Let us take these to be

$$\epsilon^{\pm}(\vec{0})^{\mu} = \frac{1}{\sqrt{2}}(0,1,\pm\mathrm{i},0) \quad \text{and} \quad \epsilon^{0}(\vec{0})^{\mu} = (0,0,0,1)\,, \tag{1.50}$$

which are eigenvectors under rotations around the z axis, i.e. eigenvectors of

$$(\mathcal{J}^{12})^{\mu}{}_{\nu} = \begin{pmatrix} 0 & 0 & 0 & 0 \\ 0 & 0 & -\mathrm{i} & 0 \\ 0 & \mathrm{i} & 0 & 0 \\ 0 & 0 & 0 & 0 \end{pmatrix}. \tag{1.51}$$

These have the Lorentz invariant normalization

$$\epsilon^{r*}(\vec{p})_{\mu}\epsilon^{s}(\vec{p})^{\mu} = -\delta^{rs}\,. \tag{1.52}$$

The polarisation vectors also obey the relations

$$\sum_s \epsilon^s(\vec{p})^{\mu}\epsilon^{s*}(\vec{p})^{\nu} = -\eta^{\mu\nu} + \frac{p^{\mu}p^{\nu}}{m^2} \quad \text{and} \quad p_{\mu}\epsilon^s(\vec{p})^{\mu} = 0\,, \tag{1.53}$$

which are most easily verified in the rest frame (but of course hold in any other frame due to Lorentz covariance).

We can now define our creation operators $b^{\dagger}_{p,s}$ as before,

$$|p,\mu\rangle \equiv \sqrt{2E_p}\epsilon^s(\vec{p})^{\mu}b^{\dagger}_{s,p}\,|0\rangle\,. \tag{1.54}$$

If we take these to obey $[b_{p,s}, b^{\dagger}_{q,r}] = \delta_{rs}(2\pi)^3\delta^{(3)}(\vec{p}-\vec{q})$, we find that our one-particle states are normalized as

$$\langle p,\mu|q,\nu\rangle = 2E_p\left(\frac{p^{\mu}p^{\nu}}{m^2} - \eta^{\mu\nu}\right)(2\pi)^3\delta^{(3)}(\vec{p}-\vec{q})\,. \tag{1.55}$$

This interesting equation is easiest to interpret in the rest frame (taking $p^{\mu} = q^{\mu} = p^{\mu}_{\mathrm{rest}} \equiv (m,\vec{0})$). The states $|p_{\mathrm{rest}},\mu\rangle$ and $|p_{\mathrm{rest}},\nu\rangle$ have zero overlap when $\mu \neq \nu$ which is just a statement of the orthogonality of our state vectors. However, the right-hand side of Eq. (1.55) also gives zero when $\mu = \nu = 0$. To interpret this, first note that $|p_{\mathrm{rest}},\mu=0\rangle$ does not transform under rotations, meaning that it should be interpreted as a spin 0 state rather than spin 1. In our description of spin 1 particles, the "spin 0 state" $|p_{\mathrm{rest}},\mu=0\rangle$ has zero norm. The probability to find the system in this state is therefore always zero: it is not physical!

We can now proceed to construct a field operator $A^\mu(\vec{x})$ that should obey

$$A^\mu(\vec{x})\,|0\rangle = \int \frac{\mathrm{d}^3p}{(2\pi)^3}\frac{1}{2E_p}\mathrm{e}^{-\mathrm{i}\vec{p}\cdot\vec{x}}\,|p,\mu\rangle \quad \text{and} \quad \langle 0|\,A^\mu(\vec{x}) = \int \frac{\mathrm{d}^3p}{(2\pi)^3}\frac{1}{2E_p}\mathrm{e}^{\mathrm{i}\vec{p}\cdot\vec{x}}\,\langle p,\mu|\ . \tag{1.56}$$

In terms of the creation and annihilation operators, we find that

$$A^\mu(\vec{x}) = \int \frac{\mathrm{d}^3p}{(2\pi)^3}\frac{1}{\sqrt{2E_p}}\sum_s \left(\epsilon^s(\vec{p})^\mu b^\dagger_{p,s}\mathrm{e}^{-\mathrm{i}\vec{p}\cdot\vec{x}} + \epsilon^{s*}(\vec{p})^\mu b_{p,s}\mathrm{e}^{\mathrm{i}\vec{p}\cdot\vec{x}}\right)\ . \tag{1.57}$$

Assuming a free theory, $A(\vec{x})^\mu$ has a time-dependence (i.e. $A(x)^\mu$) that is given by replacing the exponentials in Eq. (1.57) as $\mathrm{e}^{\pm\mathrm{i}\vec{p}\cdot\vec{x}} \to \mathrm{e}^{\mp\mathrm{i}px}$.

So how do we find the conjugate momenta π^μ to A^μ (i.e. the combinations of b's and $b^\dagger$'s that satisfy canonical commutation relations with A^μ)? First, note that the equation $p_\mu\epsilon^s(\vec{p})^\mu = 0$ corresponds to $\partial_\mu A^\mu = 0$ in position space. This means that

$$\dot{A}^0 = -\vec{\nabla}\cdot\vec{A}\,, \tag{1.58}$$

i.e. A^0 is not an independent dynamical degree of freedom (its time derivative at all times, and hence its time evolution, is set by $\vec{A}(x)$). Therefore, let us try to construct π^μ such that A^0 does not have a conjugate momentum, i.e. $\pi^0 = 0$. Second, recall that for the spin 0 field ϕ we found that we could take $\partial_0\phi$ as its canonical momentum. Let us therefore try the following construction,

$$\pi^\mu \equiv -\partial^0 A^\mu + \partial^\mu A^0\,, \tag{1.59}$$

which in terms of b's and $b^\dagger$'s becomes

$$\begin{aligned}\pi^\mu(\vec{x}) = -\mathrm{i}\int \frac{\mathrm{d}^3p}{(2\pi)^2}\sqrt{\frac{E_p}{2}}\sum_s \Bigg[&\left(\epsilon^s(\vec{p})^\mu - \frac{p^\mu}{E_p}\epsilon^s(\vec{p})^0\right)\mathrm{e}^{-\mathrm{i}\vec{p}\cdot\vec{x}}b^\dagger_{p,s} \\ &- \left(\epsilon^{*s}(\vec{p})^\mu - \frac{p^\mu}{E_p}\epsilon^{*s}(\vec{p})^0\right)\mathrm{e}^{\mathrm{i}\vec{p}\cdot\vec{x}}b_{p,s}\Bigg]\end{aligned} \tag{1.60}$$

at $x^0 = 0$. Indeed, using the commutation relations of $b_{p,s}$ and $b^\dagger_{p,s}$ combined with the relations in Eq. (1.53), we arrive at just the right equal time commutation relations,

$$[A^\mu(\vec{x}\,), A^\nu(\vec{y}\,)] = [\pi^\mu(\vec{x}\,), \pi^\nu(\vec{y}\,)] = 0, \tag{1.61}$$

and

$$[A^\mu(\vec{x}\,), \pi^\nu(\vec{y}\,)] = \mathrm{i}(-\eta^{\mu\nu} + \eta^{\mu 0})\delta^{(3)}(\vec{x} - \vec{y}\,)\,. \tag{1.62}$$

That is, the spatial components satisfy $[A^i, \pi^j] \propto \mathrm{i}\delta^{ij}$ while the temporal component A^0 has vanishing equal time commutators with all A^μ's and π^μ's.

We can now invert Eqs. (1.57) and (1.60), and arrive at

$$\begin{aligned} b^\dagger_{p,s} = & -\frac{1}{\sqrt{2}}\int \mathrm{d}^3x \mathrm{e}^{\mathrm{i}\vec{p}\cdot\vec{x}}\left[\sqrt{E_p}\left(\epsilon^{*s}(\vec{p})_\mu - \frac{\epsilon^{*s}(\vec{p})_0}{E_p}p_\mu\right)A^\mu(\vec{x})\right. \\ & \left. + \frac{\mathrm{i}}{\sqrt{E_p}}\epsilon^{*s}(\vec{p})_\mu \pi^\mu(\vec{x})\right], \\ b_{p,s} = & -\frac{1}{\sqrt{2}}\int \mathrm{d}^3x \mathrm{e}^{-\mathrm{i}\vec{p}\cdot\vec{x}}\left[\sqrt{E_p}\left(\epsilon^{s}(\vec{p})_\mu - \frac{\epsilon^{s}(\vec{p})_0}{E_p}p_\mu\right)A^\mu(\vec{x})\right. \\ & \left. - \frac{\mathrm{i}}{\sqrt{E_p}}\epsilon^{s}(\vec{p})_\mu \pi^\mu(\vec{x})\right]. \end{aligned} \tag{1.63}$$

Upon plugging these expressions into the free Hamiltonian, one can eventually obtain

$$H_0 = \int \mathrm{d}^3x \left[\frac{1}{2}(\vec{\pi})^2 - \frac{1}{2}A^i(\delta_{ij}\vec{\nabla}^2 - \partial_i\partial_j)A^j + \frac{1}{2}m^2\vec{A}^2 - \frac{1}{2}m^2\Phi^2 + \vec{\pi}\cdot\vec{\nabla}\Phi\right], \tag{1.64}$$

where I have denoted

$$A^\mu = (\Phi, \vec{A}) \quad \text{and} \quad \vec{\pi} \equiv \pi^i\,. \tag{1.65}$$

To derive H_0 in the form of Eq. (1.64), I have used the relation $\partial_i\pi^i = -m^2\Phi$ which follows from Eq. (1.60). The Lagrangian is one Legendre transformation away from Eq. (1.64) and is very compact:

$$\mathcal{L}_0^{s=1} = -\frac{1}{4}F_{\mu\nu}F^{\mu\nu} + \frac{1}{2}m^2A_\mu A^\mu \tag{1.66}$$

where

$$F_{\mu\nu} \equiv \partial_\mu A_\nu - \partial_\nu A_\mu\,. \tag{1.67}$$

The equations of motion that follow from Eq. (1.66) are

$$\partial_\mu F^{\mu\nu} = -m^2A^\nu\,. \tag{1.68}$$

If we act with ∂_ν on both sides of the above equation, we find that $m^2\partial_\nu A^\nu = 0$, i.e. the constraint $\partial_\nu A^\nu = 0$ is still encoded in the Lagrangian in Eq. (1.66) for $m^2 \neq 0$. Note also that Eq. (1.68) is just the covariant form of Maxwell's equations when $m \to 0$.

Let us now recall an interesting property of particles with spin ≥ 1: The number of spin states does not match the number of helicity states. The Lagrangian in Eq. (1.66) as it stands describes one longitudinal and two transverse polarisation states of a massive spin 1 field. However, we know from Wigner's classification that the massless spin 1 particle only has two possible polarization states, meaning that the longitudinal polarization state should somehow "drop out" of Eq. (1.66) if we take $m^2 \to 0$. How does that happen?

With $m^2 = 0$, the Lagrangian in Eq. (1.66) becomes invariant under *gauge transformations*, i.e.

$$A_\mu(x) \to A_\mu(x) - \frac{1}{g}\partial_\mu\alpha(x) \tag{1.69}$$

where α is some arbitrary function, and g is a constant that I have put in for future convenience (although it could be absorbed into $\alpha(x)$ at this stage). If we choose to stay in the so-called Lorentz gauge where $\partial_\mu A^\mu = 0$, we can still do gauge transformations using α's that satisfy $\partial^2\alpha(x) = 0$. Such functions can be expanded in plane waves with dispersion $p^2 = 0$,

$$\alpha(x) = \int \frac{\mathrm{d}^3p}{(2\pi)^3}\frac{1}{\sqrt{2E_p}}\mathrm{i}\tilde{\alpha}(\vec{p})\mathrm{e}^{\mathrm{i}px} + \mathrm{c.c}\,. \tag{1.70}$$

In momentum space, such gauge transformations correspond to shifting the polarisation vectors as

$$\epsilon^s(\vec{p})^\mu \to \epsilon^s(\vec{p})^\mu + \frac{1}{g}\tilde{\alpha}(\vec{p})p^\mu\,. \tag{1.71}$$

This can then be used to completely remove the longitudinal polarisation state, since the corresponding polarisation vector satisfies $\epsilon^\mu \propto p^\mu$.

This concludes our discussion of free field theories. To recap, starting only with the quantum states allowed by Poincaré invariance, we were able to show that the classical limit of the free Hamiltonian can lead either to e.g. the Klein-Gordon equation, the Dirac equation or Maxwell's equations, depending on the spin and the mass of the particle. I have restricted this discussion to particles with spin ≤ 1 since higher spins are not so often encountered in elementary particle physics (they at least do not appear in any of the articles included in this thesis!).

2 Quantum field theory: interactions

2.1 The path integral

Before jumping into examples of interacting quantum field theories, I will introduce another piece of formal theory which is extremely convenient for explicit calculations: the path integral. Let us take a general quantum theory with basis states $|q\rangle$ that are eigenstates of a generalized coordinate $\vec{Q}$, i.e. $\vec{Q}\,|q\rangle = \vec{q}\,|q\rangle$, and let $\vec{P}$ correspond to the conjugate momenta of $\vec{Q}$ such that

$$[(\vec{Q})_i, (\vec{P})_j] = \mathrm{i}\delta_{ij}\,. \tag{1.72}$$

The δ-function is here to be read either as a Kronecker delta or a Dirac delta function depending on if i and j are discrete or continuous labels. Given an arbitrary Hamiltonian $H(\vec{Q}, \vec{P})$, let us rewrite the amplitude for an initial state $|q_\mathrm{I}\rangle$ at $t = t_\mathrm{I}$ to evolve into a final state $|q_\mathrm{F}\rangle$ at $t = t_\mathrm{F}$,

$$\mathcal{A}_{\mathrm{I}\to\mathrm{F}} = \langle q_\mathrm{F}|\,\mathrm{e}^{-\mathrm{i}(t_\mathrm{F}-t_\mathrm{I})H}\,|q_\mathrm{I}\rangle\ , \tag{1.73}$$

in a somewhat obscure way. First, we write the exponential as a product of N factors of $\mathrm{e}^{-\mathrm{i}\epsilon H}$ where $\epsilon \equiv (t_\mathrm{F} - t_\mathrm{I})/N$ is a very short time interval when N is large. Second,

we insert a complete set of coordinate eigenstates, $1 = \int \mathrm{d}\vec{q}\,|q\rangle\,\langle q|$, between each such factor. This gives

$$\mathcal{A}_{\mathrm{I}\to\mathrm{F}} = \int \mathrm{d}\vec{q}_1 \cdots \int \mathrm{d}\vec{q}_{N-1}\,\langle q_{\mathrm{F}}|\,\mathrm{e}^{-\mathrm{i}\epsilon H}\,|q_{N-1}\rangle\,\langle q_{N-1}|\ldots|q_1\rangle\,\langle q_1|\,\mathrm{e}^{-\mathrm{i}\epsilon H}\,|q_{\mathrm{I}}\rangle\ . \tag{1.74}$$

We can evaluate each individual overlap by also inserting a complete set of momentum eigenstates,

$$\begin{aligned}\langle q_{i+1}|\,\mathrm{e}^{-\mathrm{i}\epsilon H(\vec{Q},\vec{P})}\,|q_i\rangle &= \int \mathrm{d}\vec{p}_i\,\langle q_{i+1}|p_i\rangle\,\langle p_i|\,\mathrm{e}^{-\mathrm{i}\epsilon H(\vec{Q},\vec{P})}\,|q_i\rangle \\ &= \int \mathrm{d}\vec{p}_i\,\exp\left[\mathrm{i}\epsilon\left(\vec{p}_i\cdot\frac{\vec{q}_{i+1}-\vec{q}_i}{\epsilon} - H(\vec{q}_i,\vec{p}_i)\right)\right]\ ,\end{aligned} \tag{1.75}$$

where I have used that $\langle q_i|p_i\rangle = \mathrm{e}^{\mathrm{i}\vec{p}_i\cdot\vec{q}_i}$, and assumed that all $\vec{P}$'s are to the left of the $\vec{Q}$'s in $H(\vec{P},\vec{Q})$ (if they we're not we could just use Eq. (1.72) to bring H to this form plus an unimportant overall constant).

Now take $N\to\infty$ (i.e. $\epsilon\to 0$). The amplitude becomes

$$\mathcal{A}_{\mathrm{I}\to\mathrm{F}} = \int_{\vec{q}(t_{\mathrm{I}})=\vec{q}_{\mathrm{I}}}^{\vec{q}(t_{\mathrm{F}})=\vec{q}_{\mathrm{F}}} \mathcal{D}\vec{q}(t)\int\mathcal{D}\vec{p}(t)\exp\left[\mathrm{i}\int_{t_{\mathrm{I}}}^{t_{\mathrm{F}}}\mathrm{d}t\left(\vec{p}\cdot\dot{\vec{q}}-H(\vec{q},\vec{p})\right)\right]\ , \tag{1.76}$$

where the *functional integrals* sum over all classical paths between $\vec{q}(t_{\mathrm{I}}) = \vec{q}_{\mathrm{I}}$ and $\vec{q}(t_{\mathrm{F}}) = \vec{q}_{\mathrm{F}}$ (at each point in time, there is an integral over the full classical phase space).

Although the $\vec{p}\cdot\dot{\vec{q}} - H(\vec{q},\vec{p})$ in Eq. (1.76) certainly looks like a Lagrangian, it should not be interpreted as such at this point since $\vec{p}$ and $\dot{\vec{q}}$ are independent variables (and not related by the classical equation of motion $\dot{\vec{q}} = \frac{\partial H}{\partial\vec{p}}$). Let us now return to field theory, where the field operators and their conjugate momenta take the place of $\vec{Q}$ and $\vec{P}$ respectively in the above discussion. For example, for the spin 0 field, one can perform the integrals over π since they merely amount to a set of Gaussian integrals. One gets

$$\mathcal{A}_{\mathrm{I}\to\mathrm{F}} = \mathcal{N}\int\mathcal{D}\phi\,\mathrm{e}^{\mathrm{i}\int\mathrm{d}^4x\,\mathcal{L}_0^{s=0}}\ , \tag{1.77}$$

where the functional integral sums over all field configurations of $\phi(\vec{x},t)$ for $t_{\mathrm{I}} < t < t_{\mathrm{F}}$, but where the endpoints correspond to some fixed field configurations $\phi(\vec{x},t_{\mathrm{I,F}}) = \phi_{\mathrm{I,F}}(\vec{x})$.

Let us consider the transition amplitude $\mathcal{A}_{\mathrm{I}\to\mathrm{F}}$ when $t_{\mathrm{F,I}} = \pm\infty$ and when $\phi(\vec{x})_{\mathrm{I,F}}$ are whatever field configurations that minimize the energy. This amplitude, which I'll denote as $\mathcal{Z}[0]$, is the"vacuum-to-vacuum" transition amplitude and turns out to be a very important quantity in QFT. We can further define the quantity $\mathcal{Z}[J(x)]$, which is the vacuum-to-vacuum amplitude in the presence of an external source $J(x)$:

$$\mathcal{Z}[J(x)] \equiv \int\mathcal{D}\phi\,\mathrm{e}^{\mathrm{i}\int\mathrm{d}^4x[\mathcal{L}+\phi(x)J(x)]}\ . \tag{1.78}$$

The basic building block of physical quantities in QFT are the so called n-point functions

$$G(x_1,\ldots,x_n) \equiv \langle\Omega|\,\mathcal{T}\phi(x_1)\ldots\phi(x_n)\,|\Omega\rangle\ . \tag{1.79}$$

Here $|\Omega\rangle$ is the vacuum state (which in free field theory just corresponds to the empty state $|0\rangle$), and $\mathcal{T}\phi(x_1)\dots\phi(x_n)$ is the time-ordered product of the field operators $\phi(x_i)$ (i.e. they are to be ordered from left to right by ascending $(x_i)^0 = t_i$). Once you have computed the relevant n-point functions, there are standard formulae you can use to compute measurable quantities like cross-sections and decay rates. In short, if you know the n-point functions, you know in principle the physical predictions of the theory. One can show, by a similar calculation as the one above, that the n-point functions can be computed using a path integral,

$$\begin{aligned} G(x_1,\dots,x_n) &= \frac{\int \mathcal{D}\phi\, \phi(x_1)\dots\phi(x_n)\, \mathrm{e}^{\mathrm{i}\int \mathrm{d}^4x\mathcal{L}}}{\int \mathcal{D}\phi\, \mathrm{e}^{\mathrm{i}\int \mathrm{d}^4x\mathcal{L}}} \\ &= \frac{1}{\mathcal{Z}[0]}\left[(-\mathrm{i})\frac{\delta}{\delta J(x_1)}\dots(-\mathrm{i})\frac{\delta}{\delta J(x_n)}\mathcal{Z}[J]\right]_{J=0} . \end{aligned} \tag{1.80}$$

Although vacuum-to-vacuum amplitudes might seem rather dull at first sight, this shows that once we have computed $\mathcal{Z}[J]$ then we in principle know all the physical predictions of the theory!

2.2 The Wilson renormalization group

Consider again $\mathcal{Z}[J]$. What field configurations $\phi(x)$ should we actually integrate over in Eq. (1.78)? If we would integrate over *all* of them, then this implies that we allow for variations in ϕ over arbitrarily small space-time intervals (or equivalently we allow our particles to have arbitrarily high momenta). This might be asking too much of the theory (unless you are a very ambitions model builder!), and in practice there is always a highest energy scale Λ above which we expect our theory not to be valid. The cut-off scale Λ could for example be the inverse lattice spacing in a solid state theory ($\Lambda_{\text{metals}} \sim (10\,\text{Å})^{-1}$), or the electro-weak scale in the Fermi theory ($\Lambda_{\text{Fermi}} \sim 100\,\text{GeV}$). We do not yet know where the cut-off scale lies for the Standard Model (more about this in Sec. 4), but it must at least be bounded from above by the Planck scale $\Lambda_{\text{SM}} < M_{\text{Pl}}$ (at this scale, gravitational interactions, which are not included in the SM, are expected to become important). So let us modify our path integral to only integrate over Fourier modes with momenta less than some Λ,

$$\mathcal{Z}[J] = \int^{\Lambda} \mathcal{D}\phi\, \mathrm{e}^{\mathrm{i}\int \mathrm{d}^4x(\mathcal{L}+J\phi)} . \tag{1.81}$$

If we have a theory that has some number of coupling constants, we also need to do the same number of independent measurements to set the numerical values of those couplings before we can make any predictions. Should we also regard the cut-off Λ as an additional parameter of the theory to be set by some experiment? Rather, we can imagine that we could change the value of Λ slightly, and make compensating small changes in the couplings of the theory such that $\mathcal{Z}[J]$ is unchanged. This cut-off dependence of the couplings defines the Wilson Renormalization Group. Let us take the theory of a single real scalar field as an example,

$$\mathcal{L} = \frac{1}{2}(\partial\phi)^2 - V(\phi) , \tag{1.82}$$

with

$$V(\phi) = \frac{1}{2}g_2\phi^2 + \frac{1}{3!}g_3\phi^3 + \frac{1}{4!}g_4\phi^4 + \frac{1}{5!}g_5\phi^5 + \dots\,, \tag{1.83}$$

defined with some cut-off $\Lambda_{\rm H}$. Note that we need to do an infinite number of measurements to set the values of all g_i (i.e. we require an infinite number of "renormalisation conditions"). Theories with this property are traditionally called "non-renormalisable".

If we now imagine that we continuously lower the cut-off Λ while keeping $\mathcal{Z}[J]$ unchanged, the flow of the couplings is described by a set of differential equations as

$$\Lambda\frac{\mathrm{d}}{\mathrm{d}\Lambda}g_r = \Lambda^{4-r}\beta^r(\{\Lambda^{s-4}g_s\})\,, \tag{1.84}$$

where β^r are dimensionless functions of the couplings that are in principle calculable by solving $\Lambda\frac{\mathrm{d}}{\mathrm{d}\Lambda}\mathcal{Z} = 0$, and the factors of Λ are inserted by dimensional analysis. We can rewrite Eq. (1.84) in terms of the dimensionless couplings $\lambda_r \equiv \Lambda^{r-4}g_r$,

$$\Lambda\frac{\mathrm{d}}{\mathrm{d}\Lambda}\lambda_r = (r-4)\lambda_r + \beta^r(\{\lambda_s\})\,. \tag{1.85}$$

Suppose that $\bar{\lambda}_r(\Lambda)$ is the solution of Eq. (1.85) for some boundary conditions defined at $\Lambda = \Lambda_{\rm H}$. Let us look at the behaviour of small perturbations around this solution,

$$\lambda_r(\Lambda) = \bar{\lambda}_r(\Lambda) + \epsilon_r(\Lambda)\,. \tag{1.86}$$

Linearising Eq. (1.85) then gives

$$\Lambda\frac{\mathrm{d}}{\mathrm{d}\Lambda}\epsilon_r = (r-4)\epsilon_r + \left(\frac{\partial\beta^r}{\partial\lambda_s}\right)_{\lambda=\bar{\lambda}}\epsilon_s\,. \tag{1.87}$$

Unless the β^r's become very big, the first term on the RHS above essentially governs the evolution of $\epsilon^r(\Lambda)$ (except for $r = 4$). We therefore expect that

$$\epsilon^r(\Lambda) \approx \left(\frac{\Lambda}{\Lambda_{\rm H}}\right)^{r-4}\epsilon^r(\Lambda_{\rm H})\,. \tag{1.88}$$

When we lower Λ, say to $\Lambda_{\rm L}$ (which can still be much larger than energies $\Lambda_{\rm exp}$ that are directly accessible in experiments), from $\Lambda_{\rm H}$, $\epsilon^{r>4}$ become extremely suppressed when $\Lambda_{\rm H} \gg \Lambda_{\rm L}$. If we only perturbed $\lambda^{r>4}$ at $\Lambda_{\rm H}$, then the couplings would still flow towards $\bar{\lambda}$, meaning that the actual boundary conditions $\lambda^{r>4}(\Lambda_{\rm H})$ did not really matter much. Instead, $\lambda^r(\Lambda_{\rm H})$ only depend on $\lambda^{r\leq 4}(\Lambda_{\rm H})$ up to corrections of size $(\Lambda_{\rm L}/\Lambda_{\rm H})^{r-4}$, which in particular also means that $\lambda^{r>4}(\Lambda_{\rm L})$ can be entirely written in terms of $\lambda^{r\leq 4}(\Lambda_{\rm L})$. For this reason, operators associated with positive (negative) energy dimension are called *relevant* (*irrelevant*), while operators that come with dimensionless couplings are called *marginal*. The theory becomes fully determined at $\Lambda_{\rm L}$ by a few renormalization conditions (that fix the numerical values of $\lambda^{r\leq 4}(\Lambda_{\rm L})$), which is a huge improvement compared to the infinite number of renormalization conditions that are needed to fix the values of $\lambda^r(\Lambda_{\rm H})$. This is just the characteristic property of the theories that are traditionally dubbed "renormalizable". If there is enough "head room" to lower the

cut-off from Λ_{H} to $\Lambda_{\mathrm{L}} \ll \Lambda_{\mathrm{H}}$, but still having $\Lambda_{\mathrm{L}} \gg \Lambda_{\mathrm{exp}}$, then the above procedure can be used to get rid of the irrelevant information about the extreme high energy modes in the theory. This discussion is originally due to Polchinski [7].

Note that the couplings $g^{r>4}$ do not necessarily run to zero. However, they run towards some given functions of $\lambda^{r\leq 4}$ suppressed by Λ^{r-4}. Provided that $\Lambda_{\mathrm{L}} \gg \Lambda_{\mathrm{exp}}$, it turns out that all the effects of the operators associated with $\lambda^{r>4}$ can either be "absorbed" into the lower-dimensional operators by shifting the values of $\lambda^{r\leq 4}$, or are suppressed by powers of $\Lambda_{\mathrm{exp}}/\Lambda_{\mathrm{L}}$. This was proven by Appelquist and Carazzone in 1975 [8]. The above discussion tells us that when we try to write down realistic quantum field theories describing "long distance physics" far away from a physical cut-off Λ, it is justified to only include operators that come with couplings with non-negative energy dimensions. In particular, this is of course the way the Standard Model is constructed (more about this in Sec. 3), and it certainly seems to work extremely well.

The above discussion showed that $g^{r>4}(\Lambda_{\mathrm{L}})$ are largely insensitive to the boundary conditions $g^{r>4}(\Lambda_{\mathrm{H}})$. On the other hand, couplings with positive mass dimension $g^{r<4}(\Lambda_{\mathrm{L}})$ are extremely sensitive to the boundary conditions at Λ_{H}, and must be very delicately balanced in the UV limit to have a certain value at Λ_{L}. In the Standard Model there is one such parameter: the Higgs mass squared parameter $-\mu_{\mathrm{H}}^2$ (which in turn sets the scale of the electro-weak symmetry breaking Λ_{EWSB}). If we take $\Lambda_{\mathrm{H}} \sim \Lambda_{\mathrm{Pl}} \approx 10^{18}\,\mathrm{GeV}$ and use the Wilsonian renormalization group to lower the cut-off to say $\Lambda_{\mathrm{L}} \approx 10^{10}\,\mathrm{GeV}$ (any scale that is sufficiently larger than Λ_{EWSB} would just as well) to get rid of irrelevant information about the couplings associated with higher-dimensional operators, then $\mathcal{O}(1\,\mathrm{GeV}^2)$ variations in $\mu_{\mathrm{H}}^2(\Lambda_{\mathrm{L}})$ correspond to incredibly minuscule variations of $\mathcal{O}(10^{-16}\,\mathrm{GeV}^2)$ in $\mu_{\mathrm{H}}^2(\Lambda_{\mathrm{H}})$, since such variations scale as $(\Lambda_{\mathrm{L}}/\Lambda_{\mathrm{H}})^2$ according to Eq. (1.88). This is the essence of the *hierarchy problem* which is indeed one of the biggest unsolved mysteries in theoretical physics today. Namely, the Higgs mass squared parameter needs to be suspiciously fine-tuned for maintaining the hierarchy $\Lambda_{\mathrm{EWSB}}^2/\Lambda_{\mathrm{Pl}}^2 \sim 10^{-32}$ at the quantum level.

2.3 Feynman diagrams and the effective action

Having set up all this formalism, I will now go on to describe how we can in practice compute the n-point functions in perturbation theory. This brings us to the topic of Feynman diagrams, but I will also describe an alternative approach through the use of the *effective action* (which is the starting point of Paper I in this thesis). For concreteness, I will specialise to ϕ^4-theory,

$$\mathcal{L} = \underbrace{\frac{1}{2}(\partial\phi)^2 - \frac{1}{2}m^2\phi^2}_{\equiv\mathcal{L}_0} - \frac{1}{4!}\lambda\phi^4\,. \tag{1.89}$$

Let us set out to compute $\mathcal{Z}[J]$, since we can then obtain the n-point functions by applying various functional derivatives on $\mathcal{Z}[J]$. First, if $\lambda = 0$, then we can rewrite

$$\mathcal{Z}[J]_0 \equiv \mathcal{Z}[J]_{\lambda=0} = \int \mathcal{D}\phi \mathrm{e}^{\mathrm{i}\int \mathrm{d}^4x(\mathcal{L}_0 + J\phi)}\,, \tag{1.90}$$

by performing the shift

$$\phi(x) \to \phi(x) - \int \mathrm{d}^4 y J(y) D(x-y) \tag{1.91}$$

where

$$D(x-y) = \int \frac{\mathrm{d}^4 k}{(2\pi)^4} \frac{\mathrm{e}^{-\mathrm{i}k(x-y)}}{k^2 - m^2} \,. \tag{1.92}$$

The function $D(x-y)$ is the Green's function to the differential operator $(-\partial^2 - m^2)$ meaning that it satisfies

$$(-\partial^2 - m^2) D(x-y) = \delta^{(4)}(x-y) \,. \tag{1.93}$$

The $\frac{1}{2}(\partial\phi)^2$ can be replaced by $\frac{1}{2}\phi(-\partial^2)\phi$ in Eq. (1.89) through an integration by parts (plus an unimportant boundary term that we can ignore). Therefore, the shift in Eq. (1.91) results in

$$\begin{aligned} &\frac{1}{2}\phi(x)(-\partial^2 - m^2)\phi(x) + J(x)\phi(x) \to \\ &\qquad \frac{1}{2}\phi(x)(-\partial^2 - m^2)\phi(x) - \frac{1}{2}\int \mathrm{d}^4 y J(x) J(y) D(x-y) \,. \end{aligned} \tag{1.94}$$

Plugging this into Eq. (1.90) gives that

$$\mathcal{Z}[J]_0 = \mathcal{Z}[0]_0 \, \mathrm{e}^{-\frac{\mathrm{i}}{2}\int \mathrm{d}^4 x \int \mathrm{d}^4 y J(x) J(y) D(x-y)} \,. \tag{1.95}$$

If we now switch on λ, then we note that the exponential of the $-\mathrm{i}\lambda \int \phi^4/4!$ term can be replaced by functional derivatives as

$$\mathcal{Z}[J] = \mathcal{Z}[0]_0 \, \mathrm{e}^{-\mathrm{i}\frac{\lambda}{4!}\int \mathrm{d}^4 z \left[(-\mathrm{i})\frac{\delta}{\delta J(z)}\right]^4} \, \mathrm{e}^{-\frac{\mathrm{i}}{2}\int \mathrm{d}^4 x \int \mathrm{d}^4 y J(x) J(y) D(x-y)} \,. \tag{1.96}$$

Perturbation theory now proceeds by doing a Taylor expansion in λ. The terms that show up in this expansion can be very neatly represented as Feynman diagrams, and the "value" of such diagrams can be found by associating lines and their intersections with algebraic expressions. This association using the so-called the Feyman rules (depicted in Fig. 1.1):

- Each power of λ comes with four derivatives with respect to $J(z)$ and an integration over z. This is called a *vertex*, and is pictorially represented by a dot labelled by z with four outgoing legs. The associated vertex rule is $(-\mathrm{i})\lambda \int \mathrm{d}^4 z$. The $1/4!$ is not included in the Feynman rule since there are most often 4! equivalent ways of attaching the four legs to other parts of the diagram (if this is not the case then this shows up as a symmetry of the diagram whereby we should divide by an appropriate symmetry factor).
- Each factor of $\mathrm{i}D(x-y)$ is represented by a line that connects the points x and y. The factor $\mathrm{i}D(x-y)$ is called a *propagator*.

Figure 1.1: Position space Feynman rules for ϕ^4-theory.

We are more often interested in Fourier transforms of $G(x_1, \ldots, x_n)$, which corresponds to having the external particles in momentum eigenstates. In momentum space, the Feynman rule for the vertex becomes $-\mathrm{i}\lambda$, while a propagator with momentum p^μ is $\frac{\mathrm{i}}{p^2 - m^2}$.

Let us now consider $\mathcal{Z}[0]$, i.e. the full vacuum-to-vacuum transition amplitude in absence of sources. This is obtained by first performing the functional derivatives in Eq. (1.96) and then setting all J's to zero. The perturbation series in λ is then represented by the sum of all diagrams where all propagators are attached to vertices (a leg that is not attached to a vertex corresponds to a factor of J and will thus vanish). Furthermore, this series *exponentiates*. The easiest way to see this is through the symmetry factors: Each fully connected diagram D will be summed to all powers D^n. But since D^n is diagrammatically represented by n identical disconnected sub-diagrams, there is a permutation symmetry between these sub-diagrams such that we should divide by $n!$ to not over count. Each fully connected diagram D then contributes as a factor $\sum_{n=0}^{\infty} D^n/n! = \mathrm{e}^D$ in $\mathcal{Z}[0]$. By representing the sum of all fully connected diagrams as a shaded circle (see Fig. 1.2), we can write

$$\mathcal{Z}[0] = \mathcal{Z}[0]_0 \, \exp\left[\quad \right] . \tag{1.97}$$

We can now rewrite the n-point functions in Eq. (1.80) using Eq. (1.96),

$$\begin{aligned} G(x_1, \ldots, x_n) = & \frac{1}{\mathcal{Z}[0]} \lim_{J \to 0} \mathcal{Z}[0]_0 \, \mathrm{e}^{-\mathrm{i}\frac{\lambda}{4!}\int \mathrm{d}^4 z \left[(-\mathrm{i})\frac{\delta}{\delta J(z)}\right]^4} \\ & \times \left[(-\mathrm{i})\frac{\delta}{\delta J(x_1)} \ldots (-\mathrm{i})\frac{\delta}{\delta J(x_n)}\right] \mathrm{e}^{\frac{\mathrm{i}}{2}\int \mathrm{d}^4 x \int \mathrm{d}^4 y J(x) J(y) D(x-y)} . \end{aligned} \tag{1.98}$$

The functional derivatives w.r.t. $J(x_i)$ bring down propagators that will connect x_i either to another external point x_j or to some internal point (once acted upon by $\mathrm{e}^{-\mathrm{i}\frac{\lambda}{4!}\int \mathrm{d}^4 z \left[(-\mathrm{i})\frac{\delta}{\delta J(z)}\right]^4}$). Diagrammatically, this can be written as

$$G(x_1, \ldots, x_n) = \quad . \tag{1.99}$$

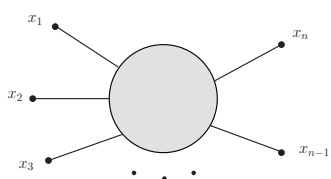

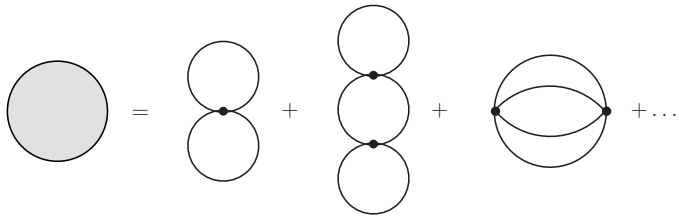

Figure 1.2: Vacuum bubbles in ϕ^4-theory.

The shaded circle here represents all possible ways of connecting the external points x_i using any number of vertices, but without disconnected vacuum bubbles (these are cancelled for by the $1/\mathcal{Z}[0]$ in front). Note that this includes disconnected diagrams, such as  for the 4-point function.

An interesting quantity to consider is the generating functional $W[J]$, defined as

$$\mathrm{i}W[J(x)] = \ln \mathcal{Z}[J(x)]\,. \tag{1.100}$$

If we apply a set of functional derivatives w.r.t. $J(x_i)$ on $W[J]$ and then set $J = 0$, we get the quantities that correspond to fully connected diagrams (i.e. the connected n-point functions). To see this, let us for example compute

$$\left[(-\mathrm{i})\frac{\delta}{\delta J(x_1)}(-\mathrm{i})\frac{\delta}{\delta J(x_2)}(-\mathrm{i})\frac{\delta}{\delta J(x_3)}(-\mathrm{i})\frac{\delta}{\delta J(x_4)}\mathrm{i}W[j]\right]_{J=0}\,. \tag{1.101}$$

Let $\delta_i \equiv (-\mathrm{i})\frac{\delta}{\delta J(x_i)}$ to simplify the notation. By noting that an odd number of derivatives on $\mathcal{Z}[J]$ will vanish when $J \to 0$, we can see that the above expression equals

$$\left\{\frac{1}{\mathcal{Z}[J]}\delta_1\delta_2\delta_3\delta_4\mathcal{Z}[J] - \frac{1}{\mathcal{Z}[J]^2}\left[(\delta_1\delta_2\mathcal{Z}[J])\,(\delta_3\delta_4\mathcal{Z}[J]) + (\text{permutations of } x_i)\right]\right\}_{J=0}$$

$$= \quad - \left(\quad + (\text{permutations of } x_i) \right) \,,$$

$$= \quad + \quad + \quad + \quad + \ldots \tag{1.102}$$

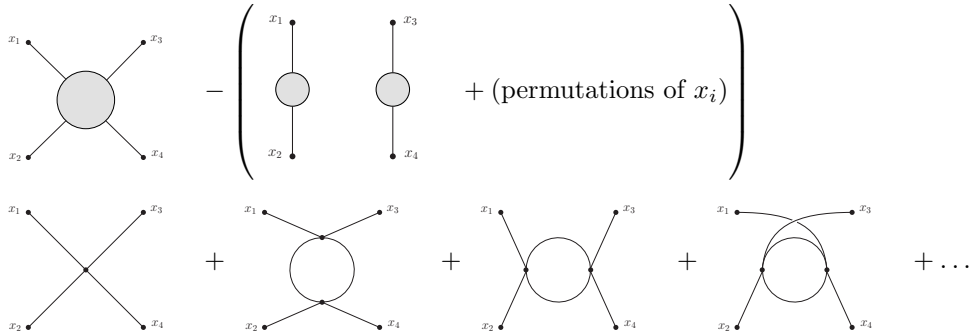

i.e. only fully connected graphs remain. The above sum also includes diagrams with corrections on the external legs, e.g.  .

Let us denote the vacuum expectation value of $\phi(x)$ in the presence of a source $J(x)$ as $\varphi(x)$,

$$\varphi(x) = \frac{\delta W}{\delta J(x)}\,. \tag{1.103}$$

Note that $\varphi(x)$ has a functional dependence on the source $J(x)$: the value of φ at a certain point in space-time x_i depends on the full functional form of J and not just $J(x_i)$.

The *effective action* $\Gamma[\varphi(x)]$ is obtained through a Legendre transform of $W[J(x)]$ that trades the functional dependence on $J(x)$ for $\varphi(x)$,

$$\Gamma[\varphi(x)] \equiv \int \mathrm{d}^4 z J(z)\varphi(z) - W[J(x)]\,. \tag{1.104}$$

The RHS here is to be read as only depending on $\varphi(x)$, meaning that $J(x)$ needs to be expressed entirely in terms of $\varphi(x)$ (which in principle can be done by inverting Eq. (1.103)). In particular, the effective action satisfies

$$\begin{aligned}\frac{\delta\Gamma[\varphi]}{\delta\varphi(x)} &= J(x) + \int \mathrm{d}^4 z \varphi(z)\frac{\partial J(z)}{\partial\varphi(x)} - \int \mathrm{d}^4 z \frac{\delta W}{\delta J(z)}\frac{\delta J(z)}{\delta\varphi(x)} \\ &= J(x)\,.\end{aligned} \tag{1.105}$$

Notice therefore that $\delta\Gamma = 0$ in the absence of sources, just like the classical action is extremised at the classical level. At a given order in perturbation theory in a weakly coupled theory, the effective action will almost look like the classical action, up to small shifts in the coupling constants and the appearance of new loop suppressed higher-dimensional interaction terms. While the interaction terms in the classical action describe classical point-like interactions, the effective action tells us how masses, interactions and field normalizations are modified by quantum fluctuations.

From this point of view, it is plausible that $\Gamma[\varphi]$ is the generating functional of fully connected diagrams without external leg corrections (so called connected and *amputated* diagrams). I will not give a proof of this here, but merely make it more plausible by explicitly computing the first few derivatives of Γ and show that the resulting expressions indeed reproduce what we would have written down from the contributing Feynman diagrams. In particular, I will do this after deriving $\Gamma[\varphi]$ to the first loop order assuming constant fields in space-time, which diagrammatically corresponds to the approximation where we neglect the momenta of the external legs (a field without "wobbles" has no momentum!).

To derive an explicit expression for $\Gamma[\varphi]$ to first loop order, let us first compute $\mathcal{Z}[J]$ using the saddle-point approximation. That is, we first find the classical field configurations ϕ_c which maximise $\int(\mathcal{L} + J\phi)$, and expand to second order around ϕ_c (since linear perturbations around ϕ_c vanish). The classical field configuration ϕ_c is given by the solution to

$$\delta\left[S + \int \mathrm{d}^4 z \phi(z) J(z)\right]_{\phi=\phi_\mathrm{c}} = 0\,, \tag{1.106}$$

where the variation is taken w.r.t. ϕ. Now, let us take

$$\phi(x) = \phi_{\rm c}(x) + \tilde{\phi}(x)\,, \tag{1.107}$$

and expand to second order in $\tilde{\phi}$:

$$\begin{aligned} S[\phi_{\rm c}+\tilde{\phi}] + \int {\rm d}^4 z J(z) \left(\phi_{\rm c}(z) + \tilde{\phi}(z)\right) \approx S[\phi_{\rm c}] + \int {\rm d}^4 J(z)\phi_{\rm c}(z) \\ + \frac{1}{2}\int {\rm d}^4 x \int {\rm d}^4 y\, \tilde{\phi}(x) \left[\frac{\delta^2 S}{\delta\phi(x)\delta\phi(y)}\right]_{\phi=\phi_{\rm c}} \tilde{\phi}(y)\,. \end{aligned} \tag{1.108}$$

If we take $\mathcal{L} = \frac{1}{2}(\partial\phi)^2 - V_0(\phi)$ then

$$\frac{1}{2}\int {\rm d}^4 x \int {\rm d}^4 y\, \tilde{\phi}(x) \left[\frac{\delta^2 S}{\delta\phi(x)\delta\phi(y)}\right]_{\phi=\phi_{\rm c}} \tilde{\phi}(y) = \int {\rm d}^4 x \frac{1}{2}\tilde{\phi}(x)\left(-\partial^2 - V_0''(\phi_{\rm c})\right)\tilde{\phi}(x)\,. \tag{1.109}$$

Therefore, to first loop order, $\mathcal{Z}[J]$ is given by

$$\begin{aligned} \mathcal{Z}[J] &\approx {\rm e}^{{\rm i}\left(S[\phi_{\rm c}] + \int {\rm d}^4 J(z)\phi_{\rm c}(z)\right)} \int \mathcal{D}\tilde{\phi} {\rm e}^{\frac{\rm i}{2}\int {\rm d}^4 x \tilde{\phi}\left(-\partial^2 - V_0''(\phi_{\rm c})\right)\tilde{\phi}} \\ &= {\rm e}^{{\rm i}\left(S[\phi_{\rm c}] + \int {\rm d}^4 J(z)\phi_{\rm c}(z)\right)} \frac{C}{\sqrt{\det\left(-\partial^2 - V_0''(\phi_{\rm c})\right)}}\,, \end{aligned} \tag{1.110}$$

where I have on the second line used the standard result for Gaussian integrals. Here, C is an unimportant constant. Note that although $J(z)$ only appears explicitly in one place in the expression above, there is also an implicit dependence on J in $\phi_{\rm c}$. We can now use

$$\det(\dots) = {\rm e}^{{\rm Tr}\log(\dots)}\,, \tag{1.111}$$

to arrive at an expression for $W[J]$ at one-loop:

$$W[J] \approx S[\phi_{\rm c}] + \int {\rm d}^4 J(z)\phi_{\rm c}(z) + \frac{\rm i}{2}{\rm Tr}\log\left(-\partial^2 - V_0''(\phi_{\rm c})\right)\,, \tag{1.112}$$

where the trace refers to

$${\rm Tr}\log\left(-\partial^2 - V_0''(\phi_{\rm c})\right) = \int {\rm d}^4 z \int \frac{{\rm d}^4 k}{(2\pi)^4} \log\left(k^2 - V_0''(\phi_{\rm c}(z))\right)\,. \tag{1.113}$$

The expectation value φ becomes

$$\varphi(x) = \frac{\delta W}{\delta J(x)} = \phi(x)_{\rm c} + \frac{\rm i}{2}\int {\rm d}^4 z \frac{\delta\phi_{\rm c}(z)}{\delta J(x)} \int \frac{{\rm d}^4 k}{(2\pi)^2} \frac{1}{k^2 - V_0''\left(\phi_{\rm c}(z)\right)}\,. \tag{1.114}$$

Since $\varphi(x) = \phi_{\rm c}(x) + (\text{higher order})$, we can replace $\phi_{\rm c}(z)$ by $\varphi(z)$ in the second term and inside the trace in Eq. (1.112). A few lines of algebra reveal the one-loop effective action:

$$-\Gamma[\varphi(x)] = S[\varphi(x)] + \frac{\rm i}{2}\int {\rm d}^4 z \int \frac{{\rm d}^4 k}{(2\pi)^4} \log\left(k^2 - V_0''(\varphi(z))\right) \tag{1.115}$$

This remarkably simple formula captures all one-loop quantum corrections to the classical action.

Consider now what happens when we take $\varphi(x) = \varphi$ to be constant in x. Then

$$-\Gamma[\varphi] = -VT \cdot V_{\text{eff}}(\varphi), \tag{1.116}$$

where VT is the total volume of space-time and $V_{\text{eff}}(\varphi)$ is the *one-loop effective potential*,

$$V_{\text{eff}}(\varphi) = V_0(\varphi) - \frac{\mathrm{i}}{2}\int \frac{\mathrm{d}^4k}{(2\pi)^4}\log\left(k^2 - V_0''(\varphi)\right) . \tag{1.117}$$

Often, $V_0''(\varphi) \equiv m^2(\varphi)$ is referred to the "field dependent mass" since it corresponds to the mass of the field in presence of the constant background field φ. As an example, let us take the tree-level scalar potential

$$V_0(\varphi) = \frac{1}{2}m^2\varphi^2 + \frac{1}{3!}\gamma\varphi^3 + \frac{1}{4!}\lambda\varphi^4 , \tag{1.118}$$

such that the tree-level vertex rules for tri-linear and quartic interactions are $-\mathrm{i}\gamma$ and $-\mathrm{i}\lambda$ respectively (also, a tree-level "mass insertion" is given by $-\mathrm{i}m^2$). The terms that show up in each n-derivative $V_{\text{eff}}^{(n)}(0)$ all have diagrammatic counterparts,

$$\begin{aligned}
-\mathrm{i}V_{\text{eff}}^{(1)}(0) =& \frac{1}{2}(-\mathrm{i}\gamma)\int \frac{\mathrm{d}^4k}{(2\pi)^4}\frac{\mathrm{i}}{k^2-m^2} = \\
-\mathrm{i}V_{\text{eff}}^{(2)}(0) =& -\mathrm{i}m^2 + \frac{1}{2}(-\mathrm{i}\gamma)^2\int \frac{\mathrm{d}^4k}{(2\pi)^4}\left(\frac{\mathrm{i}}{k^2-m^2}\right)^2 + \frac{1}{2}(-\mathrm{i}\lambda)\int \frac{\mathrm{d}^4k}{(2\pi)^4}\frac{\mathrm{i}}{k^2-m^2} \\
=& \quad + \quad + \\
-\mathrm{i}V_{\text{eff}}^{(3)}(0) =& -\mathrm{i}\gamma + (-\mathrm{i}\gamma)^3\int \frac{\mathrm{d}^4k}{(2\pi)^4}\left(\frac{\mathrm{i}}{k^2-m^2}\right)^3 + \frac{3}{2}(-\mathrm{i}\gamma)(-\mathrm{i}\lambda)\int \frac{\mathrm{d}^4k}{(2\pi)^4}\left(\frac{\mathrm{i}}{k^2-m^2}\right)^2 \\
=& \quad + \quad + 3\cdot \\
-\mathrm{i}V_{\text{eff}}^{(4)}(0) =& -\mathrm{i}\lambda + 3(-\mathrm{i}\gamma)^4\int \frac{\mathrm{d}^4k}{(2\pi)^4}\left(\frac{\mathrm{i}}{k^2-m^2}\right)^4 \\
&+ 6(-\mathrm{i}\gamma)^2(-\mathrm{i}\lambda)\int \frac{\mathrm{d}^4k}{(2\pi)^4}\left(\frac{\mathrm{i}}{k^2-m^2}\right)^3 + \frac{3}{2}(-\mathrm{i}\lambda)^2\int \frac{\mathrm{d}^4k}{(2\pi)^4}\left(\frac{i}{k^2-m^2}\right)^2 \\
=& \quad + 3\cdot \quad + 6\cdot \quad + 3\cdot \\
&\vdots
\end{aligned} \tag{1.119}$$

The pre-factors in front of the diagrams are the number of different ways to contract the external legs. Note that all loop propagators have the same momentum, namely the loop momentum k, meaning that all external momenta are taken to zero in these expressions.

But what good is all this? After all, instead of going through the trouble of deriving V_{eff} and then taking the derivatives w.r.t. φ, we could have arrived at the expressions in Eqs. (1.119) by simply drawing the diagrams and employing the Feynman rules. Rather, the power of the effective potential comes from the fact that the integral in Eq. (1.117) can be performed directly, i.e. before taking derivatives w.r.t φ. In this way, we do not have to compute all the loop integrals in Eqs. (1.119) in the effective potential approach.

I will in the next section describe the necessary tools for performing the integrals over momenta e.g. in Eq. (1.117) or in Eqs. (1.119) (in particular, dimensional regularization and the minimal subtraction scheme). But to conclude the discussion on the effective potential, I will here simply state the result of performing the integral in Eq. (1.117), but for a general renormalizable four-dimensional quantum field theory with fields with spin ≤ 1:

$$V_{\text{eff}}(\varphi_k) = V_0(\varphi_k) + \frac{1}{2(4\pi)^2}\sum_i (-1)^{2s_i}(2s_i+1)m_i^4(\varphi_k)\left(\log\frac{m_i^2(\varphi_k)}{\mu^2} - k_{s_i}\right) . \quad (1.120)$$

This was derived in [9] and is known as the Coleman-Weinberg potential. Here, the sum is taken over all mass eigenstates i in the theory, where s_i is the spin and $m_i^2(\varphi_k)$ is the field dependent squared mass of particle i in presence of the background fields φ_k (which corresponds to $V_0''(\varphi)$ in Eq. (1.117)). In Eq. (1.120), μ is the renormalisation scale and k_{s_i} are renormalisation scheme dependent constants[5].

The derivatives of the Coleman-Weinberg potential give the connected and amputated one-loop n-point functions in the zero external momentum approximation. Although no loop integrals are present in Eq. (1.120), it is still often very cumbersome to directly compute V_{eff} from Eq. (1.120) and then take the derivatives in the context of theories with many fields. In Eq. (1.120), all scalar fields φ_k need to be taken as non-zero background fields before computing $V_{\text{eff}}^{(n)}$ (even if only a small subset of φ_k will acquire vacuum expectation values in the end). Therefore, it is far from trivial to compute $m_i^2(\varphi_k)$, since these are the eigenvalues of large and non-sparse mass matrices. Alternatively, V_{eff} can be computed directly before going to the mass eigenbasis, but this involves the equally cumbersome task of computing the logarithm of large and non-sparse mass matrices. This brings us to Paper I in this thesis. There, we derive closed form "ready to use" analytical expressions of $V_{\text{eff}}^{(n)}$ at one-loop in terms of the tree-level couplings in a general renormalisable four-dimensional field theory with any number of fields with spins ≤ 1. This tool is very useful in theories with many scalar fields (such as the models considered in Paper II and Paper II), where a diagrammatic approach to one-loop corrections would be inconvenient due to the large number of diagrams.

[5] In the $\overline{MS}$ scheme we have that $k_0 = k_{\frac{1}{2}} = \frac{3}{2}$ and $k_1 = \frac{5}{6}$. See [10].

2.4 Loops and the continuum renormalisation group

Suppose we are interested in the connected and amputated four-point function at one-loop in ϕ^4-theory. Diagrammatically, this corresponds to

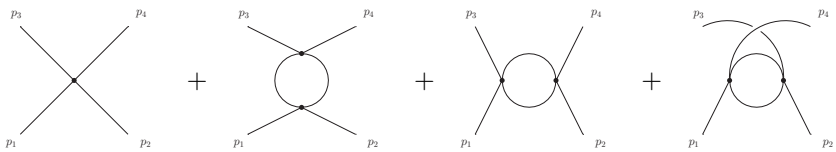

. (1.121)

For example, the first loop diagram is

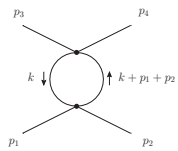

$$= \frac{(-\mathrm{i}\lambda)^2}{2} \int \frac{\mathrm{d}^4 k}{(2\pi)^4} \frac{\mathrm{i}}{k^2 - m^2} \frac{\mathrm{i}}{(k + p_1 + p_2)^2 - m^2} \,. \tag{1.122}$$

This integral should be performed with some finite cut-off Λ. We can in principle use the Wilson renormalisation group to change Λ to whatever energy scale we want, but as long as Λ is much larger than the masses and momenta of all particles involved, simple dimensional analysis tells us that the expression Eq. (1.122) depends on Λ as

$$\sim \left(\lambda^2 \ln \frac{\Lambda^2}{(p_i^2\text{'s and } m^2\text{'s})} + \text{const.} + \mathcal{O}(\Lambda^{-1}) \right) . \tag{1.123}$$

Higher powers of the logarithm, $\ln^n \Lambda^2$, will appear at higher loop orders. I will assume that we have chosen Λ to a sufficiently large value such that all terms with inverse powers of Λ can be dropped in this expression. In the end, we will want to express the bare parameter λ in our theory in terms of the physical parameter λ_p, which is the finite interaction strength that actual ϕ particles are measured to experience for some given momenta p_i. We can do this by setting the sum of the diagrams in Eq. (1.121) equal to $-\mathrm{i}\lambda_\mathrm{p}$ and then inverting this expression to $\mathcal{O}(\lambda^2)$. When λ in this way is expressed in terms of λ_p, we will find that λ has a logarithmic dependence on Λ that cancels the $\ln \Lambda$'s from the loop integrals.

In this sense, the cut-off Λ only served as a regulator of the loop integrals that in the end always drops out of the physical quantities. If we so like, we could alternatively use other regularisation schemes if they lead to simpler calculations. A far more convenient regularisation scheme is the so called dimensional regularisation, where we integrate over all momenta, but perform the integrals in $4 - 2\epsilon$ dimensions (where ϵ is taken to be a very small number). The loop integral in Eq. (1.122) will then contain a "divergent" $\frac{1}{\epsilon}$ piece that is cancelled by a $\frac{1}{\epsilon}$ dependent term in the bare parameter λ. Let us do this calculation explicitly.

First, we can do Feynman's trick and use the relation

$$\frac{1}{AB} = \int_0^1 \mathrm{d}x \frac{1}{(xA + (1-x)B)^2} \,, \tag{1.124}$$

to bring Eq. (1.122) into

$$\frac{\lambda^2}{2}\int_0^1 \mathrm{d}x \int \frac{\mathrm{d}^d k}{(2\pi)^d}\frac{1}{D^2}\,. \tag{1.125}$$

The denominator D is

$$\begin{aligned} D &= (1-x)(k^2-m^2) + x\left((k+p_1+p_2)^2 - m^2\right) \\ &= (k+x(p_1+p_2))^2 \underbrace{+x(1-x)s - m^2}_{\equiv -\Delta(s)}\,, \end{aligned} \tag{1.126}$$

where $s \equiv (p_1+p_2)^2$. We then perform the change of variables $l^\mu \equiv (k+x(p_1+p_2))^\mu$, such that Eq. (1.125) becomes

$$\frac{\lambda^2}{2}\int_0^1 \mathrm{d}x \int \frac{\mathrm{d}^d l}{(2\pi)^d}\frac{1}{(l^2-\Delta)^2}\,. \tag{1.127}$$

We can now go to Euclidean space[6] setting $l^0 = \mathrm{i}l^0_{\mathrm{E}}$ and $l^i = l^i_{\mathrm{E}}$, in particular such that $l^2 = -l^2_{\mathrm{E}}$. Then, going to d-dimensional polar coordinates, Eq. (1.127) becomes

$$\mathrm{i}\frac{\lambda^2}{2}\frac{1}{(2\pi)^d}\int \mathrm{d}\Omega_d \int_0^1 \mathrm{d}x \frac{1}{2}\int_0^\infty \mathrm{d}(l^2_{\mathrm{E}})\frac{(l^2_{\mathrm{E}})^{\frac{d-2}{2}}}{(l^2_{\mathrm{E}}+\Delta)^2}\,. \tag{1.128}$$

The d-dimensional solid angle $\int \mathrm{d}\Omega_d$ is

$$\int \mathrm{d}\Omega_d = \frac{2\pi^{\frac{d}{2}}}{\Gamma(\frac{d}{2})}\,, \tag{1.129}$$

where $\Gamma(a) \equiv \int_0^\infty \mathrm{d}x\, x^{a-1}\mathrm{e}^{-x}$ is the Euler gamma function. The integral over l^2_{E} can be performed by changing the integration variable to $y \equiv \frac{l^2_{\mathrm{E}}}{l^2_{\mathrm{E}}+\Delta}$, and using the standard integral

$$\int_0^1 \mathrm{d}y\, y^{\alpha-1}(1-y)^{\beta-1} = \frac{\Gamma(\alpha)\Gamma(\beta)}{\Gamma(\alpha+\beta)}\,. \tag{1.130}$$

This leads to

$$\int_0^\infty \mathrm{d}(l^2_{\mathrm{E}})\frac{(l^2_{\mathrm{E}})^{\frac{d-2}{2}}}{(l^2_{\mathrm{E}}+\Delta)^2} = \Delta^{\frac{d}{2}-2}\Gamma\left(\frac{d}{2}\right)\Gamma\left(2-\frac{d}{2}\right)\,. \tag{1.131}$$

We also note that λ is dimensionless only in $d=4$ dimensions. For the action to be dimensionless in d dimensions, the kinetic term demands that the scalar field ϕ has a mass dimension of $\frac{d}{2}-1$, which in turn leads to that λ has mass dimension $4-d$. Let us therefore put in an explicit (arbitrary) energy scale μ by making the replacement

$$\lambda \to \lambda\mu^{4-d}\,, \tag{1.132}$$

[6] As it stands, the integral in Eq. (1.127) can hit the pole $l^2 = \Delta$, and it is not obvious that we so straightforwardly can do this so-called Wick rotation into Euclidean space. However, had I been more rigorous in the previous section, we would have seen that we only get the correct time-ordering in Eq. (1.79) if we add an infinitesimal imaginary part $+\mathrm{i}\varepsilon$ to all inverse propagators, which in the process also justifies the Wick rotation. See any quantum field theory text book for a more rigorous treatment of this.

such that we can still think of λ as being dimensionless for $d \neq 4$. We can put all this together, and a few lines of algebra shows that Eq. (1.128) equals

$$\mathrm{i}\mu^{4-d} \cdot \frac{\lambda^2}{2} \int_0^1 \mathrm{d}x \, \frac{\Gamma\left(2-\frac{d}{2}\right)}{(4\pi)^{\frac{d}{2}}} \left(\frac{\mu^2}{\Delta}\right)^{2-\frac{d}{2}} . \tag{1.133}$$

The overall factor of μ^{4-d} just reflects the mass dimension of the 4-point function in d dimensions. Let us now set $d = 4 - 2\epsilon$, and expand in ϵ. In particular, we will need to use

$$\Gamma(\epsilon) = \frac{1}{\epsilon} - \gamma_{\mathrm{E}} + \mathcal{O}(\epsilon) \tag{1.134}$$

where $\gamma_{\mathrm{E}} \approx 0.577$ is the Euler-Mascheroni constant. Expanding Eq. (1.133) in ϵ gives

$$\mathrm{i}\mu^{2\epsilon} \frac{\lambda^2}{2(4\pi)^2} \int_0^1 \mathrm{d}x \, \left[\frac{1}{\epsilon} - \gamma_{\mathrm{E}} + \ln 4\pi - \ln \frac{\Delta(s)}{\mu^2} + \mathcal{O}(\epsilon)\right] . \tag{1.135}$$

Similarly, the other two loop diagrams in Eq. (1.121) are obtained by replacing s in the above formula by $t \equiv (p_1 - p_3)^2$ and $u \equiv (p_1 - p_4)^2$ respectively.

Suppose that, for some given reference kinematic variables s_0, t_0 and u_0, the interaction strength is measured to be $\lambda_{\mathrm{p}}(s_0, t_0, u_0)$. We therefore have that

$$\begin{aligned} -\mathrm{i}\lambda_{\mathrm{p}}(s_0,t_0,u_0) = &-\mathrm{i}\mu^{2\epsilon}\Bigg[\lambda - \frac{3\lambda^2}{2(4\pi)^2}\left(\frac{1}{\epsilon} - \gamma_{\mathrm{E}} + \ln 4\pi\right) \\ &+ \frac{\lambda^2}{2(4\pi)^2}\int_0^1 \mathrm{d}x \, \left(\ln\frac{\Delta(s_0)}{\mu^2} + \ln\frac{\Delta(t_0)}{\mu^2} + \ln\frac{\Delta(u_0)}{\mu^2}\right)\Bigg] . \end{aligned} \tag{1.136}$$

The overall factor $\mu^{2\epsilon} \to 1$ as $\epsilon \to 0$ so it can be ignored from now on. The above relation can easily be inverted to $\mathcal{O}(\lambda^2)$ to express the bare coupling λ in terms of the physical interaction strength λ_{p}. In particular, we find that λ has a piece $\propto \frac{1}{\epsilon}$ that renders the above expression finite for $\epsilon \to 0$.

By fixing λ using a particular measurement of $\lambda_{\mathrm{p}}(s_0, t_0, u_0)$, we can now use our calculation to predict the value of the interaction strength at some other kinematic variables s, t and u to $\mathcal{O}(\lambda_{\mathrm{p}}^2)$,

$$\begin{aligned} \lambda_{\mathrm{p}}(s,t,u) = &\lambda_{\mathrm{p}}(s_0,t_0,u_0) \\ &+ \frac{\lambda_{\mathrm{p}}(s_0,t_0,u_0)^2}{2(4\pi)^2}\int_0^1 \mathrm{d}x \, \left(\ln\frac{\Delta(s)}{\Delta(s_0)} + \ln\frac{\Delta(t)}{\Delta(t_0)} + \ln\frac{\Delta(u)}{\Delta(u_0)}\right) . \end{aligned} \tag{1.137}$$

Look how nice this expression is! It is perfectly finite, and all dependence on the fictitious ϵ and μ are completely gone. The first term on the RHS is to be fixed by a measurement, while the second term gives clear but non-trivial prediction for the momentum dependence of the physical scattering amplitude that is entirely due to quantum fluctuations.

However, computing observables is in general messy, so the above method to renormalise is often very cumbersome. In practice, we instead usually define our renormalized

couplings through some subtraction scheme. In particular, in the "modified minimal subtraction" scheme $\overline{MS}$, we define the renormalised coupling $\lambda_{\overline{MS}}$ through

$$\lambda \equiv \lambda_{\overline{MS}} + \frac{3\lambda^2}{2(4\pi)^2}\left(\frac{1}{\epsilon} - \gamma_{\mathrm{E}} + \ln 4\pi\right) \tag{1.138}$$

where the second term is constructed such that it cancels both the $\frac{1}{\epsilon}$ piece in Eq. (1.136) and the constant $\propto -\gamma_{\mathrm{E}} + \ln 4\pi$ that anyway always drops out when computing observables. The physical interaction strength $\lambda_{\mathrm{p}}(s,t,u)$ is now related to $\lambda_{\overline{MS}}$ as

$$\lambda_{\mathrm{p}}(s,t,u) = \lambda_{\overline{MS}} + \frac{\lambda_{\overline{MS}}^2}{2(4\pi)^2}\int_0^1 \mathrm{d}x\,\left(\ln\frac{\Delta(s)}{\mu^2} + \ln\frac{\Delta(t)}{\mu^2} + \ln\frac{\Delta(u)}{\mu^2}\right). \tag{1.139}$$

Note that $\lambda_{\overline{MS}}$ is defined with a particular value of μ in mind. If we change μ slightly, it is always possible to a compensating shift in $\lambda_{\overline{MS}}$ such that $\lambda_{\mathrm{p}}(s,t,u)$ is unchanged. This defines the *continuum renormalisation group*. In fact, we can figure out how $\lambda_{\overline{MS}}(\mu)$ should vary with μ such that $\lambda_{\mathrm{p}}(s,t,u)$ is unchanged by simply demanding that $\mu\frac{\mathrm{d}}{\mathrm{d}\mu}\lambda_{\mathrm{p}}(s,t,u) = 0$. The above equation then leads to

$$\mu\frac{d}{d\mu}\lambda_{\overline{MS}} = \frac{3\lambda_{\overline{MS}}^2}{(4\pi)^2} \equiv \beta_\lambda\,., \tag{1.140}$$

which is a simple differential equation that can be solved for $\lambda_{\overline{MS}}(\mu)$. In a general interaction field theory, each coupling λ_i comes with its own β_{λ_i}-function that describes how the coupling must vary with the renormalisation scale μ such that observables are rendered μ-independent. In Paper II, the results rely heavily on the use of the continuum renormalisation group.

2.5 Effective field theory

I will in this section introduce the concept of effective field theories, which is the formal way of getting rid of (or "integrating out") high-momentum degrees of freedom that are irrelevant for low-energy physics. The purpose of this is to introduce some of the tools used in Paper II in this thesis.

Both Paper II and Paper III concern a class of so-called Grand Unification Theories (or GUTs for short), that aim to explain certain features of the Standard Model by postulating a larger symmetry that would only become manifest at very high energies $\Lambda_{\mathrm{GUT}} \gg \Lambda_{\mathrm{EW}}$. This will be explained in more detail in Sec. 4, but here I want to first focus on a problem that generically occurs in calculations beyond tree-level in such theories: the appearance of large logarithms that can spoil the convergence of the perturbative series.

Recall from the previous section that in loop calculations, logarithms of the ratio between masses and the renormalization scale, i.e. $\log(m^2/\mu^2)$, generally appear. We are free to pick the value of the renormalization scale μ, but we better pick it such that

	$\mathrm{U}(1)_\mathrm{A}$	$\mathrm{U}(1)_\mathrm{B}$
L, $\tilde{L}$	$+1$	0
Q_L, $\tilde{Q}_\mathrm{L}$	$-1/2$	$+1/3$
Q_R, $\tilde{Q}_\mathrm{R}$	$-1/2$	$-1/3$

Table 1.1: $\mathrm{U}(1)_\mathrm{A} \times \mathrm{U}(1)_\mathrm{B}$ charges in a toy version of the non-supersymmetric trinification model in Paper II.

$\mu \sim m$, so it is justified to do an expansion in $\lambda \log(m^2/\mu^2)$. However, in GUTs, we typically have a set of heavy particles with masses $m_\mathrm{H} \sim \Lambda_\mathrm{GUT}$ along side with the "light" particles in the Standard Model which all have masses $m_\mathrm{L} \lesssim \Lambda_\mathrm{EW}$. In this situation there is no consistent choice of the value of μ such that both $\log(m_\mathrm{H}^2/\mu^2)$ and $\log(m_\mathrm{L}^2/\mu^2)$ are small.

In the end, we are interested in if the electro-weak scale physics looks anything like that of the Standard Model, and what kind of signatures beyond the Standard Model that characterises the given GUT. The strategy we employ in this situation goes as follows: We first take $\mu \sim \Lambda_\mathrm{GUT}$ and compute all the n-point functions corresponding to relevant and marginal interactions[7] involving only external light particles. We then write down an "effective theory" $\mathcal{L}_\mathrm{eff}$ involving only light fields, where the coupling constants are matched such that the n-point functions are all reproduced to the desired accuracy. In this way, the effects of the heavier particles are encoded in the point-like interactions described by $\mathcal{L}_\mathrm{eff}$. This can be shown (see e.g. [11]) to be equivalent to performing the integrals over the heavy fields in the path integral, and this process is therefore referred to as "integrating out" the heavy fields. We can then evolve the couplings in the effective theory using the continuum renormalization group in $\mathcal{L}_\mathrm{eff}$ to $\mu \sim \Lambda_\mathrm{EW}$.

To illustrate this, let us consider a toy version of the non-supersymmetric trinification model in Paper II, with three complex scalar fields $\tilde{L}$, $\tilde{Q}_\mathrm{L}$ and $\tilde{Q}_\mathrm{R}$, and three Weyl fermions L, Q_L and Q_R. Trinification will be introduced in Sec. 4.3, where these fields will be the analogues of the 3-by-3-by-3 scalar multiplets $(\tilde{L}^i)^l{}_r$, $(\tilde{Q}^i_\mathrm{L})^c{}_l$ and $(\tilde{Q}^i_\mathrm{R})^r{}_c$, and the Weyl fermions $(L^i)^l{}_r$, $(Q^i_\mathrm{L})^c{}_l$ and $(Q^i_\mathrm{R})^r{}_c$.

This toy model gets a very similar structure to the theory in Paper II if we impose a $\mathrm{U}(1)_\mathrm{A} \times \mathrm{U}(1)_\mathrm{B}$ symmetry (which I will take to be global in this toy example) with charges shown in Tab. 1.1, and a $\mathbb{Z}_3$ symmetry that simultaneously cyclically permutes the elements of $\{\tilde{L}, \tilde{Q}_\mathrm{L}, \tilde{Q}_\mathrm{R}\}$ and $\{L, Q_\mathrm{L}, Q_\mathrm{R}\}$. The charge assignment in Tab. 1.1 forbids direct mass terms for the fermions. The most general renormalisable Lagrangian that respects this symmetry is

$$\mathcal{L} = \mathcal{L}_\mathrm{kinetic} + \mathcal{L}_\mathrm{Yukawa} - V\,, \tag{1.141}$$

where

$$\mathcal{L}_\mathrm{Yukawa} = -y\left[\tilde{L}Q_\mathrm{L}Q_\mathrm{R} + (\mathbb{Z}_3 \text{ permutations})\right] + \text{c.c.}\,, \tag{1.142}$$

[7] We could also include irrelevant interactions if we are interested in effects from irrelevant operators. The first step in the GUTs considered in this thesis is however to see to what extent the Standard Model can be found as a low-energy limit, and only the marginal and relevant operators are needed for this.

and

$$V = \left(-\mu_{\rm S}^2|\tilde{L}|^2 + \frac{1}{4}\lambda|\tilde{L}|^4 + \alpha|\tilde{L}|^2|\tilde{Q}_{\rm L}|^2 + (\mathbb{Z}_3 \text{ permutations})\right) + \gamma\left(\tilde{L}\tilde{Q}_{\rm L}\tilde{Q}_{\rm L} + \text{c.c.}\right), \tag{1.143}$$

$\mathcal{L}_{\rm kinetic}$ contains the standard kinetic terms. The scalar potential has a minimum where

$$\langle\tilde{Q}_{\rm L,R}\rangle = 0\,, \quad \langle\tilde{L}\rangle = \frac{v}{\sqrt{2}} \text{ with } \mu_{\rm S}^2 = \frac{\lambda v^2}{4}\,, \tag{1.144}$$

for which $\mathrm{U}(1)_{\rm A}$ is spontaneously broken. Here, $\tilde{Q}_{\rm L,R}$ arrange themselves into the mass eigenstates

$$\tilde{Q}_\pm = \frac{1}{\sqrt{2}}\left(\tilde{Q}_{\rm L} \pm \tilde{Q}_{\rm R}^*\right), \tag{1.145}$$

with masses

$$m_\pm^2 = \left(\frac{\alpha}{2} \pm \frac{\gamma}{v\sqrt{2}}\right)v^2\,. \tag{1.146}$$

We can also write

$$\tilde{L}(x) = \frac{1}{\sqrt{2}}\left(\rho(x) + v\right)\mathrm{e}^{\mathrm{i}\frac{a(x)}{v}} \tag{1.147}$$

where $a(x)$ is the massless field (i.e. the Goldstone boson) associated with the spontaneous breaking of $\mathrm{U}(1)_{\rm A}$ (Goldstone bosons are further discussed in Sec. 3.1). Note that, since $\tilde{L} \to \mathrm{e}^{\mathrm{i}\omega_{\rm A}}\tilde{L}$ under $\mathrm{U}(1)_{\rm A}$, $a(x)$ transforms as $a \to a + v\omega_{\rm A}$. This shift symmetry protects $a(x)$ from acquiring a mass.

In the fermion sector, $Q_{\rm L,R}$ combine into a massive Dirac spinor

$$Q = \begin{pmatrix} Q_{\rm L} \\ Q_{\rm R}^\dagger \end{pmatrix}, \quad m_Q = \frac{yv}{\sqrt{2}}\,, \tag{1.148}$$

while L stays massless. Note, however, that there is no symmetry that force L to stay massless at higher loop orders. It is convenient to put L into a four-component Majorana spinor

$$\Psi = \begin{pmatrix} L \\ L^\dagger \end{pmatrix}. \tag{1.149}$$

In particular, one can now show that $\mathcal{L}_{\rm Yukawa}$ contains the interaction terms

$$\mathcal{L}_{\rm Yukawa} \supset \frac{y}{\sqrt{2}}\tilde{Q}_+\bar{Q}\Psi - \frac{y}{\sqrt{2}}\tilde{Q}_-\bar{Q}\gamma^5\Psi + \text{c.c.} \tag{1.150}$$

Let us now consider what happens when we integrate out the massive fields Q, $\tilde{Q}_\pm$ and ρ at one-loop. The lowest order terms allowed in the effective Lagrangian of L and a are

$$\begin{aligned}\mathcal{L}_{\rm eff} =& Z_L\mathrm{i}L^\dagger\bar{\sigma}^\mu\partial_\mu L + Z_a\frac{1}{2}(\partial a)^2 - \left(\frac{1}{2}m_L\mathrm{e}^{-2\mathrm{i}\frac{a}{v}}LL + \text{c.c.}\right) \\ =& \frac{1}{2}Z_L\mathrm{i}\bar{\Psi}\partial\!\!\!/\Psi + Z_a\frac{1}{2}(\partial a)^2 + \frac{1}{2}m_L\cos\frac{2a}{v}\,\bar{\Psi}\Psi - \frac{1}{2}\mathrm{i}m_L\sin\frac{2a}{v}\,\bar{\Psi}\gamma^5\Psi\,,\end{aligned} \tag{1.151}$$

where m_L and $Z_{L,a}$ are to be matched to the couplings μ_S^2, y, λ and α in the original theory. At tree level, the matching conditions are

$$m_L = 0\,, \quad Z_{a,L} = 1\,. \tag{1.152}$$

However, at loop level, these conditions will in general change. Consider for example the Ψ 2-point function at one-loop in the original theory. The one-loop diagrams that contribute to this are shown in Fig. 1.3. The sum of those diagrams in the $\overline{MS}$

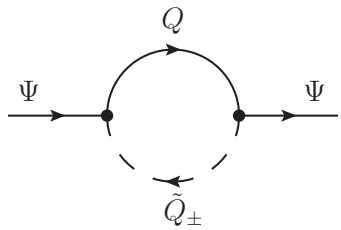

Figure 1.3: One-loop diagram that contributes to m_L in Eq. (1.151).

subtraction scheme is

$$\not{p} \cdot \mathrm{i}\frac{y^2}{(4\pi)^2}\int_0^1 \mathrm{d}x\, x \log\frac{\sqrt{\Delta_+(p^2)\Delta_-(p^2)}}{\mu^2} + \mathrm{i}\frac{y^2 m_Q}{2(4\pi)^2}\int_0^1 \mathrm{d}x \log\frac{\Delta_+(p^2)}{\Delta_-(p^2)}\,. \tag{1.153}$$

where

$$\Delta_\pm(p^2) = -x(1-x)p^2 + xm_\pm^2 + (1-x)m_Q^2 \tag{1.154}$$

and p^μ is the momentum of the Ψ particle ($\not{p} = \gamma_\mu p^\mu$). Since $m_L = 0$ at tree-level, the second term in Eq. (1.153) with $p^2 = 0$ directly gives the one-loop value of $-\mathrm{i}m_L$ in the effective theory, or

$$m_L = -\frac{y^2 m_Q}{2(4\pi)^2}\int_0^1 \mathrm{d}x \log\frac{xm_+^2 + (1-x)m_Q^2}{xm_-^2 + (1-x)m_Q^2}\,, \tag{1.155}$$

at one-loop order. We also find that $Z_{L,a}$ both deviate from 1 at this loop order, and we should therefore perform the field redefinitions $L \to Z_L^{-\frac{1}{2}} L$ and $a \to Z_a^{-\frac{1}{2}} a$ to have canonically normalized kinetic terms. However, since $m_L = 0$ at tree-level, this field renormalization does not affect the mass of L at one-loop[8]. Note also that the contribution in Eq. (1.155) is independent of the renormalization scale μ, even though the diagrams in Fig. 1.3 individually are logarithmically divergent. These divergences cancel between the diagrams since they come with opposite signs (this sign difference can be traced back to the γ^5 in Eq. (1.150)).

[8]This point was realized by the late Erik Gustafsson and me when we worked on the one-loop matching of the fermion sector of the model considered in Paper II.

	Field	$SU(3)_C$	$SU(2)_L$	$U(1)_Y$
Left-handed Weyl fermions	L_L^i	**1**	**2**	$-1/2$
	e_R^{ci}	**1**	**1**	1
	Q_L^{ci}	**3**	**2**	$1/6$
	u_R^{ci}	$\bar{\mathbf{3}}$	**1**	$-2/3$
	d_R^{ci}	$\bar{\mathbf{3}}$	**1**	$1/3$
Scalar	Φ	**1**	**2**	$1/2$
Gauge bosons	G	**8**	**1**	0
	W	**1**	**3**	0
	B	**1**	**1**	0

Table 1.2: Standard Model fields and their representations under the SM gauge group. The index i takes values 1, 2 and 3, and refers to the generation. The fields $G_\mu^{a=1,\ldots,8}$, $W_\mu^{a=1,2,3}$ and B_μ in the bottom three rows are the gauge fields for the $SU(3)_C$, $SU(2)_L$ and $U(1)_Y$ groups respectively.

3 The Standard Model

In this section I will give a condensed overview of the Standard Model (SM) of particle physics. The SM is the quantum field theory that combines the theory of electro-weak interactions [12, 13, 14] with the theory of Quantum Chromo Dynamics (QCD) which describes the strong interactions [15, 16, 17]. It provides a truly remarkable agreement between theory and experiment. If one accounts for neutrino masses, the SM has $\mathcal{O}(20)$ free parameters which on the one hand, on aesthetic grounds, might be considered too many for a supposedly fundamental theory of nature. On the other hand, this number becomes very small when compared to the ~ 40000 measurements listed by the Particle Data Group [18], out of which essentially none show significant deviations from what the SM predicts.

The SM is a gauge theory based on the gauge group

$$SU(3)_C \times SU(2)_L \times U(1)_Y \,, \tag{1.156}$$

with the field content summarised in Tab. 1.2. We construct its Lagrangian by first summing the free field Lagrangians for each field, and then adding all possible renormalisable interaction terms that are allowed by the imposed symmetry. We get

$$\mathcal{L}_{SM} = \mathcal{L}_{Gauge-kinetic} + \mathcal{L}_{Yukawa} - V_{Higgs} \tag{1.157}$$

where $\mathcal{L}_{Gauge-kinetic}$ contains the kinetic terms and the gauge interactions, $\mathcal{L}_{Yukawa}$ contains the interaction terms between the Higgs doublet and the fermions, and V_{Higgs} is the scalar potential. In particular, V_{Higgs} is constructed such that potential energy is minimized for a non-zero vacuum expectation value of the Higgs doublet which spontaneously breaks the electro-weak symmetry $SU(2)_L \times U(1)_Y$ into the familiar $U(1)_{e.m.}$ gauge symmetry of electromagnetism (this and its consequences is the so-called *Higgs mechanism* [19, 20, 21, 22]). The electro-weak symmetry breaking comes with non-trivial consequences in each of the three sectors in Eq. (1.157), which I will now go through one-by-one.

3.1 Scalar sector

The most general renormalisable scalar potential of the SM Higgs doublet is very simple,

$$V_{\text{Higgs}}(\Phi) = -\mu^2 \Phi^\dagger \Phi + \lambda (\Phi^\dagger \Phi)^2 \,. \tag{1.158}$$

The minimum of the potential is given by

$$\langle \Phi^\dagger \Phi \rangle = \frac{\mu^2}{2\lambda} \equiv \frac{v^2}{2} \,, \tag{1.159}$$

for $\mu^2 > 0$. The scalar potential makes no reference to whether electro-weak symmetry is global or local, so let me first proceed as if it was global. Let us label the components of Φ as

$$\Phi = \frac{1}{\sqrt{2}} \begin{pmatrix} \phi_1 + \mathrm{i}\phi_2 \\ \phi_3 + \mathrm{i}\phi_4 \end{pmatrix} . \tag{1.160}$$

A general global $\mathrm{SU}(2)_\mathrm{L} \times \mathrm{U}(1)_\mathrm{Y}$ transformation with real parameters $\omega_\mathrm{L}^{1,2,3}$ and ω_Y is realised on Φ as $\Phi \to \exp\left[\frac{\mathrm{i}}{2}(\omega_\mathrm{L}^a \sigma^a + \omega_\mathrm{Y})\right] \Phi$, or

$$\begin{aligned} \frac{1}{\sqrt{2}} \begin{pmatrix} \phi_1 + \mathrm{i}\phi_2 \\ \phi_3 + \mathrm{i}\phi_4 \end{pmatrix} \to & \frac{1}{\sqrt{2}} \begin{pmatrix} \phi_1' + \mathrm{i}\phi_2' \\ \phi_3' + \mathrm{i}\phi_4' \end{pmatrix} \\ & = \exp\left[\frac{\mathrm{i}}{2} \begin{pmatrix} \omega_\mathrm{L}^3 + \omega_\mathrm{Y} & \omega_\mathrm{L}^1 - \mathrm{i}\omega_\mathrm{L}^2 \\ \omega_\mathrm{L}^1 + \mathrm{i}\omega_\mathrm{L}^2 & -\omega_\mathrm{L}^3 + \omega_\mathrm{Y} \end{pmatrix} \right] \frac{1}{\sqrt{2}} \begin{pmatrix} \phi_1 + \mathrm{i}\phi_2 \\ \phi_3 + \mathrm{i}\phi_4 \end{pmatrix} , \end{aligned} \tag{1.161}$$

in terms of the components of Φ. We can use such a transformation to bring the general $\langle \Phi \rangle$,

$$\langle \Phi \rangle = \frac{1}{\sqrt{2}} \begin{pmatrix} \langle \phi_1 \rangle + \mathrm{i}\langle \phi_2 \rangle \\ \langle \phi_3 \rangle + \mathrm{i}\langle \phi_4 \rangle \end{pmatrix} , \quad \sum_{i=1}^{4} \langle \phi_i^2 \rangle = v^2 \,, \tag{1.162}$$

e.g. into the simpler form

$$\langle \Phi \rangle = \frac{1}{\sqrt{2}} \begin{pmatrix} 0 \\ v \end{pmatrix} . \tag{1.163}$$

$\omega_\mathrm{L}^{1,2,3}$ and ω_Y are in general independent transformation parameters. However, if there are symmetries that are unbroken by Eq. (1.163), we can find the corresponding constraints on $\omega_\mathrm{L}^{1,2,3}$ and ω_Y by finding the combinations that leave $\langle \Phi \rangle$ in Eq. (1.163) invariant. It is sufficient to do this infinitesimally, which gives

$$0 \stackrel{!}{=} \delta \langle \Phi \rangle = \frac{\mathrm{i}}{2} \begin{pmatrix} \omega_\mathrm{L}^3 + \omega_\mathrm{Y} & \omega_\mathrm{L}^1 - \mathrm{i}\omega_\mathrm{L}^2 \\ \omega_\mathrm{L}^1 + \mathrm{i}\omega_\mathrm{L}^2 & -\omega_\mathrm{L}^3 + \omega_\mathrm{Y} \end{pmatrix} \frac{1}{\sqrt{2}} \begin{pmatrix} 0 \\ v \end{pmatrix} . \tag{1.164}$$

This is solved by $\omega_\mathrm{L}^{1,2} = 0$ and $\omega_\mathrm{L}^3 = \omega_\mathrm{Y} \equiv \omega_\mathrm{e.m.}$. In a representation independent setting, the unbroken symmetry is then the subset

$$\omega_\mathrm{L}^a T_\mathrm{L}^a + \omega_\mathrm{Y} Y \supset \omega_\mathrm{e.m.} (T_\mathrm{L}^3 + Y) \equiv \omega_\mathrm{e.m.} T_\mathrm{e.m.} \,, \tag{1.165}$$

where we identify the single unbroken generator $T_\mathrm{e.m.} \equiv T_\mathrm{L}^3 + Y$. This generates the $\mathrm{U}(1)_\mathrm{e.m.}$ symmetry of electromagnetism.

Note that the choice in Eq. (1.163) is not unique, and we could equally well have picked for example $\langle\Phi\rangle \propto \begin{pmatrix} v \\ 0 \end{pmatrix}$ for which we would have found an unbroken $\mathrm{U}(1)_{\mathrm{e.m.}}$ group generated by $T^3_{\mathrm{L}} - Y$. This merely amounts to shuffling how the physical fields are expressed in terms of the initial fields in the Lagrangian. The physical states themselves are however indifferent to the specific form of $\langle\Phi\rangle$ (precisely because of the electro-weak symmetry). It is in fact a quite nice property of the SM Higgs sector, that is not often shared with models with extended Higgs sectors, that the SM Higgs doublet can break $\mathrm{SU}(2)_{\mathrm{L}} \times \mathrm{U}(1)_{\mathrm{Y}}$ *only* into $\mathrm{U}(1)_{\mathrm{e.m.}}$ and nothing else.

Each of the three broken generators (times 'i') acting on $\langle\Phi\rangle$ defines an equipotential (or "flat") direction in field space, and field oscillations in these three directions therefore correspond to massless bosons[9]: These are the Nambu-Goldstone bosons [24, 25] associated with the breaking $\mathrm{SU}(2)_{\mathrm{L}} \times \mathrm{U}(1)_{\mathrm{Y}} \to \mathrm{U}(1)_{\mathrm{e.m.}}$. For $\langle\Phi\rangle$ on the form in Eq. (1.163), the broken generators are $T^3_{\mathrm{L}} - Y$, T^1_{L} and T^2_{L} for which we can associate ϕ_4, ϕ_2 and ϕ_1 in Eq. (1.160) respectively as the Goldstone bosons.

Recall from Sec. 1.5 that for free massless spin-1 fields, we could use the gauge symmetry to get rid of their longitudinal polarization states. When the gauge fields are coupled to other fields (such as the Higgs doublet), these other fields must also transform under the gauge symmetry. To "fix the gauge", we can therefore instead impose constraints on these other fields, rather than on the gauge fields themselves. In particular, in the case of spontaneously broken gauge symmetries, we can perform a gauge transformation in each space-time point to completely cancel out the Goldstone fields (this corresponds to the so called "unitary gauge"). For example, for general $\phi_i(x)$, we can always choose $\omega_{\mathrm{L}}^{1,2,3}(x)$ and $\omega_{\mathrm{Y}}(x)$ in Eq. (1.161) to set $\phi'_{1,2,4}(x) = 0$. The price we have to pay for getting rid of the Goldstone bosons is that we no longer have the freedom to "gauge away" the longitudinal polarisation state of the gauge bosons corresponding to spontaneously broken gauge generators. However, we will see in the next section that this is still consistent with the discussion on spin-1 fields in Sec. 1.5, since precisely these gauge bosons become massive once $\langle\Phi\rangle \neq 0$.

Let me also write $\phi'_3(x) = v + h(x)$ such that $h(x) = 0$ in the vacuum. In the unitary gauge, we therefore have

$$\Phi(x) = \frac{1}{\sqrt{2}} \begin{pmatrix} 0 \\ v + h(x) \end{pmatrix} , \tag{1.166}$$

such that

$$V_{\mathrm{Higgs}} = \lambda v^2 h^2 + \lambda v h^3 + \frac{1}{4}\lambda h^4 + \mathrm{const.} \tag{1.167}$$

Excitations in the field $h(x)$ therefore correspond to massive scalar particles (with mass $m_h^2 = 2\lambda v^2$). This particle is the Higgs boson, and was the final particle in the SM that were experimentally verified [26, 27]. Its mass is measured to be 125.09 ± 0.24 GeV [18] which together with $v = 246$ GeV (which can be extracted from the Fermi constant) fixes the values of all interaction strengths in Eq. (1.167). In particular, we have the tree-level relation $\lambda = m_h^2/2v^2 \approx 0.13$.

[9] If this one-sentence-proof isn't convincing enough for you, then you can find three more proofs of the Goldstone theorem in [23].

Let me finally end this section by commenting on the slight abuse of language that I have employed so far regarding spontaneously broken gauge symmetries. In the case of a global symmetry, the Goldstone fields really do span the manifold of different but physically equivalent vacua, meaning that the ground state is truly degenerate (which is the characteristic feature of spontaneous symmetry breaking). However, for a gauge symmetry, all points on this vacuum manifold do correspond to the same physical vacuum which is therefore unique. Instead of having degenerate vacuum states, there is a redundancy (i.e. a gauge redundancy) in our description of the single unique vacuum state.

3.2 Gauge-kinetic sector

The gauge-kinetic terms in the SM are

$$\begin{aligned}\mathcal{L}_{\text{Gauge}-\text{kinetic}} = &\,\mathrm{i}L_{\mathrm{L}}^{i\dagger}\bar{\sigma}^{\mu}D_{\mu}L_{\mathrm{L}}^{i} + \mathrm{i}e_{\mathrm{R}}^{i\dagger}\bar{\sigma}^{\mu}D_{\mu}e_{\mathrm{R}}^{i} + \mathrm{i}Q_{\mathrm{L}}^{i\dagger}\bar{\sigma}^{\mu}D_{\mu}Q_{\mathrm{L}}^{i} \\ &+ \mathrm{i}u_{\mathrm{R}}^{i\dagger}\bar{\sigma}^{\mu}D_{\mu}u_{\mathrm{R}}^{i} + \mathrm{i}d_{\mathrm{R}}^{i\dagger}\bar{\sigma}^{\mu}D_{\mu}d_{\mathrm{R}}^{i} + |D_{\mu}\Phi|^{2} \\ &- \frac{1}{4}B_{\mu\nu}B^{\mu\nu} - \frac{1}{4}W_{\mu\nu}^{a}W^{a\mu\nu} - \frac{1}{4}G_{\mu\nu}^{a}G^{a\mu\nu}\,,\end{aligned} \tag{1.168}$$

where I have explicitly indicated the generation index i on the fermions, and the gauge adjoint index a on the gauge boson field strengths in the bottom line. Spinor and fundamental gauge indices are implicit. The covariant derivatives can all be read off from the field representations in Tab. 1.2 by plugging in the appropriate representation for the generators $T_{\mathrm{L,C}}^{a}$ and hypercharge Y into

$$D_{\mu} = \partial_{\mu} - \mathrm{i}g_{\mathrm{C}}G_{\mu}^{a}T_{\mathrm{C}}^{a} - \mathrm{i}g_{\mathrm{L}}W_{\mu}^{a}T_{\mathrm{L}}^{a} - \mathrm{i}g_{\mathrm{Y}}B_{\mu}Y\,. \tag{1.169}$$

Here, $g_{\mathrm{C,L,Y}}$ are the gauge couplings for $\mathrm{SU}(3)_{\mathrm{C}}$, $\mathrm{SU}(2)_{\mathrm{L}}$ and $\mathrm{U}(1)_{\mathrm{Y}}$ respectively. In particular, the covariant derivative of the Higgs doublet is

$$D_{\mu}\Phi = \left(\partial_{\mu} - \mathrm{i}g_{\mathrm{L}}W_{\mu}^{a}\frac{\sigma^{a}}{2} - \frac{\mathrm{i}}{2}g_{\mathrm{Y}}B_{\mu}\right)\Phi\,. \tag{1.170}$$

Consider now evaluating the $|D_{\mu}\Phi|^{2}$ term in Eq. (1.168) for $\Phi = \langle\Phi\rangle = \frac{1}{\sqrt{2}}\begin{pmatrix}0\\v\end{pmatrix}$,

$$\begin{aligned}|D_{\mu}\langle\Phi\rangle|^{2} &= \frac{v^{2}}{8}\left|\begin{pmatrix} g_{\mathrm{L}}W_{\mu}^{3} + g_{\mathrm{Y}}B_{\mu} & g_{\mathrm{L}}(W_{\mu}^{1} - \mathrm{i}W_{\mu}^{2}) \\ g_{\mathrm{L}}(W_{\mu}^{1} + \mathrm{i}W_{\mu}^{2}) & -g_{\mathrm{L}}W_{\mu}^{3} + g_{\mathrm{Y}}B_{\mu}\end{pmatrix}\begin{pmatrix}0\\1\end{pmatrix}\right|^{2} \\ &= \frac{g_{\mathrm{L}}^{2}v^{2}}{4}\left|\frac{W_{\mu}^{1} + \mathrm{i}W_{\mu}^{2}}{\sqrt{2}}\right|^{2} + \frac{v^{2}}{8}\begin{pmatrix}W_{\mu}^{3} & B_{\mu}\end{pmatrix}\begin{pmatrix} g_{\mathrm{L}}^{2} & -g_{\mathrm{L}}g_{\mathrm{Y}} \\ -g_{\mathrm{L}}g_{\mathrm{Y}} & g_{\mathrm{Y}}^{2}\end{pmatrix}\begin{pmatrix}W_{\mu}^{3}\\B_{\mu}\end{pmatrix}\,.\end{aligned} \tag{1.171}$$

The first term here provides a mass $m_{W}^{2} = \frac{1}{4}g_{\mathrm{L}}^{2}v^{2}$ for the W boson,

$$W_{\mu}^{\pm} \equiv \frac{1}{\sqrt{2}}(W_{\mu}^{1} \mp \mathrm{i}W_{\mu}^{2})\,. \tag{1.172}$$

The states $W^\pm$ have electric charge ± 1 which can be verified by seeing how they change under an infinitesimal $\mathrm{U}(1)_{\mathrm{e.m.}}$ transformation. The second term in Eq. (1.171) needs to be diagonalised in order to find the mass eigenstates and their corresponding masses. We find that there is one massless gauge boson which corresponds to the gauge field A_μ of $\mathrm{U}(1)_{\mathrm{e.m.}}$,

$$A_\mu \equiv \frac{g_{\mathrm{L}} B_\mu + g_{\mathrm{Y}} W_\mu^3}{\sqrt{g_{\mathrm{Y}}^2 + g_{\mathrm{L}}^2}}\,, \tag{1.173}$$

and a massive electrically neutral gauge boson

$$Z_\mu \equiv \frac{-g_{\mathrm{L}} W_\mu^3 + g_{\mathrm{Y}} B_\mu}{\sqrt{g_{\mathrm{Y}}^2 + g_{\mathrm{L}}^2}}\,, \tag{1.174}$$

with mass $m_Z^2 = \frac{1}{4}(g_{\mathrm{L}}^2 + g_{\mathrm{Y}}^2)v^2$. The masses of the electro-weak gauge bosons are measured [18] to be

$$m_W = 80.385 \pm 0.015\,\mathrm{GeV}\,, \quad m_Z = 91.1876 \pm 0.021\,\mathrm{GeV}\,. \tag{1.175}$$

The interactions between the physical gauge bosons and the other fields can now be found by expressing the covariant derivative in Eq. (1.169) in terms of $W_\mu^\pm$, Z_μ and A_μ:

$$\begin{aligned} D_\mu = \partial_\mu &- \mathrm{i} g_{\mathrm{C}} G_\mu^a T_{\mathrm{C}}^a - \mathrm{i}\frac{1}{\sqrt{2}} g_{\mathrm{L}} \left(T_{\mathrm{L}}^+ W^+ + T_{\mathrm{L}}^- W^-\right) \\ &- \mathrm{i}\frac{g_{\mathrm{Y}}^2 Y - g_{\mathrm{L}}^2 T_{\mathrm{L}}^3}{\sqrt{g_{\mathrm{L}}^2 + g_{\mathrm{Y}}^2}} Z_\mu - \mathrm{i}\frac{g_{\mathrm{L}} g_{\mathrm{Y}}}{\sqrt{g_{\mathrm{L}}^2 + g_{\mathrm{Y}}^2}} (T_{\mathrm{L}}^3 + Y) A_\mu\,, \end{aligned} \tag{1.176}$$

where I have abbreviated $T_{\mathrm{L}}^\pm \equiv T_{\mathrm{L}}^1 \pm \mathrm{i} T_{\mathrm{L}}^2$. We can here identify the electromagnetic coupling as

$$e \equiv \frac{g_{\mathrm{L}} g_{\mathrm{Y}}}{\sqrt{g_{\mathrm{L}}^2 + g_{\mathrm{Y}}^2}}\,. \tag{1.177}$$

3.3 Fermion sector

Given the field representations in Tab. 1.2, one can check that any fermion mass term would violate the SM gauge symmetry. Rather, all fermion masses in the SM are due to interactions between the fermions and the vacuum expectation value of the Higgs doublet. The most general set of such interactions is

$$\mathcal{L}_{\mathrm{Yukawa}} = -(y_e)^{ij} \Phi^\dagger L_{\mathrm{L}}^i e_{\mathrm{R}}^{\mathrm{c}j} - (y_d)^{ij} \Phi^\dagger Q_{\mathrm{L}}^i d_{\mathrm{R}}^{\mathrm{c}j} - (y_u)^{ij} \tilde{\Phi}^\dagger Q_{\mathrm{L}}^i u_{\mathrm{R}}^{\mathrm{c}j} + \mathrm{c.c.} \tag{1.178}$$

Here,

$$\tilde{\Phi} \equiv \mathrm{i}\sigma^2 \Phi^*\,, \tag{1.179}$$

transforms as a doublet under $\mathrm{SU}(2)_{\mathrm{L}}$ but with opposite hypercharge Y from Φ. We can label the components of the fermion $\mathrm{SU}(2)_{\mathrm{L}}$ doublets L_{L}^i and Q_{L}^i as

$$L_{\mathrm{L}}^i = \begin{pmatrix} \nu_{\mathrm{L}}^i \\ e_{\mathrm{L}}^i \end{pmatrix}\,, \quad Q_{\mathrm{L}}^i = \begin{pmatrix} u_{\mathrm{L}}^i \\ d_{\mathrm{L}}^i \end{pmatrix}\,, \tag{1.180}$$

motivated by their electric charges (i.e. by the eigenvalues of $T^3_{\rm L}+Y$). Now, let us look at Eq. (1.178) for $\Phi=\langle\Phi\rangle=\frac{1}{\sqrt{2}}\begin{pmatrix}0\\v\end{pmatrix}$ (meaning that $\langle\tilde{\Phi}\rangle=\frac{1}{\sqrt{2}}\begin{pmatrix}v\\0\end{pmatrix}$). We then get the terms

$$-\frac{v}{\sqrt{2}}(y_e)^{ij}e^i_{\rm L}e^{{\rm c}j}_{\rm R}-\frac{v}{\sqrt{2}}(y_d)^{ij}d^i_{\rm L}d^{{\rm c}j}_{\rm R}-\frac{v}{\sqrt{2}}(y_u)^{ij}u^i_{\rm L}u^{{\rm c}j}_{\rm R}+{\rm c.c.}\,, \tag{1.181}$$

which provide all fermions with their masses except the neutrinos $\nu^i_{\rm L}$. The mass eigenstates are related to the interaction eigenstates through the unitary transformations

$$\begin{aligned}
\begin{pmatrix}e_{\rm L},e^{\rm c}_{\rm R}\\ \mu_{\rm L},\mu^{\rm c}_{\rm R}\\ \tau_{\rm L},\tau^{\rm c}_{\rm R}\end{pmatrix}&=\begin{pmatrix}\\ V^e_{\rm L,R}\\ \\ \end{pmatrix}\begin{pmatrix}e^1_{\rm L},e^{\rm c1}_{\rm R}\\ e^2_{\rm L},e^{\rm c2}_{\rm R}\\ e^3_{\rm L},e^{\rm c3}_{\rm R}\end{pmatrix}\\
\begin{pmatrix}d_{\rm L},d^{\rm c}_{\rm R}\\ s_{\rm L},s^{\rm c}_{\rm R}\\ b_{\rm L},b^{\rm c}_{\rm R}\end{pmatrix}&=\begin{pmatrix}\\ V^d_{\rm L,R}\\ \\ \end{pmatrix}\begin{pmatrix}d^1_{\rm L},d^{\rm c1}_{\rm R}\\ d^2_{\rm L},d^{\rm c2}_{\rm R}\\ d^3_{\rm L},d^{\rm c3}_{\rm R}\end{pmatrix}\\
\begin{pmatrix}u_{\rm L},u^{\rm c}_{\rm R}\\ c_{\rm L},c^{\rm c}_{\rm R}\\ t_{\rm L},t^{\rm c}_{\rm R}\end{pmatrix}&=\begin{pmatrix}\\ V^u_{\rm L,R}\\ \\ \end{pmatrix}\begin{pmatrix}u^1_{\rm L},u^{\rm c1}_{\rm R}\\ u^2_{\rm L},u^{\rm c2}_{\rm R}\\ u^3_{\rm L},u^{\rm c3}_{\rm R}\end{pmatrix}
\end{aligned} \tag{1.182}$$

where the unitary matrices $V^{e,d,u}_{\rm L,R}$ are chosen such that they diagonalize the Yukawa matrices $y_{e,d,u}$ as

$$\frac{v}{\sqrt{2}}(V^{e,d,u}_{\rm L})^{\rm T}y_{e,d,u}V^{e,d,u}_{\rm R}={\rm diag}(m_{e,d,u},m_{\mu,s,c},m_{\tau,b,t})\,. \tag{1.183}$$

Let us finally write $\mathcal{L}_{\rm Yukawa}$ in Eq. (1.178) in terms of the fermion mass eigenstates assuming the unitary gauge. This gives

$$\begin{aligned}
\mathcal{L}_{\rm Yukawa}&=-\sum_f m_f\left(1+\frac{h}{v}\right)f_{\rm L}f^{\rm c}_{\rm R}+{\rm c.c}\\
&=-\sum_f m_f\left(1+\frac{h}{v}\right)\bar{f}f
\end{aligned} \tag{1.184}$$

where f runs over all massive fermions in the SM,

$$f\in\{e,\mu,\tau,d,s,b,u,c,t\}\,. \tag{1.185}$$

The top line in Eq. (1.184) is given in terms of left-handed Weyl fermions, while the bottom line is given in terms of the more conventional four-component Dirac spinors

$$f\equiv\begin{pmatrix}f_{\rm L}\\ f_{\rm R}\end{pmatrix}\,, \tag{1.186}$$

where $f_{\rm R}\equiv f^{{\rm c}\dagger}_{\rm R}$.

The change of basis in Eq. (1.182) has non-trivial effects only in the interaction terms between the fermions and $W^\pm$, since all other terms in the SM are fermion flavour

diagonal. Using the results from the previous section, we find the interaction terms

$$\begin{aligned}\mathcal{L}_{\text{Gauge-kinetic}} &\supset \frac{g_{\text{L}}}{\sqrt{2}} W_\mu^+ \left(\nu_{\text{L}}^{i\dagger} \bar{\sigma}^\mu e_{\text{L}}^i + u_{\text{L}}^{i\dagger} \bar{\sigma}^\mu d_{\text{L}}^i \right) + \text{c.c.} \\ &= \frac{g_{\text{L}}}{\sqrt{2}} W_\mu^+ \left[(V_{\text{L}}^e \nu_{\text{L}})^{i\dagger} \bar{\sigma}^\mu \tilde{e}_{\text{L}}^i + (V_{\text{L}}^u V_{\text{L}}^{d\dagger})_{ij} \tilde{u}_{\text{L}}^{i\dagger} \bar{\sigma}^\mu \tilde{d}_{\text{L}}^j \right] + \text{c.c.}\end{aligned} \tag{1.187}$$

where

$$\tilde{e}_{\text{L}}^i = (e_{\text{L}}, \mu_{\text{L}}, \tau_{\text{L}}) \,, \; \tilde{d}_{\text{L}}^i = (d_{\text{L}}, s_{\text{L}}, b_{\text{L}}) \text{ and } \tilde{u}_{\text{L}}^i = (u_{\text{L}}, c_{\text{L}}, t_{\text{L}}) \,, \tag{1.188}$$

are the charged fermion mass eigenstates. With massless neutrinos, we can simply absorb V_{L}^e into the definition of the neutrino flavours (i.e. the neutrino flavour eigenstates are defined through $W^\pm$ interactions). For quarks on the other hand, we see from Eq. (1.188) that interactions with the W can change the flavour of (left-handed) quarks. The tendency to change quark flavour is encoded in the Cabibbo–Kobayashi–Maskawa (CKM) matrix [28, 29]

$$V_{\text{CKM}} \equiv V_{\text{L}}^u V_{\text{L}}^{d\dagger} \,. \tag{1.189}$$

Although $\mathcal{L}_{\text{Yukawa}}$ at first sight appear to contain a large number parameters, we see only a few of these are physical, namely the nine fermion masses and the elements of V_{CKM} (for massless neutrinos). Furthermore, there is a residual phase freedom in particular for the six left-handed quarks that can be used to rotate away five unphysical complex phases of V_{CKM} (we can rotate away one less phase than the number of quark flavours since a simultaneous phase redefinition with a common phase of all quarks does not redefine any of the elements of V_{CKM}). Therefore, V_{CKM} can be expressed in terms of three angles and one complex phase.

One can easily accommodate the neutrino masses with the field content of the SM by adding the terms

$$-\frac{(y_\nu)^{ij}}{\Lambda} \left(\tilde{\Phi}^\dagger L_{\text{L}}^i \right) \left(\tilde{\Phi}^\dagger L_{\text{L}}^j \right) + \text{c.c.} = -\frac{v^2}{2\Lambda} (y_\nu)^{ij} \left(1 + \frac{h}{v} \right)^2 \nu_{\text{L}}^i \nu_{\text{L}}^j + \text{c.c.} \tag{1.190}$$

to $\mathcal{L}_{\text{SM}}$. This is the well known Weinberg operator [30], and is the only gauge invariant operator with a mass dimension of 5 that can be built out of the SM fields. I have therefore put in an explicit energy scale Λ such that $(y_\nu)^{ij}$ are dimensionless. This term generates neutrino Majorana masses of the order v^2/Λ for $y_\nu \sim \mathcal{O}(1)$, i.e. naturally small w.r.t. to the electro-weak scale if Λ is large. The neutrino masses lead to an additional V_{L}^ν in the first term in the second line of Eq. (1.187), which in turn gives the lepton analogue of V_{CKM} (this is known as the PMNS-matrix [31, 32]). However, Majorana mass terms $\frac{1}{2} m_\nu (\nu_{\text{L}} \nu_{\text{L}} + \text{c.c})$ are not invariant under rephasing of the neutrino fields, so we only have the freedom to rotate away 3 phases (by picking the phases of e_{L}, μ_{L} and τ_{L}) in the PMNS-matrix. The PMNS-matrix is therefore in general expressed in terms of three mixing angles and three complex phases.

3.4 The mysterious flavour structure

Up until this point, all structure has more or less followed from the imposed gauge symmetry and the field content: The Higgs doublet mass parameter $-\mu^2$ sets the energy

Fermion	Mass (GeV)	Mass (m_e)
u	$\begin{pmatrix} 2.2 & ^{+0.6}_{-0.4} \end{pmatrix} \cdot 10^{-3}$	4.3
d	$\begin{pmatrix} 4.7 & ^{+0.5}_{-0.4} \end{pmatrix} \cdot 10^{-3}$	9.2
e	$(0.5109989461 \pm 0.0000000031) \cdot 10^{-3}$	1
c	1.28 ± 0.03	2500
s	$\begin{pmatrix} 96 & ^{+8}_{-4} \end{pmatrix} \cdot 10^{-3}$	190
μ	$(106.6483745 \pm 0.0000024) \cdot 10^{-3}$	210
t	173.5 ± 1.1	340000
b	$4.18\ ^{+0.04}_{-0.03}$	8200
τ	1.77686 ± 0.00012	3500

Table 1.3: Observed charged fermion masses. The numbers are taken from [18].

scale of the electro-weak symmetry breaking, and correspondingly, gauge bosons corresponding to the broken symmetry generators, and the Higgs boson, obtain masses of the order of this symmetry breaking scale. The electro-weak symmetry breaking provides the fermions with their masses through their interactions with the Higgs vacuum. All fermions can obtain their mass through dimension-4 operators except for the neutrinos, which can at best obtain masses from dimension-5 operators which must therefore be suppressed by another energy scale Λ (that in the SM is completely unrelated to the electro-weak symmetry breaking scale). We therefore expect the neutrinos to be extremely light compared to the electro-weak scale, which indeed matches what is seen in experiments.

But what are we to expect for the numerical values of the fermion masses? A naive guess would be that all Yukawa couplings are $\mathcal{O}(1)$ such that all fermions have masses around $\frac{v}{\sqrt{2}}$. Another less naive guess would be that all Yukawa couplings (and hence all fermion masses) are very small, because of the *chiral symmetry* that appears in the absence of fermion Dirac masses (this is the symmetry of independent phase rotations of all left-handed and right-handed fermions respectively). If the Yukawa couplings are all small, the chiral symmetry protects them from large quantum corrections. It would in this sense be "natural" [33] to have fermion masses much smaller than the electro-weak scale.

Neither of these two guesses agree by themselves with the observed fermion masses (which I have listed in Tab. 1.3). While the top quark indeed has a mass very close to $\frac{v}{\sqrt{2}} \approx 174$ GeV (in fact, suspiciously close!), the lightest fermion in the SM (i.e. the electron) is roughly 10^{-5} times lighter than this. This is even though all fermion masses enter on a complete equal footing, at least from the viewpoint of the SM.

Also, the form of V_{CKM} is completely unconstrained by the imposed symmetries of the SM (it is only predicted to be unitary). However, the measured [18] absolute values the V_{CKM} entries reveal a non-trivial structure for which there is no explanation to be

found within the SM:

$$\begin{pmatrix} |V_{ud}| & |V_{us}| & |V_{ub}| \\ |V_{cd}| & |V_{cs}| & |V_{cb}| \\ |V_{td}| & |V_{ts}| & |V_{tb}| \end{pmatrix} = \begin{pmatrix} 0.97417 \pm 0.00021 & 0.2248 \pm 0.0006 & 0.00409 \pm 0.00039 \\ 0.220 \pm 0.005 & 0.995 \pm 0.016 & 0.0405 \pm 0.00015 \\ 0.0082 \pm 0.0006 & 0.0400 \pm 0.0027 & 1.009 \pm 0.031 \end{pmatrix}$$
$$= \begin{pmatrix} |\cos\theta_{\mathrm{C}}| & |\sin\theta_{\mathrm{C}}| & 0 \\ |\sin\theta_{\mathrm{C}}| & |\cos\theta_{\mathrm{C}}| & 0 \\ 0 & 0 & 1 \end{pmatrix} + \mathcal{O}(10^{-2}) \tag{1.191}$$

with $\sin\theta_{\mathrm{C}} \approx 0.225$. I.e. to $\mathcal{O}(1\%)$ accuracy, the third quark family has diagonal gauge interactions, leaving behind a 2-by-2 mixing between the lightest two quark families.

These flavour structures might have a natural explanation if the SM is extended by additional scalar fields. With such an increased field content it becomes possible to impose additional symmetries on the model. The most well-studied such model is the 2 Higgs Doublet Model (2HDM), where a second Higgs doublet is added to the SM. This leads to a very diverse phenomenology (see e.g. [34] and references therein), in particular due to discrete discrete symmetries that can be imposed. To add even more Higgs doublets might at first seem rather unmotivated, since there is still plenty of room in the phenomenologically viable regions of the 2HDM parameter space. But for example, in a model with 3 Higgs doublets (3HDM), the number of realisable symmetries on the scalar potential [35, 36] vastly exceeds that of the 2HDM [37, 38, 39, 40], and the more constraining symmetries lead to 3HDMs that are simpler in their structure than popular 2HDM realizations. In Paper IV we propose a 3HDM where we impose the most constraining Abelian symmetry possible (which is $\mathrm{U}(1) \times \mathrm{U}(1)$ in 3HDMs [35, 36]) with the purpose of partly explaining the flavour structure of the SM fermions. There, the $\mathrm{U}(1) \times \mathrm{U}(1)$ charges are assigned such that the first two doublets (H_1 and H_2 in the paper) give rise to the masses of the up-type and down-type quarks, respectively, in the two lightest quark families, while the third doublet H_3 couples exclusively to the bottom and the top quark. This directly leads to the 2-by-2 Cabibbo form of V_{CKM}. Furthermore, if we "tune" the vacuum expectation values such that $\langle|H_{1,2}|^2\rangle \ll \langle|H_3|^2\rangle$, we simultaneously get a SM-like Higgs boson in the scalar mass spectrum, and two light and one heavy quark family[10]. In addition, this model predicts new scalar particles that couple mainly to strange and charm quarks, and in the paper we propose a search strategy for the lightest charged scalar in the model which utilises the $c\bar{s}$ fusion channel.

[10] Allegedly, Howard Georgi is to have said that one should have "not more than one half of an idea per paper" [41]. In this spirit, we only use $\langle|H_{1,2}|^2\rangle \ll \langle|H_3|^2\rangle$ to explain the quark mass hierarchies, but leave the lepton sector very SM-like. I.e. in this model, the electron, the muon and the tau all get their masses from $\langle H_3\rangle$ which is most often $\lesssim 246$ GeV.

4 Physics above the electro-weak scale

4.1 Supersymmetry

The hierarchy problem (which was mentioned in Sec. 2.2) refers to the problem of the seemingly unnatural hierarchy between the electro-weak scale and the UV cut-off scale for the SM $\Lambda_{\rm SM}$ (which is usually assumed to be very large, $\Lambda_{\rm SM} \lesssim \Lambda_{\rm Pl} \sim 10^{18}$ GeV). This hierarchy is strange within the context of the SM by itself since the electro-weak scale is set by the Higgs mass squared parameter $-\mu^2$ which is quadratically sensitive to $\Lambda_{\rm SM}$ (as argued in Sec. 2.2). This is because there is no symmetry in the UV limit of the SM that forbids the $|\Phi|^2$ operator. Such a symmetry is hard to imagine, but it turns out that *supersymmetry* (SUSY) can do the job.

I will in this section introduce the very basics of supersymmetry, which is required for Paper III in this thesis. This section is heavily based on [42].

Supersymmetry is most appropriately thought of as an extension of the Poincaré algebra (see Sec. 1.1). In its minimal version, the generators of the Poincaré group P^μ and $J^{\mu\nu}$ are augmented by one pair of fermionic generators Q^α and $Q^{\dagger\dot\alpha}$ (which are in the $(\frac{1}{2},0)$ and $(0,\frac{1}{2})$ representations of the Lorentz group respectively). This is the so-called $\mathcal{N}=1$ supersymmetry, where $\mathcal{N}$ refers to number of $\{Q,Q^\dagger\}$ pairs. The Poincaré algebra (Eq. (1.2)) is extended by

$$\begin{gathered}\{Q^\alpha, Q^{\dagger\dot\alpha}\} = -2(\bar\sigma^\mu)^{\alpha\dot\alpha}P_\mu\,, \quad \{Q^\alpha, Q^\beta\} = \{Q^{\dagger\dot\alpha}Q^{\dagger\dot\beta}\} = 0 \\ [Q_\alpha, P^\mu] = 0\,, \quad [Q^\dagger_{\dot\alpha}, P^\mu] = 0\end{gathered} \tag{1.192}$$

which is the SUSY algebra. We should now go back all the way to Wigner's classification (Sec. 1.2), and see what the one-particle states are that form representations of the SUSY algebra. In particular, since Q^α is fermionic, we have that $Q\,|\text{boson}\rangle = |\text{fermion}\rangle$ and $Q\,|\text{fermion}\rangle = |\text{boson}\rangle$. Fermionic and bosonic states that are related in this way are referred to as "super partners"[11]. The particle representations of the $\mathcal{N}=1$ SUSY algebra are "super-multiplets", each consisting of two particles differing in spin by $\frac{1}{2}$. The Q^α's commute with P^2 (since they commute with P^μ), so the particles in each supermultiplet must have the same mass (for exact supersymmetry). They must also form the same representations under internal symmetries.

The generators of the Poincaré group can be represented on space-time x^μ as

$$P^\mu \to -\mathrm{i}\partial^\mu\,, \quad J^{\mu\nu} \to x^\mu\partial^\nu - x^\nu\partial^\mu\,. \tag{1.193}$$

We can extend space-time with a pair of Grassmann valued 2-component coordinates θ^α and $\theta^{\dagger\dot\alpha}$, to form the so called *superspace* $\{x^\mu, \theta^\alpha, \theta^{\dagger\dot\alpha}\}$. Q^α and $Q^{\dagger\dot\alpha}$ can now be

[11] However, supersymmetry does not always imply that for each fermionic particle there is corresponding bosonic particle. In so called non-linearly realized supersymmetry [43], the superpartner of the fermion is instead a two-fermion state which is therefore is bosonic.

represented on superspace as

$$Q^\alpha \to -\mathrm{i}\frac{\partial}{\partial\theta_\alpha} + (\theta^\dagger\bar\sigma^\mu)^\alpha\partial_\mu\,, \quad Q^{\dagger\dot\alpha} \to \mathrm{i}\frac{\partial}{\partial\theta^\dagger_{\dot\alpha}} - (\bar\sigma^\mu\theta)^{\dot\alpha}\partial_\mu\,. \tag{1.194}$$

An arbitrary scalar function of the superspace coordinates transform under supersymmetry (with fermionic parameters ϵ^α) as

$$\begin{aligned}\sqrt{2}\delta_\epsilon S(x^\mu,\theta,\theta^\dagger) = &-\mathrm{i}(\epsilon Q + \epsilon^\dagger Q^\dagger)S \\ &= S(x^\mu + \mathrm{i}\epsilon\sigma^\mu\theta^\dagger + \mathrm{i}\epsilon^\dagger\bar\sigma^\mu\theta, \theta+\epsilon, \theta^\dagger+\epsilon^\dagger) - S(x^\mu,\theta,\theta^\dagger)\end{aligned} \tag{1.195}$$

so supersymmetry transformations can be viewed as translations in superspace.

However, S is a reducible representation, and can be constrained in a few ways consistent with SUSY. In particular, if we form

$$D^\dagger{}_{\dot\alpha} \equiv -\frac{\partial}{\partial\theta^{\dagger\dot\alpha}} + \mathrm{i}(\theta\sigma^\mu)_{\dot\alpha}\partial_\mu, \tag{1.196}$$

then one can verify that if a superfield Φ satisfies

$$D^\dagger{}_{\dot\alpha}\Phi = 0\,, \tag{1.197}$$

then Φ also satisfies Eq. (1.197) after a supersymmetry transformation. Fields that satisfy Eq. (1.197) are called chiral superfields. Another constraint consistent with supersymmetry is

$$V^* = V\,, \tag{1.198}$$

which yields so called vector superfields.

The solution to Eq. (1.197) is

$$\begin{aligned}\Phi &= \Phi(y,\theta) \\ &= \phi(y) + \sqrt{2}\theta\psi(y) + \theta\theta F(y)\,,\end{aligned} \tag{1.199}$$

with $y^\mu \equiv x^\mu + \mathrm{i}\theta^\dagger\bar\sigma^\mu\theta$. Therefore, each chiral superfield contains a complex scalar ϕ and a 2-component Weyl fermion ψ. It also contains an auxiliary field $F(y)$ which will turn out to be a non-propagating degree of freedom (we will see that F lacks a kinetic term).

It turns out [42] that a vector superfield V can always be put in the form

$$V = \theta^\dagger\bar\sigma^\mu\theta A_\mu + \theta^\dagger\theta^\dagger\theta\lambda + \theta\theta\theta^\dagger\lambda^\dagger + \frac{1}{2}\theta\theta\theta^\dagger\theta^\dagger D\,. \tag{1.200}$$

This corresponds to the so-called Wess-Zumino gauge. We can see from this that the vector multiplet contains a vector field A^μ and a fermion (a "gaugino") λ. Similarly to F in Φ, the auxiliary field D in V does not correspond to propagating particles since it lacks a kinetic term.

One can check from Eq. (1.195) that F transforms as a total derivative w.r.t. x^μ under SUSY transformations. Note also that any holomorphic function of Φ (i.e. a function only of Φ but not of Φ^*) $W(\Phi)$ is also a chiral superfield. Therefore, the terms

$$\int \mathrm{d}^4x \int \mathrm{d}^2\theta\, W(\Phi) + \text{c.c.} \tag{1.201}$$

are real and invariant under SUSY transformations. (The integrals $\int \mathrm{d}^2\theta$ only receive a non-zero contribution from $\theta\theta$ component of $W(\Phi)$.)

Eq. (1.195) can also be used to show that the $\theta^2\theta^{\dagger 2}$ component D of a vector superfield V does not transform under SUSY transformations. We can therefore obtain SUSY invariant action terms by integrating V over $\theta^2\theta^{\dagger 2}$. In particular, $\Phi^*\Phi$ satisfies the reality condition in Eq. (1.198) and is therefore a vector superfield. The terms

$$\int \mathrm{d}^4x \int \mathrm{d}^2\theta \int \mathrm{d}^2\theta^\dagger \Phi^*\Phi = \int \mathrm{d}^4x \left(|\partial\phi|^2 + \mathrm{i}\psi^\dagger \bar{\sigma}^\mu \partial_\mu \psi + F^* F \right) , \tag{1.202}$$

are therefore SUSY invariant. I have on the RHS explicitly performed the integrals over θ or $\theta^\dagger$, whereby we see that we can recover the standard kinetic terms for ϕ and ψ, but no kinetic term for F (as promised).

If we now for example take $W(\Phi) = \frac{1}{2}\mu\Phi^2 + \frac{1}{3!}\lambda\Phi^3$, then the terms from Eq. (1.201) can be shown to be

$$\int \mathrm{d}^4x \left(\mu\phi F - \frac{1}{2}\mu\psi\psi + \frac{1}{2}\lambda\phi^2 F - \lambda\phi\psi\psi \right) + \text{c.c.} \tag{1.203}$$

We can add these terms to the terms in Eq. (1.202), and find the equations of motion for F as

$$F + \mu^*\phi^* + \frac{1}{2}\lambda^*\phi^{*2} = 0\,. \tag{1.204}$$

This can be used to remove F in the action in Eq. (1.203), giving

$$\begin{aligned} S = \int \mathrm{d}^4x \Big[& |\partial\phi|^2 + \mathrm{i}\psi^\dagger\bar{\sigma}^\mu\partial_\mu\psi - \frac{1}{2}\left(\mu\psi\psi + \text{c.c.}\right) \\ & - \left|\mu + \frac{1}{2}\lambda\phi\right|^2 |\phi|^2 - \left(\lambda\phi\psi\psi + \text{c.c.}\right) \Big] . \end{aligned} \tag{1.205}$$

Note that ψ and ϕ have the same mass, and also e.g. that the $|\phi|^4$ and the $\phi\psi\psi$ interactions have related strengths. One can check that, as a consequence of this, the one-loop contributions to the masses of ψ and ϕ vanish.

The fact that the masses of the fields in this toy model do not receive quantum corrections is just a special case of more general SUSY non-renormalisation theorems [44, 45], which state that no superpotential parameters do (meaning that they are cut-off independent contrary to e.g. the Higgs squared mass parameter). If the electro-weak scale is given by a superpotential parameter in a supersymmetrised version of the SM, its smallness compared to any UV cut-off would therefore be less awkward.

However, there is obviously no manifest supersymmetry at the electro-weak scale, since we simply do not see any of the superpartners of the fields in Tab. 1.2 (i.e. fields with the same mass and quantum numbers but different spins). It is however not difficult to write down a theory with an approximate supersymmetry that still retains many of the nice features of exact SUSY. Consider modifying a SUSY theory by adding operators with mass dimension $d < 4$ (which come with couplings of positive mass dimensions). These are the so called soft SUSY breaking terms. Suppose that all such couplings are related to some energy scale $\Lambda_{\text{soft}} \ll \Lambda_{\text{UV}}$. Then, at least, all SUSY breaking effects such as the mass splitting between particles in the same supermultiplets, or radiative corrections to the electro-weak scale, can at most be $\mathcal{O}(\Lambda_{\text{soft}})$ rather than $\mathcal{O}(\Lambda_{\text{UV}})$.

Soft SUSY breaking parameters are often introduced to parametrise our ignorance about the mechanism that broke SUSY in the first place. However, given that this mechanism might be completely unrelated to the superpotential, one can argue that if the electro-weak scale is set by superpotential parameters, such as e.g. in the Minimal Supersymmetric Standard Model (MSSM), the natural scale for the electro-weak scale would still be at Λ_{UV} and not at Λ_{soft}. This is the so called μ-problem of the MSSM. A very nice feature of the supersymmetric trinification model in Paper III is that only the Grand Unification scale (more about this in the next section) is set by superpotential parameters, while all subsequent symmetry breaking scales (including the electro-weak scale) are completely determined by soft SUSY breaking parameters only.

4.2 Grand unification

We have seen from Eq. (1.190) that the neutrino masses force us to introduce another scale Λ in the SM, in addition to the electro-weak scale that is set by the Higgs mass squared parameter. The neutrino (Majorana) mass terms are the only terms in the SM that do not preserve lepton number, meaning that we might want to think of Λ as the energy scale associated with lepton number violation. The actual values of the neutrino masses $m_{\nu_{1,2,3}}$ are notoriously difficult to measure and are therefore not known. However, neutrino oscillation experiments can quite accurately measure the differences between the squared masses, which are found to be

$$\begin{aligned} m_{\nu_2}^2 - m_{\nu_1}^2 &= (7.53 \pm 0.18) \cdot 10^{-5}\,\text{eV}^2 \approx [8.67 \pm 0.10\,\text{meV}]^2\,, \\ |m_{\nu_3}^2 - m_{\nu_2}^2| &= \begin{cases} (2.45 \pm 0.05) \cdot 10^{-3}\,\text{eV}^2 \approx [(49.9 \pm 0.5)\,\text{meV}]^2 & \text{(NH)} \\ (2.52 \pm 0.05) \cdot 10^{-3}\,\text{eV}^2 \approx [(50.1 \pm 0.5)\,\text{meV}]^2 & \text{(IH)} \end{cases}, \end{aligned} \tag{1.206}$$

where the numbers are taken from [18]. Here, (NH) and (IH) refers to normal ($m_{\nu_3} > m_{\nu_2} > m_{\nu_1}$) and inverted ($m_{\nu_2} > m_{\nu_1} > m_{\nu_3}$) mass hierarchy respectively. In particular, this implies a lower bound on the mass of heaviest neutrino species at ~ 50 meV. If we assume that $(y_\nu)^{ij} \sim \mathcal{O}(0.1\text{–}1)$, then we can translate this into an estimate of an upper bound on Λ as

$$\Lambda \sim \frac{v^2}{m_\nu} \lesssim 10^{15-16}\ \text{GeV}\,. \tag{1.207}$$

This is a very interesting energy scale! Not only is it just a few orders of magnitude below the Plank scale $\Lambda_{\text{Pl}} \sim 10^{18}$ GeV. It also coincides with another energy scale that

can be indirectly inferred from the SM, namely the scale of *gauge coupling unification*.

The gauge couplings in the SM take on the values

$$\alpha_3 \equiv \frac{g_{\rm C}^2}{4\pi} \approx \frac{1}{8.5} \ , \ \alpha_2 \equiv \frac{g_{\rm L}^2}{4\pi} \approx \frac{1}{29} \ , \ \alpha_1 \equiv \frac{g_{\rm Y}^2}{4\pi} \approx \frac{1}{101} \tag{1.208}$$

for a renormalisation scale $\mu = m_Z$ (we also have $\alpha_{\rm e.m.} \equiv \frac{e^2}{4\pi} \approx \frac{1}{128}$ at this scale). Note that this value of α_1 is specific to the normalisation of the hypercharges in Tab. 1.2. For reasons that will become clear later, let me change the hypercharges $\hat{Y}$ to a different normalization such that

$$\hat{Y} = \sqrt{\frac{3}{5}} Y \, . \tag{1.209}$$

The new hypercharge gauge coupling is $\hat{g}_{\rm Y} = \sqrt{\frac{5}{3}} g_{\rm Y}$, such that

$$\hat{\alpha}_1 \equiv \frac{\hat{g}_{\rm Y}^2}{4\pi} \approx \frac{1}{60} \, , \tag{1.210}$$

at $\mu = m_Z$. With the SM field content, the corresponding β-functions are

$$\beta(\hat{\alpha}_1) = \frac{41}{10} \cdot \frac{\hat{\alpha}_1^2}{2\pi} \ , \ \beta(\alpha_2) = -\frac{19}{6} \cdot \frac{\alpha_2^2}{2\pi} \ , \ \beta(\alpha_3) = -7 \cdot \frac{\alpha_3^2}{2\pi} \tag{1.211}$$

with $\beta(\alpha_i) \equiv \mu \frac{\rm d}{{\rm d}\mu} \alpha_i$, which we can use to run the gauge couplings towards higher energies. See e.g. [3] for the computation of the β-functions in Eq. (1.211). The solutions to these evolution equations (for the boundary conditions in Eqs. (1.208) and (1.210) for $\mu = m_Z$) are shown in figure 1.4. This figure reveals something interesting: At an energy scale of about $\mu \sim 10^{14-16}$ GeV, the gauge couplings acquire almost the same value. Note that the running is logarithmically slow, meaning that the energy scale, at which two curves in figure 1.4 intersect, is *exponentially* sensitive both to their slopes (given by their β-functions) and their boundary values at $\mu = m_Z$. It might therefore seem unlikely coincidental not only that the gauge couplings almost unify, but also that the unification scale roughly coincides with the new physics energy scale that can be inferred from neutrino masses.

A natural question we can now ask is: Could there be a symmetry reason for the gauge coupling unification? That is, can we construct a model where there is a symmetry that enforce a common value for the gauge couplings, and that gets spontaneously broken at a scale $\Lambda_{\rm GUT} \sim 10^{14-16}$ GeV?

The answer is of course that such models exist, and they go under the name Grand Unification Theories (GUTs). The minimal grand unified construction is based on the observation that the SM gauge group can be found as a subgroup of SU(5)[46]. In particular, the generator of the hypercharge subgroup now comes out with the normalization of $\sqrt{\frac{3}{5}}$ in Eq. (1.209), such that a manifest SU(5) gauge symmetry implies

$$\hat{\alpha}_1 = \alpha_2 = \alpha_3 \, . \tag{1.212}$$

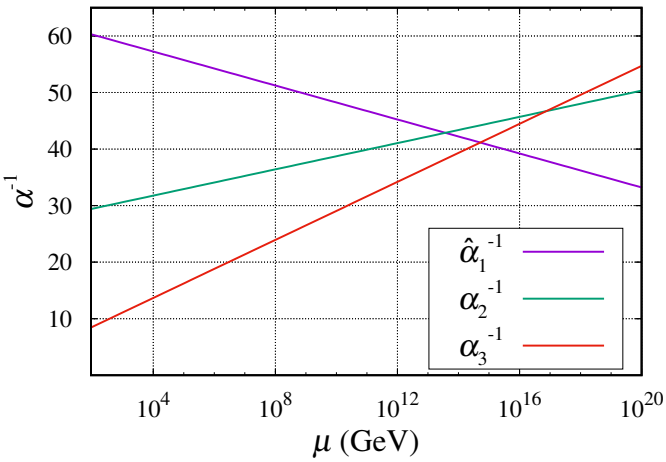

Figure 1.4: Gauge coupling scale evolution in the Standard Model.

The unification of the SM gauge group into a simple Lie group also explains another curiosity of the SM, namely the particular hypercharges of the SM fermions. In the SM, we are a priori completely free to pick the $\mathrm{U}(1)_\mathrm{Y}$ charges (and by extension the electric charges) of the fields. In this sense, the electric charges of the proton and the electron are independent quantities in the SM, and it may thus seem like a numerical coincidence that these charges are so delicately balanced against each other. This is on the contrary a natural consequence in GUTs.

The fermions $d_\mathrm{R}^{\mathrm{c}i}$ and L_L^i can be grouped into the $\bar{\mathbf{5}}^i$ representation, while $u_\mathrm{R}^{\mathrm{c}i}$, Q_L^i and $e_\mathrm{R}^{\mathrm{c}i}$ together furnish a $\mathbf{10}^i$ (i.e. the anti-symmetric bi-fundamental) representation of SU(5). The Higgs doublet Φ needs to be supplemented with an exotic colour triplet scalar field such that they together can form a $\mathbf{5}$. Furthermore, it turns out that the breaking $\mathrm{SU}(5) \to \mathrm{SU}(3)_\mathrm{C} \times \mathrm{SU}(2)_\mathrm{L} \times \mathrm{U}(1)_\mathrm{Y}$ can be induced by a vacuum expectation in a scalar multiplet in the $\mathbf{24}$ (i.e. in the adjoint) representation. This vacuum expectation value should be of the order of Λ_GUT, and provides $\mathcal{O}(\Lambda_\mathrm{GUT})$ masses to all fields that are not in the SM.

SU(5) GUTs also come with a very striking experimental signature that is absent in the SM, namely that of *proton decay*. Since quarks and leptons sit in common gauge multiplets, there exist exotic heavy gauge bosons that transform quarks into leptons and vice versa (just like gluons in the SM change the colour charge of the quarks). We can quite straightforwardly estimate the proton lifetime from this. At the GeV scale, such processes would be described by baryon number violating effective operators that are obtained from integrating out the heavy gauge bosons. These operators must at least be of mass-dimension 6, meaning that the decay amplitude is proportional to $\Lambda_\mathrm{GUT}^{-2}$. The decay width Γ_p is proportional to the square of the amplitude, and dimensional

analysis tells us where to put in extra factors of the proton mass $m_{\rm p}$:

$$\Gamma_{\rm p} \sim m_{\rm p} \cdot \left(\frac{m_{\rm p}}{\Lambda_{\rm GUT}}\right)^4 . \tag{1.213}$$

The proton lifetime $\tau_{\rm p}$ is the inverse of $\Gamma_{\rm p}$, and can therefore be related to $\Lambda_{\rm GUT}$ as

$$\Lambda_{\rm GUT} \sim m_{\rm p} \left(m_{\rm p}\tau_{\rm p}\right)^{\frac{1}{4}} . \tag{1.214}$$

Proton decay has been extensively looked for but never observed, which can be translated into lower limits of $\tau_{\rm p}$. In particular, the mean partial lifetime due to $p \to e^+\pi^0$ is constrained [18] as

$$\tau_{\rm p} > 8.2 \cdot 10^{33} \text{ years} \approx 3.9 \cdot 10^{65} \text{ GeV}^{-1} . \tag{1.215}$$

This leads to an estimate of a lower bound on the grand unification scale as

$$\Lambda_{\rm GUT} > 2 \cdot 10^{16} \text{ GeV} . \tag{1.216}$$

Although both this limit and the limit in Eq. (1.207) were very crudely estimated, we see that there is a potential tension between them. More detailed calculations [47] indeed show that the simplest SU(5) realisations are ruled out experimentally, while $\Lambda_{\rm GUT}$ is tightly constrained in other versions.

4.3 Trinification

We can now ask if it is possible to achieve grand unification where the proton is still very stable (such that the bound in Eq. (1.216) on $\Lambda_{\rm GUT}$ does not apply). Indeed, the *trinification* [48] grand unified scheme can achieve this. The trinification gauge group is

$$\mathrm{SU}(3)^3 \equiv [\mathrm{SU}(3)_{\rm C} \times \mathrm{SU}(3)_{\rm L} \times \mathrm{SU}(3)_{\rm R}] \rtimes \mathbb{Z}_3 , \tag{1.217}$$

where $\mathrm{SU}(3)_{\rm C}$ is the familiar colour group of QCD, while $\mathrm{SU}(3)_{\rm L} \times \mathrm{SU}(3)_{\rm R}$ extends the electro-weak gauge group. The $\mathbb{Z}_3$ symmetry refers to a cyclic permutation symmetry of the representations of the three SU(3) groups, which enforces a common value of the corresponding gauge couplings. It has a total of $3 \cdot 8 = 24$ generators $T^{1,\ldots,8}_{\rm L,R,C}$ which in the fundamental representations correspond to $\frac{1}{2}\lambda^{1,\ldots,8}$ (with λ^a being the Gell-Mann matrices).

Each generation of SM fermions can be embedded into three bi-fundamental representations L^i, $Q^i_{\rm L}$ and $Q^i_{\rm R}$ as

$$L^i \sim (\mathbf{1},\mathbf{3},\bar{\mathbf{3}})^i \ , \ Q^i_{\rm L} \sim (\mathbf{3},\bar{\mathbf{3}},\mathbf{1})^i \ , \ Q^i_{\rm R} \sim (\bar{\mathbf{3}},\mathbf{1},\mathbf{3})^i . \tag{1.218}$$

Each L^i can be represented as a 3-by-3 matrix $(L^i)^l{}_r$ where $\mathrm{SU}(3)_{\rm L,R}$ transformations act on the l ('row') and r ('column') indices respectively ($Q_{\rm L,R}$ can of course also be similarly represented). From now on, the indices belonging to fundamental (anti-fundamental) representations will be denoted as superscripts (subscripts), e.g. such that

$[(L^i)^l{}_r]^\dagger = (L_i^\dagger)_l{}^r$. The $\mathbb{Z}_3$ in Eq. (1.217) acts on the fermions as a cyclic permutation in $\{L, Q_\mathrm{L}, Q_\mathrm{R}\}$.

Let us first look at the gauge-kinetic terms of the fermions,

$$\mathcal{L} \supset \mathrm{i}(L^\dagger{}_i)_l{}^r \bar{\sigma}^\mu \left(D_\mu L^i\right)^l{}_r + \mathrm{i}(Q_{\mathrm{L}i}^\dagger)_c{}^l \bar{\sigma}^\mu \left(D_\mu Q_\mathrm{L}^i\right)^c{}_l + \mathrm{i}(Q_{\mathrm{R}i}^\dagger)_r{}^c \bar{\sigma}^\mu \left(D_\mu Q_\mathrm{R}^i\right)^r{}_c \,, \quad (1.219)$$

where

$$\begin{aligned}
\left(D_\mu L^i\right)^l{}_r &= \left[\delta^l_{l'}\delta^{r'}_r \partial_\mu - \frac{1}{2}\mathrm{i}g_\mathrm{L} G^a_{\mathrm{L}\mu}(\lambda^a)^l{}_{l'}\delta^{r'}_r + \frac{1}{2}\mathrm{i}g_\mathrm{R} G^a_{\mathrm{R}\mu}(\lambda^a)^{r'}{}_r\delta^l_{l'}\right](L^i)^{l'}{}_{r'} \,, \\
\left(D_\mu Q_\mathrm{L}^i\right)^c{}_l &= \left[\delta^c_{c'}\delta^{l'}_l \partial_\mu - \frac{1}{2}\mathrm{i}g_\mathrm{C} G^a_{\mathrm{C}\mu}(\lambda^a)^c{}_{c'}\delta^{l'}_l + \frac{1}{2}\mathrm{i}g_\mathrm{L} G^a_{\mathrm{L}\mu}(\lambda^a)^{l'}{}_l\delta^c_{c'}\right](Q_\mathrm{L}^i)^{c'}{}_{l'} \,, \quad (1.220) \\
\left(D_\mu Q_\mathrm{R}^i\right)^r{}_c &= \left[\delta^r_{r'}\delta^{c'}_c \partial_\mu - \frac{1}{2}\mathrm{i}g_\mathrm{R} G^a_{\mathrm{R}\mu}(\lambda^a)^r{}_{r'}\delta^{c'}_c + \frac{1}{2}\mathrm{i}g_\mathrm{C} G^a_{\mathrm{C}\mu}(\lambda^a)^{c'}{}_c\delta^r_{r'}\right](Q_\mathrm{R}^i)^{r'}{}_{c'} \,,
\end{aligned}$$

where $G^a_{\mathrm{L,R,C}\mu}$ are the gauge fields associated with $\mathrm{SU}(3)_\mathrm{L,R,C}$ respectively (in particular, $G^a_{\mathrm{C}\mu}$ are the gluons in the SM), and $g_\mathrm{L,R,C}$ are their associated gauge couplings. From this we can see that the terms in Eq. (1.219) are $\mathbb{Z}_3$ invariant if the cyclic permutation in $\{L, Q_\mathrm{L}, Q_\mathrm{R}\}$ is accompanied by a cyclic permutation in $\{G_{\mathrm{L}\mu}, G_{\mathrm{C}\mu}, G_{\mathrm{R}\mu}\}$ and the gauge couplings are unified to a common value,

$$g_\mathrm{L} = g_\mathrm{R} = g_\mathrm{C} \equiv g_\mathrm{U} \,. \quad (1.221)$$

The trinification gauge group can be broken to that of the SM by vacuum expectation values in two scalar $(\mathbf{1}, \mathbf{3}, \bar{\mathbf{3}})$ fields (i.e. scalar "cousins" of L). To keep a consistent notation with Paper II and III, let me denote these two scalar multiplets as $(\tilde{L}^3)^l{}_r$ and $(\tilde{L}^2)^l{}_r$ (as you might guess, there is also a third such field $(\tilde{L}^1)^l{}_r$ in these articles). Let us take the forms of $\langle(\tilde{L}^{2,3})^l{}_r\rangle$ to be

$$\langle(\tilde{L}^3)^l{}_r\rangle = \begin{pmatrix} 0 & 0 & 0 \\ 0 & 0 & 0 \\ 0 & 0 & \frac{v}{\sqrt{2}} \end{pmatrix} \,, \quad \langle(\tilde{L}^2)^l{}_r\rangle = \begin{pmatrix} 0 & 0 & 0 \\ 0 & 0 & 0 \\ 0 & \frac{w}{\sqrt{2}} & 0 \end{pmatrix} \,. \quad (1.222)$$

Here, $v \neq 0$ induces the breaking

$$\mathrm{SU}(3)_\mathrm{L} \times \mathrm{SU}(3)_\mathrm{R} \to \mathrm{SU}(2)_\mathrm{L} \times \mathrm{SU}(2)_\mathrm{R} \times \mathrm{U}(1)_\mathrm{L+R} \,, \quad (1.223)$$

where $\mathrm{SU}(2)_\mathrm{L,R}$ are generated by $T^{1,2,3}_\mathrm{L,R}$ and $\mathrm{U}(1)_\mathrm{L+R}$ is generated by

$$T_\mathrm{L+R} \equiv \frac{1}{\sqrt{3}}\left(T^8_\mathrm{L} + T^8_\mathrm{R}\right) \,. \quad (1.224)$$

Furthermore, $w \neq 0$ provides the breaking $\mathrm{SU}(2)_\mathrm{R} \times \mathrm{U}(1)_\mathrm{L+R} \to \mathrm{U}(1)_\mathrm{Y}$, where we find the hypercharge generator as

$$Y \equiv -T^3_\mathrm{R} - T_\mathrm{L+R} = -T^3_\mathrm{R} - \frac{1}{\sqrt{3}}\left(T^8_\mathrm{L} + T^8_\mathrm{R}\right) \,. \quad (1.225)$$

We can label the components of $Q^i_{\mathrm{L,R}}$ as

$$Q^i_{\mathrm{L}} = \begin{pmatrix} u^i_{\mathrm{L}} & d^i_{\mathrm{L}} & D^i_{\mathrm{L}} \end{pmatrix}, \quad Q^i_{\mathrm{R}} = \begin{pmatrix} u^{\mathrm{c}i}_{\mathrm{R}} & d^{\mathrm{c}i}_{\mathrm{R}} & D^{\mathrm{c}i}_{\mathrm{R}} \end{pmatrix}, \tag{1.226}$$

motivated by their hypercharges (I have here suppressed the colour degree of freedom for clarity). The $\mathrm{SU}(2)_{\mathrm{L}}$ doublets $\begin{pmatrix} u^i_{\mathrm{L}} & d^i_{\mathrm{L}} \end{pmatrix}$ have $Y = \frac{1}{6}$ meaning that they must correspond to the SM electro-weak quark doublets (while the extra $\mathrm{SU}(2)_{\mathrm{L}}$ singlet quarks D^i_{L} have $Y = -\frac{1}{3}$ and therefore do not have any SM counterpart). Similarly, $u^{\mathrm{c}i}_{\mathrm{R}}$ have $Y = -\frac{2}{3}$, so they have to be identified with the SM $u^{\mathrm{c}i}_{\mathrm{R}}$ in Tab. 1.2. However, both $d^{\mathrm{c}i}_{\mathrm{R}}$ and $D^{\mathrm{c}i}_{\mathrm{R}}$ have $Y = \frac{1}{3}$, i.e. the same quantum numbers as the SM $d^{\mathrm{c}i}_{\mathrm{R}}$'s. Therefore, as far as the electro-weak group concerns, both d^i_{R} and D^i_{R} can play the roles of the right-handed components of the SM down-type quarks.

The components of L^i are labelled as

$$L^i = \begin{pmatrix} H_d^{+i} & H_u^{0i} & \nu^i_{\mathrm{L}} \\ H_d^{0i} & H_u^{-i} & e^i_{\mathrm{L}} \\ e^{\mathrm{c}i}_{\mathrm{R}} & \nu^{\mathrm{c}i}_{\mathrm{R}} & \Phi^i \end{pmatrix} \tag{1.227}$$

which can also be motivated by their hypercharges. Here, $e^{\mathrm{c}i}_{\mathrm{R}}$ are the only $\mathrm{SU}(2)_{\mathrm{L}}$ singlets with $Y = +1$, and must therefore correspond to $e^{\mathrm{c}i}_{\mathrm{R}}$ in Tab. 1.2. However, the two $\mathrm{SU}(2)_{\mathrm{L}}$ doublets $\begin{pmatrix} \nu^i_{\mathrm{L}} \\ e^i_{\mathrm{L}} \end{pmatrix}$ and $\begin{pmatrix} H_u^{0i} \\ H_u^{-i} \end{pmatrix}$ both have $Y = -\frac{1}{2}$ and therefore are both candidates for the SM lepton doublets. The $\mathrm{SU}(2)_{\mathrm{L}}$ doublets made out of $H_d^{0,+i}$ have hypercharge $Y = +\frac{1}{2}$, while $\nu^{\mathrm{c}i}_{\mathrm{R}}$ and Φ^i are electro-weak singlets.

Since the quarks and leptons sit in different gauge multiplets, there is no gauge-mediated proton decay in this model. However, the $\mathbb{Z}_3$ symmetry in Eq. (1.217) forces us to introduce a pair of colour charged scalar fields $\tilde{Q}_{\mathrm{L,R}}$ that are the $\mathbb{Z}_3$ conjugates of $\tilde{L}$. These fields can potentially mediate a decay of the proton through the baryon number violating interaction terms

$$(y_{\not B})^{ijk} \tilde{Q}^i_{\mathrm{L,R}} Q^j_{\mathrm{L,R}} Q^k_{\mathrm{L,R}}, \tag{1.228}$$

where the gauge indices are understood to be contracted with three-dimensional Levi-Cevita tensors. This is however not as severe as e.g. in SU(5) constructions since there the relevant couplings are gauge couplings whose values are fixed by the values of the SM gauge couplings, contrary to the above coupling constants $(y_{\not B})^{ijk}$ which can be independently tuned to be small (see e.g. [49]).

Suppose that the scales v and w in Eq. (1.222) are quite well separated with $w \ll v$. The trinification model can in this case be traded for an effective theory based on the gauge group

$$\mathrm{SU}(3)_{\mathrm{C}} \times \mathrm{SU}(2)_{\mathrm{L}} \times \mathrm{SU}(2)_{\mathrm{R}} \times \mathrm{U}(1)_{\mathrm{L+R}}, \tag{1.229}$$

at energies below v, which can be obtained by integrating out all fields obtaining $\mathcal{O}(v)$ masses. This is a well known gauge group which has been extensively studied in the past in many different realizations, most often without invoking an origin in the trinification gauge group. In fact, it is the basis for a class of models dubbed Left-Right symmetric models [50, 51, 52, 53, 54]. In such models, *parity* can be treated as an exact symmetry

that interchanges representations of $\mathrm{SU}(2)_{\mathrm{L,R}}$, and that gets spontaneously broken along side with $\mathrm{SU}(2)_{\mathrm{R}} \times \mathrm{U}(1)_{\mathrm{L+R}} \to \mathrm{U}(1)_{\mathrm{Y}}$. This is in contrast to the SM, where parity is explicitly and brutally violated since the left-handed and the right-handed components of the SM Dirac fermions have different gauge interactions. In the simplest Left-Right symmetric models, the "right-handed" fields in the SM are put into $\mathrm{SU}(2)_{\mathrm{R}}$ doublets (which requires the inclusion of right-handed neutrinos) to form parity conjugates of the SM $\mathrm{SU}(2)_{\mathrm{L}}$ doublets. In such constructions, it turns out that the $\mathrm{U}(1)_{\mathrm{L+R}}$ charges of the fermions match that of (baryon number) − (lepton number), i.e. $B-L$. For this reason, $\mathrm{U}(1)_{\mathrm{L+R}}$ is often instead written as $\mathrm{U}(1)_{\mathrm{B-L}}$. However, as already discussed, there is in trinification models an ambiguity in which fermions will correspond to the SM fermions, and in general the $\mathrm{U}(1)_{\mathrm{L+R}}$ charges do not match $B-L$. For example, the $D_{\mathrm{R}}^{ci\dagger}$ fields can potentially become the right-handed SM down-type quarks, and they are $\mathrm{SU}(2)_{\mathrm{R}}$ singlets rather than being components of $\mathrm{SU}(2)_{\mathrm{R}}$ doublets. For this reason, labelling the U(1) group in Eq. (1.229) with $B-L$ would be misleading, and we do not employ that notation in Paper II and Paper III. For phenomenological aspects of a Left-Right symmetric model derived from a trinification UV completion, see [55, 56].

One can also find a motivation for trinification from the high energy limit. Namely, the trinification gauge group $\mathrm{SU}(3)^3$ can be found as a maximal subgroup of the exceptional group E_6 [57], under which the three fermion bi-triplets in each generation can form a complete **27** representation,

$$\mathbf{27} \sim (\mathbf{1}, \mathbf{3}, \bar{\mathbf{3}}) \oplus (\mathbf{3}, \bar{\mathbf{3}}, \mathbf{1}) \oplus (\bar{\mathbf{3}}, \mathbf{1}, \mathbf{3})\,. \tag{1.230}$$

This embedding of the trinification gauge group into E_6 can be shown to be one of the phenomenologically plausible low-energy scenarios of a superstring theory with gauge group $\mathrm{E}_8 \times \mathrm{E}_8$ [58, 59], where fields transforming under one of the E_8 groups contains the SM, while fields transforming under the other E_8 group constitute a hidden sector. In turn, E_8 contains $\mathrm{E}_6 \times \mathrm{SU}(3)$ as a maximal subgroup [57], and its **248** representation branches under $\mathrm{E}_8 \to \mathrm{E}_6 \times \mathrm{SU}(3)$ as

$$\mathbf{248} \to (\mathbf{1}, \mathbf{8}) \oplus (\mathbf{78}, \mathbf{1}) \oplus (\mathbf{27}, \mathbf{3}) \oplus (\overline{\mathbf{27}}, \bar{\mathbf{3}})\,. \tag{1.231}$$

Note in particular that the **248** of E_8 contains three **27** representations of E_6 that together form an SU(3) triplet. Given that the each SM fermion generation can fit into a **27**, it is tempting to interpret the SU(3) in $\mathrm{E}_6 \times \mathrm{SU}(3)$ as acting in the space of fermion generations.

Paper II and III concern a non-supersymmetric and a supersymmetric version respectively of the above trinification model, where we indeed augment the trinification gauge symmetry by a novel global $\mathrm{SU}(3)_{\mathrm{F}}$ family symmetry that acts on the space of generations of $\tilde{L}^i$, $\tilde{Q}^i_{\mathrm{L,R}}$, L^i and $Q^i_{\mathrm{L,R}}$ (i.e. the index i on these fields belong to the fundamental representation of $\mathrm{SU}(3)_{\mathrm{F}}$). In particular, $\mathrm{SU}(3)_{\mathrm{F}}$ forces $(y_{\not B})^{ijk} \propto \epsilon^{ijk}$ such that the interaction terms in (1.228) vanish since $Q^j_{\mathrm{L,R}} Q^k_{\mathrm{L,R}}$ is symmetric under $i \leftrightarrow j$. In fact, one of the nice consequences of $\mathrm{SU}(3)_{\mathrm{F}}$ is the appearance of an accidental $\mathrm{U}(1)_{\mathrm{B}}$ baryon number symmetry that stabilizes the proton[12].

[12]However, if we have in mind the embedding $\mathrm{SU}(3)^3 \in \mathrm{E}_6$, then there must be baryon number

The Yukawa interactions become extremely constrained once $\mathrm{SU}(3)_\mathrm{F}$ is imposed. In fact, the Yukawa sector then only contains a single free parameter y_U,

$$\mathcal{L}_\mathrm{Yukawa} = y_\mathrm{U}\epsilon_{ijk}\,(\tilde{L}^i)^l{}_r\,(Q^j_\mathrm{L})^c{}_l\,(Q^k_\mathrm{R})^r{}_c + \mathrm{c.c.} + (\mathbb{Z}_3 \text{ permutations})\,, \tag{1.232}$$

from which all SM Yukawa interactions must originate (at some loop level) for this model to be viable. However, the terms in Eq. (1.232) exhibit a larger global symmetry than what was imposed. To start with, one can perform independent phase rotations e.g. on $(Q_\mathrm{L}, \tilde{Q}_\mathrm{L})$ and $(Q_\mathrm{R}, \tilde{Q}_\mathrm{R})$ respectively, while making a compensating phase rotation of $(L, \tilde{L})$. This means that the model exhibits two accidental global U(1) symmetries (which I will denote as $\mathrm{U}(1)_\mathrm{A}\times\mathrm{U}(1)_\mathrm{B}$ in the reminder of this section). In particular, opposite phase rotations of $(Q_\mathrm{L}, \tilde{Q}_\mathrm{L})$ and $(Q_\mathrm{R}, \tilde{Q}_\mathrm{R})$ respectively (with $(L, \tilde{L})$ being neutral) defines a $\mathrm{U}(1)_\mathrm{B}$ symmetry that leads to a conserved baryon number (that was alluded to in the previous paragraph). It turns out that the full $\mathrm{U}(1)_\mathrm{A}\times\mathrm{U}(1)_\mathrm{B}$ symmetry is also respected in all other sectors of both the supersymmetric and the non-supersymmetric versions of the model.

The terms in Eq. (1.232) are together also invariant under a quite non-trivial discrete symmetry that interchanges $\mathrm{SU}(3)_\mathrm{L}$ and $\mathrm{SU}(3)_\mathrm{R}$ representations. Let me for this reason temporarily divert from from our standard notation and instead denote both $\mathrm{SU}(3)_\mathrm{L,R}$ indices by s, s' etc. (one can still find which index belongs to which group from their positions on the fields). This symmetry also trades Weyl fermions for their complex conjugates, so let me also for a moment drop the dotted-undotted notation and denote indices belonging to the $(\frac{1}{2},0)$ and $(0,\frac{1}{2})$ representations of the Lorentz group as α, β etc. (it should be understood that spinor indices on undaggered and daggered Weyl fermions belong to $(\frac{1}{2},0)$ and $(0,\frac{1}{2})$ respectively). The tri-triplet fields transform under this symmetry as

$$\begin{aligned} (\tilde{L}^i)^s{}_{s'} &\to -(\tilde{L}^*_i)_{s'}{}^s\,, \quad \left[(L^i)^s{}_{s'}\right]_\alpha \to -\mathrm{i}\left[(L^\dagger_i)_{s'}{}^s\right]^\alpha\,, \\ (\tilde{Q}^i_\mathrm{L,R})^c{}_s &\to (\tilde{Q}^*_{\mathrm{R,L}\,i})_s{}^c\,, \quad \left[(Q^i_\mathrm{L,R})^c{}_s\right]_\alpha \to \mathrm{i}\left[(Q^\dagger_{\mathrm{R,L}\,i})_s{}^c\right]^\alpha\,. \end{aligned} \tag{1.233}$$

One can now check that e.g. $\epsilon_{ijk}\tilde{L}^i Q^j_\mathrm{L} Q^k_\mathrm{R}$ transforms into its complex conjugate (1.233) such that the terms in Eq. (1.232) are invariant. However, the kinetic terms for the fermions are not quite invariant under the transformations in Eq. (1.233). Take for example the kinetic term for L,

$$\mathcal{L} \supset \mathrm{i}L^\dagger{}_\alpha(\bar{\sigma}^\mu)^{\alpha\beta}L_\beta\,, \tag{1.234}$$

where I have left gauge and family indices implicit since their contractions are trivial in this term. If we now take $L_\alpha \to -\mathrm{i}L^{\dagger\alpha} = -\mathrm{i}\epsilon^{\alpha\beta}L^\dagger{}_\beta$ (and therefore $L^\dagger{}_\alpha \to \mathrm{i}L^\alpha = \mathrm{i}\epsilon^{\alpha\beta}L_\beta$), and use the identity $\epsilon^{\alpha\delta}(\bar{\sigma}^\mu)^{\gamma\delta}\epsilon^{\gamma\beta} = (\bar{\sigma}_\mu)^{\alpha\beta}$, we see that the above kinetic term is only invariant (up to a total derivative) if we simultaneously take $\partial_\mu \to \partial^\mu$. This corresponds to spatial inversion, i.e.

$$x^\mu \to x_\mu\,, \tag{1.235}$$

violating interactions involving the E_6 gauge fields, which could mediate a decay of the proton. The proton decay width would then be suppressed by the energy scale associated with the breaking $\mathrm{E}_6 \to \mathrm{SU}(3)^3$ which can be much larger than unification scale Λ_GUT (which is the energy scale associated with the breaking in Eq. (1.223)).

or $\vec{x} \to -\vec{x}$ (while $t \to t$). This discrete symmetry therefore corresponds do a so called Left-Right parity symmetry. Curiously, there are also Colour-Left and Right-Colour parity symmetries in these terms due to the presence of the $\mathbb{Z}_3$ symmetry.

One can further check that the gauge fields need to transform as

$$G^{\mu}_{\mathrm{L,R,C}} \to G_{\mathrm{R,L,C}\,\mu}\,, \tag{1.236}$$

for gauge interactions to be Left-Right parity invariant. However, the most general renormalisable scalar potential containing $\tilde{L}$, $\tilde{Q}_{\mathrm{L}}$ and $\tilde{Q}_{\mathrm{R}}$ is in general not invariant under Left-Right parity, which is why this symmetry is not considered in the non-supersymmetric trinification model in Paper II.

In the non-supersymmetric model in Paper II, the tree-level scalar potential for $\tilde{L}$ often has a global minimum where $\langle \tilde{L}^3 \rangle$ has the form in Eq. (1.222). In this paper, we first integrate out the fields that obtain large masses from $\langle \tilde{L}^3 \rangle \neq 0$, to obtain an effective Left-Right symmetric[13] model based on the gauge group in Eq. (1.229). We then show that the mass term of the $\mathrm{SU}(2)_{\mathrm{R}}$ scalar doublet $\begin{pmatrix} \tilde{e}^{1,2}_{\mathrm{R}} & \tilde{\nu}^{1,2}_{\mathrm{R}} \end{pmatrix}$ can become negative through the (continuum) renormalisation group evolution towards lower energies. This running consequently triggers the $\langle \tilde{L}^2 \rangle$ in Eq. (1.222), such that $\mathrm{SU}(2)_{\mathrm{R}} \times \mathrm{U}(1)_{\mathrm{L+R}}$ is radiatively broken to $\mathrm{U}(1)_{\mathrm{Y}}$. Furthermore, we show that this can be done with light Higgs doublets from $\tilde{L}$ still remaining in the spectrum, as required for electro-weak symmetry breaking.

In the supersymmetric trinification model in Paper III, the fields $\tilde{L}$ and L belong to the same chiral superfield which we denote as $\boldsymbol{L}$ (the same goes for $\tilde{Q}_{\mathrm{L,R}}$ and $Q_{\mathrm{L,R}}$ which belong to the chiral supermultiplets $\boldsymbol{Q}_{\mathrm{L,R}}$). With only these fields, the supersymmetric sector of the model contains only *two* free parameters, i.e. the gauge coupling g_{U} and the single real superpotential parameter $\lambda_{\boldsymbol{27}}$ defined as,

$$W_{\boldsymbol{27}} = \lambda_{\boldsymbol{27}}\, \epsilon_{ijk}\, (\boldsymbol{L}^i)^l{}_r\, (\boldsymbol{Q}^j_{\mathrm{L}})^c{}_l\, (\boldsymbol{Q}^k_{\mathrm{R}})^r{}_c\,. \tag{1.237}$$

Contrary to the non-supersymmetric version of the model, Left-Right parity is an accidental symmetry of the full supersymmetric trinification theory with $\mathrm{SU}(3)_{\mathrm{F}}$. It is manifest already at the superspace level where we can take the Left-Right transformation rules to be

$$(\boldsymbol{L}^i)^s{}_{s'} \to -(\boldsymbol{L}^*_i)_{s'}{}^s\,, \quad (\boldsymbol{Q}^i_{\mathrm{L}})^c{}_s \to (\boldsymbol{Q}^*_{\mathrm{R}\,i})_s{}^c\,, \quad (\boldsymbol{Q}^i_{\mathrm{R}})^s{}_c \to (\boldsymbol{Q}^*_{\mathrm{L}\,i})_c{}^s\,. \tag{1.238}$$

The superpotential $W_{\boldsymbol{27}}$ transforms under these transformations as

$$W_{\boldsymbol{27}} \to W^*_{\boldsymbol{27}}\,, \tag{1.239}$$

so the corresponding Lagrangian terms (see e.g. Eq. (1.201)) become Left-Right parity invariant provided that

$$\theta_\alpha \to \mathrm{i}\theta^{\dagger\alpha}\,, \quad \theta^{\dagger\,\alpha} \to \mathrm{i}\theta_\alpha \tag{1.240}$$

[13]However, as was earlier discussed, the Left-Right parity is only respected by Yukawa and gauge interactions (but not the interactions in the scalar potential) at the matching scale. Explicit Left-Right parity violation then sneaks into the gauge and Yukawa sectors via renormalisation group effects at lower energies (as can be seen e.g. by comparing values of the gauge couplings corresponding to the $\mathrm{SU}(2)_{\mathrm{L,R}}$ groups.)

such that $\theta\theta \to \theta^\dagger\theta^\dagger$.

However, the resulting scalar potential does not allow for the vacuum structures in Eq. (1.222). One way to see this is to look at the D-term contribution to the scalar potential,

$$V_D = \frac{1}{2} D^a_{\rm L} D^a_{\rm L} + (\mathbb{Z}_3 \text{ permutations}) \,, \tag{1.241}$$

where

$$D^a_{\rm L} = \frac{1}{2} g_{\rm U} \left[(\tilde{L}^*_i)_l{}^r (\lambda^a)^l{}_{l'} (\tilde{L}^i)^{l'}{}_l - (\tilde{Q}^*_{{\rm L}\,i})_c{}^l (\lambda^a)^{l'}{}_l (\tilde{Q}^i_{\rm L})^c{}_{l'} \right] . \tag{1.242}$$

Suppose we take $w = 0$ in Eq. (1.222) for simplicity. With $v \neq 0$, we see that we can put vacuum expectation values into $\tilde{Q}_{\rm L,R}$ such that $\langle D^a_{\rm L,R,C} \rangle = 0$ and consequently $V = 0$ (one can also show that F-terms do not alter this discussion). This must correspond to a global minimum of the scalar potential since $V \geq 0$ in supersymmetry. However, $\langle \tilde{Q}_{\rm L,R} \rangle \neq 0$ is unacceptable from a phenomenological point of view since it would break $\mathrm{SU}(3)_{\rm C}$ which is of course known to be unbroken in nature. Another way to see that $\langle \tilde{L} \rangle \neq 0$ is phenomenologically problematic is to note that the third generation right-handed lepton doublets $\begin{pmatrix} e^3_{\rm R} & \nu^3_{\rm R} \end{pmatrix}$ are the superpartners to Goldstone bosons from the breaking of $[\mathrm{SU}(3)]^3$. These Goldstone bosons become the longitudinal polarisation states of massive gauge bosons (with GUT scale masses), which also implies that their superpartners receive GUT-scale masses. There are therefore not enough light states to build up the all three SM lepton generations!

In Paper III we present a possible solution to this problem. There we add three new chiral superfields $\mathbf{\Delta}^a_{\rm L,R,C}$ (with scalar and fermion components $\tilde{\Delta}^a_{\rm L,R,C}$ and $\Delta^a_{\rm L,R,C}$ respectively) in adjoint representations of the SU(3) gauge groups in $\mathrm{SU}(3)^3$, i.e.

$$\mathbf{\Delta}_{\rm C} \sim (\mathbf{8}, \mathbf{1}, \mathbf{1}) \,, \quad \mathbf{\Delta}_{\rm L} \sim (\mathbf{1}, \mathbf{8}, \mathbf{1}) \,, \quad \mathbf{\Delta}_{\rm R} \sim (\mathbf{1}, \mathbf{1}, \mathbf{8}) \,, \tag{1.243}$$

that are cyclically permuted under $\mathbb{Z}_3$. Such fields are not completely unmotivated, but can be found in the **78** of E_6 [57] which is also contained in the **248** of E_8 (see Eq. (1.231)). The most general renormalisable superpotential now becomes

$$W = W_{\mathbf{27}} + W_{\mathbf{78}} \tag{1.244}$$

with

$$W_{\mathbf{78}} = \frac{1}{2} \mu_{\mathbf{78}} \mathbf{\Delta}^a_{\rm L} \mathbf{\Delta}^a_{\rm L} + \frac{1}{3!} \lambda_{\mathbf{78}} d_{abc} \mathbf{\Delta}^a_{\rm L} \mathbf{\Delta}^b_{\rm L} \mathbf{\Delta}^c_{\rm L} + (\mathbb{Z}_3 \text{ permutations}) \,, \tag{1.245}$$

where $d_{abc} = 2\mathrm{Tr}[\{T^a, T^b\} T^c]$ are the totally symmetric SU(3) coefficients. Here, the phases of $\mathbf{\Delta}_{\rm L,R,C}$ can be chosen such that $\mu_{\mathbf{78}}$ is real, leaving $\lambda_{\mathbf{78}}$ complex in general. Note that there is no renormalisable superpotential interaction term between $\mathbf{\Delta}_{\rm L,R,C}$ and the tri-triplet chiral superfields, such that they only communicate via gauge interactions (and soft SUSY breaking terms).

Left-Right parity is still respected by gauge interactions if we take the following transformation rules for the gauge adjoint chiral superfields,

$$\mathbf{\Delta}^a_{\rm L,R,C} \to \mathbf{\Delta}^{*a}_{\rm R,L,C} \,. \tag{1.246}$$

However, we only recover

$$W_{\mathbf{78}} \to W^*_{\mathbf{78}}\,, \tag{1.247}$$

in the special case where the coupling $\lambda_{\mathbf{78}}$ is real. The phase of $\lambda_{\mathbf{78}}$ therefore provides a source of explicit breaking of Left-Right parity.

The scalar potential now contains several disconnected SUSY preserving minima where each gauged SU(3) group is either unbroken or broken to SU(2) × U(1) independent of the others. In particular, there is a minimum such that

$$\langle \tilde{\Delta}^a_{\rm C} \rangle = 0\,, \quad \langle \tilde{\Delta}^a_{\rm L} \rangle = \langle \tilde{\Delta}^{\,a}_{\rm R} \rangle = \frac{v_\Delta}{\sqrt{2}} \delta^a_8\,, \tag{1.248}$$

where $v_\Delta = 2\sqrt{6}\frac{\mu_{\mathbf{78}}}{\lambda_{\mathbf{78}}}$. This leaves $\mathrm{SU}(3)_{\rm C}$ unbroken, but breaks $\mathrm{SU}(3)_{\rm L,R}$ into $\mathrm{SU}(2)_{\rm L,R} \times \mathrm{U}(1)_{\rm L,R}$ where $\mathrm{SU}(2)_{\rm L,R}$ are generated by $T^{1,\ldots,3}_{\rm L,R}$ and $\mathrm{U}(1)_{\rm L,R}$ are generated by $\frac{1}{\sqrt{3}} T^8_{\rm L,R}$. Note also that $\langle \tilde{\Delta}^a_{\rm L} \rangle = \langle \tilde{\Delta}^{*a}_{\rm R} \rangle$ only if $\lambda_{\mathbf{78}}$ is real, meaning that Left-Right parity is unbroken if it was respected by $W_{\mathbf{78}}$ in the first place.

One can now check that all fields contained in $\boldsymbol{\Delta}^a_{\rm L,R,C}$ receive GUT scale masses, i.e. of the order of v_Δ. The symmetry breaking is transmitted to the tri-triplet sector via gauge interactions, and integrating out all fields with GUT scale masses leaves behind an effective Left-Right symmetric supersymmetric effective theory based on the gauge group

$$\mathrm{SU}(3)_{\rm C} \times \mathrm{SU}(2)_{\rm L} \times \mathrm{SU}(2)_{\rm R} \times \mathrm{U}(1)_{\rm L} \times \mathrm{U}(1)_{\rm R}\,, \tag{1.249}$$

with a field content given by the branching rules of $\boldsymbol{L}$, $\boldsymbol{Q}_{\rm L}$ and $\boldsymbol{Q}_{\rm R}$.

In Paper III we also study the consequences of adding soft SUSY breaking terms to this model. As all components of $\boldsymbol{L}$, $\boldsymbol{Q}_{\rm L}$ and $\boldsymbol{Q}_{\rm R}$ are massless in the case of exact SUSY, the only mass scales in the effective theory can come from soft SUSY breaking parameters. This includes all subsequent symmetry breaking scales (in particular the energy scale for the breaking of Left-Right parity as well as the electro-weak scale). This model therefore does not exhibit a μ-problem (which was described in Sec. 4.1).

This concludes the introduction to the research papers that will now follow. Far more time could have been spent on many of the topics that have been described so far, and several topics have been completely omitted. However, this is an inevitable consequence of one my personal goals regarding this text; namely to guide the reader all the way from the basic postulates of quantum field theory up to one of the many current research frontiers in theoretical high energy physics.

References

[1] M. E. Peskin and D. V. Schroeder, *An Introduction to quantum field theory*. Addison-Wesley, Reading, USA, 1995. http://www.slac.stanford.edu/~mpeskin/QFT.html.

[2] A. Zee, *Quantum field theory in a nutshell*. Princeton University Press, 2003.

[3] M. D. Schwartz, *Quantum Field Theory and the Standard Model*. Cambridge University Press, 2014. http://www.cambridge.org/us/academic/subjects/physics/theoretical-physics-and-mathematical-physics/quantum-field-theory-and-standard-model.

[4] S. Weinberg, *The Quantum theory of fields. Vol. 1: Foundations*. Cambridge University Press, 2005.

[5] E. Wigner, "On unitary representations of the inhomogeneous lorentz group," *Annals of Mathematics* **40** no. 1, (1939) 149–204. http://www.jstor.org/stable/1968551.

[6] W. Pauli, "The connection between spin and statistics," *Phys. Rev.* **58** (Oct, 1940) 716–722. https://link.aps.org/doi/10.1103/PhysRev.58.716.

[7] J. Polchinski, "Renormalization and effective lagrangians," *Nuclear Physics B* **231** no. 2, (1984) 269 – 295. http://www.sciencedirect.com/science/article/pii/0550321384902876.

[8] T. Appelquist and J. Carazzone, "Infrared singularities and massive fields," *Phys. Rev. D* **11** (May, 1975) 2856–2861. https://link.aps.org/doi/10.1103/PhysRevD.11.2856.

[9] S. Coleman and E. Weinberg, "Radiative corrections as the origin of spontaneous symmetry breaking," *Phys. Rev. D* **7** (Mar, 1973) 1888–1910. https://link.aps.org/doi/10.1103/PhysRevD.7.1888.

[10] S. P. Martin, "Two-loop effective potential for a general renormalizable theory and softly broken supersymmetry," *Phys. Rev. D* **65** (May, 2002) 116003. https://link.aps.org/doi/10.1103/PhysRevD.65.116003.

[11] C. Burgess, "An introduction to effective field theory," *Annual Review of Nuclear and Particle Science* **57** no. 1, (2007) 329–362, hep-th/0701053. https://doi.org/10.1146/annurev.nucl.56.080805.140508.

[12] S. L. Glashow, "The renormalizability of vector meson interactions," *Nuclear Physics* **10** (1959) 107 – 117. http://www.sciencedirect.com/science/article/pii/0029558259901968.

[13] A. Salam and J. C. Ward, "Weak and electromagnetic interactions," *Il Nuovo Cimento (1955-1965)* **11** no. 4, (Feb, 1959) 568–577. https://doi.org/10.1007/BF02726525.

[14] S. Weinberg, "A model of leptons," *Phys. Rev. Lett.* **19** (Nov, 1967) 1264–1266. https://link.aps.org/doi/10.1103/PhysRevLett.19.1264.

[15] H. Fritzsch, M. Gell-Mann, and H. Leutwyler, "Advantages of the color octet gluon picture," *Physics Letters B* **47** no. 4, (1973) 365 – 368. http://www.sciencedirect.com/science/article/pii/0370269373906254.

[16] D. J. Gross and F. Wilczek, "Ultraviolet behavior of non-abelian gauge theories," *Phys. Rev. Lett.* **30** (Jun, 1973) 1343–1346. https://link.aps.org/doi/10.1103/PhysRevLett.30.1343.

[17] H. D. Politzer, "Reliable perturbative results for strong interactions?," *Phys. Rev. Lett.* **30** (Jun, 1973) 1346–1349. https://link.aps.org/doi/10.1103/PhysRevLett.30.1346.

[18] **Particle Data Group** Collaboration, C. Patrignani *et al.*, "Review of Particle Physics," *Chin. Phys.* **C40** no. 10, (2016) 100001.

[19] P. W. Anderson, "Plasmons, gauge invariance, and mass," *Phys. Rev.* **130** (Apr, 1963) 439–442. https://link.aps.org/doi/10.1103/PhysRev.130.439.

[20] F. Englert and R. Brout, "Broken symmetry and the mass of gauge vector mesons," *Phys. Rev. Lett.* **13** (Aug, 1964) 321–323. https://link.aps.org/doi/10.1103/PhysRevLett.13.321.

[21] P. W. Higgs, "Broken symmetries and the masses of gauge bosons," *Phys. Rev. Lett.* **13** (Oct, 1964) 508–509. https://link.aps.org/doi/10.1103/PhysRevLett.13.508.

[22] G. S. Guralnik, C. R. Hagen, and T. W. B. Kibble, "Global conservation laws and massless particles," *Phys. Rev. Lett.* **13** (Nov, 1964) 585–587. https://link.aps.org/doi/10.1103/PhysRevLett.13.585.

[23] J. Goldstone, A. Salam, and S. Weinberg, "Broken symmetries," *Phys. Rev.* **127** (Aug, 1962) 965–970. https://link.aps.org/doi/10.1103/PhysRev.127.965.

[24] Y. Nambu, "Axial vector current conservation in weak interactions," *Phys. Rev. Lett.* **4** (Apr, 1960) 380–382. https://link.aps.org/doi/10.1103/PhysRevLett.4.380.

[25] J. Goldstone, "Field theories with « superconductor » solutions," *Il Nuovo Cimento (1955-1965)* **19** no. 1, (Jan, 1961) 154–164. https://doi.org/10.1007/BF02812722.

[26] **ATLAS** Collaboration, G. Aad *et al.*, "Observation of a new particle in the search for the Standard Model Higgs boson with the ATLAS detector at the LHC," *Phys.Lett.* **B716** (2012) 1–29, arXiv:1207.7214 [hep-ex].

[27] **CMS** Collaboration, S. Chatrchyan *et al.*, "Observation of a new boson at a mass of 125 GeV with the CMS experiment at the LHC," *Phys. Lett.* **B716** (2012) 30–61, arXiv:1207.7235 [hep-ex].

[28] N. Cabibbo, "Unitary symmetry and leptonic decays," *Phys. Rev. Lett.* **10** (Jun, 1963) 531–533. https://link.aps.org/doi/10.1103/PhysRevLett.10.531.

[29] M. Kobayashi and T. Maskawa, "CP-violation in the renormalizable theory of weak interaction," *Progress of Theoretical Physics* **49** no. 2, (1973) 652–657. http://dx.doi.org/10.1143/PTP.49.652.

[30] S. Weinberg, "Baryon- and lepton-nonconserving processes," *Phys. Rev. Lett.* **43** (Nov, 1979) 1566–1570. https://link.aps.org/doi/10.1103/PhysRevLett.43.1566.

[31] B. Pontecorvo, "Inverse beta processes and nonconservation of lepton charge," *Sov. Phys. JETP* **7** (1958) 172–173. [Zh. Eksp. Teor. Fiz.34,247(1957)].

[32] Z. Maki, M. Nakagawa, and S. Sakata, "Remarks on the Unified Model of Elementary Particles," *Progress of Theoretical Physics* **28** (Nov., 1962) 870–880.

[33] G. Hooft, *Naturalness, Chiral Symmetry, and Spontaneous Chiral Symmetry Breaking*, pp. 135–157. Springer US, Boston, MA, 1980. https://doi.org/10.1007/978-1-4684-7571-5_9.

[34] G. Branco, P. Ferreira, L. Lavoura, M. Rebelo, M. Sher, and J. P. Silva, "Theory and phenomenology of two-higgs-doublet models," *Physics Reports* **516** no. 1, (2012) 1 – 102. http://www.sciencedirect.com/science/article/pii/S0370157312000695.

[35] V. Keus, S. F. King, and S. Moretti, "Three-higgs-doublet models: symmetries, potentials and higgs boson masses," *Journal of High Energy Physics* **2014** no. 1, (Jan, 2014) 52. https://doi.org/10.1007/JHEP01(2014)052.

[36] I. P. Ivanov, V. Keus, and E. Vdovin, "Abelian symmetries in multi-higgs-doublet models," *Journal of Physics A: Mathematical and Theoretical* **45** no. 21, (2012) 215201. http://stacks.iop.org/1751-8121/45/i=21/a=215201.

[37] C. C. Nishi, "Physical parameters and basis transformations in the two-higgs-doublet model," *Phys. Rev. D* **77** (Mar, 2008) 055009. https://link.aps.org/doi/10.1103/PhysRevD.77.055009.

[38] M. Maniatis, A. von Manteuffel, and O. Nachtmann, "CP violation in the general two-higgs-doublet model: a geometric view," *The European Physical Journal C* **57** no. 4, (Oct, 2008) 719–738. https://doi.org/10.1140/epjc/s10052-008-0712-5.

[39] S. Davidson and H. E. Haber, "Erratum: Basis-independent methods for the two-higgs-doublet model [phys. rev. d 72, 035004 (2005)]," *Phys. Rev. D* **72** (Nov, 2005) 099902. https://link.aps.org/doi/10.1103/PhysRevD.72.099902.

[40] I. P. Ivanov, "Minkowski space structure of the higgs potential in the two-higgs-doublet model. ii. minima, symmetries, and topology," *Phys. Rev. D* **77** (Jan, 2008) 015017. https://link.aps.org/doi/10.1103/PhysRevD.77.015017.

[41] J. Polchinski, "Memories of a Theoretical Physicist," arXiv:1708.09093 [physics.hist-ph].

[42] S. P. Martin, "A Supersymmetry primer," arXiv:hep-ph/9709356 [hep-ph]. [Adv. Ser. Direct. High Energy Phys.18,1(1998)].

[43] Z. Komargodski and N. Seiberg, "From linear susy to constrained superfields," *Journal of High Energy Physics* **2009** no. 09, (2009) 066. http://stacks.iop.org/1126-6708/2009/i=09/a=066.

[44] M. Grisaru, W. Siegel, and M. Roček, "Improved methods for supergraphs," *Nuclear Physics B* **159** no. 3, (1979) 429 – 450. http://www.sciencedirect.com/science/article/pii/0550321379903444.

[45] N. Seiberg, "Naturalness versus supersymmetric non-renormalization theorems," *Physics Letters B* **318** no. 3, (1993) 469 – 475. http://www.sciencedirect.com/science/article/pii/037026939391541T.

[46] H. Georgi and S. L. Glashow, "Unity of all elementary-particle forces," *Phys. Rev. Lett.* **32** (Feb, 1974) 438–441. https://link.aps.org/doi/10.1103/PhysRevLett.32.438.

[47] P. Nath and P. F. Pérez, "Proton stability in grand unified theories, in strings and in branes," *Physics Reports* **441** no. 5, (2007) 191 – 317. http://www.sciencedirect.com/science/article/pii/S0370157307000683.

[48] A. De Rújula, H. Georgi, and S. L. Glashow *, in Fifth Workshop on Grand Unification edited by K. Kang, H. Fried, and F. Frampton* (1984) .

[49] J. Sayre, S. Wiesenfeldt, and S. Willenbrock, "Minimal trinification," *Phys. Rev. D* **73** (Feb, 2006) 035013. https://link.aps.org/doi/10.1103/PhysRevD.73.035013.

[50] J. C. Pati and A. Salam, "Lepton number as the fourth "color"," *Phys. Rev. D* **10** (Jul, 1974) 275–289. https://link.aps.org/doi/10.1103/PhysRevD.10.275.

[51] R. N. Mohapatra and J. C. Pati, ""natural" left-right symmetry," *Phys. Rev. D* **11** (May, 1975) 2558–2561. https://link.aps.org/doi/10.1103/PhysRevD.11.2558.

[52] R. N. Mohapatra and J. C. Pati, "Left-right gauge symmetry and an "isoconjugate" model of CP violation," *Phys. Rev. D* **11** (Feb, 1975) 566–571. https://link.aps.org/doi/10.1103/PhysRevD.11.566.

[53] G. Senjanovic and R. N. Mohapatra, "Exact left-right symmetry and spontaneous violation of parity," *Phys. Rev. D* **12** (Sep, 1975) 1502–1505. https://link.aps.org/doi/10.1103/PhysRevD.12.1502.

[54] G. Senjanović, "Spontaneous breakdown of parity in a class of gauge theories," *Nuclear Physics B* **153** (1979) 334 – 364. http://www.sciencedirect.com/science/article/pii/0550321379906047.

[55] J. Hetzel, *Phenomenology of a left-right-symmetric model inspired by the trinification model*. PhD thesis, Inst. Appl. Math., Heidelberg, 2015. arXiv:1504.06739 [hep-ph]. https://inspirehep.net/record/1364898/files/arXiv:1504.06739.pdf.

[56] J. Hetzel and B. Stech, "Low-energy phenomenology of trinification: An effective left-right-symmetric model," *Phys. Rev. D* **91** (Mar, 2015) 055026. https://link.aps.org/doi/10.1103/PhysRevD.91.055026.

[57] R. Slansky, "Group theory for unified model building," *Physics Reports* **79** no. 1, (1981) 1 – 128. http://www.sciencedirect.com/science/article/pii/0370157381900922.

[58] P. Candelas, G. T. Horowitz, A. Strominger, and E. Witten, "Vacuum configurations for superstrings," *Nuclear Physics B* **258** (1985) 46 – 74. http://www.sciencedirect.com/science/article/pii/0550321385906029.

[59] E. Witten, "Symmetry breaking patterns in superstring models," *Nuclear Physics B* **258** (1985) 75 – 100. http://www.sciencedirect.com/science/article/pii/0550321385906030.

5 Publications and contributions

Paper I

José Eliel Camargo-Molina, António P. Morais, Roman Pasechnik, Marco O. P. Sampaio, Jonas Wessén: *All one-loop scalar vertices in the effective potential approach*, e-print: arXiv:1606.07069 [hep-ph]. *JHEP* 1608 (2016) 073

The idea of this paper was conceived mainly by Marco Sampaio (post-doc at Aveiro University in Portugal), who also derived the main results of the paper. My contribution was to cross-check these results in several toy models that were simple enough such that the derivatives of the one-loop effective potential could be taken explicitly. In particular, I realized that the contribution from the fermion loops had to be treated slightly differently since their mass-squared matrices are in general not symmetric. In terms of the writing of the manuscript, I contributed to over-all adjustments before the final version of the paper.

Paper II

J. E. Camargo-Molina, A. Morais, R. Pasechnik, J. Wessén: *On a radiative origin of the Standard Model from trinification*, e-print: arXiv:1606.03492 [hep-ph]. *JHEP* 2016 (2016) 129

This is the first paper exploring the possibility of imposing a $\mathrm{SU}(3)_{\mathrm{F}}$ family symmetry in the well known trinification model (an idea conceived by my supervisor Roman Pasechnik). I took the initiative to first implement this idea in a non-supersymmetric model, and both performed the calculations and drafted the text in sections 2–5, with the exception of section 3.5. These calculations were then cross-checked by Eliel Camargo Molina (post-doc in Lund), who also significantly improved the text as well as conceived the idea of studying the radiative breaking to the electro-weak gauge group. In section 6 (also written mainly by Eliel and me), the β-functions in the effective theory were computed by Eliel, while I implemented the simulated annealing algorithm that we used for the parameter space scans. I wrote the text and also performed the calculations of sections 7.1 and 7.3, while section 7.4 was written by Roman. Section 7.2, and also section 1 (Introduction) and section 8 (Conclusions) were collaboratively written by all authors.

Paper III

J. E. Camargo-Molina, A. Morais, A. Ordell, R. Pasechnik, M. Sampaio, J. Wessén: *Reviving trinification models through an* E_6*-extended supersymmetric GUT*, e-print: arXiv:1610.03642 [hep-ph]. Phys.Rev. D**95** (2017), 7, 075031

I made critical contributions at all stages in the construction of the model considered in this article. In particular, I realized that the model exhibits a parity symmetry. Together with the other authors, I also found the symmetry breaking chain including the global symmetries originating from $\mathrm{SU}(3)_{\mathrm{F}}$, computed the U(1) charges and the tree-level mass spectra in the models with and without the adjoint chiral superfields. I also played a major role in establishing why the model with only tri-triplet representations needs to be extended to be phenomenologically viable. I contributed to the writing of all sections in the paper.

Paper IV

J. E. Camargo-Molina, T. Mandal, R. Pasechnik, J. Wessén: *Heavy charged scalars from $c\bar{s}$ fusion: A generic search strategy applied to a 3HDM with* $\mathrm{U}(1) \times \mathrm{U}(1)$ *family symmetry*, e-print: arXiv:1711.03551 [hep-ph]. *JHEP* 2018 (2018) 024.

This paper is built on the realization by Tanumoy Mandal (Uppsala University and University of Delhi) that the $c\bar{s}$ fusion channel can be a powerful discovery channel for charged Higgs bosons. The idea of attempting to explain the flavour structure of the observed fermions by using a $\mathrm{U}(1) \times \mathrm{U}(1)$ family symmetry in a 3 Higgs Doublet Model was conceived by Eliel. Together with him, I found the concrete realization of this (i.e. that follows from the U(1) charges in table 1 in the paper), which also naturally leads to a sizeable $H^+\bar{c}s$ coupling. I did all the calculations in section 2, and wrote most of the text in that section. Sections 3 and 4 were mainly written by Tanumoy who also did the analysis described in these sections. Eliel and I wrote the text in section 5, and there we together wrote the code for the genetic algorithm that we used to scan the parameter space. In particular, I wrote the code that tested a given parameter point against experimental limits from electro-weak precision tests. All authors contributed to the writing of section 1 (Introduction) and section 6 (Summary and conclusions).

6 Further published work

During my Ph.D. I have also published the following works which are not included in the thesis, but listed here for the sake of completeness.

Paper V

Anders Irbäck, Jonas Wessén: *Thermodynamics of amyloid formation and the role of intersheet interactions*, e-print: arXiv:1601.00478 [physics.bio-ph], J. Chem. Phys. **143**, 105104 (2015).

This paper is based on the work I did as master student together with Prof. Anders Irbäck within the Computational Biology and Biological Physics group at the Depart-

ment of Astronomy and Theoretical Physics at Lund U., and was finalised during my first semester as a Ph.D. student. Anders and I wrote separate codes to be able to cross check the results of the simulations. I made the figures 1–3,5,7,8 and 10, and mainly wrote section II.C.

Paper VI

J. E. Camargo-Molina, A. Morais, R. Pasechnik, J. Wessén: *On a radiative origin of the Standard Model in non-supersymmetric trinification with global* $\mathrm{SU}(3)_{\mathrm{F}}$, PoS **LHCP2016** (2016).

I wrote this conference proceedings which outlines the results of Paper II.

Paper VII

J. E. Camargo-Molina, A. Morais, R. Pasechnik, J. Wessén: *Charged scalars from* $\mathrm{SU}(3)^3$ *theories*, e-print: arXiv:1701.02757 [hep-ph], PoS **CHARGED2016** (2017)

This conference proceedings deals with phenomenological aspects of $\mathrm{U}(1) \times \mathrm{U}(1)$ symmetric 3 Higgs Doublet Models when the U(1) charges are assigned as if the $\mathrm{U}(1) \times \mathrm{U}(1)$ symmetry is a remnant symmetry from $\mathrm{SU}(3)_{\mathrm{F}}$ in trinification. I did the calculations and most of the writing in sections 2 and 3.

7 Acknowledgements

First of all, I would like to thank the all the people in the Theoretical High Energy Physics group in Lund for the friendly and inspiring atmosphere you have provided these past few years. I have thoroughly enjoyed my time as a Ph.D. student in your group. I would in particular like to extend my gratitude for the collaboration with the master students Eric Corregan, Astrid Ordell (who later also joined our group as a Ph.D. student), Laurie Walk and Erik Gustafsson, from which I have learned a lot. The passing of Erik Gustafsson was a true tragedy, and I am confident that you Erik would have had a successful career as a theoretical physicist both due to your talent and pleasant personality, which in turn I am sure can be attributed to your wonderful family.

This thesis, and especially its introduction, has benefited greatly from thorough and accurate comments by Hans Bijnens, Roman Pasechnik, Astrid Ordell, Leif Gellersen and Eliel Camargo Molina. Thank you all very much!

It has been a pleasure to collaborate and interact with the talented researchers at the department. Thank you Roman for your guidance, as well as allowing me so freely to work on the problems I found most interesting (especially the crazy ones). Thank you Hans, and also Karol Kampf, for inviting me to work on the $\eta \to \gamma\gamma$ decay with you, from which I have learnt plenty. It is a pity that we didn't have time to finish the calculation before the due date of this thesis, but I will give it a final go in the upcoming months. (I am not fully confident that you actually need my help on this one, but I have nevertheless enjoyed the work!) Thank you Johan Rathsman for sharing your expertise in the phenomenology of extended Higgs sectors. And thank you Anders Irbäck for both introducing me to cool problems in protein physics and for your very inspiring style of doing research.

I was very lucky to start my initial research projects in such active collaborations with the post-docs António Morais and Eliel Camargo Molina. The close collaboration that would follow with you Eliel has been the best part of my Ph.D. and I really hope that we will continue to work together in one way or another.

Finally, I would like to extend my warmest thanks to my family and my girlfriend Märta for your continuous belief in my ability to go through with this (also, thank you Märta for the great suggestions for the popular science summary in the beginning of the thesis!).

And even more finally so, I would like to wish all the current Ph.D. students in the group, i.e. Christine, Joel, Leif, Astrid, Harsh, Johan, Marius, Smita and Nils, good luck with your theses!

I

All one-loop scalar vertices in the effective potential approach

José Eliel Camargo-Molina[1], António P. Morais[1,2], Roman Pasechnik[1], Marco O. P. Sampaio[2] and Jonas Wessén [1].

JHEP, 1608 (2016) 073
doi:10.1007/JHEP08(2016)073
e-Print: arXiv:1606.07069 [hep-ph]

[1] Department of Astronomy and Theoretical Physics, Lund University,
SE 223-62 Lund, Sweden.
[2] Departamento de Física da Universidade de Aveiro and CIDMA
Campus de Santiago, 3810-183 Aveiro, Portugal.

Abstract: Using the one-loop Coleman-Weinberg effective potential, we derive a general analytic expression for all the derivatives of the effective potential with respect to any number of classical scalar fields. The result is valid for a renormalisable theory in four dimensions with any number of scalars, fermions or gauge bosons. This result corresponds to the zero-external momentum contribution to a general one-loop diagram with N scalar external legs. We illustrate the use of the general result in two simple scalar singlet extensions of the Standard Model, to obtain the dominant contributions to the triple couplings of light scalar particles under the zero external momentum approximation.

1 Introduction

The Large Hadron Collider (LHC) ATLAS [1] and CMS [2] experiments, have achieved in recent years a landmark in the history of particle physics: the direct confirmation of the first known fundamental scalar in Nature. Scalar fields are frequently used in the modelling of new physics beyond the Standard Model (SM) of particle physics and in cosmology. Interesting examples are models with scalar dark matter candidates [3, 4, 5,

6, 7, 8, 9, 10, 11, 12, 13, 14, 15, 16, 17, 18], models of scalar field inflation [19, 20, 21], or even in attempts to explain the finer structure of the SM parameters through scalar flavour models[1]. Furthermore they are very often predicted as part of many Beyond the Standard Model (BSM) scenarios such as supersymmetric theories [23], models with extra dimensions [24, 25], little Higgs models [26] and grand unified theories [27, 28, 29], among many others. Searches for scalar particle states are therefore of great interest and one of the focuses of the ongoing LHC searches.

Whether the current 13 TeV run of the LHC provides us a new scalar state, such as the hypothetical state recently hinted for with a 750 GeV mass [30, 31], or whether it provides measurements of the SM Higgs self couplings, the low energy observables of these lighter scalars may receive contributions from new heavy states through radiative corrections. If the typical scale of the external momentum of the light particles involved in such observables is small compared to the masses of the hypothetical heavy particles inside the diagrams, then their contributions can be computed in the zero-external momentum approximation [32]. In that approximation, for the particular case of purely scalar operators with no derivative terms, such "heavy" contributions to the corresponding loop corrected vertices can be extracted solely from derivatives of the scalar effective potential.

The computation of the scalar effective potential for a generic Quantum Field Theory (QFT), is often performed in dimensional regularisation and mass independent renormalisation schemes such as the $\overline{\text{MS}}$ or $\overline{\text{DR}}$ schemes for simplicity. This has been reviewed at two-loop order in such schemes and in the Landau gauge in [33]. In this paper we start from the one-loop Coleman-Weinberg (CW) effective potential [34] for a generic QFT and extend the analysis to find a general analytic expression for all its derivatives (corresponding to an arbitrary number of external legs). This is done by simplifying the derivatives of the matrix-log of the field dependent mass squared matrix. It reduces to a combinatoric problem involving the tree level vertices of the theory in the tree level mass eigenbasis, and a set of totally symmetric tensors that are functions only of the physical masses of the eigenstates. Our central result consists of explicit expressions for the derivatives of the one-loop effective potential with an arbitrary number of derivatives. These expressions can be easily implemented and evaluated for any theory, either as analytic expressions or numerically (reducing to common linear algebra operations).

Though our results focus on the derivatives of the effective potential, recently there have been advances in obtaining the functional derivatives of the one-loop effective action after integrating out heavy degrees of freedom using a covariant derivative expansion [35, 36, 37, 38]. In such approach all the operators can be obtained in addition to the translation invariant operators captured by the one-loop effective potential. Nevertheless, the results have to be computed at a fixed order in the derivative expansion while our general result for the effective potential contribution is valid for an arbitrary number of scalar field derivatives.

Finally, we also apply our results in two simple scalar singlet extensions of the SM that are still phenomenologically viable. We use our results to illustrate the importance of

[1]For a review in the context of neutrino physics see for example [22].

the Next to Leading Order (NLO) radiative corrections due to a new heavy scalar, to the triple vertices in the real (RxSM) and the complex (CxSM) singlet extensions of the SM recently analysed in [39].

The structure of the paper is the following. In Sect. 2 we set conventions for a general QFT and define the various fields and respective couplings. In Sect. 3 we derive our main result by applying derivatives to the CW effective potential, where many of the technical steps are described in detail in appendix I.A. We also explicitly verify the symmetry properties of the result under the interchange of scalar indices in the remaining sub-sections for cases with up to four derivatives. In Sect. 4 we provide examples of applications and in Sect. 5 we summarise our conclusions.

2 Notations and definitions

In this article we follow the general approach of [33], and write the most general Gauged QFT Lagrangian with fields of spin up to 1. Before choosing the vacuum of the theory, i.e. before symmetry breaking, we use the following notations for the various fields[2]:

- *Scalars*: All scalar multiplets are decomposed as N_0 real scalar fields, Φ_i with $i = 1, \ldots, N_0$.
- *Fermions*: All fermion multiplets are decomposed as $N_{1/2}$ Weyl 2-spinors, Ψ_I with $I = 1, \ldots, N_{1/2}$.
- *Gauge bosons* are represented by a 4-vector with a gauge group index running over N_1 bosons in the adjoint representation of the gauge group, i.e. $\mathcal{A}^\mu_a$.

The most general renormalisable interaction Lagrangian involving the scalar sector[3] is then written as:

$$\begin{aligned} -\mathcal{L}_S &= L^i\Phi_i + \frac{1}{2!}L^{ij}\Phi_i\Phi_j + \frac{1}{3!}L^{ijk}\Phi_i\Phi_j\Phi_k + \frac{1}{4!}L^{ijkl}\Phi_i\Phi_j\Phi_k\Phi_l \,, \\ -\mathcal{L}_F &= \frac{1}{2}Y^{IJ}\Psi_I\Psi_J + \frac{1}{2}Y^{IJk}\Psi_I\Psi_J\Phi_k + \text{c.c.} \,, \\ -\mathcal{L}_{SG} &= \frac{1}{4}G^{abij}\mathcal{A}_{a\mu}\mathcal{A}^\mu_b\Phi_i\Phi_j + G^{aij}\mathcal{A}_{a\mu}\Phi_i\partial^\mu\Phi_j \,. \end{aligned} \tag{I.1}$$

We adopt the Einstein convention where repeated indices that are one up (superscript) and one down (subscript) are summed over. We also adopt the convention that repeated indices that are all down or all up are not summed over. This will become useful to define tensor components in the mass eigenstate basis. The scalar couplings in the gauge eigen-basis are denoted by $\left\{L^i, L^{ij}, L^{ijk}, L^{ijkl}\right\}$ respectively for the linear, quadratic,

[2]The kinetic terms of the various fields are canonically normalised

[3]We suppress the interaction terms without scalar fields because we will focus on the one-loop effective potential.

cubic and quartic couplings and they are totally symmetric in the scalar indices i, j, k, l. In this decomposition, they are all real.[4] The fermion quadratic and Yukawa terms are denoted by the complex numbers Y^{IJ} and Y^{IJk}, which are symmetric under interchange of fermionic indices. The gauge-scalar couplings are denoted by G^{abij} and G^{aij} (see also [33] for details).

After symmetry breaking, the scalar fields are shifted around a classical field configuration. We denote a generic classical field configuration, around which the perturbative calculations are set, by v_i and shift the fields as follows: $\Phi_i(x) = v_i + \phi_i(x)$ (now ϕ_i are the quantum scalar field fluctuations around the classical configuration v_i). Then we obtain the following Lagrangian in a basis that we define to be the Λ-basis[5]

$$\begin{aligned}
-\mathcal{L}_S &= \Lambda + \Lambda^i_{(S)}\phi_i + \frac{1}{2}\Lambda^{ij}_{(S)}\phi_i\phi_j + \frac{1}{3!}\Lambda^{ijk}_{(S)}\phi_i\phi_j\phi_k + \frac{1}{4!}\Lambda^{ijkl}_{(S)}\phi_i\phi_j\phi_k\phi_l \ , \\
-\mathcal{L}_F &= \frac{1}{2}M^{IJ}\Psi_I\Psi_J + \frac{1}{2}Y^{IJk}\Psi_I\Psi_J\phi_k + \text{c.c.} \ , \\
-\mathcal{L}_{SG} &= \frac{1}{2}\Lambda^{ab}_{(G)}\mathcal{A}_{a\mu}\mathcal{A}^\mu_b + \frac{1}{2}\Lambda^{abi}_{(G)}\mathcal{A}_{a\mu}\mathcal{A}^\mu_b\phi_i + \frac{1}{4}\Lambda^{abij}_{(G)}\mathcal{A}_{a\mu}\mathcal{A}^\mu_b\phi_i\phi_j + G^{aij}\mathcal{A}_{a\mu}\phi_i\partial^\mu\phi_j \ ,
\end{aligned} \tag{I.2}$$

where

$$\begin{aligned}
\Lambda &\equiv L^i v_i + \frac{1}{2!}L^{ij}v_iv_j + \frac{1}{3!}L^{ijk}v_iv_jv_k + \frac{1}{4!}L^{ijkl}v_iv_jv_kv_l = V^{(0)}(v_i) \ , \\
\Lambda^i_{(S)} &\equiv L^i + L^{ij}v_j + \frac{1}{2}L^{ijk}v_jv_k + \frac{1}{6}L^{ijkl}v_jv_kv_l \ , \\
\Lambda^{ij}_{(S)} &\equiv L^{ij} + L^{ijk}v_k + \frac{1}{2}L^{ijkl}v_kv_l \ , \\
\Lambda^{ijk}_{(S)} &\equiv L^{ijk} + L^{ijkl}v_l \ , \\
\Lambda^{ijkl}_{(S)} &\equiv L^{ijkl} \ ,
\end{aligned} \tag{I.3}$$

and

$$\begin{aligned}
\Lambda^{ab}_{(G)} &\equiv \frac{1}{2}G^{abij}v_iv_j \ , \\
\Lambda^{abi}_{(G)} &\equiv G^{abij}v_j \ , \\
\Lambda^{abij}_{(G)} &\equiv G^{abij} \ .
\end{aligned} \tag{I.4}$$

We have defined in Eqs. (I.3) and (I.4) the scalar mass-squared matrix, $\Lambda^{ij}_{(S)}$, the gauge boson mass-squared matrix $\Lambda^{ab}_{(G)}$ and the tree level effective potential $V^{(0)}(v_i)$. The fermion mass-squared matrix is obtained from

$$\Lambda^{IJ}_{(F)} \equiv M^{*IL}M_L{}^J = Y^{*IL}Y_L{}^J + \left(Y^{JL}Y^*_L{}^{Ik} + Y^{*IL}Y_L{}^{Jk}\right)v_k + Y^{*ILk}Y_L{}^{Jm}v_kv_m \ , \tag{I.5}$$

[4] We follow the notation in [40] where basis invariant expressions for the two-loop beta functions of the scalar couplings were derived using the two-loop effective potential.

[5] Note that the Landau gauge conditions can be used to eliminate a term $G^{aij}v_i\mathcal{A}_{a\mu}\partial^\mu\Phi_j$, up to a surface term, through an integration by parts.

where we use the fermion mass matrix defined through the shifted Lagrangian, Eq. (I.2):

$$M^{IJ} = Y^{IJ} + Y^{IJk} v_k \ . \tag{I.6}$$

Note that all (non-spacetime) Latin indices are assumed to be in Euclidean space (they are lowered and raised with the identity matrix). Another important point is that, though the fermionic tensors that appear directly in the Lagrangian are symmetric under interchange of fermionic indices, the fermion mass-squared matrix defined in Eq. (I.5) is not necessarily symmetric. In general it is, however, hermitian. Below we will define fermionic cubic and quartic effective vertices that are also hermitian with respect to the two fermionic indices.

This basis will be particularly useful to obtain expressions for the derivatives of the effective potential analytically, which are directly related to the scalar N-point functions of the theory at zero external momenta. The final results, however, will adopt a much simpler form in a third basis, which we name as the λ-basis. This is defined as the basis that diagonalises all the tree level mass-squared matrices. In the λ-basis the Lagrangian takes the form

$$\begin{aligned}
-\mathcal{L}_S &= \Lambda + \lambda^i_{(S)} R_i + \frac{1}{2} m^{2\ i}_{(S)} R_i^2 + \frac{1}{3!} \lambda^{ijk}_{(S)} R_i R_j R_k + \frac{1}{4!} \lambda^{ijkl}_{(S)} R_i R_j R_k R_l \ , \\
-\mathcal{L}_F &= \frac{1}{2} m^{IJ} \psi_I \psi_J + \frac{1}{2} y^{IJk} \psi_I \psi_J R_k + \text{c.c.} \ , \\
-\mathcal{L}_{SG} &= \frac{1}{2} m^{2\ a}_{(G)} A_{a\mu} A^\mu_a + \frac{1}{2} \lambda^{abi}_{(G)} A_{a\mu} A^\mu_b R_i + \frac{1}{4} \lambda^{abij}_{(G)} A_{a\mu} A^\mu_b R_i R_j + \lambda^{aij}_{(G)} A_{a\mu} R_i \partial^\mu R_j \ ,
\end{aligned} \tag{I.7}$$

where the rotated fields are

$$\begin{aligned}
R_i &= \left[O_{(S)}\right]^{j}_{\ i} \phi_j \\
A_{a\mu} &= \left[O_{(G)}\right]^{b}_{\ a} \mathcal{A}_{b\mu} \\
\psi_I &= \left[U^*_{(F)}\right]^{J}_{\ I} \Psi_J \ .
\end{aligned} \tag{I.8}$$

Here we must use orthogonal matrices for the bosonic rotations and unitary matrices for the fermions. If we denote, generically, such a transformation matrix for the field of type $T = \{S, G, F\}$ by $\mathcal{U}_{(T)}$ (unitary or orthogonal) then all mass-squared matrices are diagonal in this basis so the Λ-basis mass-squared matrices defined above obey

$$\mathcal{U}_{(T)} \Lambda_{(T)} \mathcal{U}^\dagger_{(T)} = \text{diag}\{m^2_{(T)a}\} \ . \tag{I.9}$$

Note that on the right hand side we have now used Latin indices from the beginning of the alphabet to denote the component of the diagonal. Whenever the type T is not specified, we follow the convention of using lower case indices from the beginning of the Latin alphabet $(a, b, c, \ldots)$ and reserve indices from the middle of the alphabet $(i, j, k, \ldots)$ for scalar field indices. Finally, note that all couplings in the λ-basis, Eq. (I.7), are now in lower case. The transformation relating them to the corresponding upper case couplings defined in Eq. (I.2) (Λ-basis) is obtained by rotating each index using the $\mathcal{U}_{(T)}$ matrix corresponding to the index type (S, F or G) as induced by the transformations in Eq. (I.8).

In the following sections it will also be useful to note that the derivatives of the various mass-squared matrices with respect to the v_i are related to the cubic and quartic couplings as follows:

$$\begin{aligned}
\partial^k \Lambda^{ij}_{(S)} &= L^{ijk} + L^{ijkl} v_l = \Lambda^{ijk}_{(S)} \ , \\
\partial^{kl} \Lambda^{ij}_{(S)} &= L^{ijkl} = \Lambda^{ijkl}_{(S)} \ , \\
\partial^k \Lambda^{IJ}_{(F)} &= \partial^k M^{*IL} M_L{}^J + M^{*IL} \partial^k M_L{}^J \ , = Y^{*ILk} M_L{}^J + M^{*IL} Y_L{}^{Jk} \equiv \Lambda^{IJk}_{(F)} \ , \\
\partial^{km} \Lambda^{IJ}_{(F)} &= Y^{*ILk} \partial^m M_L{}^J + \partial^m M^{*IL} Y_L{}^{Jk} \ , = Y^{*ILk} Y_L{}^{Jm} + Y^{*ILm} Y_L{}^{Jk} \equiv \Lambda^{IJkm}_{(F)} \ , \\
\partial^i \Lambda^{ab}_{(G)} &= G^{abij} v_j = \Lambda^{abi}_{(G)} \ , \\
\partial^{ij} \Lambda^{ab}_{(G)} &= G^{abij} = \Lambda^{abij}_{(G)} \ .
\end{aligned} \tag{I.10}$$

We use the notation $\partial_i = \frac{\partial}{\partial v_i}$, $\partial_{ij} = \frac{\partial^2}{\partial v_i \partial v_j}$ etc... for derivatives with respect to the arbitrary classical scalar field configuration v_i. If we denote generically the cubic and quartic couplings for type T (on the right hand side of each of the equations in (I.10)) by $\Lambda_{(T)abi}$ and $\Lambda_{(T)abij}$ respectively, then these relations can be written collectively as (after lowering the indices with the Euclidean metric)

$$\begin{aligned}
\partial_i \Lambda_{(T)ab} &= \Lambda_{(T)abi} \ , \\
\partial_{ij} \Lambda_{(T)ab} &= \Lambda_{(T)abij} \ .
\end{aligned} \tag{I.11}$$

3 One-loop N-point vertices at zero external momenta

In this section we present the general analytic expressions for the Nth order derivatives of the effective potential. We start from the general one-loop contribution to the effective potential in the Landau gauge that is given by [33]

$$V^{(1)} = \frac{1}{4} \sum_T (-1)^{2s_T} (1 + 2s_T) \mathrm{Tr} \left[\Lambda^2_{(T)} \left(\overline{\log} \Lambda_{(T)} - k_T \right) \right] \ . \tag{I.12}$$

Here the general loop expansion of the effective potential is defined as

$$V_{\text{eff}} \equiv \sum_n \varepsilon^n V^{(n)} \ , \tag{I.13}$$

with $\varepsilon = \hbar/(4\pi)^2$ so that $V^{(n)}$ is the n-loop effective potential. The spin of the field is denoted by s_T and we have defined $\overline{\log}(m^2) \equiv \log(m^2/\mu^2)$ with μ the renormalisation scale and k_T depends on the renormalisation scheme ($\overline{\text{MS}}$ or $\overline{\text{DR}}$) and can be specified later. The log function is defined over matrices.

We now state the general result. Further details of the proof are provided in appendix I.A. Applying the N-th order derivative operator with respect to the fields

$v_{i_1},\ldots,v_{i_N}$, in the Λ-basis, to the one-loop effective potential (with $N\geq 1$) we obtain

$$\partial_{i_1,\ldots,i_N}V^{(1)}=\partial_{i_1,\ldots,i_{N-1}}\frac{1}{4}\sum_T(-1)^{2s_T}(1+2s_T)\times \\ \times\,\mathrm{Tr}\left[\partial_{i_N}\left(\Lambda^2_{(T)}\right)\left(\overline{\log}\,\Lambda_{(T)}-k_T\right)+\Lambda^2_{(T)}\partial_{i_N}\left(\overline{\log}\,\Lambda_{(T)}\right)\right]\ . \quad \text{(I.14)}$$

In appendix I.A we prove the result that $\mathrm{Tr}\left[\Lambda^2_{(T)}\partial_i\left(\overline{\log}\,\Lambda_{(T)}\right)\right]=\frac{1}{2}\mathrm{Tr}\left[\partial_i\left(\Lambda^2_{(T)}\right)\right]$. Using this result, we can effectively lower by one the order of the derivatives acting on the $\overline{\log}$. Using this identity, the cyclic property of the trace and the fact that a function of a matrix commutes with the matrix itself we obtain

$$\partial_{i_1,\ldots,i_N}V^{(1)}=\partial_{i_1,\ldots,i_{N-1}}\sum_T\frac{(-1)^{2s_T}(1+2s_T)}{4}\mathrm{Tr}\left[\partial_{i_N}\left(\Lambda^2_{(T)}\right)\left(\overline{\log}\,\Lambda_{(T)}-k_T+\frac{1}{2}\right)\right]\ . \quad \text{(I.15)}$$

So we have reduced by one the order of the derivative that will act on the matrix-$\overline{\log}$[6]. Acting with the remaining $N-1$ derivatives we obtain an expression in the form

$$\partial_{i_1,\ldots,i_N}V^{(1)}=\frac{1}{4}\sum_T(-1)^{2s_T}(1+2s_T)\times \\ \mathrm{S}_{\{i_1\ldots i_{N-1}\}}\left[\mathrm{Tr}\sum_{p=0}^{\min\{N-1,3\}}\binom{N-1}{p}\partial^{(p+1)}_{i_1,\ldots,i_p,i_N}\left(\Lambda^2_{(T)}\right)\partial_{i_{p+1},\ldots,i_{N-1}}\left(\overline{\log}\,\Lambda_{(T)}-k_T+\tfrac{1}{2}\right)\right]\ , \quad \text{(I.16)}$$

where the innermost sum is over all possible partitions of the $\{i_1,\ldots,i_{N-1}\}$ indices in two lists and we define here the operator $\mathrm{S}_{\{i_1\ldots i_{N-1}\}}$, which denotes symmetrisation with respect to the $(N-1)$-indices in the list. Observe that in the range of the sum over p we have used the fact that the mass-squared matrix only has non-zero derivatives up to order two. The term in the product that contains derivatives acting on the square of the mass-squared matrix is simple to obtain (since it is polynomial). For notational simplicity we present the result making use of the following set of tensors

$$\sigma^{(p)}_{(T)abi_1\ldots i_p}\equiv\mathcal{U}_{(T)a}{}^{c}\,\mathcal{U}^{\dagger}_{(T)}{}^{d}{}_{b}O_{(S)}{}^{j_1}{}_{i_1}\ldots O_{(S)}{}^{j_p}{}_{i_p}\left[\partial_{j_1\ldots j_p}\left(\Lambda^2_{(T)}\right)_{cd}\right]\ . \quad \text{(I.17)}$$

The components for the non-zero cases are

$$\begin{cases}\sigma^{(1)}_{(T)abi}=m^2_{(T)a}\lambda_{(T)abi}+\lambda_{(T)abi}m^2_{(T)b}\ ,\\ \sigma^{(2)}_{(T)abij}=m^2_{(T)a}\lambda_{(T)abij}+\lambda_{(T)abij}m^2_{(T)b}+\lambda_{(T)aci}\lambda_{(T)}{}^{c}{}_{bj}+\lambda_{(T)acj}\lambda_{(T)}{}^{c}{}_{bi}\ ,\\ \sigma^{(3)}_{(T)abijk}=\lambda_{(T)acij}\lambda^c_{(T)bk}+\lambda_{(T)bcij}\lambda^c_{(T)ak}+(j\leftrightarrow k)+(i\leftrightarrow k)\ ,\\ \sigma^{(4)}_{(T)abijkl}=\lambda_{(T)acij}\lambda^c_{(T)bkl}+\lambda_{(T)bcij}\lambda^c_{(T)akl}+(j\leftrightarrow k)+(i\leftrightarrow k)\ .\end{cases} \quad \text{(I.18)}$$

[6]Note however that the matrix multiplying the $\overline{\log}$ now contains derivatives, so it no longer commutes with $\Lambda_{(T)}$ and this process cannot be continued.

Here the cubic and quartic couplings for field of type T in the λ-basis are generically denoted by $\lambda_{(T)abi}$ and $\lambda_{(T)abij}$. They are obtained from the corresponding $\Lambda_{(T)abi}$ and $\Lambda_{(T)abij}$ couplings using the $\mathcal{U}_{(T)}$ transformation matrices. For the second term in the product, Eq. (I.16), we define the following tensor:

$$\delta^{(N)}_{(T)abi_1\ldots i_N} \equiv \mathcal{U}_{(T)a}{}^{c}\mathcal{U}^{\dagger}_{(T)}{}_{b}^{d} O_{(S)}{}^{j_1}{}_{i_1}\ldots O_{(S)}{}^{j_N}{}_{i_N}\left[\partial_{j_1\ldots j_N}\left(\overline{\log}\,\Lambda_{(T)} - k_T + \frac{1}{2}\right)_{cd}\right] , \tag{I.19}$$

which, for $N > 0$, is a rotated version of the derivatives of the matrix-$\overline{\log}$. In appendix I.A we derive a general algebraic analytic expressions for the $\delta^{(N)}_{abi_1\ldots i_N}$ tensors. The general expression, Eq. (I.51), contains another set of useful tensors whose components are

$$f^{(k)}_{(T)a_1\ldots a_N} \equiv \sum_{x=1}^{N} \frac{m^{2k}_{(T)a_x}\,\overline{\log}\, m^2_{(T)a_x}}{\prod_{y\neq x}\left(m^2_{(T)a_x} - m^2_{(T)a_y}\right)} . \tag{I.20}$$

More explicitly, the first few cases that contribute to the 2, 3 and 4-point functions are (using Eqs. (I.43), (I.48) and (I.51)),

$$\begin{aligned}
\delta^{(0)}_{(T)ab} &= \delta_{ab}\left(\overline{\log}\, m^2_{(T)a} - k_T + \tfrac{1}{2}\right), \\
\delta^{(1)}_{(T)abi} &= f^{(0)}_{(T)ab}\lambda_{(T)abi}, \\
\delta^{(2)}_{(T)abij} &= f^{(0)}_{(T)abc}\left(\lambda_{(T)a}{}^{c}{}_{i}\lambda_{(T)}{}^{c}{}_{bj} + \lambda_{(T)a}{}^{c}{}_{j}\lambda_{(T)}{}^{c}{}_{bi}\right) + f^{(0)}_{(T)ab}\lambda_{(T)abij} \ , \\
\delta^{(3)}_{(T)abijk} &= 3\mathrm{S}_{\{ijk\}}\Big[2\, f^{(0)}_{(T)acdb}\lambda_{(T)a}{}^{c}{}_{i}\lambda_{(T)}{}^{cd}{}_{j}\lambda_{(T)}{}^{d}{}_{bk} + \\
&\qquad + f^{(0)}_{(T)acb}\left(\lambda_{(T)a}{}^{c}{}_{ij}\lambda_{(T)}{}^{c}{}_{bk} + \lambda_{(T)a}{}^{c}{}_{i}\lambda_{(T)}{}^{c}{}_{bjk}\right)\Big] .
\end{aligned} \tag{I.21}$$

We emphasise here that the repeated indices are summed over only once and that all repeated indices are all inside the same (suppressed) sum symbol according to the Einstein convention – the fact that several repeated indices appear simultaneously up and down is a peculiarity of the mass eigenbasis (or diagonal basis).

We finally present the general result for the derivatives of the one-loop effective potential. This is fully determined using the $\delta^{(N)}_{(T)ab,i_1\ldots i_N}$ and $\sigma^{(N)}_{(T)ab,i_1\ldots i_N}$ tensors and we obtain

$$\begin{aligned}
\partial_{i_1,\ldots,i_N} V_{\text{eff}} = \Lambda^{(N\leq 4)}_{i_1,\ldots,i_N} + \varepsilon O_{(S)}{}^{j_1}{}_{i_1}\ldots O_{(S)}{}^{j_{N-1}}{}_{i_{N-1}} O_{(S)}{}^{j_N}{}_{i_N}\sum_{T}(-1)^{2s_T}\frac{(1+2s_T)}{4}\times \\
\times \mathrm{S}_{\{j_1\ldots j_{N-1}\}}\left[\sum_{p=0}^{\min\{N-1,3\}}\binom{N-1}{p}\sigma^{(p+1)ab}_{(T)}{}_{j_1,\ldots,j_p,j_N}\delta^{(N-1-p)}_{(T)baj_{p+1},\ldots,j_{N-1}}\right] + \mathcal{O}(\varepsilon^2) .
\end{aligned} \tag{I.22}$$

In the first term of Eq. (I.22) we note that for $N > 4$ the tree level term does not exist since we are working with a renormalisable theory.

The final result, Eq. (I.22), may in principle contain infrared (IR) divergences. This is a well known issue of the effective potential [41, 42] but it is also well known that the p^2 dependent contributions to the vertices must cancel out such IR divergences. In practice one may introduce an IR regulator whenever a massless particle is present in Eq. (I.22) to safely identify and discard the IR divergences. Furthermore, typically the situation is even more favourable because: i) for external lines with massless scalar states the IR divergences must cancel because the approximation $p^2 \to 0$ for the external momenta becomes exact so the effective potential description is complete, and ii) in the examples that we will consider the only massless states are the SM-like Goldstone bosons and their couplings are such that, at one-loop, no IR divergences appear for triple vertices with the other physical scalars appearing in the external lines.

A final concern may be how to deal with particular limits with degenerate masses in Eq. (I.20). This is only an apparent issue. For all derivatives up to order four we will show, in the next subsections, that the result is always expressed in terms of $f^{(1)}$-tensors which are more regular than $f^{(0)}$ tensors. In addition expanding the $f^{(1)}$-tensors around the degenerate limit we find that, in fact, no extra divergences occur besides the IR ones.

3.1 First derivatives

The results that we have found can be directly applied to obtain the first derivatives, which are usually necessary for the tadpole conditions that define the vacuum of the theory. Then, at one-loop order they are given by

$$\begin{aligned} \partial_i V_{\text{eff}} &= \partial_i V^{(0)} + \varepsilon \partial_i V^{(1)} + \mathcal{O}(\varepsilon^2) \\ &= \Lambda_i + \varepsilon \partial_i V^{(1)} + \mathcal{O}(\varepsilon^2) \, . \end{aligned} \tag{I.23}$$

Using Eqs. (I.18), (I.19) and (I.21) in Eq. (I.16) specialised to $N = 1$, we obtain that the tadpole truncated at one-loop is

$$\partial_i V_{\text{eff}} = \Lambda_i + \varepsilon O_{(S)}{}^{j}{}_{i} \sum_T \tfrac{(-1)^{2s_T}(1+2s_T)}{2} m^2_{(T)a} \lambda_{(T)a}{}^{a}{}_{j} \left(\overline{\log} m^2_{(T)a} - k_T + \frac{1}{2} \right) + \mathcal{O}(\varepsilon^2) \, . \tag{I.24}$$

3.2 Second derivatives

The second derivatives are also straightforward to obtain in an explicit form. They are important to determine the one-loop correction to the masses of the particles. The zero external momentum contribution to the one-loop scalar two point function is obtained from

$$\begin{aligned} \partial_{kl} V_{\text{eff}} &= \Lambda_{kl} + \varepsilon O_{(S)}{}^{i}{}_{k} O_{(S)}{}^{j}{}_{l} \sum_T \tfrac{(-1)^{2s_T}(1+2s_T)}{2} \mathrm{S}_{\{ij\}} \left[\lambda^{ab}_{(T)i} \lambda_{(T)baj} \left(f^{(1)}_{(T)ab} - k_T + \frac{1}{2} \right) + \right. \\ &\quad \left. + \lambda^{a}_{(T)aij} m^2_{(T)a} \left(\overline{\log} m^2_{(T)a} - k_T + \frac{1}{2} \right) \right] + \mathcal{O}(\varepsilon^2) \end{aligned} \tag{I.25}$$

where now we have used the identity

$$m_a^2 f^{(0)}_{(T)ab_1\ldots b_n} = f^{(1)}_{(T)ab_1\ldots b_n} - f^{(0)}_{(T)b_1\ldots b_n}\delta_{aa} \ . \tag{I.26}$$

This result can be used to evaluate the one-loop pole masses associated with the propagators of the scalar states in the theory, in the zero external momentum approximation. For the special case of massless states, such as for Goldstones, where the pole conditions are evaluated at zero external momentum, the second derivatives of the effective potential provide the exact pole conditions.

3.3 Third and fourth derivatives

Applying the same procedure one obtains higher derivatives. The third derivative is

$$\begin{aligned}\partial_{lmn}V_{\rm eff} &= \Lambda_{lmn} + \varepsilon O_{(S)}{}^{i}{}_{l} O_{(S)}{}^{j}{}_{m} O_{(S)}{}^{k}{}_{n} \sum_T \tfrac{(-1)^{2s_T}(1+2s_T)}{2} \mathrm{S}_{\{ijk\}} \Big[2 f^{(1)}_{(T)abc} \lambda^{ab}_{(T)i} \lambda^{bc}_{(T)j} \lambda^{ca}_{(T)k} + \\ &\quad + 3\lambda^{ab}_{(T)ij} \lambda_{(T)bak} \left(f^{(1)}_{(T)ab} - k_T + \tfrac{1}{2} \right) \Big] + \mathcal{O}(\varepsilon^2) \ .. \end{aligned} \tag{I.27}$$

Note that, despite the apparent break down of the total symmetry under exchange of the scalar indices in the reduction leading to Eq. (I.16), the final result is manifestly symmetric as it should – see Eq. (I.27). The same procedure can be applied for the fourth derivative to obtain

$$\begin{aligned}\partial_{j_1 j_2 j_3 j_4} V^{(1)}_{\rm eff} &= \Lambda_{j_1 j_2 j_3 j_4} + \varepsilon O_{(S)}{}^{i_1}{}_{j_1} O_{(S)}{}^{i_2}{}_{j_2} O_{(S)}{}^{i_3}{}_{j_3} O_{(S)}{}^{i_4}{}_{j_4} \times \\ &\quad \times \sum_T \tfrac{(-1)^{2s_T}(1+2s_T)}{2} 3 \mathrm{S}_{\{i_1 i_2 i_3 i_4\}} \Big[\lambda^{ab}_{(T)i_1 i_4} \lambda_{(T)bai_2 i_3} \left(f^{(1)}_{(T)ab} - k_T + \tfrac{1}{2} \right) + \\ &\quad + 2 \left\{ f^{(1)}_{(T)abcd} \lambda^{ab}_{(T)i_4} \lambda_{(T)}{}^{bc}{}_{i_1} \lambda_{(T)}{}^{cd}{}_{i_2} \lambda_{(T)}{}^{d}{}_{ai_3} + 2 f^{(1)}_{(T)abc} \lambda^{ab}_{(T)i_4} \lambda_{(T)}{}^{bc}{}_{i_1 i_2} \lambda_{(T)}{}^{ca}{}_{i_3} \right\} \Big] \\ &\quad + \mathcal{O}(\varepsilon^2) \ . \end{aligned} \tag{I.28}$$

For higher order derivatives, it becomes increasingly cumbersome to simplify the expressions explicitly, to check their symmetry property. Nevertheless the full result is explicitly determined by Eq. (I.22).

To verify our general expressions, we have compared against various simple cases where the derivatives can be computed directly with MATHEMATICA. This included the SM Higgs sector and a toy model with an SU(2) gauge field, plus a Weyl fermion doublet, a Weyl fermion singlet and a scalar doublet. We also performed various checks of the one-loop tadpole conditions and mass-squared matrices in the scalar sector of the CP-conserving two Higgs doublet model.

4 Examples

The general result obtained in the previous sections, Eq. (I.22), can in principle be used for computations involving N-point scalar vertices under the approximation of small external momenta. That is the case, for example, in the construction of effective field theories by the usual matching and running procedure [38] where the heavy degrees of freedom are integrated out.[7] In principle our result can then be used to obtain all the one-loop matching conditions for a given scalar N-point vertex with no derivatives and light particles in the external lines. These are given by computing all diagrams that contain at least one heavy particle in the loop [43, 38], which is equivalent to computing all diagrams and subtracting out diagrams involving only light particles, i.e. the matching conditions capture the differences due to the heavy particle interactions. In general, in this procedure, there are contributions from loops with only heavy particles or with a mixture of heavy and light particles [37, 38, 44, 45]. These mixed contributions can be found in the internal sums over the indices corresponding to particles of type T in Eq. (I.22).

Eq. (I.22) can also be used more directly in a phenomenological context to evaluate the one-loop contributions to the effective triple couplings of light scalar states due to heavier degrees of freedom at the electroweak scale. This is interesting because the LHC is now probing the Higgs sector of the SM and the structure of its scalar potential so, in particular, Higgs-to-Higgs decays should play a primary role. We will illustrate this with a real and a complex singlet extension of the SM where one adds a real or a complex scalar field that is a singlet under the SM gauge group. There are many attractive features for this type of models. Namely, they may provide dark matter candidates [3, 4, 5, 6, 7, 8, 9, 10, 11, 12, 13, 14, 16, 17, 18], allow for electroweak baryogenesis through a strong first-order electroweak phase transition in the early universe [46, 47, 48, 49, 50] and they can provide a rich collider phenomenology [51, 52, 53, 54, 55, 56, 57, 58, 59, 60, 39, 40, 61, 62] with Higgs-to-Higgs decays or invisible decays.

The theory and phenomenology of the models that we will consider in the next subsections were recently studied in detail in [39, 40, 61]. We will use, for each model, the samples generated in [39], which contain all the latest phenomenological constraints from: collider experiments (LEP, Tevatron and LHC); electroweak precision observables; dark matter observables (direct detection and relic density upper bounds); and tree level theoretical constraints such as boundedness from below, vacuum stability (the minimum is global) and perturbative unitarity. For further details we refer the reader to [39]. We note that in those samples we have used one-loop accurate relations between the input couplings, the Vacuum Expectation Values (VEVs), masses and mixings of the mass eigenstates, with full p^2 dependence. These were computed for the CxSM in [39] and the details of the calculations for general scalar singlet extension of the SM will appear in [63]. In all our calculations we keep all the new scalar sector contributions and only the dominant SM top quark corrections as illustrated below for the triple couplings.

[7] We remind the reader that our calculations assume we are working with a renormalisable theory, thus for the particular case of matching a high scale non-renormalisable effective theory with another effective theory our general formula would have to be generalised.

The one-loop corrected couplings, $\lambda_{(S)i_1,\ldots,i_N}$, for an N-point vertex of the light scalar states corrected at one-loop by the heavy states is, under the zero external momentum approximation, given by

$$\lambda_{(S)i_1,\ldots,i_N} \quad = \quad \lambda^{(0)}_{(S)i_1,\ldots,i_N} + \varepsilon\, \partial^N_{i_1,\ldots,i_N} V^{(1)}_{\text{heavy}} \,. \tag{I.29}$$

Here the subscript "heavy" indicates that in the indices of the internal sums in the one-loop effective potential at least one index is running over heavy particles, i.e. the contributions with internal sums over only light particles are dropped out. In the remainder of this section, for ease of notation, we will keep the one-loop corrected coupling represented with no superscript, $\lambda_{(S)i_1,\ldots,i_N}$, as in Eq. (I.29). The first term, $\lambda^{(0)}_{(S)i_1,\ldots,i_N}$, consists of the tree level diagrams with heavy particles in the internal lines. For the triple couplings that we will obtain in the next section there are no tree level contributions due to the heavy states, only the tree level vertices.

4.1 The RxSM

The simplest model we consider is the real singlet extension of the SM. This is obtained by adding to the SM a real singlet S with a discrete symmetry under $S \to -S$. The (renormalisable) potential is

$$V_{\text{RxSM}} = \frac{m^2}{2} H^\dagger H + \frac{\lambda}{4}(H^\dagger H)^2 + \frac{\lambda_{HS}}{2} H^\dagger H S^2 + \frac{m_S^2}{2} S^2 + \frac{\lambda_S}{4!} S^4 \,, \tag{I.30}$$

with $m, \lambda, \lambda_{HS}, m_S$ and λ_S all real. The vacuum of the theory that is consistent with the Higgs mechanism is such that

$$H = \frac{1}{\sqrt{2}} \begin{pmatrix} G^+ \\ v + h + iG^0 \end{pmatrix} \quad \text{and} \quad S = v_S + s \,, \tag{I.31}$$

where the SM Higgs VEV is $v \approx 246$ GeV, and the singlet VEV is v_S. This model contains a symmetric phase with $v_S = 0$, in which case S is a dark matter candidate, and a broken phase with $v_S \neq 0$, which has two (visible) mass eigenstates h_1 and h_2 that are mixtures of h and S and are ordered in mass ($m_{h_1} < m_{h_2}$). We focus on the broken phase, in which the mass eigenstates are given by

$$\begin{pmatrix} h_1 \\ h_2 \end{pmatrix} = \begin{pmatrix} \cos\alpha & \sin\alpha \\ -\sin\alpha & \cos\alpha \end{pmatrix} \begin{pmatrix} h \\ s \end{pmatrix} \equiv \begin{pmatrix} R_{11} & R_{12} \\ R_{21} & R_{22} \end{pmatrix} \begin{pmatrix} h \\ s \end{pmatrix} . \tag{I.32}$$

In this model, we can evaluate the one-loop contributions to the SM-like Higgs ($h_1 \equiv h_{125}$) triple coupling and to the Higgs coupling to a pair of Goldstones (equivalently longitudinal modes of massive vector bosons), in the scenario where it is the lightest of the two scalars, $h_1 \equiv h_{125}$, and where the second Higgs, h_2, is heavy. We consider scenarios with $h_2 > 250$ GeV and we also include the top quark contributions in the zero external momentum approximation. This approximation is justified noting that the one-loop contributions due to the top quark appear through a vertex with a Higgs

and a pair of top quarks so we expect a kinematic suppression of the $p^2 \neq 0$ corrections by $m_{h_1}^2/(4m_t^2) \sim 0.13$. We also consider the heavy scalar mass, m_{h_2}, to be larger than $2m_{h_1} \sim 250$ GeV for the same reason, i.e. so that the $p^2 \to 0$ approximation is reliable.

For simplicity let us illustrate the use of Eq. (I.22) for the triple h_1 coupling. At tree level, this is given by [39]

$$\lambda^{(0)}_{(S)h_1h_1h_1} = \frac{3}{2}\lambda R_{11}^3 v + 3\lambda_{HS} R_{11}^2 R_{12} v_S + 3\lambda_{HS} R_{11} R_{12}^2 v + \lambda_S R_{12}^3 v_S \ , \quad \text{(I.33)}$$

The other non-zero tree level scalar couplings that appear in the one-loop calculation are

$$\begin{aligned}
\lambda^{(0)}_{(S)h_1h_1h_2} &= R_{11}^2 \left(\frac{3\lambda R_{21} v}{2} + \lambda_{HS} R_{22} v_S\right) + R_{12}^2(\lambda_{HS} R_{21} v + \lambda_S R_{22} v_S) + \\
&\quad + 2\lambda_{HS} R_{11} R_{12}(R_{21} v_S + R_{22} v) \ , \\
\lambda^{(0)}_{(S)h_1h_2h_2} &= R_{11}\left(\frac{3}{2}\lambda R_{21}^2 v + 2\lambda_{HS} R_{21} R_{22} v_S + \lambda_{HS} R_{22}^2 v\right) + \\
&\quad + R_{12}\left(\lambda_{HS} R_{21}^2 v_S + 2\lambda_{HS} R_{21} R_{22} v + \lambda_S R_{22}^2 v_S\right) \ , \qquad \text{(I.34)} \\
\lambda^{(0)}_{(S)h_1h_1h_2h_2} &= R_{11}^2\left(\frac{3\lambda R_{21}^2}{2} + \lambda_{HS} R_{22}^2\right) + R_{12}^2\left(\lambda_{HS} R_{21}^2 + \lambda_S R_{22}^2\right) + 4\lambda_{HS} R_{11} R_{12} R_{21} R_{22} \ .
\end{aligned}$$

To include the dominant top-quark coupling (y_t) contributions we also need the following effective fermionic couplings

$$\lambda^{(0)}_{(F)IJh_1} = R_{11} v y_t \delta_{IJ} \ , \quad \text{(I.35)}$$

$$\lambda^{(0)}_{(F)IJh_1h_1} = R_{11}^2 y_t^2 \delta_{IJ} \ , \quad \text{(I.36)}$$

with $I, J = 1, \ldots, 6$, i.e. running over three colours and two helicities for the top quark. Finally, applying Eq. (I.27) with at least one heavy particle in the sum we obtain the one-loop correction:

$$\begin{aligned}
&\partial^3_{h_1h_1h_1} V^{(1)}_{\text{heavy}} \\
&= 3 f^{(1)}_{(S)h_1h_1h_2} \lambda^{(0)}_{(S)h_1h_1h_1} \left(\lambda^{(0)}_{(S)h_1h_1h_2}\right)^2 + 3 f^{(1)}_{(S)h_1h_2h_2} \lambda^{(0)}_{(S)h_1h_2h_2} \left(\lambda^{(0)}_{(S)h_1h_1h_2}\right)^2 + \\
&\quad + f^{(1)}_{(S)h_2h_2h_2} \left(\lambda^{(0)}_{(S)h_2h_2h_2}\right)^3 + \left(f^{(1)}_{(S)h_2h_2} - k_T + \tfrac{1}{2}\right) \lambda^{(0)}_{(S)h_1h_1h_2h_2} \lambda^{(0)}_{(S)h_1h_1h_2} + \\
&\quad - 6 R_{11}^3 y_t^4 v \left[2v^2 y_t^2 f^{(1)}_{(F)ttt} + 3\left(f^{(1)}_{(F)tt} - k_T + \tfrac{1}{2}\right)\right] \ . \qquad \text{(I.37)}
\end{aligned}$$

Note that $f^{(1)}_{(F)ttt}, f^{(1)}_{(S)h_2h_2h_2}, \ldots$ are the loop functions defined in Eq. (I.20) for $k = 1$, with the indices in subscript (h_i or t) denoting which masses are used to evaluate them. Note also that the top quark contribution takes the same form as for the SM Higgs multiplied by a factor of R_{11} for each h_1 in the external legs. This is expected in this type of scalar singlet extensions of the SM. This comes from the fact that the coupling

of each h_i to SM particles is simply suppressed by a factor given by the overlap of the SM Higgs doublet fluctuation h with the corresponding mass eigenstate – see Eqs. (I.31) and (I.32).

Similarly, we can obtain a simple expression for the one-loop correction for the h_1GG triple coupling. The result is expressed through the following tree level vertices (here G denotes one of the three real Goldstone degrees of freedom):

$$\begin{aligned}\lambda^{(0)}_{(S)h_iGG} &= \frac{1}{2}\lambda R_{i1} v + \lambda_{HS} R_{i2} v_S \\ \lambda^{(0)}_{(S)h_ih_jGG} &= \frac{1}{2}\lambda R_{i1} R_{j1} + \lambda_{HS} R_{i2} R_{j2} \ . \end{aligned} \tag{I.38}$$

Then we have

$$\begin{aligned}&\partial^3_{h_1GG} V^{(1)}_{\text{heavy}} \\ =\ & 2 f^{(1)}_{(S)h_1h_2G} \lambda^{(0)}_{(S)h_1h_1h_2} \lambda^{(0)}_{(S)h_2GG} \lambda^{(0)}_{(S)h_1GG} + \\ &+ \left(f^{(1)}_{(S)h_2h_2G} \lambda^{(0)}_{(S)h_1h_2h_2} + f^{(1)}_{(S)h_2GG} \lambda^{(0)}_{(S)h_1GG} \right) \left(\lambda^{(0)}_{(S)h_2GG} \right)^2 + \\ &+ \frac{3}{4} \Big[2\lambda^{(0)}_{(S)h_1h_2GG} \lambda^{(0)}_{(S)h_1h_1h_2} \left(f^{(1)}_{(S)h_1h_2} - k_T + \tfrac{1}{2} \right) + \\ &+ \lambda^{(0)}_{(S)h_2h_2GG} \lambda^{(0)}_{(S)h_1h_2h_2} \left(\overline{\log} m^2_{h_2} - k_T + \tfrac{3}{2} \right) + 2\lambda^{(0)}_{(S)h_1h_2GG} \lambda^{(0)}_{(S)h_2GG} \left(\overline{\log} m^2_{h_2} - k_T + \tfrac{1}{2} \right) \Big] \\ &- 6 R_{11} v y_t^4 \left(\overline{\log} m^2_t - k_T + \tfrac{3}{2} \right) \ , \end{aligned} \tag{I.39}$$

where again, in the last line, the top quark contribution is the SM-like term multiplied by one R_{11} factor due to the h_1 in the external leg. For other one-loop corrected vertices the steps to follow are similar, but to avoid overshadowing the discussion we omit the detailed expressions in the next section. In all our examples we work in the $\overline{\text{MS}}$ scheme ($k_T = 3/2$) and choose the renormalisation scale to be the Higgs boson mass, i.e. $\mu = 125$ GeV.

In Fig. I.1 we present a sample of points from the parameter space scan of this model generated in [39], with all the constraints applied as discussed in the beginning of Sect. 4. We show the two triple couplings for the light degrees of freedom in units of v as a function of the mass of the new heavy scalar (m_{h_2}). On the left panels we have the SM-like Higgs triple coupling and on the right we have the Higgs-Goldstone-Goldstone coupling, which corresponds to the coupling of the Higgs to a pair of longitudinally polarised vector bosons. The top panels show two layers. In green we display the tree level value of the triple coupling and in blue the one-loop correction. The bottom panels show the one-loop corrected triple couplings with a colour code showing the relative magnitude of the one-loop contribution.

On the bottom left panel we see that the corrections to the Higgs triple coupling in most of the parameter space are typically[8] $\lesssim 20\%$, except for a region for larger masses

[8]Note, however, that there are plenty of points with much smaller corrections because the colour scale is such that lighter points are on top of darker points.

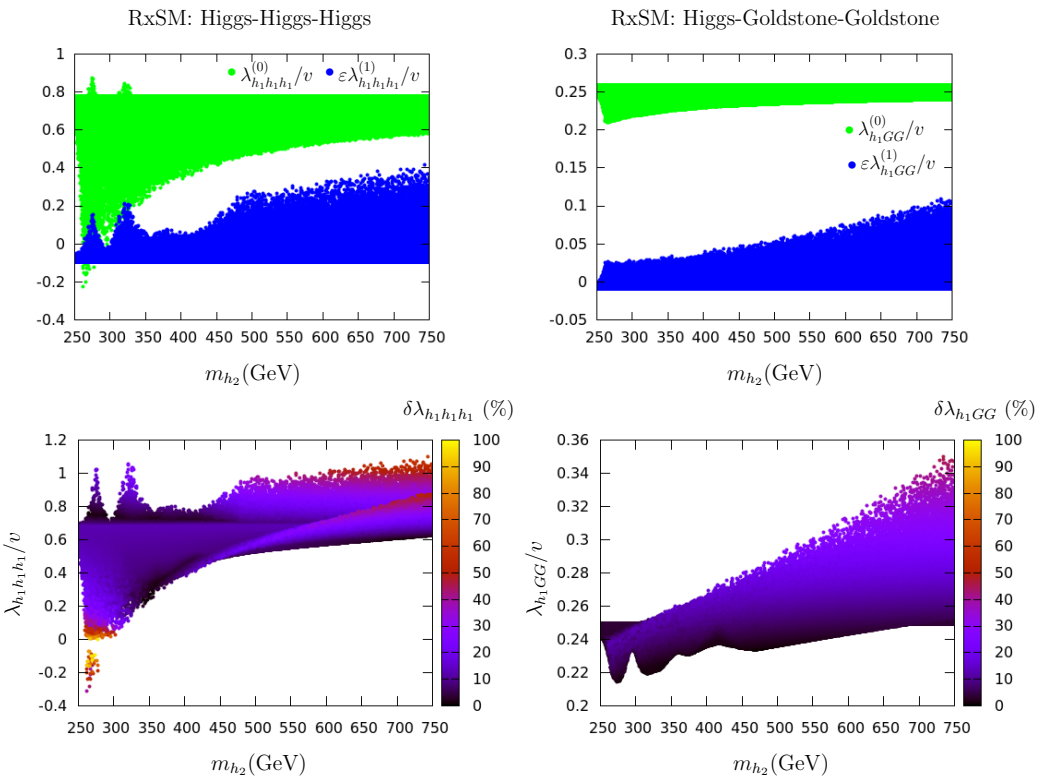

Figure I.1: *One loop contributions from a heavy scalar in the RxSM*: The top left panels display the light SM-like Higgs (h_1) triple coupling in units of v at tree level (green) and the one-loop correction due to the heavy Higgs (h_2) as a function of its mass (blue). In the right hand side panel the colour code is the same except that we display the corresponding quantities for the Higgs-Goldstone-Goldstone coupling. In the bottom panels, we present the same points with the one loop corrected couplings on the vertical axis. The colour scale is the percentage of shift due to the one loop corrections to the couplings.

$m_{h_2} \gtrsim 500$ GeV where the one-loop corrections can become of the order of[9] $\sim 50\%$. A future precise measurement of the Higgs triple coupling through Higgs pair production will constrain the deviations of this coupling from the SM value. Thus, in the high mass regions, it will be particularly important to take into account the one-loop corrections due to the new heavy scalar singlet state. Note, however, that the Higgs pair production process is rather small in the SM [64] and even at the high luminosity stage of the LHC it will be challenging to measure it very accurately [65]. Nevertheless the experimental collaborations are performing dedicated searches and these will provide increasingly tighter bounds for this process – see e.g. [66].

The bottom right panel shows a similar pattern for the Higgs coupling to longitudinally polarised vector bosons. For $m_{h_2} \gtrsim 500$ GeV there are scenarios where the corrections to the Higgs-Vector-Vector triple couplings can be larger than 25%. Thus we would expect

[9]Note also that we have cut out from the bottom left panel of Fig. I.1 points where $\lambda_{h_1h_1h_1}/v \to$ is small because the definition of the relative shift $\delta_{h_1h_1h_1}$ becomes singular.

that improved measurements of the off-shell decay of the SM-like Higgs to vector bosons would again constrain the contribution from the heavy scalar singlet and, consequently, the parameter space of this model.

4.2 The CxSM

The theory and phenomenology of the complex singlet extension of the SM has recently been studied in detail in [39, 40, 61]. In this model the Lagrangian of the SM is extended only in the Higgs sector by a complex singlet field $\mathbb{S} = S + iA$. Its scalar potential is

$$V_{\text{CxSM}} = \frac{m^2}{2} H^\dagger H + \frac{\lambda}{4}(H^\dagger H)^2 + \frac{\delta_2}{2} H^\dagger H |\mathbb{S}|^2 + \frac{b_2}{2}|\mathbb{S}|^2 + \frac{d_2}{4}|\mathbb{S}|^4 + \left(\frac{b_1}{4}\mathbb{S}^2 + a_1 \mathbb{S} + \text{c.c.}\right) , \tag{I.40}$$

where all parameters are real and the terms in parenthesis softly break a U(1) symmetry of the other terms. The doublet and the complex singlet are, respectively,

$$H = \frac{1}{\sqrt{2}} \begin{pmatrix} G^+ \\ v + h + iG^0 \end{pmatrix} \quad \text{and} \quad \mathbb{S} = \frac{1}{\sqrt{2}} \left[v_S + s + i(v_A + a) \right] , \tag{I.41}$$

with $v \approx 246$ GeV the SM Higgs VEV, and $\{v_S, v_A\}$ respectively the VEVs of the real and imaginary parts of the complex singlet. The potential in Eq.(I.40) is $\mathbb{Z}_2$ symmetric under $A \to -A$. As a consequence, there are two possible minima that break electroweak symmetry consistently with the Higgs mechanism. If $v_S \neq 0, v_A = 0$ then h, s mix into a pair of scalars that are visible at colliders and A does not couple to the other SM-particles, so it is a dark candidate. If both $v_S \neq 0, v_A \neq 0$ then h, s, a all mix and we have three scalars that are visible at colliders (one of them being the observed SM-like Higgs). We focus only on the dark matter phase of this model where we denote the masses of the visible Higgs bosons by m_{h_1} and m_{h_2}, and the mass of the dark matter candidate by m_D.

In the case of the dark phase of the singlet extension of the SM we can have a new ingredient in the light spectrum of the theory. We consider the scenario where, again, $m_{h_2} > 250$ GeV, $m_{h_1} = 125$ GeV is the SM-like Higgs boson, but now there is a dark matter candidate that we choose to be light, $m_D < 90$ GeV. Thus, besides the Higgs triple coupling, the one-loop corrections due to the heavy state h_2 now affect the Higgs-dark-dark triple coupling. For this vertex, the one-loop corrections are only due to the scalar sector since the dark particle does not couple, at tree level, with the SM particles. This coupling is very important for dark matter observables, namely the calculation of the relic density that is left over after freeze out in the early Universe, the cross-section for direct detection in underground experiments and invisible decays at colliders. The former two severely constrain the parameter space allowed for the model.

In Fig. I.2 we present a sample of points from the parameter space scan of this model generated in [39], with all the constraints applied as discussed in the beginning of Sect. 4. The top panels are for the Higgs triple coupling, $\lambda_{h_1 h_1 h_1}/v$, and the bottom panels for

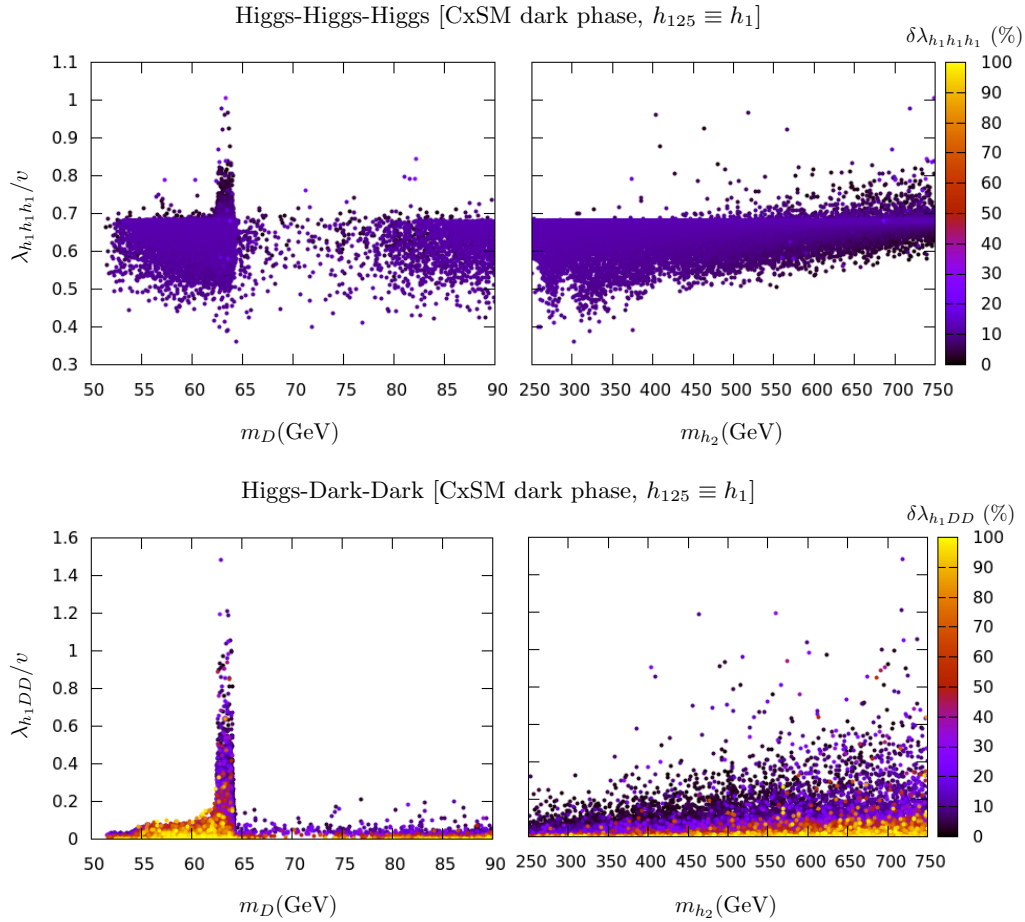

Figure I.2: *One loop contributions from a heavy scalar in the dark phase of the CxSM*: The panels show several projections with triple couplings on the vertical axis versus the dark matter particle mass, m_D (left column) or the heavy scalar mass m_{h_2} (right panel). The colour code on each row is the same for the left and the right panels as well as the triple coupling on the vertical axis.

the Higgs-dark-dark triple coupling λ_{h_1DD}/v. We first note that in the left panels there is a peak around $m_D \sim m_{h_1}/2$ corresponding to the kinematic region where dark matter annihilates efficiently into Higgs bosons in the early Universe, so the triple couplings are allowed to be larger while the relic density does not become larger than the combination of the observational values from the WMAP and Planck satellites [67, 68]. The loss in density to the right of this threshold is also because of the LUX dark matter direct detection bounds [69], which are stronger in the region ~ 20 GeV to ~ 70 GeV but become progressively less restrictive outside this window.

We observe in the top panel that all scenarios in the scan have a one-loop contribution to the Higgs triple coupling that is typically $\lesssim 20-30\%$. In the bottom panel, however, we see that the correction to the Higgs-dark-dark coupling can become as large as the tree level one. This typically happens for points where the tree level contribution is

already small, so that the one-loop contribution can enhance it. Since this sample of points was generated with tree level dark matter observables, the potentially large one-loop corrections can exclude such parameter space points or bring back other points excluded by the tree level analysis.

5 Conclusions

In this article we have obtained the derivatives of the one-loop CW effective potential with respect to the scalar fields up to an arbitrary number of derivatives. Our central result, Eq. (I.22), was derived for an arbitrary renormalisable quantum field theory in four space-time dimensions. We have first found that it is possible to obtain exact expressions for such derivatives, in a closed form, in the tree level mass eigenbasis. This was done using the CW effective potential in mass independent renormalisation schemes in the Landau gauge. The general result follows from the properties of the matrix-log and suitable combinatorics. It remains valid in an arbitrary basis after applying suitable basis transformations.

Our result can in principle be used to compute effective field theory scalar operators without derivatives with any number of light scalar external legs when integrating out heavy degrees of freedom. It can also be used directly to compute one-loop corrections due to heavy states to scalar interaction vertices. In this context we have analysed two scalar singlet extensions (the RxSM and the dark phase of the CxSM) to observe the effect of a new heavy scalar on the low energy phenomenology of the SM-like 125 GeV Higgs boson and of a light dark matter candidate. We have found that in some cases the corrections to the SM-like Higgs self-coupling and the coupling to vector bosons can be comparable to the tree level value. This shows the importance of computing the full one-loop corrections for these models. Most importantly, the corrections to the coupling between the SM-like Higgs and the dark matter candidate in the dark phase of the CxSM can be large. This can take some scenarios out of the phenomenological viable region, due to one-loop shifts to the dark matter observables that are already constrained, or bring back scenarios that were excluded in a tree level analysis.

Finally, it would be interesting to study whether our general analytic result could be extended to the derivatives of the two-loop effective potential or if it could be generalised to non-renormalisable theories.

Acknowledgements

A. P. M. and M.S. acknowledge the THEP group at Lund University, where part of this work was developed, for all support and hospitality. J. E. C.-M., R. P. and J. W. acknowledge the warm hospitality of the Gr@v group at Aveiro University. The work by J. E. C.-M. was supported by the Crafoord Foundation. A. P. M. and M.S. are funded by FCT through the grants SFRH/BPD/97126/2013 and SFRH/BPD/ 69971/2010 re-

spectively. R. P. and J. W. were partially supported by the Swedish Research Council, contract number 621-2013-428. The work in this paper is also supported by the CIDMA project UID/MAT/04106/2013.

I.A All Nth order derivatives of the matrix-$\overline{\log}$ term

In Sec. 3 we have summarised the ingredients needed to obtain the zero external momenta contributions to the scalar N-point functions from the derivatives of the effective potential. Here we provide details on how to obtain the general result for the $\delta^{(N)}_{abi_1\ldots i_N}$ tensors from the derivatives of the matrix-$\overline{\log}$. It is indeed instructive to start by deriving the lower order cases first, on one hand because $N = 1, 2$ are special, and on the other hand because it is then easier to observe the pattern to generalise it to higher orders. For notational simplicity, to avoid carrying around factors of μ^2, we use units of mass such that $\mu^2 = 1$. In this case $\overline{\log}$ is equivalent to the log function. The final result will remain valid with the μ^2 dependence simply appearing in masses inside the $\overline{\log}$ factors.

I.A.1 $N = 1$

The quantity we seek is (suppressing for convenience the indices of $\Lambda_{(T)}$, i.e. using matrix notation)

$$\begin{aligned}
\partial_i\overline{\log}\,\Lambda_{(T)} &= -\partial_i \sum_{n=1}^{+\infty} \frac{(-1)^n}{n} \left(\Lambda_{(T)} - \mathbf{1}\right)^n \\
&= \sum_{n=1}^{+\infty} \frac{(-1)^{n+1}}{n} \sum_{q=1}^{n} \left(\Lambda_{(T)} - \mathbf{1}\right)^{q-1} \overset{q^{th}term}{\partial_i\Lambda_{(T)}} \left(\Lambda_{(T)} - \mathbf{1}-\right)^{n-1-q} \\
&= \sum_{n=1}^{+\infty} \frac{(-1)^{n+1}}{n} \sum_{q=1}^{n} \left(\Lambda_{(T)} - \mathbf{1}\right)^{q-1} \overset{q^{th}term}{\Lambda_{(T,3)i}} \left(\Lambda_{(T)} - \mathbf{1}\right)^{n-1-q} . \quad \text{(I.42)}
\end{aligned}$$

Here we have used the matrix series representation of the matrix log and defined the set of matrices $[\Lambda_{(T,3)i}]_{ab} \equiv \Lambda_{(T)abi}$, which are the cubic vertices of field of type T in the Λ-basis. Note that on the second line we have obtained n terms by applying the Leibniz rule for the derivative operator acting on the product of n equal terms. Each term is obtained by replacing $\left(\Lambda_{(T)} - \mathbf{1}\right) \to \partial_i\Lambda_{(T)}$ in the the term appearing in position q of the product (named $q^{th}term$). Using the definition of the $\delta^{(N)}_{abi_1\ldots i_N}$ tensors, Eq. (I.21), and inserting the orthogonality/unitarity relations for the transformation matrices $\mathcal{U}_{(T)}$

several times between products of matrices[10], we have

$$\begin{aligned}
\delta^{(1)}_{(T)abi} &= \sum_{n=1}^{+\infty}\frac{(-1)^{n+1}}{n}\sum_{q=1}^{n}\left[\left(\mathbf{m^2_{(T)}}-\mathbf{1}\right)^{q-1}\right]_a^{\ c}\ \overset{q^{th}\,term}{\lambda_{(T)c\ i}^{\ \ d}}\ \left[\left(\mathbf{m^2_{(T)}}-\mathbf{1}\right)^{n-q}\right]_{db} \\
&= \lambda_{(T)abi}\sum_{n=1}^{+\infty}\frac{(-1)^{n+1}}{n}\sum_{q=1}^{n}\left(m^2_{(T)a}-1\right)^{q-1}\left(m^2_{(T)b}-1\right)^{n-q} \\
&= \lambda_{(T)abi}f^{(0)}_{(T)ab}\,. \qquad \text{(I.43)}
\end{aligned}$$

In the last line we have used the $N=1$ case of the following general formula

$$\begin{aligned}
& f\left[x_1,\ldots,x_N\right] \\
\equiv\ & \sum_{n=1}^{+\infty}\frac{(-1)^{n+1}}{n}\sum_{P_1=0}^{n-N}\sum_{P_2=0}^{n-N-P_1}\cdots\sum_{P_{N-1}=0}^{n-N-\sum_{i=1}^{N-1}P_i}(x_1-1)^{P_1}(x_2-1)^{P_2}\ldots(x_N-1)^{n-N-\sum_{i=1}^{N}P_i} \\
=\ & \sum_{i=1}^{N}\frac{\overline{\log}\,x_i}{\prod_{k\neq i}(x_i-x_k)}\,, \qquad \text{(I.44)}
\end{aligned}$$

which relates to the $f^{(0)}_{(T)abi_1\ldots i_N}$ tensors defined in Eq. (I.20).

I.A.2 $N=2$

In this case, the two derivatives will either produce two cubic vertices or a quartic as follows

$$\begin{aligned}
\partial_{ij}\overline{\log}\,\Lambda_{(T)} &= \partial_{ij}\sum_{n=1}^{+\infty}\frac{(-1)^{n+1}}{n}\left(\Lambda_{(T)}-\mathbf{1}\right)^n \\
&= \sum_{n=1}^{+\infty}\frac{(-1)^{n+1}}{n}\left[\sum_{q=1}^{n}\left(\Lambda_{(T)}-\mathbf{1}\right)^{q-1}\ \overset{q^{th}\,term}{\partial_{ij}\Lambda_{(T)}}\ \left(\Lambda_{(T)}-\mathbf{1}\right)^{n-q}+\right. \qquad \text{(I.45)} \\
&+ \sum_{p=1}^{n-1}\sum_{p<q\leq n}\left(\Lambda_{(T)}-\mathbf{1}\right)^{p-1}\ \overset{p^{th}\,term}{\partial_i\Lambda_{(T)}}\ \left(\Lambda_{(T)}-\mathbf{1}\right)^{q-p-1}\ \overset{q^{th}\,term}{\partial_j\Lambda_{(T)}}\ \left(\Lambda_{(T)}-\mathbf{1}\right)^{n-q}+ \\
&+ \left.\sum_{p=1}^{n-1}\sum_{p<q\leq n}\left(\Lambda_{(T)}-\mathbf{1}\right)^{p-1}\ \overset{p^{th}\,term}{\partial_j\Lambda_{(T)}}\ \left(\Lambda_{(T)}-\mathbf{1}\right)^{q-p-1}\ \overset{q^{th}\,term}{\partial_i\Lambda_{(T)}}\ \left(\Lambda_{(T)}-\mathbf{1}\right)^{n-q}\right]\,.
\end{aligned}$$

Clearly, the term with the second derivative is similar to the $N=1$ case up to a replacement of the cubic by a quartic $\lambda_{(T)abij}$ vertex. The last term, however, introduces

[10] For a lighter notation, from here on, we use $\mathbf{m^2_{(T)}}$ to denote the diagonal mass-squared matrix $\mathrm{diag}\{m^2_{(T)}\}$.

a new case. Applying again the definition of the $\delta^{(N)}_{abi_1\ldots i_N}$ tensors we have

$$\begin{aligned}
&\delta^{(2)}_{(T)abij} \\
&= \sum_{n=1}^{+\infty} \frac{(-1)^{n+1}}{n} \left[\sum_{q=1}^{n} \left[\left(\mathbf{m^2_{(T)}} - \mathbf{1} \right)^{q-1} \right]_a{}^c \lambda_{(T)c}{}^d{}_{ij} \left[\left(\mathbf{m^2_{(T)}} - \mathbf{1} \right)^{n-q} \right]_{db} + \right. \qquad \text{(I.46)} \\
&+ \sum_{p=1}^{n-1} \sum_{p<q\leq n} \left[\left(\mathbf{m^2_{(T)}} - \mathbf{1} \right)^{p-1} \right]_a{}^c \lambda_{(T)c}{}^d{}_i \left[\left(\mathbf{m^2_{(T)}} - \mathbf{1} \right)^{q-1-p} \right]_d{}^e \lambda_{(T)e}{}^f{}_j \left(\mathbf{m^2_{(T)}} - \mathbf{1} \right)^{n-q}_{fb} \\
&\left. + \sum_{p=1}^{n-1} \sum_{p<q\leq n} \left[\left(\mathbf{m^2_{(T)}} - \mathbf{1} \right)^{p-1} \right]_a{}^c \lambda_{(T)c}{}^d{}_j \left[\left(\mathbf{m^2_{(T)}} - \mathbf{1} \right)^{q-1-p} \right]_d{}^e \lambda_{(T)e}{}^f{}_i \left(\mathbf{m^2_{(T)}} - \mathbf{1} \right)^{n-q}_{fb} \right] .
\end{aligned}$$

This can be further simplified using the definition of the $f^{(0)}_{(T)abi_1\ldots i_N}$ tensors

$$\begin{aligned}
&\delta^{(2)}_{(T)abij} \\
&= \lambda_{(T)abij} \sum_{n=1}^{+\infty} \frac{(-1)^{n+1}}{n} \left[\sum_{q=1}^{n} \left(m^2_{(T)a} - 1 \right)^{q-1} \left(m^2_{(T)b} - 1 \right)^{n-q} \right] + \qquad \text{(I.47)} \\
&+ \lambda_{(T)a}{}^d{}_i \lambda_{(T)b}{}^d{}_j \sum_{n=1}^{+\infty} \frac{(-1)^{n+1}}{n} \left[\sum_{p=1}^{n-1} \sum_{p<q\leq n} \left(m^2_{(T)a} - 1 \right)^{p-1} \times \right. \\
&\qquad \left. \times \left(m^2_{(T)d} - 1 \right)^{q-1-p} \left(m^2_{(T)b} - 1 \right)^{n-q} \right] + (i \leftrightarrow j) \\
&= f^{(0)}_{(T)ab} \lambda_{(T)abij} + f^{(0)}_{(T)abc} \left(\lambda_{(T)a}{}^c{}_i \lambda_{(T)}{}^c{}_{bj} + \lambda_{(T)a}{}^c{}_j \lambda_{(T)}{}^c{}_{bi} \right) . \qquad \text{(I.48)}
\end{aligned}$$

I.A.3 $N \geq 3$

From the $N = 2$ case, it is now clear that the general result for $N \geq 3$ will be a sum of terms that are generalised versions of the last term we found for $N = 2$, Eq. (I.48). This looks like a chain of vertices attached to an $f^{(0)}_{(T)acb}$ tensor (where we have used its total symmetry under exchange of any two indices) with an internal contraction (through the index c) and two external indices a, b fixed. To obtain the general expression we note the following rules (which follow from applying the differential operator to the series expansion of the matrix-$\overline{\log}$ for general N):

- For each N, the result is a sum over terms containing an $f^{(0)}_{(T)ac_1\ldots c_m b}$ tensor. The allowed values of m are such that[11] $\left[\frac{N-1}{2}\right] \leq m \leq N-1$.

[11] We denote the integer part of an number X by $[X]$.

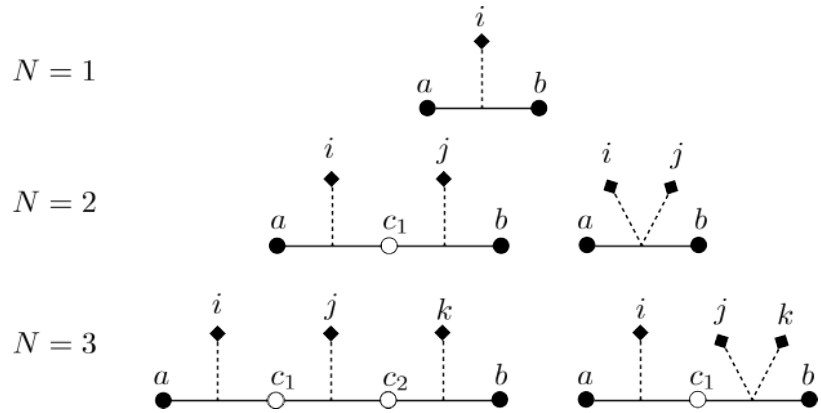

Figure I.3: *Diagrams representing the possible terms appearing in the* $\delta^{(N)}_{abi_1\ldots i_N}$ *tensors.*

- Each $f^{(0)}_{(T)ac_1\ldots c_m b}$ is the base of a chain with two ends fixed a, b where we attach (through internal contractions with the c_i indices) cubic or quartic vertices following the pattern

$$f^{(0)}_{(T)ac_1\ldots c_m b} \times \lambda_{(T)a}{}^{c_1}{}_{\{L_1\}} \lambda^{c_2 c_3}_{(T)\ \{L_2\}} \cdots \lambda^{c_{m-1} c_m}_{(T)\qquad\{L_m\}} \lambda_{(T)}{}^{c_m}{}_{b\{L_{m+1}\}}. \tag{I.49}$$

  Each $\{L_k\}$ contains either one index (for cubic vertices) or a pair of indices (for quartic vertices) from the list $\{i_1, \ldots, i_N\}$. Note that $m+1$ counts the number of cubic vertices in the chain.

- The relative position of the internal vertices (without an a or b index) is only relevant for the purpose of counting multiplicities. The internal contractions of such vertices with the c_i indices in $f^{(0)}_{(T)ac_1\ldots c_m b}$ (which is totally symmetric) automatically symmetrises the result. Thus, it is enough to multiply one representative case by the combinatorial factor under the constraint that the ends of the chain are fixed. Later we can just symmetrise over $\{i_1, \ldots, i_N\}$ to obtain the correct result.

The possible types of terms can be better visualised through graphs as presented in Fig. I.3 for the first three cases. The bottom solid lines with Latin indices $\{a, b, c_i\}$ represent the $f^{(0)}_{(T)ac_1\ldots c_m b}$ base chain. The dashed lines represent the λ_T coupling tensor (one line for cubic or two lines for quartic) with the external scalar indices $\{i, j, \ldots\}$ denoted with diamonds. The external indices $\{a, b\}$ that are uncontracted are denoted with a solid circle, whereas the c_i indices contracted between adjacent $\lambda_{(T)}$ couplings are denoted by open circles.

The problem then reduces to the computation of combinatorial factors. The natural way of organising the result is to start with the case $m + 1 = N$ (where all vertices in the chain are cubic) and then at each step (after reducing m by one) we delete a cubic vertex and replace another cubic vertex by a quartic[12] – from left to right in Fig. I.3.

[12]This guarantees that the number of i_k indices is always the same.

This rule is very important since it defines the number of cubic and quartic vertices at each order $n \equiv N-1-m$ in the sum. For the purpose of counting it is in fact convenient to use n instead of m. This counts the number of quartic vertices in the chain, so it runs from $n = 0$ to $[N/2]$ (simultaneously m runs from $m = N-1$ to $[(N-1)/2]$). To obtain the correct multiplicities for the general expression one notes that:

- At order n, the number of ways of distributing the n quartic vertices by the $N-n$ vertices in the chain (before deciding about the positions of the i_k indices) is $\binom{N-n}{n}$. As already noted, the relative position of internal vertices in Eq. (I.49) is only relevant for the purpose of counting multiplicities. Since the internal c_i contractions with the $f^{(0)}_{(T)ac_1\ldots c_m b}$ tensor automatically symmetrise the expression under the internal positions, it is enough to multiply one representative case by the combinatorial factor. The only possibilities (and the respective multiplicites) are as follows:

  1. *Two quartic vertices are external* - Here we need to choose $n-2$ positions out of the remaining $N-n-2$ internal positions (regardless of ordering), to distribute the remaining quartic vertices, i.e. $\binom{N-n-2}{n-2}$.
  2. *One quartic vertex in the left external position and one cubic in the right one* - In this case, what remains is to choose $n-1$ internal positions out of the remaining $N-n-2$ to distribute the remaining quartic vertices, i.e. $\binom{N-n-2}{n-1}$.
  3. *Cubic vertex in the left external position and a quartic in the right one* - This is just a flipped case, compared to the previous one, so it has the same multiplicity.
  4. *Two cubic vertices are external* - In this case we need to distribute all n quartic vertices by $N-n-2$ positions, i.e. $\binom{N-n-2}{n}$.

  We note that if we sum the multiplicities of these four cases we obtain $\binom{N-n}{n}$, which is precisely the number of ways of distributing n quartic vertices among $N-n$ available positions.

- The final step consists of assigning the $i_1, \ldots, i_N$ indices to the free positions $\{L_k\}$ in each vertex (internal or external). Since the cubic vertices only have one free index to fill, it is easier to use them to start the counting. At order n there are $N-2n$ indices to assign to cubic vertices, so there are $N(N-1)\ldots(N-2n+1) = N!/(2n)!$ ways of distributing them[13]. Finally we are left with $2n$ indices to distribute among the n quartic vertices. This corresponds to the number of different ways of arranging the $2n$ indices in groups of 2. However we must note that in this case the ordering of the two indices within each pair is irrelevant, since the quartic vertices come from a second derivative operator. The combinatorial factor is

$$\binom{2n}{2}\binom{2n-2}{2}\ldots 1 = \frac{(2n)!}{2!(2n-2)!} \times \frac{(2n-2)!}{2!(2n-4)!} \times \ldots 1 = \frac{(2n)!}{2^n} \,. \tag{I.50}$$

[13]Note that now the ordering is relevant. It corresponds to different terms in the expansion of the differential operator (when the Leibniz rule is applied), acting on the polynomials that appear in the series expansion of the matrix-$\overline{\log}$.

Multiplying this factor by the first one, we obtain that the total multiplicity due to the distribution of the indices $\{i_1 \dots i_N\}$ among the various $\{L_k\}$ is

$$\frac{N!}{2^n} \, .$$

Gathering all the multiplicities we can finally write the general expression for $N > 2$:

$$\begin{aligned}
\delta^{(N)}_{(T)abi_1\dots i_N} \;=\; & \mathrm{S}_{\{i_p\}} \sum_{n=0}^{\left[\frac{N}{2}\right]} \frac{N!}{2^n} f^{(0)}_{(T)ac_1\dots c_{N-1-n}b} \left[\binom{N-n-2}{n} \lambda_{(T)a}{}^{c_1}{}_{i_1} \dots \lambda^{c_{N-1-n}}_{(T)}{}_{bi_N} + \right. \\
& + \binom{N-n-2}{n-1} \left(\lambda_{(T)a}{}^{c_1}{}_{i_1 i_2} \dots \lambda^{c_{N-1-n}}_{(T)}{}_{bi_N} + \lambda_{(T)a}{}^{c_1}{}_{i_1} \dots \lambda^{c_{N-1-n}}_{(T)}{}_{bi_{N-1}i_N} \right) \\
& \left. + \binom{N-n-2}{n-2} \lambda_{(T)a}{}^{c_1}{}_{i_1 i_2} \dots \lambda^{c_{N-1-n}}_{(T)}{}_{bi_{N-1}i_N} \right] \, . \qquad \text{(I.51)}
\end{aligned}$$

Here the internal terms that are suppressed using ... are to be replaced by the internal vertices according to the pattern in Eq. (I.49) in any order[14]. Also note that whenever the binomial factor is not defined (such that the corresponding chain is inconsistent), the corresponding term is to be deleted. For example for $n = 0$, only the first term is defined (it is a term with cubic vertices only).

[14] As explained before the $\mathrm{S}_{\{i_p\}}$ takes care of covering all possible cases.

References

[1] **ATLAS** Collaboration, G. Aad *et al.*, "Observation of a new particle in the search for the Standard Model Higgs boson with the ATLAS detector at the LHC," *Phys.Lett.* **B716** (2012) 1–29, arXiv:1207.7214 [hep-ex].

[2] **CMS** Collaboration, S. Chatrchyan *et al.*, "Observation of a new boson at a mass of 125 GeV with the CMS experiment at the LHC," *Phys.Lett.* **B716** (2012) 30–61, arXiv:1207.7235 [hep-ex].

[3] V. Silveira and A. Zee, "Scalar phantoms," *Phys.Lett.* **B161** (1985) 136.

[4] J. McDonald, "Gauge singlet scalars as cold dark matter," *Phys.Rev.* **D50** (1994) 3637–3649, arXiv:hep-ph/0702143 [HEP-PH].

[5] C. Burgess, M. Pospelov, and T. ter Veldhuis, "The Minimal model of nonbaryonic dark matter: A Singlet scalar," *Nucl.Phys.* **B619** (2001) 709–728, arXiv:hep-ph/0011335 [hep-ph].

[6] M. Bento, O. Bertolami, R. Rosenfeld, and L. Teodoro, "Selfinteracting dark matter and invisibly decaying Higgs," *Phys.Rev.* **D62** (2000) 041302, arXiv:astro-ph/0003350 [astro-ph].

[7] H. Davoudiasl, R. Kitano, T. Li, and H. Murayama, "The New minimal standard model," *Phys.Lett.* **B609** (2005) 117–123, arXiv:hep-ph/0405097 [hep-ph].

[8] A. Kusenko, "Sterile neutrinos, dark matter, and the pulsar velocities in models with a Higgs singlet," *Phys.Rev.Lett.* **97** (2006) 241301, arXiv:hep-ph/0609081 [hep-ph].

[9] J. van der Bij, "The Minimal non-minimal standard model," *Phys.Lett.* **B636** (2006) 56–59, arXiv:hep-ph/0603082 [hep-ph].

[10] X.-G. He, T. Li, X.-Q. Li, J. Tandean, and H.-C. Tsai, "Constraints on Scalar Dark Matter from Direct Experimental Searches," *Phys.Rev.* **D79** (2009) 023521, arXiv:0811.0658 [hep-ph].

[11] M. Gonderinger, Y. Li, H. Patel, and M. J. Ramsey-Musolf, "Vacuum Stability, Perturbativity, and Scalar Singlet Dark Matter," *JHEP* **1001** (2010) 053, arXiv:0910.3167 [hep-ph].

[12] Y. Mambrini, "Higgs searches and singlet scalar dark matter: Combined constraints from XENON 100 and the LHC," *Phys.Rev.* **D84** (2011) 115017, arXiv:1108.0671 [hep-ph].

[13] X.-G. He, B. Ren, and J. Tandean, "Hints of Standard Model Higgs Boson at the LHC and Light Dark Matter Searches," *Phys.Rev.* **D85** (2012) 093019, arXiv:1112.6364 [hep-ph].

[14] M. Gonderinger, H. Lim, and M. J. Ramsey-Musolf, "Complex Scalar Singlet Dark Matter: Vacuum Stability and Phenomenology," *Phys.Rev.* **D86** (2012) 043511, arXiv:1202.1316 [hep-ph].

[15] J. Elias-Miro, J. R. Espinosa, G. F. Giudice, H. M. Lee, and A. Strumia, "Stabilization of the Electroweak Vacuum by a Scalar Threshold Effect," *JHEP* **1206** (2012) 031, arXiv:1203.0237 [hep-ph].

[16] J. M. Cline, K. Kainulainen, P. Scott, and C. Weniger, "Update on scalar singlet dark matter," *Phys.Rev.* **D88** (2013) 055025, arXiv:1306.4710 [hep-ph].

[17] E. Gabrielli, M. Heikinheimo, K. Kannike, A. Racioppi, M. Raidal, *et al.*, "Towards Completing the Standard Model: Vacuum Stability, EWSB and Dark Matter," *Phys.Rev.* **D89** (2014) 015017, arXiv:1309.6632 [hep-ph].

[18] S. Profumo, M. J. Ramsey-Musolf, C. L. Wainwright, and P. Winslow, "Singlet-Catalyzed Electroweak Phase Transitions and Precision Higgs Studies," arXiv:1407.5342 [hep-ph].

[19] A. H. Guth, "The Inflationary Universe: A Possible Solution to the Horizon and Flatness Problems," *Phys. Rev.* **D23** (1981) 347–356.

[20] A. D. Linde, "A New Inflationary Universe Scenario: A Possible Solution of the Horizon, Flatness, Homogeneity, Isotropy and Primordial Monopole Problems," *Phys. Lett.* **B108** (1982) 389–393.

[21] A. H. Guth and S. Y. Pi, "Fluctuations in the New Inflationary Universe," *Phys. Rev. Lett.* **49** (1982) 1110–1113.

[22] S. F. King and C. Luhn, "Neutrino Mass and Mixing with Discrete Symmetry," *Rept. Prog. Phys.* **76** (2013) 056201, arXiv:1301.1340 [hep-ph].

[23] S. P. Martin, "A Supersymmetry primer," *Adv.Ser.Direct.High Energy Phys.* **21** (2010) 1–153, arXiv:hep-ph/9709356 [hep-ph].

[24] I. Antoniadis, "A Possible new dimension at a few TeV," *Phys.Lett.* **B246** (1990) 377–384.

[25] N. Arkani-Hamed, S. Dimopoulos, and G. Dvali, "The Hierarchy problem and new dimensions at a millimeter," *Phys.Lett.* **B429** (1998) 263–272, arXiv:hep-ph/9803315 [hep-ph].

[26] N. Arkani-Hamed, A. G. Cohen, and H. Georgi, "Electroweak symmetry breaking from dimensional deconstruction," *Phys.Lett.* **B513** (2001) 232–240, arXiv:hep-ph/0105239 [hep-ph].

[27] S. Dimopoulos, S. Raby, and F. Wilczek, "Supersymmetry and the Scale of Unification," *Phys.Rev.* **D24** (1981) 1681–1683.

[28] L. E. Ibanez and G. G. Ross, "Low-Energy Predictions in Supersymmetric Grand Unified Theories," *Phys.Lett.* **B105** (1981) 439.

[29] J. R. Ellis, S. Kelley, and D. V. Nanopoulos, "Probing the desert using gauge coupling unification," *Phys.Lett.* **B260** (1991) 131–137.

[30] T. A. collaboration, "Search for resonances decaying to photon pairs in 3.2 fb^{-1} of pp collisions at $\sqrt{s} = 13$ TeV with the ATLAS detector,".

[31] **CMS** Collaboration, C. Collaboration, "Search for new physics in high mass diphoton events in proton-proton collisions at 13TeV,".

[32] J. R. Ellis, G. Ridolfi, and F. Zwirner, "Radiative corrections to the masses of supersymmetric Higgs bosons," *Phys. Lett.* **B257** (1991) 83–91.

[33] S. P. Martin, "Two loop effective potential for a general renormalizable theory and softly broken supersymmetry," *Phys.Rev.* **D65** (2002) 116003, arXiv:hep-ph/0111209 [hep-ph].

[34] S. R. Coleman and E. J. Weinberg, "Radiative Corrections as the Origin of Spontaneous Symmetry Breaking," *Phys. Rev.* **D7** (1973) 1888–1910.

[35] A. Drozd, J. Ellis, J. Quevillon, and T. You, "The Universal One-Loop Effective Action," arXiv:1512.03003 [hep-ph].

[36] B. Henning, X. Lu, and H. Murayama, "How to use the Standard Model effective field theory," *JHEP* **01** (2016) 023, arXiv:1412.1837 [hep-ph].

[37] F. del Aguila, Z. Kunszt, and J. Santiago, "One-loop effective lagrangians after matching," *Eur. Phys. J.* **C76** no. 5, (2016) 244, arXiv:1602.00126 [hep-ph].

[38] B. Henning, X. Lu, and H. Murayama, "One-loop Matching and Running with Covariant Derivative Expansion," arXiv:1604.01019 [hep-ph].

[39] R. Costa, M. Mühlleitner, M. O. P. Sampaio, and R. Santos, "Singlet Extensions of the Standard Model at LHC Run 2: Benchmarks and Comparison with the NMSSM," arXiv:1512.05355 [hep-ph].

[40] R. Costa, A. P. Morais, M. O. P. Sampaio, and R. Santos, "Two-loop stability of a complex singlet extended Standard Model," *Phys. Rev.* **D92** no. 2, (2015) 025024, arXiv:1411.4048 [hep-ph].

[41] J. Elias-Miro, J. R. Espinosa, and T. Konstandin, "Taming Infrared Divergences in the Effective Potential," *JHEP* **08** (2014) 034, arXiv:1406.2652 [hep-ph].

[42] S. P. Martin, "Taming the Goldstone contributions to the effective potential," *Phys. Rev.* **D90** no. 1, (2014) 016013, arXiv:1406.2355 [hep-ph].

[43] C. P. Burgess, "Introduction to Effective Field Theory," *Ann. Rev. Nucl. Part. Sci.* **57** (2007) 329–362, arXiv:hep-th/0701053 [hep-th].

[44] S. A. R. Ellis, J. Quevillon, T. You, and Z. Zhang, "Mixed Heavy-Light Matching in the Universal One-Loop Effective Action," arXiv:1604.02445 [hep-ph].

[45] J. Fuentes-Martin, J. Portoles, and P. Ruiz-Femenia, "Integrating out heavy particles with functional methods: a simplified framework," arXiv:1607.02142 [hep-ph].

[46] A. Menon, D. Morrissey, and C. Wagner, "Electroweak baryogenesis and dark matter in the nMSSM," *Phys.Rev.* **D70** (2004) 035005, arXiv:hep-ph/0404184 [hep-ph].

[47] S. J. Huber, T. Konstandin, T. Prokopec, and M. G. Schmidt, "Electroweak Phase Transition and Baryogenesis in the nMSSM," *Nucl.Phys.* **B757** (2006) 172–196, arXiv:hep-ph/0606298 [hep-ph].

[48] S. Profumo, M. J. Ramsey-Musolf, and G. Shaughnessy, "Singlet Higgs phenomenology and the electroweak phase transition," *JHEP* **0708** (2007) 010, arXiv:0705.2425 [hep-ph].

[49] V. Barger, D. J. Chung, A. J. Long, and L.-T. Wang, "Strongly First Order Phase Transitions Near an Enhanced Discrete Symmetry Point," *Phys.Lett.* **B710** (2012) 1–7, arXiv:1112.5460 [hep-ph].

[50] J. R. Espinosa, T. Konstandin, and F. Riva, "Strong Electroweak Phase Transitions in the Standard Model with a Singlet," *Nucl.Phys.* **B854** (2012) 592–630, arXiv:1107.5441 [hep-ph].

[51] A. Datta and A. Raychaudhuri, "Next-to-minimal Higgs: Mass bounds and search prospects," *Phys.Rev.* **D57** (1998) 2940–2948, arXiv:hep-ph/9708444 [hep-ph].

[52] R. Schabinger and J. D. Wells, "A Minimal spontaneously broken hidden sector and its impact on Higgs boson physics at the large hadron collider," *Phys.Rev.* **D72** (2005) 093007, arXiv:hep-ph/0509209 [hep-ph].

[53] O. Bahat-Treidel, Y. Grossman, and Y. Rozen, "Hiding the Higgs at the LHC," *JHEP* **0705** (2007) 022, arXiv:hep-ph/0611162 [hep-ph].

[54] V. Barger, P. Langacker, and G. Shaughnessy, "Collider Signatures of Singlet Extended Higgs Sectors," *Phys.Rev.* **D75** (2007) 055013, arXiv:hep-ph/0611239 [hep-ph].

[55] V. Barger, P. Langacker, M. McCaskey, M. J. Ramsey-Musolf, and G. Shaughnessy, "LHC Phenomenology of an Extended Standard Model with a Real Scalar Singlet," *Phys.Rev.* **D77** (2008) 035005, arXiv:0706.4311 [hep-ph].

[56] V. Barger, P. Langacker, M. McCaskey, M. Ramsey-Musolf, and G. Shaughnessy, "Complex Singlet Extension of the Standard Model," *Phys.Rev.* **D79** (2009) 015018, arXiv:0811.0393 [hep-ph].

[57] D. O'Connell, M. J. Ramsey-Musolf, and M. B. Wise, "Minimal Extension of the Standard Model Scalar Sector," *Phys.Rev.* **D75** (2007) 037701, arXiv:hep-ph/0611014 [hep-ph].

[58] R. S. Gupta and J. D. Wells, "Higgs boson search significance deformations due to mixed-in scalars," *Phys.Lett.* **B710** (2012) 154–158, arXiv:1110.0824 [hep-ph].

[59] A. Ahriche, A. Arhrib, and S. Nasri, "Higgs Phenomenology in the Two-Singlet Model," *JHEP* **1402** (2014) 042, arXiv:1309.5615 [hep-ph].

[60] C.-Y. Chen, S. Dawson, and I. Lewis, "Exploring Resonant di-Higgs production in the Higgs Singlet Model," arXiv:1410.5488 [hep-ph].

[61] R. Coimbra, M. O. Sampaio, and R. Santos, "ScannerS: Constraining the phase diagram of a complex scalar singlet at the LHC," *Eur.Phys.J.* **C73** (2013) 2428, arXiv:1301.2599.

[62] T. Robens and T. Stefaniak, "Status of the Higgs Singlet Extension of the Standard Model after LHC Run 1," *Eur. Phys. J.* **C75** (2015) 104, arXiv:1501.02234 [hep-ph].

[63] M. O. P. Sampaio. to appear.

[64] J. Baglio, A. Djouadi, R. Gröber, M. M. Mühlleitner, J. Quevillon, and M. Spira, "The measurement of the Higgs self-coupling at the LHC: theoretical status," *JHEP* **04** (2013) 151, arXiv:1212.5581 [hep-ph].

[65] **CMS** Collaboration, C. Collaboration, "Higgs pair production at the High Luminosity LHC,".

[66] T. A. collaboration, "Search for Higgs boson pair production in the $b\bar{b}\gamma\gamma$ final state using pp collision data at $\sqrt{s} = 13$ TeV with the ATLAS detector,".

[67] **Planck Collaboration** Collaboration, P. Ade *et al.*, "Planck 2013 results. XVI. Cosmological parameters," *Astron.Astrophys.* (2014) , arXiv:1303.5076 [astro-ph.CO].

[68] **WMAP** Collaboration, G. Hinshaw *et al.*, "Nine-Year Wilkinson Microwave Anisotropy Probe (WMAP) Observations: Cosmological Parameter Results," *Astrophys.J.Suppl.* **208** (2013) 19, arXiv:1212.5226 [astro-ph.CO].

[69] **LUX Collaboration** Collaboration, D. Akerib *et al.*, "First results from the LUX dark matter experiment at the Sanford Underground Research Facility," *Phys.Rev.Lett.* **112** (2014) 091303, arXiv:1310.8214 [astro-ph.CO].

II

On a radiative origin of the Standard Model from Trinification

José Eliel Camargo-Molina[1], António P. Morais[1,2], Roman Pasechnik[1], and Jonas Wessén[1].

JHEP, 1609 (2016) 129
doi:10.1007/JHEP09(2016)129
e-Print: arXiv:1606.03492 [hep-ph]
LU-TP-16-32

[1] Department of Astronomy and Theoretical Physics, Lund University,
SE 223-62 Lund, Sweden.
[2] Departamento de Física da Universidade de Aveiro and CIDMA
Campus de Santiago, 3810-183 Aveiro, Portugal.

Abstract: In this work, we present a trinification-based grand unified theory incorporating a global SU(3) family symmetry that after a spontaneous breaking leads to a left-right symmetric model. Already at the classical level, this model can accommodate the matter content and the quark Cabbibo mixing in the Standard Model (SM) with only one Yukawa coupling at the unification scale. Considering the minimal low-energy scenario with the least amount of light states, we show that the resulting effective theory enables dynamical breaking of its gauge group down to that of the SM by means of radiative corrections accounted for by the renormalisation group evolution at one loop. This result paves the way for a consistent explanation of the SM breaking scale and fermion mass hierarchies.

1 Introduction

The discovery of the Higgs boson at the Large Hadron Collider (LHC) [1, 2] and continuous studies of its properties have revealed an intriguing consistency of experimental results with the Standard Model (SM) predictions. This highlights yet another major

step in precision verification of the SM structure. Besides being a big phenomenological success as a fundamental theory of particle physics, the SM as an effective theory still allows for possibilities for new interactions and particles (such as Dark Matter, right-handed neutrinos, heavy Higgs boson partners, new gauge interactions, among others) at energy scales much larger then the electroweak (EW) scale. This kind of new physics might bring answers to current open questions and could be detected already at the LHC. In addition, the origin of the large set of measured (not predicted!) fermion mass and mixing parameters as well as the Higgs boson mass and self-couplings still remains as one of the most interesting open questions to date. Furthermore, there is still no explanation for the characteristic hierarchies in the measured fermion mass spectrum.

In order to get a better understanding of these long-standing issues in the framework of quantum field theory, one naturally considers the SM as a low-energy approximation of a bigger and more symmetric (unified) theory whose dynamics at high energies is implicitly encoded in the observed structure of the SM.

An important example of such a grand unified theory (GUT) based upon the trinified gauge group $\mathrm{SU}(3)_\mathrm{L} \times \mathrm{SU}(3)_\mathrm{R} \times \mathrm{SU}(3)_\mathrm{C} \equiv [\mathrm{SU}(3)]^3$ (also known as trinification) was proposed by De Rújula, Georgi and Glashow (RGG-model) back in 1984 [3]. Since then, trinified extensions of the SM have been traditionally considered as good bets for a GUT, both with and without supersymmetry (SUSY) [4, 5, 6, 7, 8, 9], due to many attractive features (for a good introduction into trinification GUTs, see [10] and references therein).

The gauge trinification $[\mathrm{SU}(3)]^3 \rtimes \mathbb{Z}_3$ is a maximal subgroup of E_6, where $\mathbb{Z}_3$ is the group of cyclic (L,R,C)-permutations (for a comprehensive discussion of E_6-inspired GUT scenarios, see e.g. Refs. [11, 12, 13, 14, 15, 16, 17, 18, 19, 20, 21, 22, 23, 24, 25, 26, 27, 28, 29, 30, 31, 32, 33, 34, 35, 36, 37]). Typically, this model is considered to be a low-energy limit of the heteroic $\mathrm{E}_8 \times \mathrm{E}_8'$ string theory [38] as well as the $\mathcal{N} = 4$ supergravity [39]. It naturally incorporates the left-right (LR) symmetric gauge interactions [40] as well as the gauge couplings' unification at a GUT scale. All matter fields (including the Higgs fields) can be elegantly arranged into bi-fundamental representations where each family belongs to a **27**-plet, $\mathbf{27} = (\mathbf{3}, \overline{\mathbf{3}}, \mathbf{1}) \oplus (\mathbf{1}, \mathbf{3}, \overline{\mathbf{3}}) \oplus (\overline{\mathbf{3}}, \mathbf{1}, \mathbf{3})$, being the fundamental representation of the E_6 group [11, 41]. Remarkably, no adjoint Higgs fields are needed to break $\mathrm{SU}(3)_\mathrm{L} \times \mathrm{SU}(3)_\mathrm{R}$ down to the electroweak (EW) symmetry group of the SM, $\mathrm{SU}(2)_\mathrm{L} \times \mathrm{U}(1)_\mathrm{Y}$. The spontaneous breaking of trinification with at least two Higgs **27**-plets yields the standard GUT-scale prediction for the weak mixing angle, $\sin^2\theta_W = 3/8$, which leads to quantization of the $\mathrm{U}(1)_\mathrm{Y}$ hypercharge in the SM (e.g. resulting in electron charge being exactly opposite to the proton charge) and provides a consistent explanation of parity violation in the SM. As was shown in Refs. [42, 43] it is possible to achieve naturally light neutrinos via a seesaw mechanism as well. Moreover, in the RGG formulation, the model accommodates any quark mixing angles [44] and a natural suppression of proton decay [4, 8].

However, many existing realizations of the RGG model suffer from severe issues with phenomenology, a considerable amount of particles in its spectrum and many (e.g. Yukawa) parameters. One particular issue, common to most of the well-known GUTs, is an un-

motivated strong hierarchy between the trinification and the EW symmetry breaking scales as well as hierarchies in the SM fermion mass spectrum. In addition, the existing minimal SUSY-based trinification [44] has problems in avoiding TeV-scale lepton masses without imposing higher-dimensional operators, large Higgs representations or an artificial and simultaneous fine tuning of many parameters. At the same time, realistic calculations including quantum corrections are cumbersome due to a large number of scalar particles and gauge bosons in any $[\mathrm{SU}(3)]^3$-symmetric theory. These issues left the trinification-based models among the least-developed GUT scenarios so far.

To be consistent with SM phenomenology, a number of additional U(1) groups emerging in E_6 (or E_8) breaking [45] should be consistently broken at intermediate steps by the conventional Higgs mechanism. Having a few **27** Higgs multiplets coupled to fermions which acquire several low-scale vacuum expectation values (VEVs), may resolve this issue. However, those interactions induce potentially large flavour-changing neutral current processes which are severely restricted by experiment, and a large degree of fine tuning is required.

Due to a huge hierarchy in the mass spectra, at low energy scales heavy d.o.f.'s have to be integrated out at each intermediate symmetry breaking scale giving rise to a new effective model having a fewer amount of light fields in the spectrum. Depending on the symmetry breaking scheme and the hierarchy in the initial $[\mathrm{SU}(3)]^3$ GUT model parameters, one may end up with a few possible low-energy effective models having different light particle content.

One possible development would be to consider a mechanism for Yukawa couplings unification, severely reducing the number of free parameters at the GUT scale [15, 16]. Similarly to the gauge couplings, the unified Yukawa coupling would then give rise to several different couplings by means of radiative corrections via the renormalisation group (RG) evolution and loop-induced operators, which may reproduce the SM fermion mass and mixing hierarchies at low energies. In this way, family symmetries acting in the space of fermion generations [46] are known to provide a convenient tool for generating the necessary patterns in fermion spectra [16, 47]. In particular, such symmetries help to avoid GUT-scale lepton masses in trinification-type models.

An example of an effective LR-symmetric scenario with very interesting phenomenology has been discussed in Ref. [48]. There the authors introduce the gauge group $\mathrm{SU}(3)_\mathrm{C} \times \mathrm{SU}(2)_\mathrm{L} \times \mathrm{SU}(2)_\mathrm{R} \times \mathrm{U}(1)_{\mathrm{B}-\mathrm{L}}$ as originating at lower energies from the trinification model with two $\mathbb{Z}_2$-even and odd Higgs **27**-plets. However, the properties of the Yukawa sector in this model rely on additional higher-dimensional representations of E_6 such as (anti)symmetric **351** reps.

In this work, we consider an alternative non-SUSY trinification model $[\mathrm{SU}(3)]^3 \rtimes \mathbb{Z}_3$ augmented by a $\mathrm{SU}(3)_\mathrm{F}$ global family symmetry which acts both on fermion and scalar multiplets. The latter are thus incorporated in a symmetric way essentially inspired by SUSY. Our scenario is however manifestly non-supersymmetric and it does not invoke any higher-dimensional reps or extra singlets besides lowest **27**-plets of E_6. The scenario we present is naturally inspired by a reduction $\mathrm{E}_8 \to \mathrm{E}_6 \times \mathrm{SU}(3)$ where the remnant SU(3) is identified with a global family symmetry $\mathrm{SU}(3)_\mathrm{F}$ at the trinification breaking

scale. The symmetry group is spontaneously broken down to a LR-symmetric model with an extra $\mathrm{SU}(2)_\mathrm{F} \times \mathrm{U}(1)_\mathrm{X} \times \mathrm{U}(1)_\mathrm{Z} \times \mathrm{U}(1)_\mathrm{B}$ global symmetry that is a remnant of the $\mathrm{SU}(3)_\mathrm{F}$ and an accidental $\mathrm{U}(1)_\mathrm{A} \times \mathrm{U}(1)_\mathrm{B}$ symmetry in the high-scale trinification theory.

As we show in the present work, this model inherits all the important features of trinified GUTs and resolves some of their known difficulties. In the considered implementation of the family symmetry together with the trinification model, all Yukawa couplings are manifestly unified into a single coupling at the GUT scale, and the number of free scalar self-couplings in the scalar potential is remarkably low, making a complete RG analysis of this model feasible. Many of the relevant interactions in the low-energy effective theory emerge radiatively at one (or higher) loop level, bringing a potential explanation to a variety of hierarchies in the SM parameters. However, a detailed calculation of such quantities is beyond the scope of this paper and left for future work. Simultaneously, the family symmetry forbids proton decay due to an appearance of an accidental $\mathrm{U}(1)_\mathrm{B}$ symmetry and protects the light SM fermion sector from large radiative corrections offering potentially interesting phenomenological consequences. Another feature of this model, that we show in this work, is that the $\mathrm{SU}(2)_\mathrm{R} \times \mathrm{U}(1)_{\mathrm{L+R}}$ subgroup gets broken radiatively to $\mathrm{U}(1)_\mathrm{Y}$ at a much lower scale in a natural way for a large region of the parameter space of the GUT-scale trinification model.

In Sect. 2, we introduce the high-scale trinification model augmented by the family symmetry. In Sect. 3, we discuss in detail the first symmetry breaking stage down to a low-energy LR-symmetric effective theory. In Sect. 4, we describe the effective model and the matching of effective couplings in order to study, in Sect. 5, under which circumstances the effective theory shows radiative breaking of the $\mathrm{SU}(2)_\mathrm{R} \times \mathrm{U}(1)_{\mathrm{L+R}}$ symmetry. In Sect. 6, we perform a parameter space scan to find the regions where the radiative symmetry breaking happens in the simplest feasible scenario. In Sect. 7 we discuss, in the light of our results, under which conditions it could be possible to reproduce the SM mass spectra. Concluding remarks are given in Sect. 8.

1.1 A quick note on notations

In the text that follows, we employ the following notations:

- Fundamental representations carry superscript indices while anti-fundamental representations carry subscript indices.
- Fundamental and anti-fundamental indices of SU(3) groups are denoted with lower case letters, while fundamental and anti-fundamental indices under SU(2) groups are denoted with upper case letters.
- $\mathrm{SU}(3)_\mathrm{K}$ and $\mathrm{SU}(2)_\mathrm{K}$ (anti-)fundamental indices are denoted by $k, k', k_1, k_2 \ldots$ and $K, K', K_1, K_2 \ldots$ for $K = L, R, C$, respectively.
- Indices belonging to (anti-)fundamental representations of $\mathrm{SU}(3)_\mathrm{F}$ and $\mathrm{SU}(2)_\mathrm{F}$ are denoted by $i, j, k \ldots$ and $I, J, K \ldots$ respectively.

- If a field transforms both under gauge and global symmetry groups, the index corresponding to the global one is placed within the parenthesis around the field, while the indices corresponding to the gauge symmetries are placed outside.
- Global symmetry groups will be indicated by $\{\dots\}$.

For example, $(L^i)^l_r$ is a $\mathbf{3}\otimes\mathbf{3}\otimes\bar{\mathbf{3}}$ representation of $\mathrm{SU}(3)_\mathrm{L}\times\mathrm{SU}(3)_\mathrm{R}\times\{\mathrm{SU}(3)_\mathrm{F}\}$, and $(\tilde{l}_\mathrm{R}{}^I)_R$ is a $\mathbf{2}\otimes\bar{\mathbf{2}}$ representation of $\mathrm{SU}(2)_\mathrm{R}\times\{\mathrm{SU}(2)_\mathrm{F}\}$, where $\mathrm{SU}(3)_\mathrm{F}$ and $\mathrm{SU}(2)_\mathrm{F}$ are global family symmetry groups.

2 The GUT-scale $[\mathrm{SU}(3)]^3\rtimes\mathbb{Z}_3\times\{\mathrm{SU}(3)_\mathrm{F}\}$ model

The fields in the high-scale trinification model form representations of the symmetry group

$$[\mathrm{SU}(3)_\mathrm{L}\times\mathrm{SU}(3)_\mathrm{R}\times\mathrm{SU}(3)_\mathrm{C}]\rtimes\mathbb{Z}_3\times\{\mathrm{SU}(3)_\mathrm{F}\}, \tag{II.1}$$

as shown in Tab. II.1, and consist of three Weyl fermion multiplets (L, Q_L, Q_R), three scalar multiplets ($\tilde{L}$, $\tilde{Q}_\mathrm{L}$, $\tilde{Q}_\mathrm{R}$) and gauge bosons (G_L, G_R, G_C). Here, $\mathrm{SU}(3)_\mathrm{F}$ is a global family symmetry acting on the space of fermion and scalar field generations, while $\mathrm{SU}(3)_\mathrm{L}\times\mathrm{SU}(3)_\mathrm{R}\times\mathrm{SU}(3)_\mathrm{C}$ is the standard trinification gauge group. Although our model is not supersymmetric, we employ a notation inspired by SUSY, since we have the same group representations in the scalar and fermion sectors. The fermions and scalars both form bi-triplet representations under the gauge group, but *tri*-triplets under the full symmetry group (including the $\mathrm{SU}(3)_\mathrm{F}$)[1].

The $\mathbb{Z}_3$ symmetry refers to the cyclic permutation of the fields

$$\begin{aligned}
G_\mathrm{L}&\overset{\mathbb{Z}_3}{\to}G_\mathrm{C}, & L&\overset{\mathbb{Z}_3}{\to}Q_\mathrm{L}, & \tilde{L}&\overset{\mathbb{Z}_3}{\to}\tilde{Q}_\mathrm{L},\\
G_\mathrm{C}&\overset{\mathbb{Z}_3}{\to}G_\mathrm{R}, & Q_\mathrm{L}&\overset{\mathbb{Z}_3}{\to}Q_\mathrm{R}, & \tilde{Q}_\mathrm{L}&\overset{\mathbb{Z}_3}{\to}\tilde{Q}_\mathrm{R},\\
G_\mathrm{R}&\overset{\mathbb{Z}_3}{\to}G_\mathrm{L}, & Q_\mathrm{R}&\overset{\mathbb{Z}_3}{\to}L, & \tilde{Q}_\mathrm{R}&\overset{\mathbb{Z}_3}{\to}\tilde{L}.
\end{aligned} \tag{II.2}$$

which in turn enforces the gauge coupling unification. This symmetry combined with the global $\mathrm{SU}(3)_\mathrm{F}$ also dramatically reduces the number of possible terms in the scalar potential as well as in the fermion sector of the theory.

The most general renormalizable scalar potential for the trinification model reads

$$V=V_1+V_2+V_3 \tag{II.3}$$

[1]Gauging the family $\mathrm{SU}(3)_\mathrm{F}$ in an E_8 inspired scenario would effectively mean the doubling the number of chiral and scalar multiplets as is required by the anomaly cancellation condition. In this paper, however, we avoid such a huge complication by treating the family symmetry as a global one, as a first step.

	$\mathrm{SU}(3)_\mathrm{L}$	$\mathrm{SU}(3)_\mathrm{R}$	$\mathrm{SU}(3)_\mathrm{C}$	$\{\mathrm{SU}(3)_\mathrm{F}\}$
fermions				
L	$\mathbf{3}$	$\bar{\mathbf{3}}$	$\mathbf{1}$	$\mathbf{3}$
Q_L	$\bar{\mathbf{3}}$	$\mathbf{1}$	$\mathbf{3}$	$\mathbf{3}$
Q_R	$\mathbf{1}$	$\mathbf{3}$	$\bar{\mathbf{3}}$	$\mathbf{3}$
scalars				
$\tilde{L}$	$\mathbf{3}$	$\bar{\mathbf{3}}$	$\mathbf{1}$	$\mathbf{3}$
$\tilde{Q}_\mathrm{L}$	$\bar{\mathbf{3}}$	$\mathbf{1}$	$\mathbf{3}$	$\mathbf{3}$
$\tilde{Q}_\mathrm{R}$	$\mathbf{1}$	$\mathbf{3}$	$\bar{\mathbf{3}}$	$\mathbf{3}$
gauge bosons				
G_L	$\mathbf{8}$	$\mathbf{1}$	$\mathbf{1}$	$\mathbf{1}$
G_R	$\mathbf{1}$	$\mathbf{8}$	$\mathbf{1}$	$\mathbf{1}$
G_C	$\mathbf{1}$	$\mathbf{1}$	$\mathbf{8}$	$\mathbf{1}$

Table II.1: Field content of the GUT-scale trinification model. The fermionic fields are left-handed Weyl fermions.

where

$$\begin{aligned}
V_1 = &-\mu^2 (\tilde{L}^i)^l_r \, (\tilde{L}^*_i)^r_l + \lambda_1 \left[(\tilde{L}^i)^l_r \, (\tilde{L}^*_i)^r_l \right]^2 \\
&+ \lambda_2 (\tilde{L}^i)^l_r \, (\tilde{L}^j)^{l'}_{r'} \, (\tilde{L}^*_j)^r_l \, (\tilde{L}^*_i)^{r'}_{l'} \\
&+ \lambda_3 (\tilde{L}^i)^l_r \, (\tilde{L}^j)^{l'}_{r'} \, (\tilde{L}^*_i)^{r'}_l \, (\tilde{L}^*_j)^r_{l'} \\
&+ \lambda_4 \, (\tilde{L}^i)^l_r \, (\tilde{L}^j)^{l'}_{r'} \, (\tilde{L}^*_j)^{r'}_l \, (\tilde{L}^*_i)^r_{l'} \\
&+ \quad (\mathbb{Z}_3 \text{ permutations}), \\
V_2 = &\, \alpha_1 \, (\tilde{L}^i)^l_r \, (\tilde{L}^*_i)^r_l \, (\tilde{Q}_\mathrm{L}{}^j)^c_{l'} \, (\tilde{Q}^*_{\mathrm{L}j})^{l'}_c \\
&+ \alpha_2 \, (\tilde{L}^i)^l_r \, (\tilde{L}^*_j)^r_l \, (\tilde{Q}_\mathrm{L}{}^j)^c_{l'} \, (\tilde{Q}^*_{\mathrm{L}i})^{l'}_c \\
&+ \alpha_3 \, (\tilde{L}^i)^l_r \, (\tilde{L}^*_i)^r_{l'} \, (\tilde{Q}_\mathrm{L}{}^j)^c_l \, (\tilde{Q}^*_{\mathrm{L}j})^{l'}_c \\
&+ \alpha_4 \, (\tilde{L}^i)^l_r \, (\tilde{L}^*_j)^r_{l'} \, (\tilde{Q}_\mathrm{L}{}^j)^c_l \, (\tilde{Q}^*_{\mathrm{L}i})^{l'}_c \\
&+ \quad (\mathbb{Z}_3 \text{ permutations}),
\end{aligned} \tag{II.4}$$

and

$$V_3 = \gamma \, \epsilon_{ijk} \, (\tilde{L}^i)^l_r \, (\tilde{Q}_\mathrm{L}{}^j)^c_l \, (\tilde{Q}_\mathrm{R}{}^k)^r_c + \text{c.c.} \tag{II.5}$$

The scalar potential thus contains two dimensionfull parameters, mass parameter μ and trilinear coupling γ, and eight quartic couplings $\lambda_{1,\ldots,4}$ and $\alpha_{1,\ldots,4}$ which can be taken to be real without loss of generality.

Due to the interplay between $\mathrm{SU}(3)_\mathrm{F}$ and $\mathbb{Z}_3$, combined with the trinification gauge group, the fermion sector in the model only contains one single Yukawa coupling,

$$\begin{aligned}
\mathcal{L}_\mathrm{Fermion} = \quad & -y \, \epsilon_{ijk} \, (\tilde{L}^i)^l_r \, (Q_\mathrm{L}{}^j)^c_l \, (Q_\mathrm{R}{}^k)^r_c + \text{c.c.} \\
& + \quad (\mathbb{Z}_3 \text{ permutations}).
\end{aligned} \tag{II.6}$$

The trinification Yukawa coupling y can be taken to be real since any complex phase may be absorbed into the definition of the fermion fields.

	$\mathrm{U}(1)_\mathrm{A}$	$\mathrm{U}(1)_\mathrm{B}$
L, $\tilde{L}$	$+1$	0
Q_L, $\tilde{Q}_\mathrm{L}$	$-1/2$	$+1/3$
Q_R, $\tilde{Q}_\mathrm{R}$	$-1/2$	$-1/3$
$G_{\mathrm{L,R,C}}$	0	0

Table II.2: Charge assignment under the accidental symmetries.

Once all the renormalizable terms invariant under the trinification gauge group and the global $\mathrm{SU}(3)_\mathrm{F}$ symmetry are written, one can notice that the terms are also invariant under an accidental $\{\mathrm{U}(1)_\mathrm{A} \times \mathrm{U}(1)_\mathrm{B}\}$ symmetry. A convenient charge assignment under the accidental U(1) groups is shown in Tab. II.2, where one immediately recognizes $\mathrm{U}(1)_\mathrm{B}$ as giving rise to a conserved baryon number. Furthermore, $\mathrm{U}(1)_\mathrm{B}$ will stay unbroken at lower scales (including the SM), since $\tilde{L}$ is uncharged under $\mathrm{U}(1)_\mathrm{B}$ and no other fields will develop VEVs throughout the evolution to the EW scale. Though the symmetry would still allow for the proton to decay into coloured scalars $\tilde{Q}_{\mathrm{L,R}}$, we will see that all the coloured scalar states acquire their masses of the order of the unification scale (i.e. much larger than the proton mass), making such a proton decay kinematically impossible. Meanwhile, the heavy coloured scalars are relevant for generation of loop-induced lepton mass terms at the matching scale in the low-energy effective model as will be discussed in more detail below.

3 Spontaneous trinification breaking down to a LR-symmetric model

In this paper, we would like to explore whether after the spontaneous symmetry breaking (SSB) of the trinification gauge symmetry, it will be possible for the effective LR-symmetric model to break down to the SM gauge group by means of the RG evolution of the corresponding couplings, in particular, mass parameters. In order to do that, one has to explore first the SSB of the group in Eq. (II.1) (also taking into account the accidental $\{\mathrm{U}(1)_\mathrm{A} \times \mathrm{U}(1)_\mathrm{B}\}$ symmetry). The most straightforward way to break trinification is when only one component in $\tilde{L}$ acquires a real non-zero VEV, namely,

$$\langle (\tilde{L}^i)^l_r \rangle = \delta^i_3 \delta^l_3 \delta^3_r \frac{v_3}{\sqrt{2}} = \begin{pmatrix} 0 & 0 & 0 \\ 0 & 0 & 0 \\ 0 & 0 & \frac{v_3}{\sqrt{2}} \end{pmatrix}^{i=3} , \tag{II.7}$$

where the l (r) index labels the rows (columns), while $\langle \tilde{Q}_L \rangle = \langle \tilde{Q}_R \rangle = 0$. As will be shown in Sect. 3.5, this often corresponds to the global minimum of the potential in Eq. (II.3), assuming no $\mathrm{SU}(3)_\mathrm{C}$ breaking VEVs. The extremal conditions (i.e. the requirement that the first derivatives of the scalar potential vanish in the minimum) allow us to rewrite μ in terms of v_3 as follows

$$\mu^2 = (\lambda_1 + \lambda_2 + \lambda_3 + \lambda_4)\, v_3^2 \,. \tag{II.8}$$

By applying a general infinitesimal gauge transformation on $\langle(\tilde{L}^i)^l_r\rangle$, we find that the following subset of the trinification gauge symmetry generators leaves that vacuum invariant:

$$T_{\rm C}^{1,\ldots,8}\,, \qquad T_{\rm L}^{1,2,3}\,, \qquad T_{\rm R}^{1,2,3}\,, \qquad T_{\rm L+R} \equiv \frac{2}{\sqrt{3}}\left(T_{\rm L}^8 + T_{\rm R}^8\right)\,. \tag{II.9}$$

Therefore, the vacuum (II.7) spontaneously breaks the trinification gauge group to the LR-symmetric gauge group $\mathrm{SU}(3)_{\rm C} \times \mathrm{SU}(2)_{\rm L} \times \mathrm{SU}(2)_{\rm R} \times \mathrm{U}(1)_{\rm L+R}$. Before the SSB, the global symmetry group is the full symmetry group $\mathrm{SU}(3)_{\rm C} \times \mathrm{SU}(3)_{\rm L} \times \mathrm{SU}(3)_{\rm R} \times \mathrm{SU}(3)_{\rm F} \times \mathrm{U}(1)_{\rm A} \times \mathrm{U}(1)_{\rm B}$. When applying a general infinitesimal global symmetry transformation on the vacuum given by Eq. (II.7), we find that the following generators leave it invariant

$$T_{\rm F}^{1,2,3}\,, \qquad T_{\rm X} \equiv \frac{2}{\sqrt{3}}\left(T_{\rm L}^8 - T_{\rm R}^8 - 2T_{\rm F}^8\right)\,, \qquad T_{\rm Z} \equiv \frac{2}{3}\left(T_{\rm A} + \sqrt{3}T_{\rm F}^8\right)\,, \tag{II.10}$$

in addition to $T_{\rm B}$ and the generators in Eq. (II.9). Here, we have constructed $T_{\rm X,Z}$ such that they are orthogonal to $T_{\rm L+R}$ and chosen their normalisation for convenience. However, any other two linearly independent combinations of $T_{\rm X,Z}$ and $T_{\rm L+R}$ that are also linearly independent of $T_{\rm L+R}$, generate an unbroken $\{\mathrm{U}(1) \times \mathrm{U}(1)\}$ symmetry. Therefore, after the SSB, in addition to the unbroken gauge group, the symmetry $\{\mathrm{SU}(2)_{\rm F} \times \mathrm{U}(1)_{\rm X} \times \mathrm{U}(1)_{\rm Z} \times \mathrm{U}(1)_{\rm B}\}$ remains unbroken as well. In summary, the VEV setting (II.7) leads to the SSB pattern

$$\begin{gathered}
\mathrm{SU}(3)_{\rm L} \times \mathrm{SU}(3)_{\rm R} \times \mathrm{SU}(3)_{\rm C} \times \{\mathrm{SU}(3)_{\rm F} \times \mathrm{U}(1)_{\rm A} \times \mathrm{U}(1)_{\rm B}\} \\
\downarrow \\
\mathrm{SU}(3)_{\rm C} \times \mathrm{SU}(2)_{\rm L} \times \mathrm{SU}(2)_{\rm R} \times \mathrm{U}(1)_{\rm L+R} \times \{\mathrm{SU}(2)_{\rm F} \times \mathrm{U}(1)_{\rm X} \times \mathrm{U}(1)_{\rm Z} \times \mathrm{U}(1)_{\rm B}\}\,,
\end{gathered} \tag{II.11}$$

and the basic properties of the resulting effective LR-symmetric model will be studied below in detail.

3.1 Colour-singlet scalar sector

The colour-singlet scalars (CSS) are contained in $\tilde{L}$ which is the tri-triplet representation $\mathbf{3} \otimes \bar{\mathbf{3}} \otimes \mathbf{3}$ of $\mathrm{SU}(3)_{\rm L} \times \mathrm{SU}(3)_{\rm R} \times \{\mathrm{SU}(3)_{\rm F}\}$. It therefore contains 54 real degrees of freedom. The VEV structure (II.7) breaks nine gauge symmetry generators, meaning that one identifies nine massless real d.o.f.'s in the CSS mass spectrum that become the longitudinal polarisation states of nine massive gauge bosons. In addition, the non-gauge part of the symmetry group is reduced from $\mathrm{SU}(3)_{\rm F} \times \mathrm{U}(1)_{\rm A} \times \mathrm{U}(1)_{\rm B}$ down to $\mathrm{SU}(2)_{\rm F} \times \mathrm{U}(1)_{\rm X} \times \mathrm{U}(1)_{\rm Z} \times \mathrm{U}(1)_{\rm B}$ so that the CSS spectrum, after the SSB, also contains four corresponding Goldstone d.o.f.'s. These so-called "global Goldstone" bosons remain as physical massless scalar d.o.f.'s. However, at energy scales much lower than v_3, these are effectively decoupled from all other light fields (including the SM fields) since their interactions are always suppressed by powers of v_3. The decoupling of global Goldstone bosons is further discussed in Sect. 4.4. The mass eigenstates and the corresponding squared masses of the CSS after $(\tilde{L}^3)^3_3$ develops a VEV, are listed in Tab. II.3. Local

Fields	$(\text{Mass})^2$	$(L+R, X, Z)$	Comment
$(\tilde{L}^I)^L_R$	$-(\lambda_2+\lambda_3+\lambda_4)\,v_3^2$	$(0,0,+1)$	
$(\tilde{L}^I)^3_R$	$m_R^2 \equiv -(\lambda_2+\lambda_3)\,v_3^2$	$(-1,-1,+1)$	
$(\tilde{L}^3)^L_R$	$m_h^2 \equiv -(\lambda_3+\lambda_4)\,v_3^2$	$(0,+2,0)$	
$(\tilde{L}^I)^L_3$	$-(\lambda_2+\lambda_4)\,v_3^2$	$(+1,-1,+1)$	
$\mathrm{Re}[(\tilde{L}^3)^3_3]$	$2(\lambda_1+\lambda_2+\lambda_3+\lambda_4)\,v_3^2$	$(0,0,0)$	
$\mathrm{Im}[(\tilde{L}^3)^3_3]$	0	$(0,0,0)$	Gauge Goldstone
$(\tilde{L}^3)^L_3$	0	$(+1,+1,0)$	Gauge Goldstone
$(\tilde{L}^3)^3_R$	0	$(-1,+1,0)$	Gauge Goldstone
$(\tilde{L}^I)^3_3$	0	$(0,-2,+1)$	Global Goldstone

Table II.3: Mass eigenstates in $\tilde{L}$ after the SSB of the trinification group, and the corresponding tree-level squared masses and U(1) charges. All states have zero baryon number here. In Sect. 4, we consider the LR-symmetric low-energy effective model with $(\tilde{L}^I)^3_R \equiv (\tilde{l}_{\mathrm{R}}{}^I)_R$ and $(\tilde{L}^3)^L_R \equiv \tilde{h}^L_R$ assuming that $m^2_{R,h} \ll v_3^2$ while all other masses are heavy, i.e. $\sim v_3$.

stability of the minima in the CSS sector is obtained when these squared masses are non-negative. Combined with the requirement that $\mu^2 > 0$, this is ensured when

$$\lambda_1+\lambda_2+\lambda_3+\lambda_4 > 0\,, \qquad \lambda_2+\lambda_3 \leq 0\,, \qquad \lambda_2+\lambda_4 \leq 0\,, \qquad \lambda_3+\lambda_4 \leq 0\,. \quad \text{(II.12)}$$

3.2 Coloured scalar sector

When $\tilde{L}$ acquires a VEV according to Eq. (II.7), all coloured scalar (CS) d.o.f.'s become massive. The mass eigenstates and masses are listed in Tab. II.4. Requiring that the squared masses must be non-negative constrains the parameters in V_2 and V_3 as

$$\begin{aligned} \alpha_1 &\geq 2(\lambda_1+\lambda_2+\lambda_3+\lambda_4)\,, \\ \alpha_1+\alpha_2 &\geq 2(\lambda_1+\lambda_2+\lambda_3+\lambda_4)\,, \\ \alpha_1+\alpha_3-\frac{|\gamma|}{\sqrt{2}v_3} &\geq 2(\lambda_1+\lambda_2+\lambda_3+\lambda_4)\,, \\ \alpha_1+\alpha_2+\alpha_3+\alpha_4 &\geq 2(\lambda_1+\lambda_2+\lambda_3+\lambda_4)\,. \end{aligned} \quad \text{(II.13)}$$

3.3 Gauge boson sector

After the SSB, nine gauge bosons become massive. Their masses are determined by the trinification gauge coupling g as indicated in Tab. II.5. They can be conveniently grouped into two doublets (one for each $\mathrm{SU}(2)_{\mathrm{L,R}}$)

$$V_{\mathrm{L}\mu}{}^L \equiv \frac{1}{\sqrt{2}}\begin{pmatrix} G_{\mathrm{L}}{}^6+\mathrm{i}G_{\mathrm{L}}{}^7 \\ G_{\mathrm{L}}{}^4+\mathrm{i}G_{\mathrm{L}}{}^5 \end{pmatrix}_\mu\,, \quad V_{\mathrm{R}\mu}{}^R \equiv \frac{1}{\sqrt{2}}\begin{pmatrix} G_{\mathrm{R}}{}^6+\mathrm{i}G_{\mathrm{R}}{}^7 \\ G_{\mathrm{R}}{}^4+\mathrm{i}G_{\mathrm{R}}{}^5 \end{pmatrix}_\mu\,, \quad \text{(II.14)}$$

and one singlet

$$V_{\mathrm{s}\mu} \equiv \frac{1}{\sqrt{2}}\left(G_{\mathrm{L}}{}^8 - G_{\mathrm{R}}{}^8\right)_\mu\,. \quad \text{(II.15)}$$

Fields	(Mass)^2	$(L+R, X, Z, B)$
$(\tilde{Q}_{\rm L}{}^I)^c_L$	$\frac{1}{2}\left[\alpha_1 - 2(\lambda_1+\lambda_2+\lambda_3+\lambda_4)\right] v_3^2$	$(-1/3, -1, 0, +1/3)$
$(\tilde{Q}_{\rm R}{}^I)^R_c$	$\frac{1}{2}\left[\alpha_1 - 2(\lambda_1+\lambda_2+\lambda_3+\lambda_4)\right] v_3^2$	$(+1/3, -1, 0, -1/3)$
$(\tilde{Q}_{\rm L}{}^3)^c_L$	$\frac{1}{2}\left[\alpha_1 + \alpha_2 - 2(\lambda_1+\lambda_2+\lambda_3+\lambda_4)\right] v_3^2$	$(-1/3, +1, -1, +1/3)$
$(\tilde{Q}_{\rm R}{}^3)^R_c$	$\frac{1}{2}\left[\alpha_1 + \alpha_2 - 2(\lambda_1+\lambda_2+\lambda_3+\lambda_4)\right] v_3^2$	$(+1/3, +1, -1, -1/3)$
$(\tilde{Q}^I_{\rm LR\pm})^c$	$\frac{1}{2}\left[\alpha_1 + \alpha_3 \pm \frac{\gamma}{\sqrt{2}v_3} - 2(\lambda_1+\lambda_2+\lambda_3+\lambda_4)\right] v_3^2$	$(+2/3, 0, +1/3)$
$(\tilde{Q}_{\rm L}{}^3)^c_3$	$\frac{1}{2}\left[\alpha_1 + \alpha_2 + \alpha_3 + \alpha_4 - 2(\lambda_1+\lambda_2+\lambda_3+\lambda_4)\right] v_3^2$	$(+2/3, +2, -1, +1/3)$
$(\tilde{Q}_{\rm R}{}^3)^3_c$	$\frac{1}{2}\left[\alpha_1 + \alpha_2 + \alpha_3 + \alpha_4 - 2(\lambda_1+\lambda_2+\lambda_3+\lambda_4)\right] v_3^2$	$(-2/3, +2, -1, -1/3)$

Table II.4: Mass eigenstates in $\tilde{Q}_{\rm L}$ and $\tilde{Q}_{\rm R}$ after the SSB of the trinification symmetry group, and the corresponding tree-level squared masses and U(1) charges. Here, $(\tilde{Q}^I_{\rm LR\pm})^c \equiv \frac{1}{\sqrt{2}}\left[(\tilde{Q}_{\rm L}{}^I)^c_3 \pm \epsilon^{IJ}(\tilde{Q}^*_{\rm R\,J})^c_3\right]$.

3.4 Fermion sector

The fermions $(L^i)^l_r$, $(Q_{\rm L}{}^i)^c_l$ and $(Q_{\rm R}{}^i)^r_c$ couple to the scalars $(\tilde{L}^i)^l_r$, $(\tilde{Q}_{\rm L}{}^i)^c_l$ and $(\tilde{Q}_{\rm R}{}^i)^r_c$ via the Yukawa interactions given in Eq. (II.6). In particular, the VEV leads to a Dirac mass term for one fermionic $\mathrm{SU}(2)_{\rm F}$ doublet. The corresponding down-type Dirac state is built out of $(Q_{\rm L}{}^I)^c_3$ and $(Q^\dagger_{\rm R}{}_I)^c_3$ as follows

$$(\mathcal{D}_{\rm H}{}^I)^c \equiv \begin{pmatrix} (Q_{\rm L}{}^I)^c_3 \\ \epsilon^{IJ}(Q^\dagger_{\rm R}{}_J)^c_3 \end{pmatrix} . \tag{II.16}$$

The U(1) charges of $\mathcal{D}_{\rm H}$ are shown in Tab. II.6.

3.5 Finding the global minimum through homotopy continuation

If we restrict ourselves to the case of two generations of colour singlet scalars $\tilde{L}^i$ getting VEVs, the most general VEV setting after accounting for gauge [43] and family symmetries can be written as[2]

$$\langle(\tilde{L}^1)^l_r\rangle = \frac{1}{\sqrt{2}}\begin{pmatrix} v^1 & 0 & 0 \\ 0 & v^2 & 0 \\ 0 & 0 & v^3 \end{pmatrix}, \qquad \langle(\tilde{L}^2)^l_r\rangle = \frac{1}{\sqrt{2}}\begin{pmatrix} v^5 & 0 & v^6 \\ 0 & 0 & 0 \\ v^7 & 0 & v^8 \end{pmatrix} . \tag{II.17}$$

Note that, due to $\mathbb{Z}_3$, this choice is physically equivalent to assuming only VEVs in two generations of either $\tilde{Q}_{\rm L}$ or $\tilde{Q}_{\rm R}$.

As discussed in the previous sections, we are interested in the case where only one real scalar field aqcuires a non-zero VEV. The question remains as to whether this is indeed the global minimum of the scalar potential or if the global minimum has a different set of non-zero VEVs and therefore a different symmetry breaking chain takes place.

[2]Using the $\mathrm{SU}(2)_{\rm F} \subset \mathrm{SU}(3)_{\rm F}$ family symmetry we can "rotate away" one of the VEVs of the general case shown in Ref. [43].

Fields	$(\text{Mass})^2$	$(L+R, X)$	Comment
${G_{\text{C}}}_{\mu}^{1\ldots8}$	0	$(0,0)$	Gauge field of $\text{SU}(3)_{\text{C}}$
${G_{\text{L}}}_{\mu}^{1\ldots3}$	0	$(0,0)$	Gauge field of $\text{SU}(2)_{\text{L}}$
${G_{\text{R}}}_{\mu}^{1\ldots3}$	0	$(0,0)$	Gauge field of $\text{SU}(2)_{\text{R}}$
$\frac{1}{\sqrt{2}}\left({G_{\text{L}}}^{8} + {G_{\text{R}}}^{8}\right)_{\mu}$	0	$(0,0)$	Gauge field of $\text{U}(1)_{\text{L+R}}$
${V_{\text{L}}}_{\mu}^{L}$	$\frac{1}{4}g^2\, v_3^2$	$(+1,+1)$	
${V_{\text{R}}}_{\mu}^{R}$	$\frac{1}{4}g^2\, v_3^2$	$(+1,-1)$	
${V_{\text{s}}}_{\mu}$	$\frac{2}{3}g^2\, v_3^2$	$(0,0)$	

Table II.5: Gauge boson states after the SSB of the trinification group. All gauge boson states are uncharged under $\{\text{U}(1)_{\text{Z}} \times \text{U}(1)_{\text{B}}\}$.

Using the homotopy continuation method through HOM4PS2 [49], we performed a random scan over 5000 parameter points satisfying the conditions in Eqs. (II.12) and (II.13). The homotopy continuation method finds all the solutions of systems of polynomial equations, in this case the minimisation conditions of the tree-level potential (II.3) for the VEV setting in Eq. (II.58).

For all the points in the scan, the global minimum was always the one for which $v^3 \equiv v \neq 0$ and $v^{i\neq 3} = 0$, even for parameter points where other minima were present. In other words, for the model described here if we require that there exists a minimum with one real field acquiring a VEV then, excluding pathological cases that might have been missed in the numerical analysis, that minimum is the global one.

The most general case where a third generation is also allowed to acquire VEVs could not be treated with HOM4PS2 due to a complicated system of equations outpacing our computational resources. However, a purely numerical minimisation was performed over a second scan of parameter space leading to the same result as for the case of two generations. Given a parameter point that satisfies the positive scalar mass-squares condition in the one VEV minima, the numerical minimisation procedure was started in a random point in field space, whereby the minimum of the potential was found by a simple steepest-descent method. For the minima obtained in this way, we computed the gauge boson mass spectrum and observed that it numerically matched the masses in Tab. II.5. By pretending that $\text{SU}(3)_{\text{F}}$ is gauged, we computed the number of unbroken global symmetry generators by counting the number of "new" massless gauge bosons, and could in all cases conclude that it matched the number of global symmetry generators in the effective LR-symmetric model. Therefore, we believe that the all of these minima are related to the one VEV minima in Eq. (II.7) by a symmetry transformation, and are hence physically equivalent.

Fields	$(\text{Mass})^2$	$(L+R, X, Z, B)$	Comment
$(\mathcal{D}_{\rm H}{}^I)^c$	$\frac{1}{2}y^2v_3^2$	$(+2/3, 0, 0, +1/3)$	Dirac fermion

Table II.6: The first and second generation $\mathrm{SU}(2)_{\rm L}\times\mathrm{SU}(2)_{\rm R}$-singlet quarks make up an $\mathrm{SU}(2)_{\rm F}$-doublet Dirac fermion that gets a tree-level mass at the trinification breaking scale. All other fermionic d.o.f.'s in $(L^i)^l_r$, $(Q_{\rm L}{}^i)^c_l$ and $(Q_{\rm R}{}^i)^r_c$ are massless at tree-level.

4 The low-scale effective LR-symmetric model

4.1 Minimal particle content of the effective model

The trinification group is spontaneously broken by the VEV v_3 in Eq. (II.7) to the following symmetry

$$\mathrm{SU}(3)_{\rm C}\times\mathrm{SU}(2)_{\rm L}\times\mathrm{SU}(2)_{\rm R}\times\mathrm{U}(1)_{\rm L+R}\times\{\mathrm{SU}(2)_{\rm F}\times\mathrm{U}(1)_{\rm X}\times\mathrm{U}(1)_{\rm Z}\times\mathrm{U}(1)_{\rm B}\}. \quad \text{(II.18)}$$

The decomposition of $\tilde{L}$ in terms of representations of the group (II.18) can be written as

$$\begin{aligned}(\tilde{L}^i)^l_r =&\delta^i_I\left[\delta^l_L\delta^R_r\,(\tilde{H}^I)^L_R+\delta^l_L\delta^3_r\,(\tilde{l}_{\rm L}{}^I)^L+\delta^l_3\,\delta^R_r(\tilde{l}_{\rm R}{}^I)_R+\delta^l_3\delta^3_r\,\tilde{\Phi}^I\right]\\&+\delta^i_3\left[\delta^l_L\delta^R_r\,\tilde{h}^L_R+\delta^l_L\delta^3_r\,\tilde{l}^{s\,L}_{\rm L}+\delta^L_3\delta^R_r\,\tilde{l}^s_{\rm R}{}_R+\delta^l_3\delta^3_r\left(\tilde{\Phi}^s+\frac{v_3}{\sqrt{2}}\right)\right].\end{aligned} \quad \text{(II.19)}$$

Here, $\tilde{l}^s_{\rm L,R}$ and $\mathrm{Im}[\tilde{\Phi}^s]$ are the gauge Goldstone d.o.f.'s that become the longitudinal polarisation states of the heavy vector bosons listed in Tab. II.5, wheras $\tilde{\Phi}^I$ is the "global" Goldstone boson. Similarly, the fermion multiplet L can be written in terms of reps of the new symmetry group as follows

$$\begin{aligned}(L^i)^l_r =&\delta^i_I\left[\delta^l_L\delta^R_r\,(H^I)^L_R+\delta^l_L\delta^3_r\,(l_{\rm L}{}^I)^L+\delta^l_3\delta^R_r\,(l_{\rm R}{}^I)_R+\delta^l_3\delta^3_r\,\Phi^I\right]\\&+\delta^i_3\left[\delta^l_L\delta^R_r\,(H^s)^L_R+\delta^l_L\delta^3_r\,l^{s\,L}_{\rm L}+\delta^l_3\delta^R_r\,l^s_{\rm R}{}_R+\delta^l_3\delta^3_r\,\Phi^s\right].\end{aligned} \quad \text{(II.20)}$$

Moreover, the decomposition of the trinification quark multiplets, $Q_{\rm L}$ and $Q_{\rm R}$, reads

$$\begin{aligned}(Q_{\rm L}{}^i)^c_l =&\delta^i_I\left[\delta^L_l\,(\mathcal{Q}_{\rm L}{}^I)^c_L+\delta^3_l\,(D_{\rm L}{}^I)^c\right]+\delta^i_3\left[\delta^L_l\,\mathcal{Q}^{s\,c}_{{\rm L}L}+\delta^3_l\,D^{s\,c}_{\rm L}\right],\\(Q_{\rm R}{}^i)^r_c =&\delta^i_I\left[\delta^r_R\,(\mathcal{Q}_{\rm R}{}^I)^R_c+\delta^r_3(D_{\rm R}{}^I)_c\right]+\delta^i_3\left[\delta^r_R\,\mathcal{Q}^{s\,R}_{{\rm R}c}+\delta^r_3\,D^s_{{\rm R}c}\right],\end{aligned} \quad \text{(II.21)}$$

and similarly for $\tilde{Q}_{\rm L,R}$.

As mentioned in Sect. 3, we want to explore whether a radiatively induced breaking down to the SM gauge group can happen for the proposed model. As will be discussed later in detail, in order for that to happen, we need to have at least one $\mathrm{SU}(2)_{\rm R}$ and one $\mathrm{SU}(2)_{\rm L}$ scalar doublet in the effective theory so that the $\mathrm{SU}(2)_{\rm R}$-doublet mass parameter can run negative. With this in mind, and considering the simplest possible scenario, we will focus our attention on a subset of the parameter space where after the trinification symmetry is broken, the scalar spectrum comprises two very light states, namely,

$$\tilde{h}^L_R\equiv(\tilde{L}^3)^L_R \qquad \text{and} \qquad (\tilde{l}_{\rm R}{}^I)_R\equiv(\tilde{L}^I)^3_R\,, \quad \text{(II.22)}$$

in addition to the global Goldstone field $\tilde{\Phi}^I \equiv (\tilde{L}^I)^3_3$. The remaining scalars either get masses of $\mathcal{O}(v_3)$ or get "eaten" by heavy gauge bosons. For this particular case, one can integrate out all the heavy scalars ending up with a simpler effective theory containing the light and massless fields only. In the fermion sector, the fields $(Q_{\rm L}{}^I)^c_3$ and $(Q_{\rm R}{}^I)^3_c$ can also be integrated out as they make up the heavy Dirac fermions shown in Tab. II.6. The fields that are present in the effective theory are shown in Tab. II.7.

In order to parametrize the relevant regions of parameter space giving rise to such a minimal particle content of the effective model, let us define small dimensionless δ and ε parameters as follows

$$\varepsilon \equiv -\lambda_2 - \lambda_3\,, \quad \delta \equiv -\lambda_3 - \lambda_4, \tag{II.23}$$

such that $m^2_{\tilde{R}} = \varepsilon v_3^2$ and $m^2_{\tilde{h}} = \delta v_3^2$. We will then construct the effective LR-symmetric model assuming $\varepsilon \ll 1$ and $\delta \ll 1$. At higher orders in perturbation theory, other tree-level couplings (such as α_i and γ) will enter in the full expressions for $m^2_{\tilde{h},\tilde{R}}$. To still keep these states sufficiently light at the matching scale will then further constrain the parameter space as the simple assumptions $\varepsilon, \delta \ll 1$ will not suffice. This is further discussed in Sec. 7.2.

In the LR-symmetric effective model, the fields interact with gauge bosons according to their representations under the gauge groups as given in Tab. II.7, with strengths determined by the gauge couplings $g_{\rm L}$, $g_{\rm R}$, $g_{\rm C}$ and $g_{\rm L+R}$. At the matching scale v_3, these are related to the trinification gauge coupling g as

$$g_{\rm L} = g_{\rm R} = g_{\rm C} = g\,, \quad g_{\rm L+R} = \sqrt{\frac{3}{8}}g\,. \tag{II.24}$$

4.2 Matching of the scalar potential parameters

The GUT-scale scalar potential V should be matched onto the most general renormalizable scalar potential for $\tilde{h}^L_R$, $(\tilde{l}_{\rm R}{}^I)_R$ and $\tilde{\Phi}^I$ in the low-energy LR-symmetric model:

$$\begin{aligned}
V_{LR} = {} & m_h^2\,|\tilde{h}|^2 + m_R^2\,|\tilde{l}_{\rm R}|^2 + m_{\tilde{\Phi}}^2\,|\tilde{\Phi}|^2 \\
& + \lambda_a\,|\tilde{h}|^4 + \lambda_b\,|\tilde{l}_{\rm R}|^4 + \lambda_c\,|\tilde{\Phi}|^4 + \lambda_d\,|\tilde{h}|^2|\tilde{\Phi}|^2 + \lambda_e\,|\tilde{l}_{\rm R}|^2|\tilde{\Phi}|^2 + \lambda_f\,|\tilde{l}_{\rm R}|^2|\tilde{h}|^2 \\
& + \lambda_g\,(\tilde{l}_{\rm R}{}^I)_{R_1}\;(\tilde{l}^*_{{\rm R}I})^{R_2}\;\tilde{h}^{L}_{R'_1}\;\tilde{h}^{*R'_2}_{L}\quad \epsilon^{R_1R'_1}\,\epsilon_{R_2R'_2} \\
& + \lambda_h\,(\tilde{l}_{\rm R}{}^{I_1})_R\;(\tilde{l}^*_{{\rm R}J_1})^{R}\;\tilde{\Phi}^{I_2}\;\tilde{\Phi}^*_{J_2}\quad \epsilon_{I_1I_2}\,\epsilon^{J_1J_2} \\
& + \lambda_i\,(\tilde{l}_{\rm R}{}^{I_1})_{R_1}\;(\tilde{l}_{\rm R}{}^{I_2})_{R'_1}\;(\tilde{l}^*_{{\rm R}J_1})^{R_2}\;(\tilde{l}^*_{{\rm R}J_2})^{R'_2}\quad \epsilon_{I_1I_2}\,\epsilon^{J_1J_2}\,\epsilon_{R_2R'_2}\,\epsilon^{R_1R'_1} \\
& + \lambda_j\,\tilde{h}^{L_1}_{R_1}\;\tilde{h}^{L'_1}_{R'_1}\;\tilde{h}^{*R_2}_{L_2}\;\tilde{h}^{*R'_2}_{L'_2}\quad \epsilon_{L_1L'_1}\,\epsilon^{L_2L'_2}\,\epsilon_{R_2R'_2}\,\epsilon^{R_1R'_1}
\end{aligned} \tag{II.25}$$

The tree-level matching conditions in the scalar sector are obtained by requiring that the n-point functions with external scalars in the high-scale and the low-scale theory coincide at tree-level at the matching scale μ_m, which we take to be the trinification

breaking scale v_3. In this case, we get all relations between the high scale parameters $\{v_3, \lambda_{1,3}, \epsilon, \delta\}$, and the low-scale parameters $\{m^2_{h,R,\tilde{\Phi}}, \lambda_{a,\ldots,j}\}$ from the two-point functions (i.e. from the masses squared) and the four-point functions (quartic couplings). We compute the four-point functions taking the limit of small external momenta (compared to v_3 scale), since we are only interested in the matching of the renormalizable operators. Any momentum dependence in the four-point functions in the low-scale theory would instead be attributed to (non-renormalizable) derivative interactions. We do not take these higher order derivative operators into account since they presumably would have a negligible effect in the infrared behaviour of the theory. Thus, the matching conditions are

$$\begin{aligned}
&m_h^2 = \delta v^2\,, \quad m_R^2 = \varepsilon v^2\,, \quad m_{\tilde{\Phi}}^2 = 0\,,\\
&\lambda_c = \lambda_d = \lambda_e = \lambda_h = 0\,,\\
&\lambda_g = -2\lambda_3\,, \quad \lambda_i = \frac{1}{2}\varepsilon\,, \quad \lambda_j = \frac{1}{2}\delta\,,\\
&\lambda_a = \lambda_1 - \lambda_3 - \varepsilon - \delta - \frac{(\lambda_1 - \lambda_3 - \varepsilon)^2}{\lambda_1 - \lambda_3 - \varepsilon - \delta} \approx -2\delta + \mathcal{O}(\varepsilon^2, \varepsilon\delta, \delta^2)\,,\\
&\lambda_b = \lambda_1 - \lambda_3 - \varepsilon - \delta - \frac{(\lambda_1 - \lambda_3 - \delta)^2}{\lambda_1 - \lambda_3 - \varepsilon - \delta} \approx -2\varepsilon + \mathcal{O}(\varepsilon^2, \varepsilon\delta, \delta^2)\,,\\
&\lambda_f = 2\left[\lambda_1 + \lambda_3 - \frac{(\lambda_1 - \lambda_3 - \varepsilon)(\lambda_1 - \lambda_3 - \delta)}{\lambda_1 - \lambda_3 - \varepsilon - \delta}\right] \approx 4\lambda_3 + \mathcal{O}(\varepsilon^2, \varepsilon\delta, \delta^2)\,.
\end{aligned} \tag{II.26}$$

Interestingly, all λ_1's cancel out in the matching conditions, provided that ε and δ are sufficiently small, which means that λ_1 does not affect the values of the couplings in the effective LR-symmetric model at tree-level. This can be seen as a consequence of $\tilde{h}^L_R$, $(\tilde{l}_{\mathrm{R}}{}^I)_R$ and $\tilde{\Phi}^I$ becoming Goldstone bosons of the O(54) $\to$ O(53) breaking that is induced in the CSS sector by the v_3 VEV in the limit λ_2, λ_3, $\lambda_4 \to 0$ (since they are Goldstone bosons in this limit, they must decouple from the scalar potential in the same limit).

4.3 Fermion sector

Though the trinification theory only contains one Yukawa coupling, many terms are allowed by the symmetry group of the LR-symmetric effective model in the fermion sector:

$$\begin{aligned}
\mathcal{L}^{(LR)}_{\text{Fermion}} = {} & Y_\alpha\, (\tilde{l}^*_{\mathrm{R}I})^R\, (l_{\mathrm{R}}{}^I)_R\, \Phi^s + Y_\beta\, (\tilde{l}^*_{\mathrm{R}I})^R\, l^s_{\mathrm{R}R}\, \Phi^I + Y_\gamma\, (\tilde{l}_{\mathrm{R}}{}^I)_R\, (\mathcal{Q}_{\mathrm{R}}{}^J)^R\, D^s_{\mathrm{L}}\, \epsilon_{IJ}\\
& + Y_\delta\, \tilde{h}^{*R}_L\, (H^s)^L_R\, \Phi^s + Y_\epsilon\, \tilde{h}^{*R}_L\, l^{s\,L}_{\mathrm{L}}\, l^s_{\mathrm{R}R} + Y_\zeta\, \tilde{h}^L_R\, (\mathcal{Q}_{\mathrm{L}}{}^I)_L\, (\mathcal{Q}_{\mathrm{R}}{}^J)^R\, \epsilon_{IJ}\\
& + Y_\eta\, \tilde{\Phi}^*_I\, \Phi^I \Phi^s + \frac{m_{\Phi^s}}{2}\, \Phi^s \Phi^s + \text{c.c.}
\end{aligned} \tag{II.27}$$

The matching conditions for the Yukawa couplings are rather easy at tree-level, as only two of them are found to have non-vanishing values at the matching scale. This does not mean that the other couplings are not present in the effective theory and it would

be a subject of a future study to calculate the matching conditions at higher orders where they might not necessarily vanish. However, for the purpose of this work, which is to explore a potential for the radiative breaking of the LR symmetry down to the SM gauge group, the tree-level approximation is expected to be sufficient. In this case, the matching conditions are such that

$$Y_\zeta = -y \qquad \text{and} \qquad Y_\gamma = y\,, \tag{II.28}$$

while $Y_{\alpha,\beta,\delta,\epsilon,\eta} = 0$. Furthermore, the β-functions in Appendix II.A indicate that the Yukawa couplings that are zero at the matching scale will also remain zero at lower scales, since $\beta_{Y_i} \propto Y_i$.

With the matching conditions defined above, the parameters of the effective LR-symmetric model can be determined from a reduced set of parameters of the GUT-scale theory. The vacuum stability constraints (II.12) and (II.13) can be then translated as well to reduce further the allowed parameter space for the effective theory. With this framework in mind, the question remains as to whether the remaining symmetries of the effective theory can be broken radiatively by one-loop RG running at a lower scale leading to an effective model which approaches the SM.

4.4 Decoupling of "global" Goldstone bosons

It can be shown, on very general grounds that Goldstone bosons appearing due to the spontaneous breaking of a global symmetry at a scale v_3, have negligibly small interactions at scales $\mu \ll v_3$ [50, 51]. This decoupling is obvious if one chooses a specific exponential representation of the Goldstone d.o.f.'s, which comes at expense of manifest renormalisability. In this work, we have instead chosen the simple (but equivalent) linear representation of the global Goldstone d.o.f.'s $\tilde{\Phi}^I$ such that renormalisability (but not decoupling) is manifest in the GUT-scale trinification theory. Nevertheless, with the results from the three previous sections, we can see explicitly how $\tilde{\Phi}^I$ decouple at scales well below v_3.

Firstly, we notice that $\tilde{\Phi}^I$ decouples from the scalar potential at the matching scale since $m_{\tilde{\Phi}} = 0$ and $\lambda_c = \lambda_d = \lambda_e = \lambda_h = 0$. Instead, one finds that for the matching to agree at non-zero Goldstone boson momenta, one has to introduce derivative interactions among the Goldstone bosons as well as between the Goldstone bosons and non-Goldstone fields. These derivative interactions necessarily have dim > 4 and hence must be suppressed by the trinification breaking scale $\sim v_3$. Since these operators presumably will be increasingly irrelevant in the infrared, we simply omit them from our LR-symmetric effective Lagrangian.

In the trinification fermion sector shown in Eq. (II.6), one can check that the only Yukawa interactions involving $\tilde{\Phi}^I$ that are non-zero at tree-level also involve the heavy quark fields $(Q_{\mathrm{L}}{}^I)^c_3$ and $(Q_{\mathrm{R}}{}^I)^3_c$ (which are integrated out at the trinification breaking scale). In addition, in the effective theory, one new Yukawa interaction with $\tilde{\Phi}^I$ is allowed by symmetry (Y_η in Eq. (II.27)), but it vanishes at the matching scale. The cor-

	$\mathrm{SU}(2)_\mathrm{L}$	$\mathrm{SU}(2)_\mathrm{R}$	$\mathrm{SU}(3)_\mathrm{C}$	$\mathrm{U}(1)_{\mathrm{L+R}}$	$\{\mathrm{SU}(2)_\mathrm{F}\}$	$\{\mathrm{U}(1)_\mathrm{X}\}$	$\{\mathrm{U}(1)_\mathrm{Z}\}$	$\{\mathrm{U}(1)_\mathrm{B}\}$
fermions								
H	$\mathbf{2}$	$\bar{\mathbf{2}}$	$\mathbf{1}$	0	$\mathbf{2}$	0	$+1$	0
l_L	$\mathbf{2}$	$\mathbf{1}$	$\mathbf{1}$	$+1$	$\mathbf{2}$	-1	$+1$	0
l_R	$\mathbf{1}$	$\bar{\mathbf{2}}$	$\mathbf{1}$	-1	$\mathbf{2}$	-1	$+1$	0
Φ	$\mathbf{1}$	$\mathbf{1}$	$\mathbf{1}$	0	$\mathbf{2}$	-2	$+1$	0
$\mathcal{Q}_\mathrm{L}$	$\bar{\mathbf{2}}$	$\mathbf{1}$	$\mathbf{3}$	$-1/3$	$\mathbf{2}$	-1	0	$+1/3$
$\mathcal{Q}_\mathrm{R}$	$\mathbf{1}$	$\mathbf{2}$	$\bar{\mathbf{3}}$	$+1/3$	$\mathbf{2}$	-1	0	$-1/3$
H^s	$\mathbf{2}$	$\bar{\mathbf{2}}$	$\mathbf{1}$	0	$\mathbf{1}$	$+2$	0	0
l^s_L	$\mathbf{2}$	$\mathbf{1}$	$\mathbf{1}$	$+1$	$\mathbf{1}$	$+1$	0	0
l^s_R	$\mathbf{1}$	$\bar{\mathbf{2}}$	$\mathbf{1}$	-1	$\mathbf{1}$	$+1$	0	0
Φ^s	$\mathbf{1}$	$\mathbf{1}$	$\mathbf{1}$	0	$\mathbf{1}$	0	0	0
$\mathcal{Q}^s_\mathrm{L}$	$\bar{\mathbf{2}}$	$\mathbf{1}$	$\mathbf{3}$	$-1/3$	$\mathbf{1}$	$+1$	-1	$+1/3$
$\mathcal{Q}^s_\mathrm{R}$	$\mathbf{1}$	$\mathbf{2}$	$\bar{\mathbf{3}}$	$+1/3$	$\mathbf{1}$	$+1$	-1	$-1/3$
D^s_L	$\mathbf{1}$	$\mathbf{1}$	$\mathbf{3}$	$+2/3$	$\mathbf{1}$	$+2$	-1	$+1/3$
D^s_R	$\mathbf{1}$	$\mathbf{1}$	$\bar{\mathbf{3}}$	$-2/3$	$\mathbf{1}$	$+2$	-1	$-1/3$
scalars								
$\tilde{h}$	$\mathbf{2}$	$\bar{\mathbf{2}}$	$\mathbf{1}$	0	$\mathbf{1}$	$+2$	0	0
$\tilde{l}_\mathrm{R}$	$\mathbf{1}$	$\bar{\mathbf{2}}$	$\mathbf{1}$	-1	$\mathbf{2}$	-1	$+1$	0
$\tilde{\Phi}$	$\mathbf{1}$	$\mathbf{1}$	$\mathbf{1}$	0	$\mathbf{2}$	-2	$+1$	0
gauge bosons								
G_L	$\mathbf{3}$	$\mathbf{1}$	$\mathbf{1}$	0	$\mathbf{1}$	0	0	0
G_R	$\mathbf{1}$	$\mathbf{3}$	$\mathbf{1}$	0	$\mathbf{1}$	0	0	0
G_C	$\mathbf{1}$	$\mathbf{1}$	$\mathbf{8}$	0	$\mathbf{1}$	0	0	0
$G_{\mathrm{L+R}}$	$\mathbf{1}$	$\mathbf{1}$	$\mathbf{1}$	0	$\mathbf{1}$	0	0	0

Table II.7: Field content of the effective LR-symmetric model.

responding β-function, β_{Y_η}, is proportional to Y_η, meaning that the vanishing matching condition also forces $Y_\eta = 0$ at lower scales.

Having shown the disappearance of scalar and Yukawa interactions with $\tilde{\Phi}^I$, only gauge interactions remain. However, since $\tilde{\Phi}^I$ is a gauge singlet, it will neither interact via gauge interactions nor contribute to the running of the gauge couplings in the effective LR-symmetric model.

5 Breaking of $\mathrm{SU}(2)_\mathrm{R} \times \mathrm{U}(1)_{\mathrm{L+R}}$ in the effective model

In order to reproduce the phenomenology of the SM at low energies, the gauge $\mathrm{SU}(2)_\mathrm{R} \times \mathrm{U}(1)_{\mathrm{L+R}}$ subgroup needs to be broken to the SM hypercharge group $\mathrm{U}(1)_\mathrm{Y}$. One of the persistent issues in high energy models is the fact that the vastly different energy scales associated have to be given through input parameters. One way of dealing with this issue is to introduce the possibility of radiative symmetry breaking, i.e SSB triggered by the RG evolution of the model. This is a standard way of understanding, for example, EW symmetry breaking in the MSSM where the running of $m^2_{H_u}$ drives the breaking of $\mathrm{SU}(2)_\mathrm{L} \times \mathrm{U}(1)_\mathrm{Y}$ [52, 53, 54]. The question remains as to whether this model offers

a possibility of breaking $\mathrm{SU}(2)_\mathrm{R} \times \mathrm{U}(1)_\mathrm{L+R}$ through the RG running of m_R^2 and the rest of parameters of the effective model with initial conditions coming from tree-level matching of the high energy theory. This will give us the possibility of checking under which conditions (for the high-energy input parameters) this radiative breaking can be induced.

For this purpose, we consider two separate scenarios. In scenario I, we study the properties of a minimum in the scalar potential of the effective LR-symmetric model where $\mathrm{SU}(2)_\mathrm{R} \times \mathrm{U}(1)_\mathrm{L+R}$ is broken to the analogous of $\mathrm{U}(1)_\mathrm{Y}$ in the SM, (i.e. the EW gauge group $\mathrm{SU}(2)_\mathrm{L} \times \mathrm{U}(1)_\mathrm{Y}$ is unbroken in this minimum). To study the model at the electro-weak scale, where $\mathrm{SU}(2)_\mathrm{L} \times \mathrm{U}(1)_\mathrm{Y}$ is broken, a second step of matching and running would have to be performed to discover whether there is a sign change of the Higgs squared mass parameter inducing the electro-weak symmetry breaking. In scenario II, we instead study minima with a more complicated VEV structure such that $\mathrm{SU}(2)_\mathrm{L} \times \mathrm{SU}(2)_\mathrm{R} \times \mathrm{U}(1)_\mathrm{L+R}$ is directly broken down to $\mathrm{U}(1)_\mathrm{E.M.}$. This is accomplished by suitable VEVs both in $\tilde{h}$ and in $\tilde{l}_\mathrm{R}$. The VEV in $\tilde{l}_\mathrm{R}$ needs to be larger than the Higgs VEV to keep the W' and Z' bosons heavy, but not too large as to ruin the convergence the perturbative expansion through large logarithms of the ratio between the two VEVs. If this ratio would become too large, Scenario I is more appropriate.

5.1 Scenario I: Breaking to the SM gauge group

Let us first understand what are the conditions necessary for $\mathrm{SU}(2)_\mathrm{R} \times \mathrm{U}(1)_\mathrm{L+R}$ breaking through non-vanishing VEV for the scalar field $\tilde{l}_\mathrm{R}$,

$$\langle (\tilde{l}_\mathrm{R}{}^I)_R \rangle = \delta_2^I \delta_R^2 \frac{w}{\sqrt{2}} = \begin{pmatrix} 0 & 0 \\ 0 & \frac{w}{\sqrt{2}} \end{pmatrix}, \tag{II.29}$$

where w is taken to be real. The extremal condition for such a VEV setting reads

$$-m_R^2 = \lambda_b w^2. \tag{II.30}$$

This leaves the following gauged U(1) generator unbroken,

$$T_\mathrm{Y} = T_\mathrm{R}^3 + \frac{1}{2} T_\mathrm{L+R}, \tag{II.31}$$

which can be identified as the SM hypercharge generator. In addition, Eq. (II.29) leaves four global U(1) generators unbroken,

$$T_\mathrm{D} \equiv \frac{1}{2}\left(T_\mathrm{X} - T_\mathrm{L+R}\right), \quad T_\mathrm{E} \equiv T_\mathrm{F}^3 + \frac{1}{2} T_\mathrm{Z}, \quad T_\mathrm{G} \equiv \frac{1}{2}\left(T_\mathrm{Z} + T_\mathrm{L+R}\right), \quad T_\mathrm{B}. \tag{II.32}$$

Thus, the VEV (II.29) breaks the LR symmetry group (II.18) down to

$$\mathrm{SU}(3)_\mathrm{C} \times \mathrm{SU}(2)_\mathrm{L} \times \mathrm{U}(1)_\mathrm{Y} \times \{\mathrm{U}(1)_\mathrm{D} \times \mathrm{U}(1)_\mathrm{E} \times \mathrm{U}(1)_\mathrm{G} \times \mathrm{U}(1)_\mathrm{B}\}. \tag{II.33}$$

which will also be the symmetry group of a SM-like effective model that is obtained when the heavy particles in the effective LR-symmetric model are integrated out.

Fields	$(\text{Mass})^2$	(Y, D, E)	Comment
$\tilde{h}_1^L$	$m_{h_2}^2 \equiv m_h^2 + \frac{1}{2}(\lambda_g - \lambda_f)w^2$	$(-1/2, +1, 0)$	
$\tilde{h}_2^L$	$m_{h_1}^2 \equiv m_h^2 - \frac{1}{2}\lambda_f w^2$	$(+1/2, +1, 0)$	
$(\tilde{l}_{\rm R}{}^1)_1$	$m_{r_2}^2 \equiv 2\lambda_i w^2$	$(-1, 0, +1)$	
$\text{Re}[(\tilde{l}_{\rm R}{}^2)_2]$	$m_{r_1}^2 \equiv 2\lambda_b w^2$	$(0, 0, 0)$	
$(\tilde{l}_{\rm R}{}^2)_1$	0	$(-1, 0, 0)$	Gauge Goldstone
$\text{Im}[(\tilde{l}_{\rm R}{}^2)_2]$	0	$(0, 0, 0)$	Gauge Goldstone
$(\tilde{l}_{\rm R}{}^1)_2$	0	$(0, 0, +1)$	Global Goldstone

Table II.8: Mass eigenstates in $\tilde{h}$ and $\tilde{l}_{\rm R}$ after SSB of the LR symmetry by $\tilde{l}_{\rm R}$ VEV, the corresponding tree-level masses and U(1) charges. All scalars are uncharged under the $\{\text{U}(1)_{\rm G} \times \text{U}(1)_{\rm B}\}$ global symmetry.

The scalar mass eigenstates in the minimum described by Eq. (II.30) are shown in Tab. II.8. Notice, in particular, that the scalar spectrum contains one massless complex d.o.f. that is the "global" Goldstone boson from the breaking of the global part of the LR symmetry. We expect this to decouple at scales $\mu \ll w$, similarly to how $\tilde{\Phi}^I$ decouples for $\mu \ll v$.

The gauge fields after SSB of the LR symmetry are mixed and give rise to the massive and massless states shown in Tab. II.9. The massless states are the gauge fields of the unbroken gauge symmetries, and the massive gauge fields are the combinations

$$W'^{\pm}{}_{\mu} = \frac{1}{\sqrt{2}}\left(G_{\rm R}{}^1 \mp \imath G_{\rm R}{}^2\right)_{\mu}\,, \quad Z'^0{}_{\mu} = \cos\theta_V\, G_{\text{L+R}\mu} - \sin\theta_V\, G_{\rm R}{}^3_{\mu} \tag{II.34}$$

with $\tan\theta_V = g_{\rm R}/2g_{\text{L+R}}$. The hypercharge gauge coupling $g_{\rm Y}$ becomes

$$g_{\rm Y} = \frac{2\, g_{\rm R}\, g_{\text{L+R}}}{\sqrt{4g_{\text{L+R}}^2 + g_{\rm R}^2}}. \tag{II.35}$$

For general values of the Yukawa couplings in Eq. (II.27), many fermion fields become massive once $\langle\tilde{l}_{\rm R}\rangle \neq 0$. However, in the approximation employed in this work, i.e. tree-level matching and one-loop RG evolution, most of the Yukawa couplings are zero and only one Dirac fermion becomes massive in the effective LR-symmetric model (shown in Tab. II.10). This fermion is a Dirac state

$$\mathcal{D}_{\rm s}{}^c \equiv \begin{pmatrix} D_{\rm L}^{s\,c} \\ (\mathcal{Q}_{\rm R}^{\dagger\,1})_c^2 \end{pmatrix} \tag{II.36}$$

and, when integrated out, leaves behind three $\text{SU}(2)_{\rm L}$ doublet quarks and six $\text{SU}(2)_{\rm L}$ singlet quarks that will make up the SM quark sector.

5.2 Scenario II: Breaking directly to $\text{U}(1)_{\text{E.M.}}$

A second possible scenario is that in which both $(\tilde{l}_{\rm R}{}^I)_R$ and $\tilde{h}_R^L$ develop VEVs, which would directly trigger $\text{SU}(2)_{\rm L} \times \text{SU}(2)_{\rm R} \times \text{U}(1)_{\text{L+R}} \to \text{U}(1)_{\text{E.M.}}$. Although this case is

Fields	$(\text{Mass})^2$	Y	Comment
${G_{\text{C}}}_{\mu}^{1,\ldots,8}$	0	0	Gauge field of $\text{SU}(3)_{\text{C}}$
${G_{\text{L}}}_{\mu}^{1,2,3}$	0	0	Gauge field of $\text{SU}(2)_{\text{L}}$
$s_{\theta_V} {G_{\text{L+R}}}_{\mu} + c_{\theta_V} {G_{\text{R}}}_{\mu}^{3}$	0	0	Gauge field of $\text{U}(1)_{\text{Y}}$
${W'^{\pm}}_{\mu}$	$m^2_{W'} \equiv \frac{1}{4} g^2_{\text{R}} w^2$	± 1	
${Z'^{0}}_{\mu}$	$m^2_{Z'} \equiv \left(g^2_{\text{L+R}} + \frac{1}{4} g^2_{\text{R}} \right) w^2$	0	

Table II.9: Gauge boson mass eigenstates and their hypercharges after the spontaneous LR symmetry breaking. All gauge bosons are uncharged under the global $\{\text{U}(1)_{\text{D}} \times \text{U}(1)_{\text{E}} \times \text{U}(1)_{\text{G}} \times \text{U}(1)_{\text{B}}\}$ group. Here, $c_{\theta_V} \equiv \cos\theta_V$ and $s_{\theta_V} \equiv \sin\theta_V$.

certainly allowed by the model, and might also be triggered by RG running of effective Lagrangian parameters, there is no a priori reason that there will be any hierarchy in the VEVs of the fields consistent with the SM. This could lead to several massive gauge bosons with comparable masses which would immediately be in conflict with what is observed experimentally. So far, only the SM $W^{\pm}$ and Z^0 bosons have been observed, and the existing LHC bounds on extra gauge bosons [55, 56] would force an unnatural hierarchy which is precisely the problem one wants to avoid by means of radiative breaking.

Nevertheless, let us explore the conditions under which such symmetry breaking might lead to an unbroken $\text{U}(1)_{\text{E.M.}}$. The most general VEV setting, after accounting for gauge symmetries for $({\tilde{l}_{\text{R}}}^{I})_R$ and $\tilde{h}^L_R$ would be:

$$\langle ({\tilde{l}_{\text{R}}}^{I})_R \rangle = \frac{1}{\sqrt{2}} \begin{pmatrix} w_1 & w_2 \\ 0 & w_3 \end{pmatrix} \qquad \langle \tilde{h}^L_R \rangle = \frac{1}{\sqrt{2}} \begin{pmatrix} v_1 & 0 \\ 0 & v_2 \end{pmatrix}. \tag{II.37}$$

However, not all of these minima lead to a $\text{U}(1)_{\text{E.M.}}$ remaining gauge symmetry consistent with the proposed framework. To understand this, it is useful to think as if the VEVs are attained sequentially. Let us assume $({\tilde{l}_{\text{R}}}^{I})_R$ gets its VEV first. From our previous analysis we know that in order to identify $T_{\text{E.M.}} = T^3_{\text{L}} + T_{\text{Y}}$ we need $\tilde{h}^L_R$ to break down to two $\text{SU}(2)_{\text{L}}$ doublets with opposite hypercharge. This is only possible with $w_1 = w_2 = 0$ (up to any symmetry transformation on $\langle \tilde{l}_{\text{R}} \rangle$). Once $({\tilde{l}_{\text{R}}}^{I})_R$ has obtained its VEV, there are physically different VEV settings in the Higgs bi-doublet we should explore separately: $v_1 = v \neq 0$ and $v_2 = 0$ (Case A), $v_2 = v \neq 0$ and $v_1 = 0$ (Case B), and $v_1 \neq 0$ and $v_2 \neq 0$ (Case C). In the following we will explore the details of Case A and B. Case C, where both Higgs VEVs are non-zero, is cumbersome and can be left for a future work. The reason for this is that for that case the masses in the scalar sector can not be obtained analytically and the type of analysis we will do in Sect. 6.1 is not feasible without further work. We will thus take a closer look at scenario I and the first two cases described above.

Fields	$(\text{Mass})^2$	(Y, D, E)
${\mathcal{D}_{\text{s}}}^c$	$m_q^2 \equiv \frac{1}{2} Y_\gamma^2 w^2$	$(+1/3, 2/3, -1/3)$

Table II.10: Massive quark field and its quantum numbers after the $\text{SU}(2)_{\text{R}} \times \text{U}(1)_{\text{L+R}}$ breaking.

Case A

Given the VEV setting

$$\langle ({\tilde{l}_{\text{R}}}^I)_R \rangle = \begin{pmatrix} 0 & 0 \\ 0 & \frac{w}{\sqrt{2}} \end{pmatrix}, \qquad \langle \tilde{h}_R^L \rangle = \begin{pmatrix} 0 & 0 \\ 0 & \frac{v}{\sqrt{2}} \end{pmatrix}, \tag{II.38}$$

the extremal conditions become

$$\left(m_h^2 + v^2 \lambda_a - \frac{1}{2} w^2 \lambda_f \right) v = 0\,, \quad \left(m_R^2 + w^2 \lambda_b - \frac{1}{2} v^2 \lambda_f \right) w = 0. \tag{II.39}$$

With $v \neq 0$ and $w \neq 0$, there is only one unbroken gauge symmetry generator

$$T_{\text{E.M.}} = T_{\text{L}}^3 + T_{\text{R}}^3 + \frac{1}{2} T_{\text{L+R}} \tag{II.40}$$

which corresponds exactly to the generator of $\text{U}(1)_{\text{E.M.}}$ in our previous analysis with only $({\tilde{l}_{\text{R}}}^I)_R$ VEV. There are also two new U(1) global symmetries in addition to $\{\text{U}(1)_{\text{G}} \times \text{U}(1)_{\text{B}}\}$ with generators

$$T_{\text{V}} = T_{\text{X}} - T_{\text{L+R}} + 4T_{\text{L}}^3\,, \quad T_{\text{W}} = T_{\text{F}}^3 - \frac{1}{2} T_{\text{L+R}} \tag{II.41}$$

The mass eigenstates in the scalar sector after this symmetry breaking are shown in Tab. II.11. In particular, there is one real state which obtains a mass of $\mathcal{O}(v)$ when $v \ll w$, which would be the candidate for the 125 GeV SM Higgs particle.

Case B

A second possible case follows from the VEV assignment

$$\langle ({\tilde{l}_{\text{R}}}^I)_R \rangle = \begin{pmatrix} 0 & 0 \\ 0 & \frac{w}{\sqrt{2}} \end{pmatrix} \qquad \langle \tilde{h}_R^L \rangle = \begin{pmatrix} \frac{v}{\sqrt{2}} & 0 \\ 0 & 0 \end{pmatrix}. \tag{II.42}$$

The extremal conditions in this case will be

$$\left(m_H^2 + v^2 \lambda_a + \frac{1}{2} w^2 (-\lambda_f + \lambda_g) \right) v = 0\,, \quad \left(m_R^2 + w^2 \lambda_b + \frac{1}{2} v^2 (-\lambda_f + \lambda_g) \right) w = 0. \tag{II.43}$$

The mass eigenstates in the scalar sector after this symmetry breaking are shown in Tab. II.12, where as in the previous case the spectrum contains a candidate for the SM Higgs particle. The VEV setting (II.42) leaves the same gauged $\mathrm{U}(1)_{\mathrm{E.M.}}$ and global $\mathrm{U}(1)_{\mathrm{W}}$ unbroken as the vev setting in Eq. (II.38). However, the $\mathrm{U}(1)_{\mathrm{V}}$ is replaced by $\mathrm{U}(1)_{\mathrm{V}'}$ which is generated by

$$T_{\mathrm{V}'} = T_{\mathrm{X}} - T_{\mathrm{L+R}} - 4T_{\mathrm{L}}^3 \,. \tag{II.44}$$

Fields	$(\mathrm{Mass})^2$	Comment
$s_\alpha(\tilde{l}_{\mathrm{R}}{}^2)_1 - c_\alpha \tilde{h}_1^2$	$\frac{1}{2}(v^2+w^2)\lambda_g$	
$(\tilde{l}_{\mathrm{R}}{}^1)_1$	$\frac{1}{2}v^2\lambda_g + 2w^2\lambda_i$	
$\tilde{h}_1^1$	$\frac{1}{2}w^2\lambda_g + 2v^2\lambda_j$	
$c_\eta \Re[\tilde{h}_2^2] + s_\eta \Re[(\tilde{l}_{\mathrm{R}}{}^2)_2]$	$v^2\lambda_a + w^2\lambda_b + \sqrt{\dots}$	
$c_\eta \Re[(\tilde{l}_{\mathrm{R}}{}^2)_2] - s_\eta \Re[\tilde{h}_2^2]$	$v^2\lambda_a + w^2\lambda_b - \sqrt{\dots}$	$\sim \mathcal{O}(v^2)$ for $\tan\alpha \sim 0$
$(\tilde{l}_{\mathrm{R}}{}^1)_2$	0	Global Goldstone
$\tilde{h}_2^1$	0	Gauge Goldstone
$\Im[\tilde{h}_2^2]$	0	Gauge Goldstone
$\Im[(\tilde{l}_{\mathrm{R}}{}^2)_2]$	0	Gauge Goldstone
$c_\alpha(\tilde{l}_{\mathrm{R}}{}^2)_1 + s_\alpha \tilde{h}_1^2$	0	Gauge Goldstone

Table II.11: Case A: Mass eigenstates in $\tilde{h}$ and $\tilde{l}_{\mathrm{R}}$ after SSB of the LR symmetry group to $\mathrm{U}(1)_{\mathrm{E.M.}}$ and the corresponding tree-level masses. Here, $\sqrt{\dots} = \sqrt{(v^2\lambda_a - w^2\lambda_b)^2 + (vw\lambda_f)^2}$, $c_\alpha = \cos\alpha$, $s_\alpha = \sin\alpha$ with $\tan\alpha = v/w$ and $c_\eta = \cos\eta$, $s_\eta = \sin\eta$ with η being the corresponding mixing angle whose explicit form we omit for simplicity.

6 Numerical results

The main question to answer for the proposed framework is whether for a consistent set of parameters of the trinification theory, the RG running in the effective LR-symmetric theory can trigger the radiative breaking of $\mathrm{SU}(2)_{\mathrm{R}} \times \mathrm{U}(1)_{\mathrm{L+R}}$, and for what regions in parameter space this happens. In addition, we will explore under which circumstances we can get close to a realistic SM-like scalar sector, with a light $\mathrm{SU}(2)_{\mathrm{L}}$ scalar doublet with hypercharge $Y = +1/2$ remaining in the spectrum at lower energies (which potentially can induce EW symmetry breaking). The resulting low-scale mass spectrum after the radiative symmetry breaking will depend on our choice of initial parameters only, but the connection between the initial values of the parameters and the resulting mass spectrum is not obvious. In order to explore it, we implemented a parameter scanning framework using numerical integration of the RG equations together with a simulated annealing (SA) procedure to scan over the possible initial values of high-scale parameters.

We calculated one-loop β-functions for the effective LR-symmetric model using the package `pyr@te` [57], which are written in Appendix II.A.

Fields	$(\text{Mass})^2$	Comment
$c_\alpha \Re[\tilde{h}_2^1] + s_\alpha \Re[(\tilde{l}_{\mathrm{R}}{}^2)_1]$	$-\frac{1}{2}(v^2+w^2)\lambda_g$	
$s_\alpha \Im[(\tilde{l}_{\mathrm{R}}{}^2)_1] - c_\alpha \Im[\tilde{h}_2^1]$	$-\frac{1}{2}(v^2+w^2)\lambda_g$	
$(\tilde{l}_{\mathrm{R}}{}^1)_1$	$-\frac{1}{2}v^2\lambda_g + 2w^2\lambda_i$	
$\tilde{h}_2^2$	$-\frac{1}{2}w^2\lambda_g + 2v^2\lambda_j$	
$c_\kappa \Re[\tilde{h}_1^1] + s_\kappa \Re[(\tilde{l}_{\mathrm{R}}{}^2)_2]$	$v^2\lambda_a + w^2\lambda_b + \sqrt{\dots}$	
$c_\kappa \Re[(\tilde{l}_{\mathrm{R}}{}^2)_2] - s_\kappa \Re[\tilde{h}_1^1]$	$v^2\lambda_a + w^2\lambda_b - \sqrt{\dots}$	$\sim \mathcal{O}(v^2)$ for $\tan\alpha \sim 0$
$(\tilde{l}_{\mathrm{R}}{}^1)_2$	0	Global Goldstone
$\tilde{h}_1^2$	0	Gauge Goldstone
$\Im[\tilde{h}_1^1]$	0	Gauge Goldstone
$\Im[(\tilde{l}_{\mathrm{R}}{}^2)_2]$	0	Gauge Goldstone
$-s_\alpha \Re[\tilde{h}_2^1] + c_\alpha \Re[(\tilde{l}_{\mathrm{R}}{}^2)_1]$	0	Gauge Goldstone
$c_\alpha \Im[(\tilde{l}_{\mathrm{R}}{}^2)_1] + s_\alpha \Im[\tilde{h}_2^1]$	0	Gauge Goldstone

Table II.12: Case B: Mass eigenstates in $\tilde{h}$ and $\tilde{l}_{\mathrm{R}}$ after SSB of the LR symmetry group directly to $\mathrm{U}(1)_{\mathrm{E.M.}}$ and the corresponding tree-level masses. Here, $\sqrt{\dots} = \sqrt{(v^2\lambda_a - w^2\lambda_b)^2 + v^2w^2(\lambda_g - \lambda_f)^2}$, $c_\alpha = \cos\alpha$, $s_\alpha = \sin\alpha$ with $\tan\alpha = v/w$ and $c_\kappa = \cos\kappa$, $s_\kappa = \sin\kappa$ with κ being the corresponding mixing angle whose explicit form we omit for simplicity.

6.1 Parameter scan

Effectively, we would like to explore a five-dimensional parameter subspace of the high-scale model $\{\lambda_3, \varepsilon, \delta, g, y\}$ assuming we have fixed the scale at which trinification is broken and imposed the constraints in Eq. (II.12). This is due to the fact that in the effective LR-symmetric model after tree-level matching, the β-functions only depend on those parameters as seen in Eq. (II.26). Once a consistent set of high-scale model parameters is found, the matching can be performed and the RG equations can be numerically integrated yielding a scale dependence of the effective model parameters. The running starts from the matching scale μ_m, which is chosen to be the trinification breaking VEV,

$$\mu_m = v_3, \tag{II.45}$$

since the heavy states in the trinification theory that we integrate out have masses of $\mathcal{O}(v_3)$. The running is then terminated at a lower scale μ_r, which is defined as

$$\mu_r = \sqrt{\frac{|m_R^2(\mu_r)| + |m_h^2(\mu_r)|}{2}}, \tag{II.46}$$

since, at this scale, there are again states with masses of the same order as the renormalisation scale. These states then have to be integrated out before we can run down even further. Depending on the initial values at a high scale, m_R^2 may have run negative at this scale, thus triggering the radiative symmetry breaking we are looking for. However, we have to guarantee that, at the stopping scale μ_r, the minimisation conditions for the VEV setting described in Eq. (II.29) are satisfied (i.e. that all the squared masses in Tab. II.8 are positive).

Simulated annealing

In order to find viable parameter space points in the high-scale theory, we implemented the SA algorithm together with the numerical integration of β functions. The SA is a method for estimating the global minimum of a given function $E(\{p_i\})$ in a multi-dimensional parameter space $\{p_i\}$ [58].

If we interpret the function $E(\{p_i\})$ as the energy of a system whose physical state is defined by $\{p_i\}$, and imagine that the system is in thermal contact with a heat bath with temperature T, we can let this system approach its equilibrium state by employing the Metropolis algorithm. That is, we start with a random set of initial parameters, and propose random updates $\{p_i\} \to \{p'_j\}$ that are accepted with probability

$$P_{\text{acc}}(\{p_i\} \to \{p'_i\}) = \begin{cases} 1 & \text{if } E(\{p'_i\}) < E(\{p_i\}) \\ \mathrm{e}^{(E(\{p_i\})-E(\{p'_i\}))/T} & \text{otherwise,} \end{cases} . \tag{II.47}$$

Given a constant T, this procedure fulfils detailed balance w.r.t. the canonical ensemble $\mathcal{P}(\{p_i\}) \propto \mathrm{e}^{-E(\{p_i\})/T}$, which in the limit $T \to \infty$ is a flat distribution where all $\{p_i\}$ are equally likely, while in the limit $T \to 0$ becomes highly peaked for the ground states of the system, i.e. the states $\{p_i\}$ that minimise $E(\{p_i\})$.

The SA works by initialising the system at a large temperature, and then running the Metropolis algorithm while slowly (i.e. adiabatically) decreasing the temperature until $T \sim 0$. In this way, $E(\{p_i\})$ is minimised and the corresponding parameter space points $\{p_i\}$ are found. This procedure has the advantage of being easy to implement while also being less prone to get stuck in local minima compared to for example a gradient descent method since local energy barriers can be overcome by "thermal fluctuations".

For the purpose of this work we defined

$$E = \begin{cases} 10 & \text{if } m_R^2(\mu) > 0 \,\forall\, \mu \in (m_Z, \mu_m) \\ 5 + \frac{\min(m_i^2)}{\max(|m_i^2|)} & \text{if } m_j^2 < 0 \text{ for some } j \\ 2\frac{\min(m_{h_i}^2)}{\min(m_q^2, m_{Z'}^2, m_{W'}^2)} + \frac{\min(m_{h_i}^2)}{\max(m_q^2, m_{r_2}^2, m_{Z'}^2, m_{W'}^2)} & \text{if } m_R^2(\mu_r) < 0 \text{ and } m_j^2(\mu_r) > 0 \end{cases} \tag{II.48}$$

where $E = E(\lambda_3, \epsilon, \delta, g, y)$ and $m_i^2 = (m_q^2, m_{h_i}^2, m_{R_i}^2, m_{Z'}^2, m_{W'}^2)$ are the masses after radiative symmetry breaking evaluated at the scale μ_r. Minimisation of this function guarantees that we find parameter space points where m_R^2 runs negative while also introducing a bias towards parameters that yield a light Higgs-like $\mathrm{SU}(2)_{\mathrm{L}}$ doublet.

Choosing the trinification breaking scale

One of the free parameters of the proposed framework is the scale at which trinification symmetry is spontaneously broken. This scale, which is the starting point for all the

successive symmetry breakings at low scales, is defined only by the trinification breaking VEV (II.7). In order to get an idea of what scales are sensible to explore, we integrated the one-loop RG equations for gauge couplings in the effective LR-symmetric model, an easy task due to the fact that at one-loop the β-functions only depend on the gauge couplings themselves. It was possible then to relate the trinification breaking scale to the measured values of the SM $\mathrm{SU(2)_L}$, $\mathrm{U(1)_Y}$ and $\mathrm{SU(3)_C}$ gauge couplings. We found that for a trinification breaking scale of $\mu_m = 10^{12.2}$ GeV, the boundary condition of $g_0 = 0.61$ leads roughly to the SM values at m_Z. In Fig. II.1 we show the result from integrating the gauge coupling β-functions from μ_m down to m_Z. Because the β-functions only depend on the gauge couplings at one-loop, this running is valid for any parameter space point with $g_0 = 0.61$ as boundary condition. We show in the same plot

$$g_{\mathrm{Y}}(\mu) \equiv \frac{2\, g_{\mathrm{R}}\, g_{\mathrm{L+R}}}{\sqrt{4 g_{\mathrm{L+R}}^2 + g_{\mathrm{R}}^2}} \tag{II.49}$$

which would be the matching condition for g_1, the hypercharge gauge coupling, as function of the scale μ. Note however that in Fig. II.1, the running is performed all the way down to the EW scale m_Z, without decoupling the massive states at μ_r. A more accurate calculation would implement this intermediate step, which would alter the slopes of the lines in Fig. II.1 at scales below μ_r. Therefore, this calculation should only serve as a very rough estimate of the numerical values of the matching scale (and the value of the trinification gauge coupling at this scale).

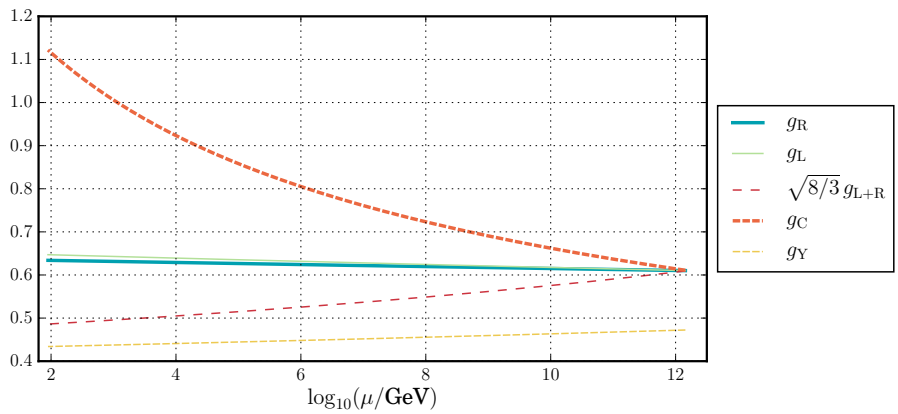

Figure II.1: One-loop RG evolution of gauge couplings in the effective LR-symmetric model and matching condition for the hypercharge coupling g_{Y} with $g_0 = 0.61$. A trinification breaking scale of $\mu_m \approx 10^{12.2}$ GeV leads to roughly SM values for $g_{\mathrm{L}} \equiv g_2$, $g_{\mathrm{C}} \equiv g_3$ and $g_{\mathrm{Y}} \equiv g_1$ at $\mu \approx m_Z$.

6.2 Regions of parameter space with radiative breaking

Using the framework described above we found 22081 parameter space points by running our implementation of the SA algorithm allowing for high-scale parameters within the unitarity bounds and for a trinification breaking scale of $\mu_m = 10^{12.2}$ GeV. Remarkably,

we found that the considered model naturally contains large parameter space regions where $\mathrm{SU}(2)_\mathrm{R}\times\mathrm{U}(1)_\mathrm{L+R}$ is radiatively broken down to $\mathrm{U}(1)_\mathrm{Y}$ while a light Higgs doublet remains in the spectrum at the stopping scale μ_r. In Fig. II.2 we show the allowed regions in several slices of the high-scale parameter space. Most of the features of these regions can be explained by the structure of the mass-parameter β-functions in Eqs. (II.84) and (II.83). Our algorithm selects points where m_R^2 would have a positive β-function so that it could run to negative values at low scales. For example, we see that the allowed parameter space region always satisfies $\epsilon < \delta$ which translates into the inequality $m_R^2 < m_h^2$ at the matching scale. Although one can find points for which (II.84) is positive and $\epsilon > \delta$, for such points m_h^2 value runs negative before m_R^2 does. This would trigger an unwanted simultaneous breaking of $\mathrm{SU}(2)_\mathrm{L}$ and $\mathrm{SU}(2)_\mathrm{R}$ with the same VEV, as opposed to the desired situation where the VEV responsible for $\mathrm{SU}(2)_\mathrm{R}\times\mathrm{U}(1)_\mathrm{L+R}\to\mathrm{U}(1)_\mathrm{Y}$ is much larger than the Higgs VEV that triggers the EW symmetry breaking.

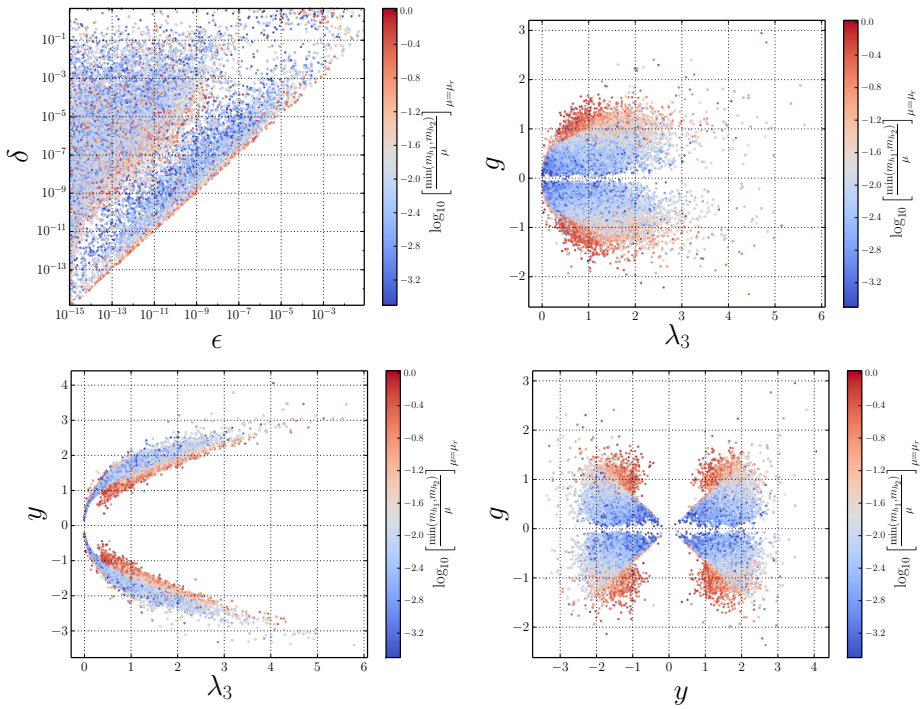

Figure II.2: Regions of the high-scale model parameter space with the radiative $\mathrm{SU}(2)_\mathrm{R}\times\mathrm{U}(1)_\mathrm{L+R}$ symmetry breaking down to $\mathrm{U}(1)_\mathrm{Y}$ by RG evolution in the effective LR-symmetric model. The ranges for the scan were chosen such as to preserve the unitarity property at tree-level. The colours indicate the lightness of the lightest Higgs doublet compared to the renormalization scale at the stopping scale μ_r.

We selected the most promising candidates from the results of the scan by requiring the maximal hierarchy between a light Higgs-like doublet and heavy exotic particles at the scale μ_r while having parameters within the perturbativity constraints. In Fig. II.3 we

show the running of mass parameters before and after the radiative $\mathrm{SU}(2)_\mathrm{R} \times \mathrm{U}(1)_{\mathrm{L+R}}$ symmetry breaking for a benchmark point satisfying those conditions. We find that it is possible to find some mass hierarchy at the symmetry breaking scale, with a Higgs-like scalar doublet coming from $\tilde{h}$ with masses up to two orders of magnitude lighter than the rest of the mass spectrum. In addition, we also observe that a complex scalar coming from $\tilde{l}_\mathrm{R}$ prefers to have a small mass at μ_r (this is the dark solid curve in Fig. II.3, corresponding to $m^2_{r_2}$ in Tab. II.8). This scalar is a singlet under $\mathrm{SU}(2)_\mathrm{L}$ while having unit hypercharge, meaning that it will have unit electric charge after EW symmetry breaking. At present, it is not clear to what extent this state accumulates a much larger mass when evolving from μ_r down to the EW scale.

Although the gauge couplings of the effective LR-symmetric model start with the same values due to the matching conditions and the $\mathbb{Z}_3$ symmetry in the high-scale model, the RG evolution induces a splitting as seen in Fig. II.1. It is interesting to note that although we did not impose the boundary condition $g_0 = 0.6$ for the SA algorithm, the allowed points in parameter space seem to be consistent with the boundary condition as seen in the upper right plot in Fig. II.2. We also note from Fig. II.1 that there is an approximate relation $g_\mathrm{L} \approx g_\mathrm{R}$ that is exact at the matching scale, while a small splitting between g_L and g_R is generated in the low energy limit. This observation points towards an approximate $\mathbb{Z}_2$ symmetry between the $\mathrm{SU}(2)_\mathrm{L}$ and $\mathrm{SU}(2)_\mathrm{R}$ gauge groups. In fact, we can trace the origin of the radiative $\mathbb{Z}_2$ breaking to the scalar sector in the effective model, where the choice of keeping only $\tilde{l}_\mathrm{R}$ and $\tilde{h}$ leads to $\beta_{g_\mathrm{L}} \neq \beta_{g_\mathrm{R}}$. This is because only $\tilde{h}$ transforms under $\mathrm{SU}(2)_\mathrm{L}$ (while both $\tilde{l}_\mathrm{R}$ and $\tilde{h}$ transform under $\mathrm{SU}(2)_\mathrm{R}$).

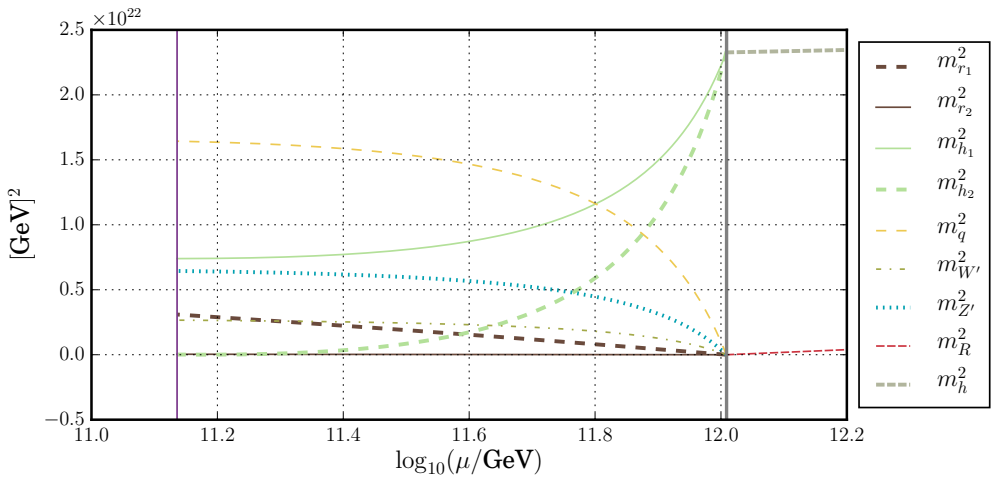

Figure II.3: One-loop RG evolution of the mass parameters before and after the radiative $\mathrm{SU}(2)_\mathrm{R} \times \mathrm{U}(1)_{\mathrm{L+R}}$ symmetry breaking down to $\mathrm{U}(1)_\mathrm{Y}$ for an example point. The two vertical lines mark the scales at which m^2_R first runs negative (right) and the scale μ_r at which the RG running is terminated (left), respectively.

This serves to prove that in the proposed framework it is possible to trigger the full symmetry breaking down to the SM gauge group by means of the trinification breaking VEV (II.7) only, while at the same time generating a desired hierarchy at low energy

scales. In other words, in the model proposed in this work, the RG evolution makes it possible to have a highly symmetric trinification model whose gauge group is naturally broken down to the SM gauge group.

For the alternative case of breaking directly to $\mathrm{U}(1)_{\mathrm{E.M.}}$ discussed in Sect. 5.2 we performed a similar analysis as we did above by preparing a SA scan to find parameter space points looking for a possibility for the radiative breaking to $\mathrm{U}(1)_{\mathrm{E.M.}}$. For case A (discussed in Sect. 5.2) 6080 points were produced during three weeks where both m_h^2 and m_R^2 ran negative. However, none of the points showed positive squared masses in the scalar sector, i.e. no points were found where the desired vacuum was a minimum of the scalar potential. Similarly, for case B (discussed in Sect. 5.2) we run a SA scan that produced 32631 points, again with none of them showing stable minima with the desired radiative symmetry breaking. What this means is that as far as our analysis could tell, when m_h^2 and m_R^2 became negative through RG running, the true minimum of the scalar potential did not exhibit $\mathrm{U}(1)_{\mathrm{E.M.}}$ as a remaining symmetry, thus making it unviable as a phenomenological model within the proposed framework.

7 Discussion and future work

7.1 Fermion sector at one-loop

In the present analysis, many Yukawa couplings (and also the Majorana mass m_{Φ^s}) in the effective LR-symmetric model are zero simply due to the tree-level matching procedure. However, this will no longer be true once the matching and running are performed at a higher loop level. Although the full one-loop matching and two-loop running analysis is necessary to obtain precise numerical values that is planned for a future work, it is interesting to understand which diagrams will lead to non-vanishing matching conditions for some of the parameters in Eq. (II.27).

We first note that m_{Φ^s} receives a non-zero contribution from the diagram in Fig. II.4, with the trinification VEV in Eq. (II.7). From this we can estimate that m_{Φ^s} will be suppressed with respect to the trinification breaking scale v_3 as

$$m_{\Phi^s}^{(1-\mathrm{loop})} \sim \left(\frac{y^3}{(4\pi)^2} \cdot \frac{\gamma}{v_3} \right) v_3. \tag{II.50}$$

If the trinification Yukawa coupling y and the scalar tri-linear coupling γ are sufficiently large, it might be appropriate to integrate out Φ^s along with the heavy trinification-scale quarks in Tab. II.6, so that it no longer appears in the effective LR-symmetric model. If instead y and γ are small, the suppression factor in Eq. (II.50) can easily be very small such that $m_{\Phi^s} \sim m_h, m_R$. At present, as was shown in Sect. 6, we see no preference for neither large nor small values of y and γ, and both possibilities thus remain open.

Next, we turn to the Yukawa interactions that are generated by the diagrams in Fig. II.5. These diagrams are of interest when the external leg $\tilde{L}$ corresponds to one of the two

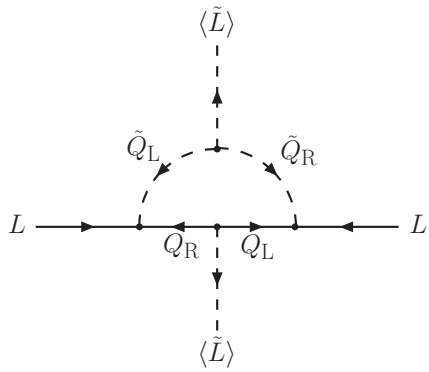

Figure II.4: A diagram in the trinification theory that constitutes the one-loop contribution to the matching onto the Majorana Φ^s mass, m_{Φ^s}, in the effective LR-symmetric model.

remaining scalars in the effective LR-symmetric model, namely $\tilde{h}$ and $\tilde{l}_{\rm R}$. One can then show that the diagram is non-vanishing when the external fermion legs are such that the loop corresponds to Yukawa interactions of the types

$$\begin{aligned} &(\tilde{l}^*_{{\rm R}I})^R\ (l_{\rm R}{}^I)_R\,\Phi^s + \text{c.c.}\,, \\ &(\tilde{l}^*_{{\rm R}I})^R\ (l_{\rm R}{}^s)_R\,\Phi^I + \text{c.c.}\,, \\ &\tilde{h}^{*R}_L\ (l_{\rm L}{}^s)^L\,(l_{\rm R}{}^s)_R + \text{c.c.}\,, \end{aligned} \tag{II.51}$$

i.e. the Yukawa couplings Y_γ, Y_δ and Y_η receive a non-zero contribution at one-loop. In particular, when $\langle\tilde{l}_{\rm R}\rangle \neq 0$ the upper two interaction terms in Eq. (II.51) will provide masses to two generations of right-handed neutrinos. Note, however, that right-handed neutrinos receive a *Dirac* mass that is formed together with two generations of Φ. We can identify the last interaction term in Eq. (II.51) as containing the Yukawa term for SM leptons of the third generation.

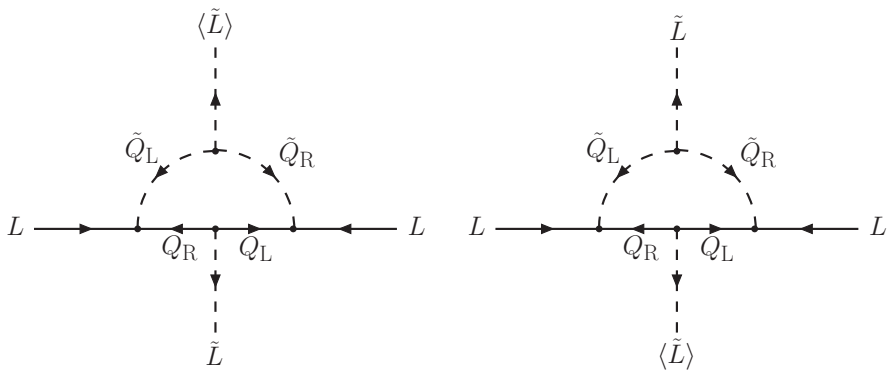

Figure II.5: These two diagrams give rise to Yukawa terms that, in turn, provide Dirac masses for two generations of right-handed neutrinos and Φ's, as well as for SM leptons of the third generation.

7.2 One-loop corrections to masses of light scalars

Although we have performed tree-level matching down to an effective theory, its important to understand whether the scalars $\tilde{h}_R^L$, $(\tilde{l}_{\rm R}{}^I)_R$ can remain light as soon as the higher-order corrections are considered. In general, this may not be the case and thus it would no longer be justified to keep those light scalars in the low-energy theory. Even if the corrections would keep the scalars sufficiently light, the particular values for their masses also affect the RG flow potentially leading to different conclusions regarding the radiative LR-symmetry breaking.

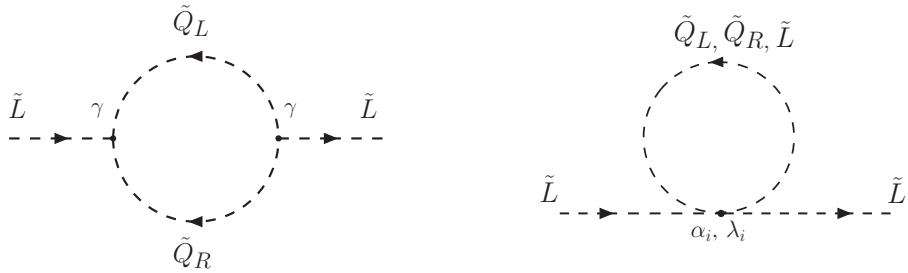

Figure II.6: Class of diagrams with a non-vanishing contribution to m_h^2 and m_R^2 in the trinification theory.

It turns out that the only non-vanishing one-loop contributions (in the zero external momenta approximation) to m_h^2 and m_R^2 come from the type of diagrams shown in Fig. II.6. Any other topology will either (i) be forbidden by the trinification symmetry (such as fermion loops), or (ii) vanish once the zero momentum approximation is taken into account.

The tri-linear coupling γ plays an important role in the one-loop matching conditions. Namely, it determines the size of the one-loop corrections to m_h^2 and m_R^2 coming from the left panel in Fig. II.6. It thus suffices to make $\gamma/v_3 \ll 1$ in order to keep those corrections small[3]. For the second type of diagrams in Fig. II.6 (right), the corrections become functions of λ_i but also α_i (the tree-level masses are only functions of λ_i). As long as the coloured scalars remain heavy, choosing appropriate values for α_i would give us enough freedom for $\tilde{h}_R^L$, $(\tilde{l}_{\rm R}{}^I)_R$ to remain light.

In the tree-level study of the model that has been presented here, we thus assume that the scalars are light leaving the specifics of the physical mechanism which appropriately tunes the values for γ and α_i as well as the corresponding effect on the RG evolution for future work. However, we expect that the qualitative conclusions reached in this work would still be valid when accounting for the higher-order corrections due to the

[3]The model presented here, while inspired by SUSY, is not supersymmetric. However, as long as SUSY is concerned, $\gamma/v_3 \ll 1$ condition could be justified by γ corresponding to a soft-SUSY breaking term whose natural values are around the SUSY breaking scale.

fact that, as discussed in section 6, the regions of the effective theory parameter space where the radiative LR-symmetry breaking takes place are quite broad.

7.3 The low-energy LR-symmetric model with additional light Higgs-doublets

We have shown that the proposed model brings an intriguing possibility of the radiative $\mathrm{SU(2)_R} \times \mathrm{U(1)_{L+R}} \to \mathrm{U(1)_Y}$ breaking. To do this, we integrated out the maximal number of fields in the high scale trinification theory in order to make the effective LR-symmetric model as simple as possible. Although the radiative symmetry breaking in such a toy model is realized, we show in this section that in order to accurately generate all fermion masses in the SM, we need to consider the case where more scalars are present in the effective theory. This is due to the fact that some mass terms are forbidden by the global group that remains unbroken in the scenario considered in Sect. 4. However, we note that the interplay between scalar mass parameters and their β-functions allowing m_R^2 to run negative, will still be present when integrating out fewer Higgs doublets. Although a more detailed study will be needed to find explicit regions of parameter space with the radiative symmetry breaking, we expect that the qualitative conclusions in Sect. 6 will not be changed.

SM quarks

Trinification	effective LR-symmetric model	$\mathrm{U(1)_E}$	$\mathrm{U(1)_G}$
$(Q_{\mathrm{L}}{}^2)^c_2$	$(\mathcal{Q}_{\mathrm{L}}{}^2)^c_2$	$-1/2$	$-1/6$
$(Q_{\mathrm{L}}{}^3)^c_1$	$(\mathcal{Q}_{\mathrm{L}}{}^s)^c_1$	$-1/2$	$-2/3$
$(Q_{\mathrm{L}}{}^3)^c_2$	$(\mathcal{Q}_{\mathrm{L}}{}^s)^c_2$	$-1/2$	$-2/3$
$(Q^\dagger_{\mathrm{R}}{}_3)^c_1$	$(\mathcal{Q}^{\dagger\ s}_{\mathrm{R}})^1_c$	$+1/2$	$+1/3$
$(Q^\dagger_{\mathrm{R}}{}_3)^c_2$	$(\mathcal{Q}^{\dagger\ s}_{\mathrm{R}})^2_c$	$+1/2$	$+1/3$
$(Q^\dagger_{\mathrm{R}}{}_3)^c_3$	$(D^{\dagger\ s}_{\mathrm{R}})^3{}_c$	$+1/2$	$+5/6$

Table II.13: Components in the trinification quark tri-triplets (and the corresponding fields in the effective LR-symmetric model) that should build up the left- and right-handed components of the lightest SM u, d, s quarks. In the current realisation of the model, the mass terms for these quarks are forbidden by the global $\{\mathrm{U(1)_E} \times \mathrm{U(1)_G}\}$ group that is left unbroken by the two Higgs VEVs.

With tree-level matching (and one-loop running) the only non-zero Yukawa coupling with SM particles is Y_ζ in Eq. (II.27). Arranging the $\tilde{h}$ and $\tilde{l}_{\mathrm{R}}$ VEVs as in Eq. (II.37), we see that, through this term, v_1 gives masses to two up-type quarks which could be identified with the top and charm quarks of the SM. On the other hand, the VEV v_2 gives a mass to one down-type quark (which can be identified with the bottom quark) and also a contribution to the mass of the heavy down-type quark in Tab. II.10. However, there still remain one up-type and two down-type quarks that are massless at tree-level, which should be identified with the lightest *u, d, s* quarks in the SM. The corresponding left-handed and right-handed components are shown in Tab. II.13

along with their charges under the global group $\{\mathrm{U}(1)_\mathrm{E} \times \mathrm{U}(1)_\mathrm{G}\}$, which is unbroken by the Higgs VEVs in Eq. (II.37). Since none of the Q_L fields have the same global U(1) charges as any of the $Q_\mathrm{R}^\dagger$ fields in Tab. II.13, it is not possible to generate Dirac masses for the *u, d, s* quarks since those mass terms would violate $\{\mathrm{U}(1)_\mathrm{E} \times \mathrm{U}(1)_\mathrm{G}\}$. However, there is a simple way to accommodate these masses. For regions of parameter space with light Higgs doublets in the effective LR-symmetric model, their VEVs would break $\{\mathrm{U}(1)_\mathrm{E} \times \mathrm{U}(1)_\mathrm{G}\}$ enabling the radiative generation of the light quark mass terms.

Colour singlet fermions

As in the quark sector, many colour neutral fermion mass terms are forbidden by the global group that is left unbroken by the two Higgs VEVs. By looking at the global U(1) charges of the components of the colour neutral fermions, we find that the only electrically charged and electrically neutral fermions that can participate in a fermion bilinear term are contained in

$$\begin{aligned}
\psi_\mathrm{C} &= \big(\ (l_\mathrm{R}{}^s)_1 \quad (l_\mathrm{L}{}^s)^1 \quad (H^2)^1_2 \ \big|\ (H^s)^1_2 \quad (H^s)^2_1 \quad (l_\mathrm{R}{}^2)_1 \ \big)^T, \\
\psi_\mathrm{N} &= \big(\ (l_\mathrm{R}{}^s)_2 \quad (H^2)^1_1 \quad (H^2)^2_2 \quad \Phi^2 \quad (l_\mathrm{L}{}^s)^2 \ \big|\ (l_\mathrm{R}{}^2)_2 \quad (H^s)^1_1 \quad (H^s)^2_2 \quad \Phi^s \ \big)^T,
\end{aligned} \tag{II.52}$$

respectively. For all other colour neutral fermions, there is no fermion field with opposite U(1) charges such that they together could form a mass term. In particular, note that $\psi_{\mathrm{C,N}}$ contain no first generation colour singlet fermions.

Generally, we can then write the mass terms for the colour neutral fermions as

$$\frac{1}{2}\psi_\mathrm{C}^T\, M_\mathrm{C} \psi_\mathrm{C} + \frac{1}{2}\psi_\mathrm{N}^T\, M_\mathrm{N} \psi_\mathrm{N} + \text{c.c.} \tag{II.53}$$

Upon demanding invariance under the global U(1) groups (and of course $\mathrm{U}(1)_\mathrm{E.M.}$), we find that the mass matrices $M_{\mathrm{C,N}}$ have the following structure:

$M_\mathrm{C} =$ 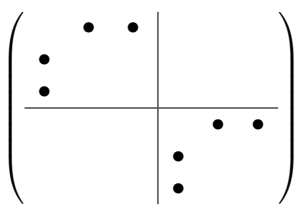 , $M_\mathrm{N} =$ 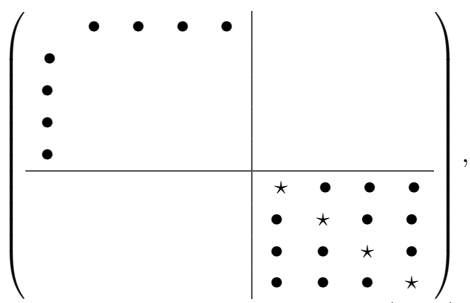 , (II.54)

where entries marked with a '•' ('⋆') denote the Dirac (Majorana) contributions that are allowed to be non-zero. These would amount to two electrically charged massive Dirac fermions (which we would have to identify with the τ-lepton and muon in the SM), one massive electrically neutral Dirac fermion, and four electrically neutral Weyl fermions that receive both Dirac and Majorana mass contributions.

The tri-triplet $(L^i)^l_r$ contains twelve electrically charged Weyl fermions, meaning that we will still have eight electrically charged Weyl fermions whose mass terms are forbidden by the unbroken global group. Out of the remaining fifteen electrically neutral components in $(L^i)^l_r$, at least nine Weyl fermions are necessarily massless. To make more components in $(L^i)^l_r$ massive (to evade obvious inconsistencies with phenomenology), we have to include more Higgs doublets in the effective LR-symmetric model originating from the high-scale trinification theory.

7.4 CKM mixing with additional Higgs doublets

In the previous section, we have seen that in order to explain the observed fermionic mass spectra, more components of $\tilde{L}$ should be kept in the effective LR-symmetric model. By looking at the CSS mass spectra, we see that this will be possible when

$$\lambda_{2,3,4} \ll \lambda_1 \,, \tag{II.55}$$

in which case the fields

$$(\tilde{L}^I)^L_R \,, \quad (\tilde{L}^I)^3_R \,, \quad (\tilde{L}^I)^L_3 \,, \quad (\tilde{L}^3)^L_R \quad , \tag{II.56}$$

would all remain in the effective LR-symmetric model (see Tab. II.3). In this case, the CSS potential exhibits an approximate O(54) symmetry. Although this increase in the number of scalar fields would lead to a substantial increase in complexity in the low-energy theory, we are confident that the radiative $\mathrm{SU(2)_R \times U(1)_{L+R} \to U(1)_Y}$ breaking will still be present as mentioned above. In this section, we show in a straightforward tree-level analysis, that the structure of the SM Cabibbo-Kobayashi-Maskawa (CKM) mixing matrix in the Cabibbo form emerges as a consequence of $\mathrm{SU(3)_F}$ if VEVs are strategically placed in the tri-doublet $(\tilde{L}^I)^L_R$. These VEVs would be allowed at lower scales when keeping the extra fields in the effective theory after SSB of trinification.

Consider the following VEV setting:

$$\langle(\tilde{L}^1)^L_R\rangle = \tfrac{1}{\sqrt{2}} \begin{pmatrix} h_1 & 0 \\ 0 & h_2 \end{pmatrix} \,, \quad \langle(\tilde{L}^2)^L_R\rangle = \tfrac{1}{\sqrt{2}} \begin{pmatrix} h_3 & 0 \\ 0 & 0 \end{pmatrix} \tag{II.57}$$

In terms of the full trinification tri-triplet $\tilde{L}$, this means that

$$\langle\tilde{L}^1\rangle = \tfrac{1}{\sqrt{2}} \begin{pmatrix} h_1 & 0 & 0 \\ 0 & h_2 & 0 \\ 0 & 0 & 0 \end{pmatrix} \,, \qquad \langle\tilde{L}^2\rangle = \tfrac{1}{\sqrt{2}} \begin{pmatrix} h_3 & 0 & 0 \\ 0 & 0 & 0 \\ 0 & w & 0 \end{pmatrix} \,, \qquad \langle\tilde{L}^3\rangle = \tfrac{1}{\sqrt{2}} \begin{pmatrix} 0 & 0 & 0 \\ 0 & 0 & 0 \\ 0 & 0 & v_3 \end{pmatrix} \,. \tag{II.58}$$

where we have also indicated the trinification and LR symmetry breaking VEVs v_3 and w. The VEV setting (II.58) leaves the group

$$\mathrm{SU(3)_C \times U(1)_{E.M.} \times \{U(1)_P \times U(1)_B\}} \tag{II.59}$$

unbroken, where the global $\mathrm{U(1)_P}$ is generated by

$$T_\mathrm{P} \equiv \frac{1}{\sqrt{3}} \left(T^8_\mathrm{R} + T^8_\mathrm{F}\right) . \tag{II.60}$$

For a consistency with the SM, we have to impose the following hierarchy between the above VEVs

$$v \gg w \gg h_{1,2,3} \sim 10^2 - 10^3\,\mathrm{GeV}\,, \tag{II.61}$$

such that $h_{1,2,3}$ would correspond to the SM-breaking Higgs VEVs. In the gauge sector, at tree level one recovers one massless (photon) state

$$A_\mu = \frac{1}{2\sqrt{2}}\Big[G_{\mathrm{L}_\mu}^{\ 8} + G_{\mathrm{R}_\mu}^{\ 8} - \sqrt{3}(G_{\mathrm{L}_\mu}^{\ 3} + G_{\mathrm{R}_\mu}^{\ 3})\Big]\,, \tag{II.62}$$

$W^\pm$ bosons

$$W_\mu^\pm = G_{\mathrm{L}_\mu}^{\ 1,2}\,, \qquad m_W^2 \simeq \frac{1}{8}\,g^2 \sum_i h_i^2\,, \tag{II.63}$$

and the Z^0 boson

$$Z_\mu^0 = \frac{1}{2\sqrt{10}}\Big[5G_{\mathrm{L}_\mu}^{\ 3} - 3G_{\mathrm{R}_\mu}^{\ 3} + \sqrt{3}(G_{\mathrm{L}_\mu}^{\ 8} + G_{\mathrm{R}_\mu}^{\ 8})\Big]\,, \qquad m_Z^2 \simeq \frac{2}{10}\,g^2 \sum_i h_i^2\,, \tag{II.64}$$

in a rough consistency with the SM. Besides, at w scale one finds heavy $W'^\pm$ and Z'^0 bosons

$$W'^\pm_{\ \mu} = G_{\mathrm{R}_\mu}^{\ 1,2}\,, \qquad m_{W'}^2 \simeq \frac{1}{8}\,g^2 w^2\,, \tag{II.65}$$

$$Z'^0_{\ \mu} = \frac{1}{\sqrt{10}}\Big[2G_{\mathrm{R}_\mu}^{\ 3} + \sqrt{3}(G_{\mathrm{L}_\mu}^{\ 8} + G_{\mathrm{R}_\mu}^{\ 8})\Big]\,, \qquad m_{Z'}^2 \simeq \frac{5}{16}\,g^2 w^2\,, \tag{II.66}$$

which can be recognised as the heavy vector states in Tab. II.9. The other nine gauge bosons corresponding to broken (by v_3) generators of $[\mathrm{SU}(3)]^2 \to [\mathrm{SU}(2)]^2$ in trinification get masses at the GUT scale $\mu_m \sim v_3$ (see Tab. II.9).

In the quark sector with $Q_{\mathrm{L}}^i = \{u_{\mathrm{L}}^i,\, d_{\mathrm{L}}^i,\, D_{\mathrm{L}}^i\}$, we obtain three weak-singlet down-type quarks $D^i = \{D,\, S,\, B\}$ that acquire large (Dirac) tree-level masses

$$m_B \simeq \tfrac{1}{\sqrt{2}} yw\,, \qquad m_D \simeq m_S \simeq \tfrac{1}{\sqrt{2}} yv\,, \tag{II.67}$$

and hence decouple from the SM. The other three down-type states $d^i = \{d,\, s,\, b\}$ remain light

$$m_d = 0\,, \qquad m_s \simeq m_b \simeq \tfrac{1}{\sqrt{2}} yh_2\,, \tag{II.68}$$

and could thus be identified with masses of down, strange and bottom quarks of the SM, respectively, such that there is no tree-level splitting between s and b quarks, and d-quark is massless. Interestingly enough, all the down-type quarks d^i and D^i practically do not mix with each other to the leading order in small h_i/v, h_i/w and w/v ratios. Note, while it is possible to introduce a non-zero tree-level splitting between s and b quarks by imposing more VEVs in neutral components of two Higgs doublets, a non-zero d-quark mass can only acquire a non-zero value by an unnaturally small VEV in

a neutral component of a third Higgs doublet, but we do not consider this situation here. All the physical up-type quarks emerge as mixures of trinification up-type quarks $u^i = \{u^1, u^2, u^3\}$ remain light

$$u = \frac{u^1 h_1 + u^2 h_3}{\sqrt{h_1^2 + h_3^2}}\,, \qquad c = \frac{-u^2 h_1 + u^1 h_3}{\sqrt{h_1^2 + h_3^2}}\,, \qquad t = u^3\,, \tag{II.69}$$

$$m_u = 0\,, \qquad m_c \simeq m_t \simeq \tfrac{1}{\sqrt{2}} y \sqrt{h_1^2 + h_3^2}\,, \tag{II.70}$$

which could be identified with masses of up u, charm c and top t quarks of the SM, respectively. Again, in the considering scenario, there is no tree-level splitting between c and t, and it can not be generated at tree level by imposing any additional VEVs. The observed substantial charm-top and strange-bottom splittings can be in principle generated radiatively by (i) RG runnings of the corresponding Yukawa couplings which will have different slopes as long as trinification symmetry is broken, and by (ii) higher-loop effects which may modify the starting values for the Yukawa couplings at the matching scale. The quark CKM mixing aquires an approximate Cabbibo form already at tree level

$$V^{\mathrm{CKM}} \simeq \begin{pmatrix} \cos\theta_C & \sin\theta_C & 0 \\ -\sin\theta_C & \cos\theta_C & 0 \\ 0 & 0 & 1 \end{pmatrix}\,, \qquad \tan\theta_C = \frac{h_1}{h_3}\,, \tag{II.71}$$

which is a remarkable feature of the family symmetry, while small observed distortions of the Cabbibo mixing could only be generated at a higher-loop level. Non-unitarity corrections to the quark CKM mixing are also suppressed by small h_i/v, h_i/w and w/v ratios. This means that phenomenological constraints on those corrections could be important for setting lower limits on hierarchies between the trinification symmetry breaking scales.

8 Conclusions

In this work we have introduced a GUT based on the trinification gauge group. By introducing a global $\mathrm{SU}(3)_{\mathrm{F}}$ family symmetry, our model resolves some of the issues with previous attempts to work with gauge trinification-based models while also considerably reduces the number of free parameters.

We found that SSB of the trinification symmetry can be triggered by the VEV of only one component of a scalar **27**-plet and that the minimum is, in a large part of the parameter space, the global one. We found that radiative breaking of gauge (i.e. $\mathrm{SU}(2)_{\mathrm{R}} \times \mathrm{U}(1)_{\mathrm{L+R}}$) and global symmetries, that are not present in the SM, was possible in the effective LR-symmetric model that is left after SSB of trinification. We did so by studying the most simple scenario (two light scalar multiplets remaining in the effective theory) where the mass-squared parameter for a scalar field charged under such symmetries could become negative by means of the RG evolution. By implementing a parameter scan algorithm using simulated annealing, we were able to efficiently scan

the parameter space of the trinification theory and found regions where the radiative breaking happens in the chosen effective LR-symmetric model.

We also explored under which circumstances the high-scale theory might reproduce the masses and hierarchies of the SM at lower energies. We found that the simple scenario used to understand the radiative symmetry breaking needs to be extended in order to get for example CKM mixing and masses for all SM fermions. By having more light scalar multiplets present in the effective theory, their VEVs could break the remaining global symmetries which forbid the necessary mass terms in the low-energy theory. We also show that if such fields are present, the proposed model has good potential to result in a realistic quark mass spectrum resembling the SM one, while keeping the ingredients necessary to trigger the radiative breaking shown in this work. It is clear then that future studies should include one-loop matching, two-loop RG running and the extra scalar multiplets in the effective theory. Although we have shown the feasibility of radiative breaking and the possibility to explain the hierarchies in mass parameters for the proposed model, in order to offer a complete consistency with the SM such extended study needs to be performed in future work.

Acknowledgments

The authors would like to thank N.-E. Bomark, E. Corrigan, W. Porod, M. Sampaio and F. Staub for insightful discussions during the development of this work. A. P. M. is supported by the FCT grant SFRH/BPD/97126/2013 and partially by the H2020-MSCA-RISE-2015 Grant agreement No StronGrHEP-690904, and by the CIDMA project UID/MAT/04106/2013. A. P. M. also acknowledges the THEP group at Lund University for all hospitality and significant support provided for the development of this work. J. E. C.-M., R. P. and J. W. acknowledge the warm hospitality of the Gr@v group at Aveiro University. The work by J. E. C.-M. was supported by the Crafoord Foundation. R. P. and J. W. were partially supported by the Swedish Research Council, contract number 621-2013-428.

II.A RG equations for the LR-symmetric theory

In this appendix we list the one-loop β-functions for the LR symmetric theory described in Section 4. The convention we will follow is that for a given coupling g, the β-function is defined as

$$\beta_g = \frac{\mathrm{d}g}{\mathrm{d}t} \tag{II.72}$$

where $t = \log(\mu)$ with μ the renormalisation scale.

II.A.1 Gauge couplings

$$(4\pi)^2\beta_{g_{\rm R}} = -\frac{2}{3}g_{\rm R}^3 \tag{II.73}$$

$$(4\pi)^2\beta_{g_{\rm L}} = -g_{\rm L}^3 \tag{II.74}$$

$$(4\pi)^2\beta_{g_{\rm L+R}} = \frac{124}{9}g_{\rm L+R}^3 \tag{II.75}$$

$$(4\pi)^2\beta_{g_{\rm C}} = -\frac{19}{3}g_{\rm C}^3 \tag{II.76}$$

II.A.2 Yukawa couplings

$$(4\pi)^2\beta_{Y_\alpha} = \left(\frac{7}{2}|Y_\alpha|^2 + |Y_\beta|^2 + 3|Y_\gamma|^2 + 2|Y_\delta|^2 - \frac{9}{4}g_{\rm R}^2 - 3g_{\rm L+R}^2\right) Y_\alpha \tag{II.77}$$

$$(4\pi)^2\beta_{Y_\beta} = \left(|Y_\alpha|^2 + 3|Y_\beta|^2 + 3|Y_\gamma|^2 + |Y_\epsilon|^2 - \frac{9}{4}g_{\rm R}^2 - 3g_{\rm L+R}^2\right) Y_\beta \tag{II.78}$$

$$(4\pi)^2\beta_{Y_\gamma} = \left(|Y_\alpha|^2 + |Y_\beta|^2 + \frac{11}{2}|Y_\gamma|^2 + |Y_\zeta|^2 - 8g_{\rm C}^2 - \frac{9}{4}g_{\rm R}^2 - \frac{5}{3}g_{\rm L+R}^2\right) Y_\gamma \tag{II.79}$$

$$(4\pi)^2\beta_{Y_\delta} = \left(2|Y_\alpha|^2 + \frac{7}{2}|Y_\delta|^2 + |Y_\epsilon|^2 + 6|Y_\zeta|^2 - \frac{9}{4}g_{\rm L}^2 - \frac{9}{4}g_{\rm R}^2\right) Y_\delta \tag{II.80}$$

$$(4\pi)^2\beta_{Y_\epsilon} = \left(|Y_\beta|^2 + |Y_\delta|^2 + 3|Y_\epsilon|^2 + 6|Y_\zeta|^2 - \frac{9}{4}g_{\rm L}^2 - \frac{9}{4}g_{\rm R}^2 - 6g_{\rm L+R}^2\right) Y_\epsilon \tag{II.81}$$

$$(4\pi)^2\beta_{Y_\zeta} = \left(\frac{1}{2}|Y_\gamma|^2 + |Y_\delta|^2 + |Y_\epsilon|^2 + 8|Y_\zeta|^2 - 8g_{\rm C}^2 - \frac{9}{4}g_{\rm L}^2 - \frac{9}{4}g_{\rm R}^2 - \frac{2}{3}g_{\rm L+R}^2\right) Y_\zeta \tag{II.82}$$

II.A.3 Scalar masses

$$
\begin{aligned}
(4\pi)^2\beta_{m_h^2} = &\left(20\lambda_a - 8\lambda_j + 2|Y_\delta|^2 + 2|Y_\epsilon|^2 + 12|Y_\zeta|^2 - \frac{9}{2}g_{\mathrm{L}}^2 - \frac{9}{2}g_{\mathrm{R}}^2\right) m_h^2 \\
&+ 4\left(\lambda_g + 2\lambda_f\right) m_R^2 - 4|Y_\delta|^2 m_{\Phi^s}^2
\end{aligned}
\tag{II.83}
$$

$$
\begin{aligned}
(4\pi)^2\beta_{m_R^2} = &\left(20\lambda_b - 8\lambda_i + 2|Y_\alpha|^2 + 2|Y_\beta|^2 + 6|Y_\gamma|^2 - \frac{9}{2}g_{\mathrm{R}}^2 - 6g_{\mathrm{L+R}}^2\right) m_R^2 \\
&+ 4\left(\lambda_g + 2\lambda_f\right) m_h^2 - 4|Y_\alpha|^2 m_{\Phi^s}^2
\end{aligned}
\tag{II.84}
$$

II.A.4 Singlet Fermion mass

$$
(4\pi)^2\beta_{m_{\Phi^s}} = 4(|Y_\alpha|^2 + |Y_\delta|^2) m_{\Phi^s}
\tag{II.85}
$$

II.A.5 Quartic couplings

$$
\begin{aligned}
(4\pi)^2\beta_{\lambda_a} = &\, 32\lambda_a^2 + 4\lambda_f^2 + 2\lambda_g^2 + 4\lambda_f\lambda_g + 16\lambda_j^2 - 16\lambda_a\lambda_j \\
&+ 4\left(|Y_\epsilon|^2 + |Y_\delta|^2 + 6|Y_\zeta|^2\right)\lambda_a \\
&- 2\left(|Y_\epsilon|^4 + |Y_\delta|^4 + 6|Y_\zeta|^4\right) \\
&- 9\left(g_{\mathrm{L}}^2 + g_{\mathrm{R}}^2\right)\lambda_a \\
&+ \frac{9}{8}g_{\mathrm{L}}^4 + \frac{3}{4}g_{\mathrm{L}}^2 g_{\mathrm{R}}^2 + \frac{9}{8}g_{\mathrm{R}}^4
\end{aligned}
\tag{II.86}
$$

$$
\begin{aligned}
(4\pi)^2\beta_{\lambda_b} = &\, 32\lambda_b^2 + 4\lambda_f^2 + 2\lambda_g^2 + 4\lambda_f\lambda_g + 16\lambda_i^2 - 16\lambda_b\lambda_i \\
&+ 4\left(|Y_\alpha|^2 + |Y_\beta|^2 + 3|Y_\gamma|^2\right)\lambda_b \\
&- 2\left(|Y_\alpha|^4 + |Y_\beta|^4 + 3|Y_\gamma|^4\right) \\
&- 3\left(3g_{\mathrm{R}}^2 + 4g_{\mathrm{L+R}}^2\right)\lambda_b \\
&+ \frac{9}{8}g_{\mathrm{R}}^4 + 3g_{\mathrm{R}}^2 g_{\mathrm{L+R}}^2 + 6g_{\mathrm{L+R}}^4
\end{aligned}
\tag{II.87}
$$

$$
\begin{aligned}
(4\pi)^2\beta_{\lambda_f} = &\, 4\lambda_f^2 + 2\lambda_g^2 + 4\left(5\lambda_f + 2\lambda_g\right)\left(\lambda_a + \lambda_b\right) - 8\left(\lambda_f + \lambda_g\right)\left(\lambda_i + \lambda_j\right) \\
&+ 2\left(|Y_\alpha|^2 + |Y_\beta|^2 + 3|Y_\gamma|^2 + |Y_\delta|^2 + |Y_\epsilon|^2 + 6|Y_\zeta|^2\right)\lambda_f \\
&- 4\left(|Y_\alpha|^2|Y_\delta|^2 + |Y_\beta|^2|Y_\epsilon|^2 + 3|Y_\gamma|^2|Y_\zeta|^2\right) \\
&- 3\left(\frac{3}{2}g_{\mathrm{L}}^2 + 3g_{\mathrm{R}}^2 + 2g_{\mathrm{L+R}}^2\right)\lambda_f + \frac{9}{4}g_{\mathrm{R}}^4
\end{aligned}
\tag{II.88}
$$

$$
\begin{aligned}
(4\pi)^2\beta_{\lambda_g} = &\lambda_g(2|Y_\alpha|^2 + 2|Y_\beta|^2 + 6|Y_\gamma|^2 + 2|Y_\delta|^2 + 2|Y_\epsilon|^2 + 12|Y_\zeta|^2) \\
&- \frac{9}{2}\lambda_g g_{\mathrm{L}}^2 + \frac{1}{2}|Y_\alpha|^2|Y_\delta|^2 + \frac{5}{2}|Y_\beta|^2|Y_\epsilon|^2 + \frac{15}{2}|Y_\gamma|^2|Y_\zeta|^2 \\
&+ 8\lambda_g\lambda_i + 8\lambda_g\lambda_j + 8\lambda_f\lambda_g + 4\lambda_b\lambda_g + 4\lambda_a\lambda_g \\
&- 9\lambda_g g_{\mathrm{R}}^2 - 6\lambda_g g_{\mathrm{L+R}}^2 + 4\lambda_g^2
\end{aligned}
\tag{II.89}
$$

$$
\begin{aligned}
(4\pi)^2\beta_{\lambda_i} = &- 16\lambda_i^2 + \lambda_g^2 + 24\lambda_b\lambda_i \\
&+ 4\left(|Y_\alpha|^2 + 3|Y_\beta|^2 + 3|Y_\gamma|^2\right)\lambda_i \\
&- \frac{1}{8}\left(|Y_\alpha|^4 + 5|Y_\beta|^4 + 3|Y_\gamma|^4\right) \\
&- 3\left(3g_{\mathrm{R}}^2 + 4g_{\mathrm{L+R}}^2\right)\lambda_i + 3g_{\mathrm{L+R}}^2 g_{\mathrm{R}}^2
\end{aligned}
\tag{II.90}
$$

$$
\begin{aligned}
(4\pi)^2\beta_{\lambda_j} = &- 16\lambda_j^2 + \lambda_g^2 + 24\lambda_a\lambda_j \\
&+ 4\left(|Y_\delta|^2 + |Y_\epsilon|^2 + 6|Y_\zeta|^2\right)\lambda_j \\
&- \frac{5}{8}\left(|Y_\delta|^4 + |Y_\epsilon|^4 + 6|Y_\zeta|^4\right) \\
&- 9\left(g_{\mathrm{R}}^2 + g_{\mathrm{L}}^2\right)\lambda_j - \frac{3}{2}g_{\mathrm{L}}^2 g_{\mathrm{R}}^2
\end{aligned}
\tag{II.91}
$$

References

[1] **ATLAS** Collaboration, G. Aad *et al.*, "Observation of a new particle in the search for the Standard Model Higgs boson with the ATLAS detector at the LHC," *Phys. Lett.* **B716** (2012) 1–29, arXiv:1207.7214 [hep-ex].

[2] **CMS** Collaboration, S. Chatrchyan *et al.*, "Observation of a new boson at a mass of 125 GeV with the CMS experiment at the LHC," *Phys. Lett.* **B716** (2012) 30–61, arXiv:1207.7235 [hep-ex].

[3] A. De Rújula, H. Georgi, and S. L. Glashow *, in Fifth Workshop on Grand Unification edited by K. Kang, H. Fried, and F. Frampton* (1984) .

[4] K. S. Babu, X.-G. He, and S. Pakvasa, "Neutrino masses and proton decay modes in SU(3) × SU(3) × SU(3) trinification," *Phys. Rev. D* **33** (Feb, 1986) 763–772. http://link.aps.org/doi/10.1103/PhysRevD.33.763.

[5] G. Lazarides and C. Panagiotakopoulos, "MSSM from SUSY Trinification," *Phys. Lett.* **B336** (1994) 190–193, arXiv:hep-ph/9403317 [hep-ph].

[6] G. Lazarides and C. Panagiotakopoulos, "MSSM and large tan β from SUSY Trinification," *Phys. Rev.* **D51** (1995) 2486–2488, arXiv:hep-ph/9407286 [hep-ph].

[7] J. E. Kim, "Z_3 orbifold construction of $SU(3)^3$ GUT with $\sin^2\theta_W^0 = \frac{3}{8}$," *Phys. Lett.* **B564** (2003) 35–41, arXiv:hep-th/0301177 [hep-th].

[8] S. Willenbrock, "Triplicated Trinification," *Phys. Lett.* **B561** (2003) 130–134, arXiv:hep-ph/0302168 [hep-ph].

[9] C. D. Carone and J. M. Conroy, "Higgsless GUT Breaking and Trinification," *Phys. Rev.* **D70** (2004) 075013, arXiv:hep-ph/0407116 [hep-ph].

[10] J. Hetzel, *Phenomenology of a left-right-symmetric model inspired by the trinification model.* PhD thesis, Inst. Appl. Math., Heidelberg, 2015.

arXiv:1504.06739 [hep-ph].
https://inspirehep.net/record/1364898/files/arXiv:1504.06739.pdf.

[11] F. Gursey, P. Ramond, and P. Sikivie, "A universal gauge theory model based on E_6," *Phys. Lett.* **B60** (1976) 177–180.

[12] Y. Achiman and B. Stech, "Quark-Lepton Symmetry and Mass Scales in an E6 Unified Gauge Model," *Phys. Lett.* **B77** (1978) 389–393.

[13] Q. Shafi, "E_6 as a Unifying Gauge Symmetry," *Phys. Lett.* **B79** (1978) 301–303.

[14] R. Barbieri, D. V. Nanopoulos, and A. Masiero, "Hierarchical Fermion Masses in E6," *Phys. Lett.* **B104** (1981) 194–198.

[15] B. Stech and Z. Tavartkiladze, "Fermion masses and coupling unification in E_6: Life in the desert," *Phys. Rev.* **D70** (2004) 035002, arXiv:hep-ph/0311161 [hep-ph].

[16] B. Stech, "Neutrino Properties from $E_6 \times SO(3) \times Z_2$," *Fortsch. Phys.* **58** (2010) 692–698, arXiv:1003.0581 [hep-ph].

[17] S. F. King, S. Moretti, and R. Nevzorov, "Exceptional Supersymmetric Standard Model," *Phys. Lett.* **B634** (2006) 278–284, arXiv:hep-ph/0511256 [hep-ph].

[18] S. F. King, S. Moretti, and R. Nevzorov, "Theory and Phenomenology of an Exceptional Supersymmetric Standard Model," *Phys. Rev.* **D73** (2006) 035009, arXiv:hep-ph/0510419 [hep-ph].

[19] S. F. King, S. Moretti, and R. Nevzorov, "Gauge Coupling Unification in the Exceptional Supersymmetric Standard Model," *Phys. Lett.* **B650** (2007) 57–64, arXiv:hep-ph/0701064 [hep-ph].

[20] F. Braam, A. Knochel, and J. Reuter, "An Exceptional SSM from E_6 Orbifold GUTs with intermediate LR symmetry," *JHEP* **06** (2010) 013, arXiv:1001.4074 [hep-ph].

[21] P. Athron, S. F. King, D. J. Miller, S. Moretti, R. Nevzorov, S. F. King, D. J. Miller, S. Moretti, and R. Nevzorov, "The Constrained E_6SSM," arXiv:0810.0617 [hep-ph].

[22] S. F. King, R. Luo, D. J. Miller, and R. Nevzorov, "Leptogenesis in the Exceptional Supersymmetric Standard Model: Flavour dependent lepton asymmetries," *JHEP* **12** (2008) 042, arXiv:0806.0330 [hep-ph].

[23] P. Athron, S. F. King, D. J. Miller, S. Moretti, and R. Nevzorov, "Predictions of the Constrained Exceptional Supersymmetric Standard Model," *Phys. Lett.* **B681** (2009) 448–456, arXiv:0901.1192 [hep-ph].

[24] P. Athron, S. F. King, D. J. Miller, S. Moretti, and R. Nevzorov, "The Constrained Exceptional Supersymmetric Standard Model," *Phys. Rev.* **D80** (2009) 035009, arXiv:0904.2169 [hep-ph].

[25] P. Athron, S. F. King, D. J. Miller, S. Moretti, and R. Nevzorov, "LHC Signatures of the Constrained Exceptional Supersymmetric Standard Model," *Phys. Rev.* **D84** (2011) 055006, arXiv:1102.4363 [hep-ph].

[26] J. P. Hall, S. F. King, R. Nevzorov, S. Pakvasa, M. Sher, R. Nevzorov, S. Pakvasa, and M. Sher, "Novel Higgs Decays and Dark Matter in the E_6SSM," *Phys. Rev.* **D83** (2011) 075013, arXiv:1012.5114 [hep-ph].

[27] P. Athron, S. F. King, D. J. Miller, S. Moretti, and R. Nevzorov, "Constrained Exceptional Supersymmetric Standard Model with a Higgs Near 125 GeV," *Phys. Rev.* **D86** (2012) 095003, arXiv:1206.5028 [hep-ph].

[28] R. Nevzorov, "E_6 inspired supersymmetric models with exact custodial symmetry," *Phys. Rev.* **D87** no. 1, (2013) 015029, arXiv:1205.5967 [hep-ph].

[29] R. Nevzorov and S. Pakvasa, "Exotic Higgs decays in the E_6 inspired SUSY models," *Phys. Lett.* **B728** (2014) 210–215, arXiv:1308.1021 [hep-ph].

[30] R. Nevzorov, "Quasifixed point scenarios and the Higgs mass in the E_6 inspired supersymmetric models," *Phys. Rev.* **D89** no. 5, (2014) 055010, arXiv:1309.4738 [hep-ph].

[31] R. Nevzorov and A. W. Thomas, "E_6 inspired composite Higgs model," *Phys. Rev.* **D92** (2015) 075007, arXiv:1507.02101 [hep-ph].

[32] P. Athron, D. Harries, R. Nevzorov, and A. G. Williams, "E_6 Inspired SUSY Benchmarks, Dark Matter Relic Density and a 125 GeV Higgs," arXiv:1512.07040 [hep-ph].

[33] S. F. King and R. Nevzorov, "750 GeV Diphoton Resonance from Singlets in an Exceptional Supersymmetric Standard Model," *JHEP* **03** (2016) 139, arXiv:1601.07242 [hep-ph].

[34] P. Athron, D. Stockinger, and A. Voigt, "Threshold Corrections in the Exceptional Supersymmetric Standard Model," *Phys. Rev.* **D86** (2012) 095012, arXiv:1209.1470 [hep-ph].

[35] Y. Kawamura and T. Miura, "Classification of Standard Model Particles in E_6 Orbifold Grand Unified Theories," *Int. J. Mod. Phys.* **A28** (2013) 1350055, arXiv:1301.7469 [hep-ph].

[36] T. G. Rizzo, "Gauge Kinetic Mixing in the E_6SSM," *Phys.Rev.* **D85** (2012) 055010, arXiv:1201.2898 [hep-ph].

[37] J. Reuter and D. Wiesler, "Distorted mass edges at LHC from supersymmetric leptoquarks," *Phys. Rev.* **D84** (2011) 015012, arXiv:1010.4215 [hep-ph].

[38] D. J. Gross, J. A. Harvey, E. J. Martinec, and R. Rohm, "The Heterotic String," *Phys. Rev. Lett.* **54** (1985) 502–505.

[39] E. Cremmer, J. Scherk, and J. H. Schwarz, "Spontaneously Broken N=8 Supergravity," *Phys. Lett.* **B84** (1979) 83–86.

[40] E. Ma, "Particle Dichotomy and Left-Right Decomposition of E_6 Superstring Models," *Phys. Rev.* **D36** (1987) 274.

[41] E. Ma, "Neutrino masses in an extended gauge model with E_6 particle content," *Phys. Lett.* **B380** (1996) 286–290, arXiv:hep-ph/9507348 [hep-ph].

[42] J. E. Kim, "Trinification with $\sin^2\theta_W = \frac{3}{8}$ and seesaw neutrino mass," *Phys. Lett.* **B591** (2004) 119–126, arXiv:hep-ph/0403196 [hep-ph].

[43] C. Cauet, H. Pas, S. Wiesenfeldt, C. Cauet, H. Pas, and S. Wiesenfeldt, "Trinification, the Hierarchy Problem and Inverse Seesaw Neutrino Masses," *Phys. Rev.* **D83** (2011) 093008, arXiv:1012.4083 [hep-ph].

[44] J. Sayre, S. Wiesenfeldt, and S. Willenbrock, "Minimal trinification," *Phys. Rev.* **D73** (2006) 035013, arXiv:hep-ph/0601040 [hep-ph].

[45] C.-S. Huang, J. Jiang, T.-j. Li, and W. Liao, "N=2 six-dimensional supersymmetric E_6 breaking," *Phys. Lett.* **B530** (2002) 218–226, arXiv:hep-th/0112046 [hep-th].

[46] H. Georgi, "Towards a Grand Unified Theory of Flavor," *Nucl. Phys.* **B156** (1979) 126–134.

[47] B. Stech, "Trinification Phenomenology and the structure of Higgs Bosons," *JHEP* **08** (2014) 139, arXiv:1403.2714 [hep-ph].

[48] J. Hetzel and B. Stech, "Low-energy phenomenology of trinification: an effective left-right-symmetric model," *Phys. Rev.* **D91** (2015) 055026, arXiv:1502.00919 [hep-ph].

[49] T. Lee, T. Li, and C. Tsai, "Hom4PS-2.0: a software package for solving polynomial systems by the polyhedral homotopy continuation method," *Computing* **83** no. 2, (2008) 109–133.

[50] C. P. Burgess, "A Goldstone boson primer," in *11th Summer School and Symposium on Nuclear Physics (NuSS 98): Effective Theories of Matter (1) Seoul, Korea, June 23-27, 1998*. 1998. arXiv:hep-ph/9812468 [hep-ph]. http://alice.cern.ch/format/showfull?sysnb=0300459.

[51] C. P. Burgess, "Goldstone and Pseudo-Goldstone Bosons in Nuclear, Particle and Condensed-Matter Physics," *Phys. Rept.* **330** (2000) 193–261, arXiv:hep-th/9808176 [hep-th].

[52] A. Dedes, A. B. Lahanas, and K. Tamvakis, "Radiative electroweak symmetry breaking in the MSSM and low-energy threshold," *Phys. Rev.* **D53** (1996) 3793–3807, arXiv:hep-ph/9504239 [hep-ph].

[53] G. Gamberini, G. Ridolfi, and F. Zwirner, "On Radiative Gauge Symmetry Breaking in the Minimal Supersymmetric Model," *Nucl.Phys.* **B331** (1990) 331–349.

[54] M. Carena, S. Pokorski, and C. E. M. Wagner, "On the unification of couplings in the minimal supersymmetric Standard Model," *Nucl. Phys.* **B406** (1993) 59–89, arXiv:hep-ph/9303202 [hep-ph].

[55] **ATLAS** Collaboration, M. Aaboud *et al.*, "Search for new resonances in events with one lepton and missing transverse momentum in pp collisions at $\sqrt{s} = 13$ TeV with the ATLAS detector," arXiv:1606.03977 [hep-ex].

[56] **ATLAS** Collaboration, "Search for new phenomena in the dilepton final state using proton-proton collisions at $\sqrt{s} = 13$ TeV with the ATLAS detector,".

[57] F. Lyonnet, I. Schienbein, F. Staub, and A. Wingerter, "PyR@TE: Renormalization Group Equations for General Gauge Theories," *Comput. Phys. Commun.* **185** (2014) 1130–1152, arXiv:1309.7030 [hep-ph].

[58] S. Kirkpatrick, C. D. Gelatt, and M. P. Vecchi, "Optimization by simulated annealing," *Science* **220** no. 4598, (1983) 671–680, http://science.sciencemag.org/content/220/4598/671.full.pdf. http://science.sciencemag.org/content/220/4598/671.

III

Reviving trinification models through an E_6-extended supersymmetric GUT

José E. Camargo-Molina[1], António P. Morais[1,2], Astrid Ordell[1], Roman Pasechnik[1], Marco O. P. Sampaio[2] and Jonas Wessén[1].

Phys.Rev. D95 (2017) no.7, 075031
doi:10.1103/PhysRevD.95.075031
e-Print: arXiv:1610.03642 [hep-ph]

[1] Department of Astronomy and Theoretical Physics, Lund University, SE 223-62 Lund, Sweden.
[2] Departamento de Física da Universidade de Aveiro and CIDMA Campus de Santiago, 3810-183 Aveiro, Portugal.

Abstract: We present a supersymmetric (SUSY) model based on trinification $[SU(3)]^3$ and family $SU(3)_F$ symmetries embedded into a maximal subgroup of E_8, where the sectors of light Higgs bosons and leptons are unified into a single chiral supermultiplet. The common origin of gauge trinification and of the family symmetry from E_8 separates the model from other trinification-based GUTs, as it protects, in particular, the Standard Model fermions from gaining mass until the electroweak symmetry is broken. Furthermore, it allows us to break the trinification symmetry via vacuum expectation values in SU(3)-adjoint scalars down to a left-right symmetric theory. Simultaneously, it ensures the unification of the gauge and Yukawa couplings as well as proton stability. Although the low-energy regime (e.g. mass hierarchies in the scalar sector determined by a soft SUSY-breaking mechanism) is yet to be established, these features are one key to revive the once very popular trinification-based GUTs.

1 Introduction

Finding a compelling theory for the unification of the fundamental interactions that is capable of reproducing known features of the Standard Model (SM) has been a major

goal of the theoretical physics community. Popular SM extensions are supersymmetric (SUSY) grand unified theories (GUTs) based on simple Lie groups such as e.g. SU(5) [1], SO(10) [2], E_6 [3], and E_7 [4]. However, many of the existing GUTs typically suffer from various issues with, e.g., proton stability, fine-tuning, and hierarchies in parameters such as fermion masses and mixings lacking a fundamental explanation, as well as with inconceivably complicated parameter spaces severely reducing their predictive power.

GUTs inspired by E_6 are becoming increasingly popular due to their rich phenomenology and their many attractive properties (see, e.g., Refs. [5, 6, 7, 8]). One such GUT scenario based upon a maximal rank-6 subgroup $[SU(3)]^3 \subset E_6$ and known as gauge trinification (T-GUT) was initially proposed by Glashow et al in 1984 [9]. The trinification symmetry is typically identified as a left-right-color product group, *i.e.*, $[SU(3)]^3 \equiv SU(3)_L \times SU(3)_R \times SU(3)_C$, and is supplemented by a cyclic permutation symmetry $\mathbb{Z}_3$ forcing the gauge couplings to unify, *i.e.* $g_U \equiv g_L = g_R = g_C$. One of the appealing features of T-GUT models is that all the matter fields, which belong to bitriplet representations (reps) of the trinification symmetry,

$$\left(\boldsymbol{L}^i\right)_r^l = \begin{pmatrix} \boldsymbol{H}_{11} & \boldsymbol{H}_{12} & \boldsymbol{e}_L \\ \boldsymbol{H}_{21} & \boldsymbol{H}_{22} & \boldsymbol{\nu}_L \\ \boldsymbol{e}_R^c & \boldsymbol{\nu}_R^c & \boldsymbol{\phi} \end{pmatrix}^i, \quad \begin{array}{l} (Q_L{}^i)_l^x = \left(\boldsymbol{u}_L^x \quad \boldsymbol{d}_L^x \quad \boldsymbol{D}_L^x\right)^i, \\ (Q_R{}^i)_x^r = \left(\boldsymbol{u}_{Rx}^c \quad \boldsymbol{d}_{Rx}^c \quad \boldsymbol{D}_{Rx}^c\right)^{\top\ i}, \end{array} \tag{III.1}$$

can be embedded into three **27**-plets of E_6 as $\mathbf{27}^i \to (\mathbf{3}, \bar{\mathbf{3}}, \mathbf{1})^i \oplus (\bar{\mathbf{3}}, \mathbf{1}, \mathbf{3})^i \oplus (\mathbf{1}, \mathbf{3}, \bar{\mathbf{3}})^i$. Here, the left, right, and color SU(3) indices are l, r, and x, respectively, while the generations are labelled by an index i (for an alternative realization containing the trinified gauge symmetry $[SU(3)]^3$, see Refs. [10, 11]). Some T-GUT versions claim to preserve baryon number naturally [12, 13] but can also be engineered to account for the baryon-antibaryon asymmetry in the Universe through heavy Higgs decays at one loop [14]. They can, in principle, accommodate any quark and lepton masses and mixing angles [12] while neutrino masses can be generated by, e.g., a radiative [13] or an inverse [15] see-saw mechanism. However, despite some progress in recent years, the T-GUT scenarios remain among the least explored extensions of the SM. One of the major theoretical challenges in building the SUSY-based T-GUTs is finding a stable vacuum with spontaneously broken gauge trinification while keeping a low number of free parameters at the GUT scale.

In order to avoid GUT-scale lepton masses, previous realizations of T-GUTs introduced either additional unmotivated Higgs multiplets [12, 16, 17, 18, 19, 20, 13, 15, 21, 22, 23, 24], whose vacuum expectation values (VEVs) provide a consistent spontaneous symmetry breaking (SSB) of trinification down to the SM gauge symmetry, or higher-dimensional operators [25, 17, 18, 20, 15]. Such constructions may, however, result in severe phenomenological contradictions with proton stability [12, 18, 13] and too many unobserved low-scale signatures [9, 25, 17, 22, 23, 26]. As a consequence, a large number of free Yukawa parameters in the superpotential has to be highly fine-tuned in order to reproduce the SM mass hierarchies [13]. A proper renormalization group (RG) analysis of a high-scale SUSY model containing a few hundreds of particles and couplings and accounting for several SSB scales down to the effective low-energy SM-like theory remains barely feasible in practice. Thus, deriving even basic features of the SM (such as fermion mass/mixing hierarchies and Higgs sector properties) as a low-energy

effective field theory (EFT) limit of a T-GUT remains a big unsolved problem (for more details, see, e.g., Ref. [27] and references therein).

In this paper, we propose a new way to resolve the problem of GUT-scale masses of the SM leptons inspired by an embedding of the trinification $[\mathrm{SU}(3)]^3 \subset \mathrm{E}_6$ and family $\mathrm{SU}(3)_\mathrm{F}$ symmetries into the maximal exceptional symmetry group E_8. A common origin of family symmetry and SM gauge symmetries from $[\mathrm{SU}(3)]^3 \times \mathrm{SU}(3)_\mathrm{F} \subset \mathrm{E}_8$ implies that, in particular, the light Higgs and lepton sectors originate from the same (tritriplet) rep of $[\mathrm{SU}(3)]^3 \times \mathrm{SU}(3)_\mathrm{F}$. Having such light Higgs-lepton unification in the E_6-extended theory (inspired by E_8) leads to a complete unification of quark and lepton Yukawa couplings for all three generations (as well as the quartic interactions of the scalar potential) at the trinification-breaking scale. This is at variance with popular SO(10) and Pati-Salam models where the unification of Yukawa couplings is restricted to the third family [28, 29, 30, 31, 32, 33, 34, 35, 36, 37, 38, 39, 40]. Such a distinct feature of the high-scale model dramatically reduces its parameter space making its complete analysis computationally simple, at least, at tree level. We have found that the proposed E_6-extended T-GUT model gives rise to an effective left-right (LR) symmetric theory with specific properties. The remnant $\mathrm{SU}(3)_\mathrm{F}$ family symmetry reduces the number of allowed terms in the LR-symmetric EFT, simplifying its matching procedure with the high-scale theory and making its RG flow analysis technically feasible. A consistent match of the LR-symmetric EFT with the SM at low scale would then strongly constrain the hierarchies in the soft SUSY-breaking sector offering new possibilities for studies of the SUSY breaking in E_6-based theories.

2 E_8-inspired family symmetry

In earlier work by some of the authors [41], it was understood that the SM gauge group can arise dynamically from a non-SUSY T-GUT in a scenario where fermions and scalars belong to the same E_6 reps [augmented by a global $\mathrm{SU}(3)_\mathrm{F}$], thus hinting at a possible presence of SUSY at (or beyond) the GUT scale. In particular, the color-neutral scalars $\tilde{L}$ (containing the Higgs scalars) and fermions L (containing the SM leptons and right-handed neutrinos) could then be naturally considered as components of $\boldsymbol{L}$. Here and below, the notations $\tilde{f}$ and f for scalar and fermion components of the superfield $\boldsymbol{f}$ are used.

Inspired by this observation, the implications of a Higgs-lepton unification in a SUSY T-GUT were explored, with *local* gauge trinification $[\mathrm{SU}(3)]^3$ and *global* family $\mathrm{SU}(3)_\mathrm{F}$ motivated by a minimal E_6 embedding into E_8 as $\mathrm{E}_6 \times \mathrm{SU}(3)_\mathrm{F} \subset \mathrm{E}_8$ [42, 43]. Indeed, such an E_6-extended trinification model inspired by its E_8 embedding can be considered as an approximation to the full gauge $[\mathrm{SU}(3)]^3 \times \mathrm{SU}(3)_\mathrm{F} \subset \mathrm{E}_8$ theory in those regions of parameter space where gauge $\mathrm{SU}(3)_\mathrm{F}$ interactions are suppressed, $g_\mathrm{F} \ll g_\mathrm{U}$. A special interest in E_8-based models originates from string theories where massless sectors are described by the $\mathrm{E}_8 \times \mathrm{E}_8'$ symmetry [44, 43].

At variance with the non-SUSY model [41], incorporating the $\mathrm{SU}(3)_\mathrm{F}$ family symmetry

in a SUSY T-GUT model with only tritriplets of $[\mathrm{SU}(3)]^3 \times \mathrm{SU}(3)_\mathrm{F}$ (specified in the first three rows of Table III.1) leads to a scalar potential containing flat directions with color-breaking VEVs. Even with the inclusion of soft breaking terms, such a model at tree level is necessarily inconsistent with the SM at low scales. Alternatively, the desired trinification SSB becomes possible in a SUSY T-GUT when relaxing $\mathrm{SU}(3)_\mathrm{F}$. However, this reintroduces GUT-scale masses for those SM leptons that are SUSY partners of the Goldstone bosons from $\tilde{L}$, due to terms such as $-\sqrt{2}g_\mathrm{U}(\tilde{L}_i^*)^r_{l_1}(T^a_\mathrm{L})^{l_1}_{l_2}(L^i)^{l_2}_r\lambda^a_\mathrm{L}$. These terms lead to gaugino-lepton mass terms of the order of the T-GUT-breaking VEV $\tilde{L}^i$. Although components in the trinification gaugino fields $\lambda^a_{\mathrm{L,R}}$ could in principle build up one generation of the SM leptons, we find such a construction unappealing both due to the reduction of the family symmetry and the abandonment of the full Higgs-lepton unification. Besides, the gaugino mass scale in this case would then be unnaturally small for a consistency with the SM lepton sector.

This gaugino-lepton mixing indeed posed a big problem for early attempts to consistently unify the Higgs and lepton sectors. However, rather than including additional copies of $\boldsymbol{L}$, we have found that the leptons are protected from obtaining GUT-scale masses via the inclusion of SU(3) adjoint superfields which, together with tritriplets $\boldsymbol{L}$, $\boldsymbol{Q}_\mathrm{L}$, and $\boldsymbol{Q}_\mathrm{R}$, are irreducible representations (irreps) of the E_8 symmetry group. This novel scenario is in the focus of our further discussion.

3 Minimal E_6-extended T-GUT model

The proposed $[\mathbb{Z}_2 \times \mathbb{Z}_3]$-symmetric E_6-extended model, where the problem of SUSY T-GUT breaking is consistently resolved, preserves all the well-known attractive features of T-GUTs. The chiral superfield content of this model transforms as (**8**,**1**), (**3**,**27**), and (**1**,**78**) of $\mathrm{SU}(3)_\mathrm{F} \times \mathrm{E}_6$, where $\mathrm{SU}(3)_\mathrm{F}$ is a global family symmetry. This set contains, in addition to the lepton and quark superfields $\boldsymbol{L}$, $\boldsymbol{Q}_\mathrm{L}$ and $\boldsymbol{Q}_\mathrm{R}$, chiral supermultiplets in the adjoint rep of $\mathrm{SU}(3)_\mathrm{A}$ (A=L,R,C,F) shown in Table III.1. The superpotential of this model reads

$$\begin{aligned} W = & \sum_{\mathrm{A=L,R,C}} \left[\lambda_{\mathbf{78}}\, d_{abc}\boldsymbol{\Delta}^a_\mathrm{A}\boldsymbol{\Delta}^b_\mathrm{A}\boldsymbol{\Delta}^c_\mathrm{A} + \mu_{\mathbf{78}}\boldsymbol{\Delta}^a_\mathrm{A}\boldsymbol{\Delta}^a_\mathrm{A}\right] \\ & + \lambda_{\mathbf{1}} d_{abc}\boldsymbol{\Delta}^a_\mathrm{F}\boldsymbol{\Delta}^b_\mathrm{F}\boldsymbol{\Delta}^c_\mathrm{F} + \mu_{\mathbf{1}}\boldsymbol{\Delta}^a_\mathrm{F}\boldsymbol{\Delta}^a_\mathrm{F} + \lambda_{\mathbf{27}}\,\varepsilon_{ijk}\boldsymbol{Q}^i_\mathrm{L}\boldsymbol{Q}^j_\mathrm{R}\boldsymbol{L}^k\,, \end{aligned} \tag{III.2}$$

where $\lambda_{\mathbf{27}}$ is the unified quark-lepton Yukawa coupling, the subscript under the couplings denotes the E_6 irreps, $d_{abc} \equiv 2\,\mathrm{Tr}\left[\{T_a, T_b\}\,T_c\right]$ are the totally symmetric SU(3) coefficients, $\boldsymbol{Q}^i_\mathrm{L}\boldsymbol{Q}^j_\mathrm{R}\boldsymbol{L}^k \equiv (Q_\mathrm{L}{}^i)^x_l (Q_\mathrm{R}{}^j)^r_x (\boldsymbol{L}^k)^l_r$, and summation over repeated indices is always implied. Furthermore, $\boldsymbol{L}$ unifies the light Higgs scalar and lepton sectors while $\boldsymbol{Q}_\mathrm{L}$ and $\boldsymbol{Q}_\mathrm{R}$ contain the SM quarks. In what follows, we refer to this model as the SUSY Higgs-unified trinification (or, shortly, SHUT) model.

Superfield		$\mathrm{SU}(3)_\mathrm{C}$	$\mathrm{SU}(3)_\mathrm{L}$	$\mathrm{SU}(3)_\mathrm{R}$	$\mathrm{SU}(3)_\mathrm{F}$
Lepton	$(\boldsymbol{L}^i)^l_r$	$\mathbf{1}$	$\mathbf{3}^l$	$\overline{\mathbf{3}}_r$	$\mathbf{3}^i$
Right-Quark	$(Q_\mathrm{R}{}^i)^r_x$	$\overline{\mathbf{3}}_x$	$\mathbf{1}$	$\mathbf{3}^r$	$\mathbf{3}^i$
Left-Quark	$(Q_\mathrm{L}{}^i)^x_l$	$\mathbf{3}^x$	$\overline{\mathbf{3}}_l$	$\mathbf{1}$	$\mathbf{3}^i$
Colour-adjoint	$\boldsymbol{\Delta}^a_\mathrm{C}$	$\mathbf{8}^a$	$\mathbf{1}$	$\mathbf{1}$	$\mathbf{1}$
Left-adjoint	$\boldsymbol{\Delta}^a_\mathrm{L}$	$\mathbf{1}$	$\mathbf{8}^a$	$\mathbf{1}$	$\mathbf{1}$
Right-adjoint	$\boldsymbol{\Delta}^a_\mathrm{R}$	$\mathbf{1}$	$\mathbf{1}$	$\mathbf{8}^a$	$\mathbf{1}$
Family-adjoint	$\boldsymbol{\Delta}^a_\mathrm{F}$	$\mathbf{1}$	$\mathbf{1}$	$\mathbf{1}$	$\mathbf{8}^a$

Table III.1: The minimal chiral superfield content of the SUSY $[\mathrm{SU}(3)]^3 \times \mathrm{SU}(3)_\mathrm{F} \subset \mathrm{E}_8$ model [with global family $\mathrm{SU}(3)_\mathrm{F}$].

The soft SUSY-breaking potential contains

$$\begin{aligned} V^\mathrm{G}_\mathrm{soft} = \Big\{ & m^2_{\mathbf{27}} \tilde{L}\tilde{L}^\dagger + m^2_{\mathbf{78}} \tilde{\Delta}^{*a}_\mathrm{L} \tilde{\Delta}^a_\mathrm{L} + \Big[b_{\mathbf{78}} \tilde{\Delta}^a_\mathrm{L} \tilde{\Delta}^a_\mathrm{L} \\ & + \; d_{abc} \big(A_{\mathbf{78}} \tilde{\Delta}^a_\mathrm{L} \tilde{\Delta}^b_\mathrm{L} \tilde{\Delta}^c_\mathrm{L} + C_{\mathbf{78}} \tilde{\Delta}^{*a}_\mathrm{L} \tilde{\Delta}^b_\mathrm{L} \tilde{\Delta}^c_\mathrm{L} \big) \\ & + \; A_G \tilde{\Delta}^a_\mathrm{L} T^a_\mathrm{L} \left(\tilde{L}^\dagger \tilde{L} + \tilde{Q}^\dagger_\mathrm{L} \tilde{Q}_\mathrm{L} \right) + \mathrm{c.c.} \Big] \Big\} \rtimes \mathbb{Z}_3 \\ & + \; \Big[A_{\mathbf{27}} \varepsilon_{ijk} \tilde{Q}^i_\mathrm{L} \tilde{Q}^j_\mathrm{R} \tilde{L}^k + \mathrm{c.c.} \Big] \end{aligned} \tag{III.3}$$

accounting for gauge adjoint scalars $\tilde{\Delta}^a_{\mathrm{L,R,C}}$, and

$$\begin{aligned} V^\mathrm{Gl}_\mathrm{soft} = {} & m^2_{\mathbf{1}} \tilde{\Delta}^{*a}_\mathrm{F} \tilde{\Delta}^a_\mathrm{F} + \big\{ b_{\mathbf{1}} \tilde{\Delta}^a_\mathrm{F} \tilde{\Delta}^a_\mathrm{F} + A_{\mathbf{1}} d_{abc} \tilde{\Delta}^a_\mathrm{F} \tilde{\Delta}^b_\mathrm{F} \tilde{\Delta}^c_\mathrm{F} + \\ & + \; A_F \tilde{\Delta}^a_\mathrm{F} \left(\tilde{L}^\dagger T^a_\mathrm{F} \tilde{L} \right) \rtimes \mathbb{Z}_3 + \mathrm{c.c.} \big\} \end{aligned} \tag{III.4}$$

for interactions involving family octets $\tilde{\Delta}^a_\mathrm{F}$, where T^a_A are the $\mathrm{SU}(3)_\mathrm{A}$ generators such that $\tilde{L}^\dagger T^a_\mathrm{L} \tilde{L} \equiv (\tilde{L}^*_k)^r_l (T^a_\mathrm{L})^l_{l'} (\tilde{L}^k)^{l'}_r$ etc, and summation over $\mathbb{Z}_3$ permutations is implied by the symbol $\rtimes \mathbb{Z}_3$. For completeness, we also include soft SUSY-breaking interactions in the fermion sector,

$$\mathcal{L}^\mathrm{ferm}_\mathrm{soft} = \Big\{ -\frac{1}{2} M_0 \tilde{\lambda}^a_\mathrm{L} \tilde{\lambda}^a_\mathrm{L} - M'_0 \tilde{\lambda}^a_\mathrm{L} \Delta^a_\mathrm{L} + \mathrm{h.c.} \Big\} \rtimes \mathbb{Z}_3 \,. \tag{III.5}$$

Here, besides the gaugino Majorana mass M_0, the symmetry allows a Dirac mass term parameterized by M'_0.

Notably, by setting all the soft SUSY-breaking parameters to zero the model still allows for the trinification SSB with a T-GUT-breaking but SUSY-preserving stable vacuum giving rise to an effective SUSY LR-symmetric model below the GUT scale. At the moment, however, it is unclear if one could generate a consistent soft SUSY-breaking and gauge symmetry SSB in such an effective model providing a large splitting between the GUT and SM energy scales as required by phenomenology. We leave this open question to further studies taking into account the generic soft SUSY-breaking sector in the considered T-GUT as specified above.

In SUSY models with Dirac gauginos (such as minimal supersymmetric SM) the additional adjoint superfields spoil the gauge couplings' unification. This problem is resolved

in the so-called minimal Dirac-gaugino supersymmetric standard model [45, 46] inspired by $SU(3)^3$ T-GUTs. In the SHUT model this problem is also resolved but, in a more elegant way, offering a framework that accommodates both the Dirac gauginos and the unified gauge coupling g_U. Furthermore, the proton is stabilized to all orders in perturbation theory due to an accidental $U(1)_B$. This global baryon symmetry is then preserved all the way down to the SM scale since none of the $(\tilde{Q}_L, \tilde{Q}_R)$ squarks carrying the baryon number ($B = +1/3, -1/3$) acquire a VEV [41] (see also Ref. [13]).

4 SUSY T-GUT symmetry breaking

The presence of family $SU(3)_F$ symmetry together with adjoint superfields $\mathbf{\Delta}^a_A$ allows for a consistent trinification SSB which is rather clean compared to older SUSY T-GUT realizations. It also provides, in particular, SM-like fermion candidates whose masses are protected from GUT-scale contributions. Choosing a VEV along the $\tilde{\Delta}^8_A$ direction yields the rank-preserving trinification SSB

$$SU(3)_A \to SU(2)_A \times U(1)_A\,, \qquad A = L, R, F\ . \tag{III.6}$$

Such a VEV choice is

$$\langle\tilde{\Delta}^8_L\rangle \equiv v_L\,, \qquad \langle\tilde{\Delta}^8_R\rangle \equiv v_R\,, \qquad \langle\tilde{\Delta}^8_F\rangle \equiv v_F \tag{III.7}$$

(where $v_L = v_R \equiv v$ is required by vacuum stability) which provides the SSB scheme

$$\begin{aligned}&[SU(3)_C \times SU(3)_L \times SU(3)_R] \rtimes \mathbb{Z}_3 \times SU(3)_F \\ &\overset{v,\,v_F}{\to} \quad SU(3)_C \times \big[SU(2)_L \times SU(2)_R \\ &\qquad \times U(1)_L \times U(1)_R\big] \rtimes \mathbb{Z}_2 \times SU(2)_F \times U(1)_F\,,\end{aligned} \tag{III.8}$$

in addition to implicit accidental symmetries such as $U(1)_B$. Here, the square brackets denote parts gathered under the permutation symmetries.

After the T-GUT symmetry breaking (III.8) the fermionic tritriplets L, Q_L, and Q_R are split into blocks revealing, e.g., massless $SU(2)_L$ [$SU(2)_R$] doublets of leptons $E_L \equiv (e_L, \nu_L)$ [$E_R \equiv (e^c_R, \nu^c_R)$] and quarks $q_L \equiv (u_L, d_L)$ [$q_R \equiv (u^c_R, d^c_R)$], whose first and second generations form $SU(2)_F$ doublets. Notably, the matching of Yukawa couplings in subsequent EFT scenarios is greatly simplified due to the unified Yukawa interactions in the considered T-GUT.

5 Left-right-symmetric effective theory

We have found that the high-scale SHUT model gives rise to a non-SUSY LR $SU(2)_L \times SU(2)_R$-symmetric EFT [Eq. III.8] as long as the quadratic and trilinear soft SUSY-breaking terms are small compared to the GUT scale. Here, we briefly discuss an

important class of its characteristic low-energy scenarios where (i) all the gauge-adjoint $\tilde{\Delta}_{\mathrm{L,R,C}}$ and the flavour-adjoint $\tilde{\Delta}_{\mathrm{F}}^{1,2,3,8}$ scalars are heavy, thus are integrated out at the T-GUT-breaking (or, simply, GUT) scale, and (ii) the fundamental scalars $\tilde{L}$ are lighter than the GUT scale and are kept in the LR-symmetric EFT. This is indeed the most natural choice as the masses of the latter are solely governed by soft SUSY-breaking interactions while those of the former also contain large $\mathcal{F}$- and $\mathcal{D}$-term contributions of the order of the GUT scale. In particular, assuming for simplicity the superpotential and soft SUSY-breaking parameters to be real, it follows from Eqs. (III.3) and (III.4) that the masses of the scalar components of the tritriplets $\boldsymbol{L}$, $\boldsymbol{Q}_{\mathrm{L}}$, and $\boldsymbol{Q}_{\mathrm{R}}$ are of the form

$$m^2_{\tilde{\varphi}_i} = m^2_{\boldsymbol{27}} + c^i_1 A_{\mathrm{G}} v + c^i_2 A_{\mathrm{F}} v_{\mathrm{F}}\,, \tag{III.9}$$

where the index i runs over all fundamental scalars and $c^i_{1,2}$ are irrational constants. We can now relate all dimensionful parameters to the T-GUT-breaking VEV as $m^2_{\boldsymbol{27}} \equiv \alpha_{\boldsymbol{27}} v^2$, $A_{\mathrm{G}} \equiv \sigma_{\mathrm{G}} v$, $A_{\mathrm{F}} \equiv \sigma_{\mathrm{F}} v$, and $v_{\mathrm{F}} \equiv \beta v$. Here, $\alpha_{\boldsymbol{27}}$, σ_{G}, $\sigma_{\mathrm{F}} \ll 1$ are small, as they parametrize unknown details of soft SUSY breaking, while $\beta \sim \mathcal{O}(1)$ such that both gauge and family SSBs occur simultaneously. This allows us to recast the scalar masses as

$$m^2_{\tilde{\varphi}_i} = v^2 \left(\alpha_{\boldsymbol{27}} + c^i_1 \sigma_{\mathrm{G}} + c^i_2 \beta \sigma_{\mathrm{F}}\right) \equiv v^2 \omega_{\tilde{\varphi}_i}\,, \quad \omega_{\tilde{\varphi}_i} \ll 1\,. \tag{III.10}$$

Interestingly, the light scalar spectrum of the effective LR-symmetric model is fully determined by three independent small parameters characterizing the soft SUSY-breaking sector and thus is protected from gaining the GUT-scale radiative corrections. Choosing, for example, $\omega_{\tilde{H}^{(3)}} \equiv \xi$, $\omega_{\tilde{E}^{(1,2)}_{\mathrm{L,R}}} \equiv \delta$, and $\omega_{\tilde{H}^{(1,2)}} \equiv \kappa$, one obtains

$$\begin{aligned}
m^2_{\tilde{H}^{(3)}} &= v^2 \xi\,, & m^2_{\tilde{H}^{(1,2)}} &= v^2 \kappa\,,\\
m^2_{\tilde{E}^{(3)}_{\mathrm{L,R}}} &= v^2 (\delta + \xi - \kappa)\,, & m^2_{\tilde{E}^{(1,2)}_{\mathrm{L,R}}} &= v^2 \delta\,,\\
m^2_{\tilde{\phi}^{(3)}} &= v^2 (2\delta + \xi - 2\kappa)\,, & m^2_{\tilde{\phi}^{(1,2)}} &= v^2 (2\delta - \kappa)\,,\\
m^2_{\tilde{q}^{(3)}_{\mathrm{L,R}}} &= \tfrac{1}{3} v^2 (\delta + 3\xi - \kappa)\,, & m^2_{\tilde{q}^{(1,2)}_{\mathrm{L,R}}} &= \tfrac{1}{3} v^2 (\delta + 2\kappa)\,,\\
m^2_{\tilde{D}^{(3)}_{\mathrm{L,R}}} &= \tfrac{1}{3} v^2 (4\delta + 3\xi - 4\kappa)\,, & m^2_{\tilde{D}^{(1,2)}_{\mathrm{L,R}}} &= \tfrac{1}{3} v^2 (4\delta - \kappa)\,.
\end{aligned} \tag{III.11}$$

where ξ, δ and κ determine all possible mass hierarchies in the scalar spectrum in the LR-symmetric EFT at the GUT scale. Together with quartic, Yukawa, and gauge couplings, they control the initial conditions and shape of the RG flow and therefore define a particular SSB scheme affecting the features of the low-energy EFT limit. For example, setting $\kappa \ll \xi \ll \delta$ one finds that $m^2_{\tilde{H}^{(1,2)}} \ll m^2_{\tilde{H}^{(3)}} \ll m^2_{\text{others}} \ll v^2$. One of the possible symmetry-breaking schemes down to the SM gauge group consists of two subsequent steps that can be induced by the VEVs $\langle \tilde{\phi}^{(3)} \rangle \equiv \langle \big(\tilde{L}^3\big)^3_3 \rangle$ and $\langle \tilde{\nu}^{(2)}_{\mathrm{R}} \rangle \equiv \langle \big(\tilde{L}^2\big)^3_1 \rangle$ at well-separated scales. This is represented by the following SSB chain:

$$\begin{aligned}
&\mathrm{SU}(3)_{\mathrm{C}} \times [\mathrm{SU}(2)_{\mathrm{L}} \times \mathrm{SU}(2)_{\mathrm{R}} \times \mathrm{U}(1)_{\mathrm{L}} \times \mathrm{U}(1)_{\mathrm{R}}] \rtimes \mathbb{Z}_2\\
&\overset{\langle \tilde{\phi}^{(3)} \rangle}{\to} \quad \mathrm{SU}(3)_{\mathrm{C}} \times [\mathrm{SU}(2)_{\mathrm{L}} \times \mathrm{SU}(2)_{\mathrm{R}}] \rtimes \mathbb{Z}_2 \times \mathrm{U}(1)_{\mathrm{L+R}}\\
&\overset{\langle \tilde{\nu}^{(2)}_{\mathrm{R}} \rangle}{\to} \quad \mathrm{SU}(3)_{\mathrm{C}} \times \mathrm{SU}(2)_{\mathrm{L}} \times \mathrm{U}(1)_{\mathrm{Y}}\,,
\end{aligned} \tag{III.12}$$

where only the gauge symmetry and $\mathbb{Z}_2$ are shown.

Consider the SSB chain (III.12) in more detail. Due to the presence of both Majorana and Dirac mass terms in the fermion-adjoint sector, with a large splitting one recovers light neutralino- and gluinolike states in the LR-symmetric EFT with masses $m_{\mathcal{S}_{\rm L,R}} \simeq m_{\mathcal{T}_{\rm L,R}} \simeq m_{\tilde{g}} \simeq 2M_0$ in terms of the soft SUSY-breaking parameter $M_0 \ll v \sim \mu_{\boldsymbol{78}}$. Here, the $\mathrm{SU}(2)_{\rm L,R}$ triplet $\mathcal{T}_{\rm L,R}$ and singlet $\mathcal{S}_{\rm L,R}$ states emerge from a decomposition of the $\mathrm{SU}(3)_{\rm L,R}$ octets as $\mathbf{8} \to \mathbf{3}_0 \oplus \mathbf{2}_1 \oplus \mathbf{2}_{-1} \oplus \mathbf{1}_0$, and $\tilde{g}$ is the lightest gluino. On the other hand, as long as $M_0 \sim \langle\tilde{\phi}^{(3)}\rangle \ll v$, these gaugino-like states will be integrated out at the $\mathcal{O}\big(\langle\tilde{\phi}^{(3)}\rangle\big)$ scale. Thus, in the resulting $\mathrm{SU}(2)_{\rm L} \times \mathrm{SU}(2)_{\rm R} \times \mathrm{U}(1)_{\rm L+R}$ EFT, the gaugino-lepton mass terms do not appear and the SM fermions are guaranteed to remain massless until the electroweak scale. Conveniently, the charges of the weak-singlet (non-SM) down-type quarks allow them to gain masses at the LR-breaking scales $\langle\tilde{\phi}^{(3)}\rangle$, $\langle\tilde{\nu}_{\rm R}^{(2)}\rangle$ via the high-scale Yukawa terms of the form $Q_{\rm L}Q_{\rm R}\tilde{L}$.

6 Significance, expectations and future work

The proposed E_6-extended SHUT model represents a promising way of unifying the light Higgs scalar and SM lepton sectors into the same supermultiplet $\boldsymbol{L}$, where [due to the trinification SSB via adjoint scalar VEVs and the family $\mathrm{SU}(3)_{\rm F}$] the SM fermions are protected from gaining masses in the high-scale model, in consistency with the SM. The inclusion of $\mathrm{SU}(3)_{\rm F}$ also results in the high-scale unification of the tree-level quark-lepton Yukawa couplings in the current framework [see $\lambda_{\boldsymbol{27}}$ in Eq. (III.2)]. Due to the emergent Yukawa and Higgs-lepton unification properties, the SHUT model has a relatively low number of free parameters at the GUT scale without introducing additional Higgs multiplets besides those in E_8 and also without assuming any universality in the soft SUSY-breaking sector. While potentially sharing some of the key features of the non-SUSY T-GUT scenario discussed in Ref. [41], the SHUT model brings a straightforward explanation to some of its seemingly arbitrary characteristics such as the presence of scalars and fermions with the same quantum numbers.

In particular, in Ref. [41] it was demonstrated that in the non-SUSY T-GUT the LR symmetry breaking down to the SM gauge group can be initiated radiatively through the RG evolution. The circumstances under which the model leads to a realistic mass spectrum at lower energies were also explored, as well as aspects of its one-loop stability. Indeed, due to the running of a mass squared of a scalar $\mathrm{SU}(2)_{\rm R/F}$ bidoublet $(\tilde{e}_{i=1,2},\, \tilde{\nu}_{i=1,2})$ to a negative value at lower scales, the SSB can be triggered in the LR-symmetric EFT with a residual global $\mathrm{SU}(2)_{\rm F}$ down to the SM gauge symmetry [cf. the last SSB step in Eq. (III.12)]. Similar low-energy features could be present in the considered SHUT model as a plausible possibility, though they are not immediately guaranteed since its mass spectra differ from that of Ref. [41]. A better understanding of the radiative symmetry breaking in the resulting LR-symmetric EFT which determines the structure of the SM-like theory at low energies should be the subject of future

studies.

In the SM-like EFT, resulting from the chain (III.12), the three lightest SM Higgs $SU(2)_L$ doublets originating from the scalar $SU(2)_L \times SU(2)_R \times SU(2)_F$ tridoublet in the LR-symmetric EFT are expected to develop VEVs breaking the electroweak symmetry. As long as this property holds true, it provides a correct mass scale for the SM quarks in the second and third generations as well as gives rise to the Cabbibo mixing pattern at tree level. While there are no tree-level Higgsino, SM lepton, and first-generation quark masses in the high-scale theory, those can, in principle, be regenerated radiatively as soon as the LR and electroweak symmetries are broken. The EFT fermion mass spectra should thus be explored at least to one-loop order in following studies.

7 Conclusions

By unifying light Higgs bosons and SM leptons in the same supermultiplet of trinification, by breaking the trinification symmetry with adjoint scalar VEVs, and by introducing a global family symmetry, the SHUT model protects the SM fermions from gaining masses until the electroweak symmetry is broken while still ensuring the proton stability. The apparent simplicity of the SHUT model, originating from its gauge, Yukawa, and Higgs-lepton unification at the trinification breaking scale, makes it a very interesting candidate for further theoretical and phenomenological studies. Depending on the chosen symmetry-breaking scheme as well as on values of the high-scale couplings and the hierarchy between them, the path down to an effective SM-like theory could lead to vast and yet unexplored low-energy phenomena. While those are yet to be understood in full detail, the SHUT model presented here shows potential for reviving the trinification GUT model building.

The first immediate task in further developments of the proposed high-scale SHUT model is to derive the basic properties of its SM-like EFT limit (at least, to one loop) and then to search for possible deviations from the characteristic SM signatures. This would allow us to set constraints on the SHUT parameter space and, possibly, to predict new smoking gun signals of new physics specific to the corresponding LR-symmetric EFT. The latter would then offer a plethora of opportunities for phenomenological studies of potentially observable beyond-SM phenomena in connection with the ongoing LHC and astroparticle physics searches.

Acknowledgments. The authors would like to thank N.-E. Bomark, C. Herdeiro, W. Porod, and F. Staub for insightful discussions in the preliminary stages of this work. J. E. C.-M. was supported by the Crafoord Foundation. A. M. and M. S. are funded by Grants of the Fundação para a Ciência e a Tecnologia (FCT), Portugal, No. SFRH/BPD/97126/2013 and No. SFRH/BPD/69971/2010 respectively. R. P., A. O., and J. W. were partially supported by the Swedish Research Council, Contract No. 621-2013-428. The work in this paper is also supported by FCT funding to CIDMA (Center for Research and Development in Mathematics and Applications), Project No. UID/MAT/04106/2013. R. P. was partially supported by the Comisión Nacional de

Investigación Científica y Tecnológica (CONICYT) project No. PIA ACT1406.

References

[1] H. Georgi and S. L. Glashow, "Unity of All Elementary Particle Forces," *Phys. Rev. Lett.* **32** (1974) 438–441.

[2] H. Fritzsch and P. Minkowski, "Unified Interactions of Leptons and Hadrons," *Annals Phys.* **93** (1975) 193–266.

[3] F. Gursey, P. Ramond, and P. Sikivie, "A Universal Gauge Theory Model Based on E6," *Phys. Lett.* **B60** (1976) 177–180.

[4] F. Gursey and P. Sikivie, "E(7) as a Universal Gauge Group," *Phys. Rev. Lett.* **36** (1976) 775.

[5] S. F. King, S. Moretti, and R. Nevzorov, "Exceptional supersymmetric standard model," *Phys. Lett.* **B634** (2006) 278–284, `arXiv:hep-ph/0511256 [hep-ph]`.

[6] S. F. King, S. Moretti, and R. Nevzorov, "Gauge coupling unification in the exceptional supersymmetric standard model," *Phys. Lett.* **B650** (2007) 57–64, `arXiv:hep-ph/0701064 [hep-ph]`.

[7] F. Braam, A. Knochel, and J. Reuter, "An Exceptional SSM from E6 Orbifold GUTs with intermediate LR symmetry," *JHEP* **06** (2010) 013, `arXiv:1001.4074 [hep-ph]`.

[8] R. Nevzorov, "E_6 inspired supersymmetric models with exact custodial symmetry," *Phys. Rev.* **D87** no. 1, (2013) 015029, `arXiv:1205.5967 [hep-ph]`.

[9] A. De Rújula, H. Georgi, and S. L. Glashow *in Fifth Workshop on Grand Unification. Editors: P. H. Frampton, H. Fried and K. Kang (World Scientific, Singapore), p. 88.* (1984) .

[10] A. G. Dias, C. A. de S. Pires, and P. S. Rodrigues da Silva, "The Left-Right SU(3)(L)xSU(3)(R)xU(1)(X) Model with Light, keV and Heavy Neutrinos," *Phys. Rev.* **D82** (2010) 035013, `arXiv:1003.3260 [hep-ph]`.

[11] M. Reig, J. W. F. Valle, and C. A. Vaquera-Araujo, "Unifying left–right symmetry and 331 electroweak theories," *Phys. Lett.* **B766** (2017) 35–40, arXiv:1611.02066 [hep-ph].

[12] K. S. Babu, X.-G. He, and S. Pakvasa, "Neutrino Masses and Proton Decay Modes in SU(3) X SU(3) X SU(3) Trinification," *Phys. Rev.* **D33** (1986) 763.

[13] J. Sayre, S. Wiesenfeldt, and S. Willenbrock, "Minimal trinification," *Phys. Rev.* **D73** (2006) 035013, arXiv:hep-ph/0601040 [hep-ph].

[14] X.-G. He and S. Pakvasa, "Baryon Asymmetry in SU(3)**3 X $Z(3)$ Trinification Model," *Phys. Lett.* **B173** (1986) 159.

[15] C. Cauet, H. Pas, and S. Wiesenfeldt, "Trinification, the Hierarchy Problem and Inverse Seesaw Neutrino Masses," *Phys. Rev.* **D83** (2011) 093008, arXiv:1012.4083 [hep-ph].

[16] M. Y. Wang and E. D. Carlson, "The Breaking of the SU(3)**3 gauge group," arXiv:hep-ph/9302215 [hep-ph].

[17] G. R. Dvali and Q. Shafi, "Gauge hierarchy in SU(3)(C) x SU(3)(L) x SU(3)-R and low-energy implications," *Phys. Lett.* **B326** (1994) 258–263, arXiv:hep-ph/9401337 [hep-ph].

[18] N. Maekawa and Q. Shafi, "Supersymmetric SU(3)**3 unification with anomalous U(1)(a) gauge symmetry," *Prog. Theor. Phys.* **109** (2003) 279–293, arXiv:hep-ph/0204030 [hep-ph].

[19] S. Willenbrock, "Triplicated trinification," *Phys. Lett.* **B561** (2003) 130–134, arXiv:hep-ph/0302168 [hep-ph].

[20] C. D. Carone, "Tri-N-ification," *Phys. Rev.* **D71** (2005) 075013, arXiv:hep-ph/0503069 [hep-ph].

[21] B. Stech, "The mass of the Higgs boson in the trinification subgroup of E6," *Phys. Rev.* **D86** (2012) 055003, arXiv:1206.4233 [hep-ph].

[22] B. Stech, "Trinification Phenomenology and the structure of Higgs Bosons," *JHEP* **08** (2014) 139, arXiv:1403.2714 [hep-ph].

[23] J. Hetzel and B. Stech, "Low-energy phenomenology of trinification: an effective left-right-symmetric model," *Phys. Rev.* **D91** (2015) 055026, arXiv:1502.00919 [hep-ph].

[24] G. M. Pelaggi, A. Strumia, and S. Vignali, "Totally asymptotically free trinification," *JHEP* **08** (2015) 130, arXiv:1507.06848 [hep-ph].

[25] P. Nath and R. L. Arnowitt, "Symmetry Breaking in Three Generation Calabi-yau Manifolds," *Phys. Rev.* **D39** (1989) 2006.

[26] G. M. Pelaggi, A. Strumia, and E. Vigiani, "Trinification can explain the di-photon and di-boson LHC anomalies," *JHEP* **03** (2016) 025, arXiv:1512.07225 [hep-ph].

[27] J. Hetzel, *Phenomenology of a left-right-symmetric model inspired by the trinification model*. PhD thesis, Ruperto-Carola-University of Heidelberg, Germany, 2015. arXiv:1504.06739 [hep-ph].

[28] T. Blazek, R. Dermisek, and S. Raby, "Predictions for Higgs and supersymmetry spectra from SO(10) Yukawa unification with mu greater than 0," *Phys. Rev. Lett.* **88** (2002) 111804, arXiv:hep-ph/0107097 [hep-ph].

[29] H. Baer and J. Ferrandis, "Supersymmetric SO(10) GUT models with Yukawa unification and a positive mu term," *Phys. Rev. Lett.* **87** (2001) 211803, arXiv:hep-ph/0106352 [hep-ph].

[30] A. Anandakrishnan and S. Raby, "Yukawa Unification Predictions with effective "Mirage" Mediation," *Phys. Rev. Lett.* **111** no. 21, (2013) 211801, arXiv:1303.5125 [hep-ph].

[31] T. Blazek, R. Dermisek, and S. Raby, "Yukawa unification in SO(10)," *Phys. Rev.* **D65** (2002) 115004, arXiv:hep-ph/0201081 [hep-ph].

[32] K. Tobe and J. D. Wells, "Revisiting top bottom tau Yukawa unification in supersymmetric grand unified theories," *Nucl. Phys.* **B663** (2003) 123–140, arXiv:hep-ph/0301015 [hep-ph].

[33] H. Baer, S. Kraml, and S. Sekmen, "Is 'just-so' Higgs splitting needed for t - b - tau Yukawa unified SUSY GUTs?," *JHEP* **09** (2009) 005, arXiv:0908.0134 [hep-ph].

[34] M. Badziak, M. Olechowski, and S. Pokorski, "Yukawa unification in SO(10) with light sparticle spectrum," *JHEP* **08** (2011) 147, arXiv:1107.2764 [hep-ph].

[35] A. Anandakrishnan, S. Raby, and A. Wingerter, "Yukawa Unification Predictions for the LHC," *Phys. Rev.* **D87** no. 5, (2013) 055005, arXiv:1212.0542 [hep-ph].

[36] A. S. Joshipura and K. M. Patel, "Yukawa coupling unification in SO(10) with positive μ and a heavier gluino," *Phys. Rev.* **D86** (2012) 035019, arXiv:1206.3910 [hep-ph].

[37] A. Anandakrishnan, B. C. Bryant, S. Raby, and A. Wingerter, "LHC Phenomenology of SO(10) Models with Yukawa Unification," *Phys. Rev.* **D88** (2013) 075002, arXiv:1307.7723 [hep-ph].

[38] A. Anandakrishnan, B. C. Bryant, and S. Raby, "LHC Phenomenology of SO(10) Models with Yukawa Unification II," *Phys. Rev.* **D90** no. 1, (2014) 015030, arXiv:1404.5628 [hep-ph].

[39] M. Badziak, M. Olechowski, and S. Pokorski, "Light staus and enhanced Higgs diphoton rate with non-universal gaugino masses and SO(10) Yukawa unification," *JHEP* **10** (2013) 088, arXiv:1307.7999 [hep-ph].

[40] M. Adeel Ajaib, I. Gogoladze, Q. Shafi, and C. S. Un, "A Predictive Yukawa Unified SO(10) Model: Higgs and Sparticle Masses," *JHEP* **07** (2013) 139, arXiv:1303.6964 [hep-ph].

[41] J. E. Camargo-Molina, A. P. Morais, R. Pasechnik, and J. Wessén, "On a radiative origin of the Standard Model from Trinification," *JHEP* **09** (2016) 129, arXiv:1606.03492 [hep-ph].

[42] R. Slansky, "Group Theory for Unified Model Building," *Phys. Rept.* **79** (1981) 1–128.

[43] M. B. Green, J. H. Schwarz, and E. Witten, *Superstring Theory, 25th Anniversary Edition*. Cambridge University Press, 2012.

[44] P. Candelas, G. T. Horowitz, A. Strominger, and E. Witten, "Vacuum Configurations for Superstrings," *Nucl. Phys.* **B258** (1985) 46–74.

[45] K. Benakli, M. Goodsell, F. Staub, and W. Porod, "Constrained minimal Dirac gaugino supersymmetric standard model," *Phys. Rev.* **D90** no. 4, (2014) 045017, arXiv:1403.5122 [hep-ph].

[46] K. Benakli, L. Darmé, M. D. Goodsell, and J. Harz, "The Di-Photon Excess in a Perturbative SUSY Model," *Nucl. Phys.* **B911** (2016) 127–162, arXiv:1605.05313 [hep-ph].

IV

Heavy charged scalars from $c\bar{s}$ fusion: A generic search strategy applied to a 3HDM with $\mathrm{U}(1) \times \mathrm{U}(1)$ family symmetry

José Eliel Camargo-Molina[1], Tanumoy Mandal[2,3], Roman Pasechnik, and Jonas Wessén[1].

JHEP, 1503 (2015) 148
doi:10.1007/JHEP03(2015)148
e-Print: arXiv:1412.6259 [hep-ph]
MCnet-14-27 LU-TP 14-44 JLAB-THY-15-1991

[1]Department of Astronomy and Theoretical Physics, Lund University, SE-223 62 Lund, Sweden
[2] Department of Physics and Astronomy, Uppsala University, Box 516, SE-751 20 Uppsala, Sweden.
[3] Department of Physics and Astrophysics, University of Delhi, Delhi 110007, India.

Abstract: We describe a class of three Higgs doublet models (3HDMs) with a softly broken $\mathrm{U}(1) \times \mathrm{U}(1)$ family symmetry that enforces a Cabibbo-like quark mixing while forbidding tree-level flavour changing neutral currents. The hierarchy in the observed quark masses is partly explained by a softer hierarchy in the vacuum expectation values of the three Higgs doublets. As a consequence, the physical scalar spectrum contains a Standard Model (SM) like Higgs boson h_{125} while exotic scalars couple the strongest to the second quark family, leading to rather unconventional discovery channels that could be probed at the Large Hadron Collider. In particular, we describe a search strategy for the lightest charged Higgs boson $H^{\pm}$, through the process $c\bar{s} \to H^{+} \to W^{+} h_{125}$, using a multivariate analysis that leads to an excellent discriminatory power against the SM background. Although the analysis is applied to the proposed class of 3HDMs, we employ a model-independent formulation such that it can be applied to any other model with the same discovery channel.

1 Introduction

The Standard Model (SM) remarkably stands as one of the most successful theories in physics. However, it can still be considered rather *ad hoc* in its nature, with unexplained features that arise from fitting the experimental data. In addition, it fails to offer an explanation to several observed natural phenomena such as dark matter, neutrino masses or baryon asymmetry in the universe. It is then natural to study extensions of the SM that, while retaining its predictive power, offer explanations or shed light into the origin of e.g. the hierarchy of fermion masses or rather specific flavour structure of the SM. There is a plethora of such beyond the SM (BSM) theories, but not many of those offer unconventional features testable at the current experiments.

One of the simplest and most studied extensions is the class of the so-called Two-Higgs Doublet Models (2HDMs) that add a second $\mathrm{SU}(2)_\mathrm{L}$ doublet to the SM (an extensive review can be found in Ref. [1]). The 2HDMs offer interesting phenomenological signatures and can lead to e.g. extra sources of CP violation, dark matter candidates and stable vacua at high energies. However, they typically introduce many new free parameters, fail to address the origin of the mass hierarchy in the fermion sector of the SM and require extra discrete symmetries to avoid tree-level Flavour Changing Neutral Currents (FCNCs).

The Three Higgs Doublet Models (3HDMs) can overcome some of those limitations (see e.g. Refs. [2, 3, 4]) and have sparked interest in recent literature (see e.g. Refs. [5, 6, 7, 8, 9, 10, 11]). While retaining most of the features of 2HDMs, 3HDMs can offer explanations to yet unexplained features of the SM with predictions testable in the current collider measurements. In particular, the increased field content makes it possible to impose higher symmetries, which in turn can lead to interesting flavour structures.

As shown in Refs. [12, 13], the most constraining realisable abelian symmetry of the scalar potential in 3HDM is $\mathrm{U}(1) \times \mathrm{U}(1)$. In this work, we promote the $\mathrm{U}(1) \times \mathrm{U}(1)$ symmetry of the scalar sector to the fermion sector, hereinafter called $\mathrm{U}(1)_\mathrm{X} \times \mathrm{U}(1)_\mathrm{Z}$, in such a way that (1) no tree-level FCNCs are present, (2) a Cabibbo-like mixing is enforced, and (3) the fermion mass hierarchies are related to a hierarchy in the three vacuum expectation values (VEVs) of the doublets. This leads to a model that, although remarkably simple due to its high symmetry, is still capable of both reproducing the current experimental data and providing the exotic collider signatures. The latter is due to the fact that, as a consequence of the model symmetries, the new scalar states (both charged and neutral) couple dominantly to the second quark family.

At the LHC, the searches for charged Higgs bosons are generally categorized into two mass regions depending on whether its mass $m_{H^\pm}$ is smaller or bigger than the top quark mass m_t. The motivation of this categorization comes from the properties of $H^\pm$ within the various 2HDM types or supersymmetric models. Usually, for a heavy charged Higgs state ($m_{H^\pm} \gtrsim m_t$), the dominant production and decay channels in the LHC context are $pp \to H^- t\bar{b}\,(H^+\bar{t}b)$ and $H^+ \to t\bar{b}$ ($H^- \to \bar{t}b$), respectively [14, 15]. Apart from this channel, production of $H^\pm$ in vector boson ($W^\pm Z$) fusion followed

by the $H^\pm \to W^\pm Z$ decay is prominent in Higgs triplet models such as the Georgi-Machacek model [16]. This channel has also been searched for by the ATLAS [17] and CMS [18] collaborations recently. Conversely, a light charged Higgs boson ($m_{H^\pm} \lesssim m_t$) that decays to $\tau\bar{\nu}$ [19, 15], $c\bar{s}$ [20, 21] or $c\bar{b}$ [22] has also been searched for at the LHC. Previously, at LEP, pair production of $H^\pm$ was considered where $H^\pm$ subsequently decays to a $W^\pm A$ pair [23, 24] (where A is a scalar with mass $m_A > 12$ GeV and predominantly decays to $b\bar{b}$ pairs).

Searches for heavy $H^\pm$ become increasingly important with the rise of the LHC center-of-mass energy and luminosity, thus it is important to explore new production and decay modes of $H^\pm$ that are predicted by various BSM theories. In this paper, we particularly focus on a new search channel where a heavy $H^\pm$ resonantly decays to a $W^\pm h_{125}$ pair after being produced in $c\bar{s}$ ($\bar{c}s$) fusion. This rather uncommon search channel leads to testable predictions of our model at current LHC energies. In Refs. [25, 26, 27], the $H^\pm \to W^\pm h_{125}$ decay is considered where the H^- (H^+) is produced in association with a $t\bar{b}$ ($\bar{t}b$) pair. In our case, H^+ is produced in the s-channel resonance through $c\bar{s}$ fusion. In Ref. [28], the possibility of sizable $c\bar{s} \to H^+$ production cross section is discussed in the SUSY context where a squark mixing can circumvent the chiral suppression of the single $H^\pm$ production. In Ref. [29], $c\bar{s} \to H^+$ production is shown to be dominant for a 2HDM with a Yukawa sector chosen such that one doublet couples strongest to the second generation. In our model, we will see that the $c\bar{s}H^+$ and $\bar{c}sH^-$ couplings are sizable due to the hierarchy in VEVs combined with the particular structure of the Yukawa sector.

In section 2, we introduce the model, its fermion and scalar sectors and their interplay as given by the $\mathrm{U(1)_X} \times \mathrm{U(1)_Z}$ symmetry, the VEV hierarchy and the spectrum of the theory. In section 3, we discuss the charged Higgs boson production and decay channels of the model and introduce a model-independent way to study $H^\pm$ production in the same unconventional channels. In section 4, we show the results of a multivariate analysis for the charged Higgs boson searches and show, by using the results of a genetic algorithm scan, that our proposed theory can produce the type of signals visible with such an analysis at the LHC. Finally, we summarize and conclude our results in section 6.

2 The model

In this work, we propose a 3HDM, with features that lead to a simple yet predictive theory. The model has a $\mathrm{U(1)_X} \times \mathrm{U(1)_Z}$ global symmetry constraining its scalar potential. This symmetry is the biggest abelian symmetry not leading to additional accidental symmetries in a 3HDM [5, 12, 13]. As a consequence, in the limit of one VEV being much larger than the other two, we can derive simple analytical formulas for masses and mixing matrices in the scalar sector and readily understand the features of the model and its physical consequences.

The $\mathrm{U(1)_X} \times \mathrm{U(1)_Z}$ is also present in the fermion sector of the theory. We choose the charge assignments to constrain the Yukawa sector in a manner consistent with the

experimental hierarchies in the quark mass spectrum while forbidding tree-level FCNCs arising from the scalar sector. The upside of this is that the mass hierarchy is directly connected to a VEV hierarchy, which needs not to be as strong as the hierarchy in the SM Yukawa parameters to explain the known quark masses.

A nice consequence is the opening of new search strategies for testing this model at the LHC. Due to the structure of the Yukawa sector, two physical charged Higgs bosons would be produced mainly through $c\bar{s}$ fusion, which can lead to good signal-to-background ratios as will be shown in section 4.

2.1 VEV hierarchy and the softly broken $\mathrm{U}(1)_\mathrm{X}\times\mathrm{U}(1)_\mathrm{Z}$ symmetry

Besides the field content of the SM, the model has two additional scalar $\mathrm{SU}(2)_\mathrm{L}$ doublets for a total of three. We will denote them by $H_{1,2,3}$, with charges shown in Table IV.1, and expand around the vacuum as

$$H_i = \begin{pmatrix} H_i^+ \\ \frac{1}{\sqrt{2}}\left(v_i + h_i + \mathrm{i}A_i\right) \end{pmatrix}, \quad i = 1,2,3\,. \tag{IV.1}$$

We will often focus on the case where $v_3 \gg v_{1,2}$. This particular limit calls for the definition of a small parameter ξ,

$$\xi \equiv \frac{\sqrt{v_1^2 + v_2^2}}{v_3}\,. \tag{IV.2}$$

After spontaneous symmetry breaking, in the limit $\xi \to 0$, there remains a $\mathrm{U}(1)_\mathrm{X} \times \mathrm{U}(1)_\mathrm{YZ}$ symmetry where $\mathrm{U}(1)_\mathrm{YZ}$ is generated by a combination of the $\mathrm{U}(1)_\mathrm{Y}$ and $\mathrm{U}(1)_\mathrm{Z}$ generators. That means that all processes violating $\mathrm{U}(1)_\mathrm{X} \times \mathrm{U}(1)_\mathrm{YZ}$ (and in particular $\mathrm{U}(1)_\mathrm{X}$) would be suppressed by some power of ξ. As we will see, in the limit that $\xi \ll 1$ it is possible to derive simple expressions for the masses and mixing matrices in the scalar sector. It is worth mentioning at this stage that, while such expressions serve as tools to understand the model's features, all scalar masses and mixing matrices will be computed fully numerically (i.e. not as expansions in ξ) when scanning the parameter space of the model.

A spontaneously broken $\mathrm{U}(1)_\mathrm{X} \times \mathrm{U}(1)_\mathrm{Z}$ global symmetry would lead to massless Goldstone bosons and constrain the model significantly when considering e.g. the precise measurements of the Z-boson width. This motivates us to softly break the symmetry by adding additional mass terms in the scalar potential. The scalar potential consistent with a softly broken $\mathrm{U}(1)_\mathrm{X} \times \mathrm{U}(1)_\mathrm{Z}$ global symmetry group can be split into fully symmetric and soft-breaking parts as $V = V_0 + V_\mathrm{soft}$, where

$$V_0 = -\sum_{i=1}^{3}\mu_i^2|H_i|^2 + \sum_{i,j=1}^{3}\left(\frac{\lambda_{ij}}{2}|H_i|^2|H_j|^2 + \frac{\lambda'_{ij}}{2}|H_i^\dagger H_j|^2\right), \quad V_\mathrm{soft} = \sum_{i=1}^{3}\frac{1}{2}(m_{ij}^2 H_i^\dagger H_j + \mathrm{c.c}) \tag{IV.3}$$

with

$$\lambda_{ij} = \lambda_{ji}\,, \quad \lambda'_{ij} = \lambda'_{ji}\,, \quad m^2_{ij} = m^2_{ji}\,, \tag{IV.4}$$

$$\lambda'_{11} = \lambda'_{22} = \lambda'_{33} = 0\,, \quad m^2_{11} = m^2_{22} = m^2_{33} = 0\,. \tag{IV.5}$$

All parameters in the scalar potential can be taken real without any loss of generality. This is due to the fact that the parameters in V_0 are real by construction, while any phases on m^2_{ij} can be eliminated by field redefinitions of the three Higgs doublets. As a consequence the scalar sector of the model has no choice but to be CP-conserving.

For convenience we define

$$\tilde{\lambda}_{ij} = (\lambda_{ij} + \lambda'_{ij})\,. \tag{IV.6}$$

Finally, assuming that $v_{1,2,3} \neq 0$ and requiring that the first derivative of V vanishes, we can write

$$\mu_i^2 = \sum_{j=1}^{3} \left[\frac{1}{2} \tilde{\lambda}_{ij} v_j^2 + m^2_{ij} \frac{v_j}{v_i} \right]\,. \tag{IV.7}$$

2.2 Extending the $\mathrm{U}(1)_\mathrm{X} \times \mathrm{U}(1)_\mathrm{Z}$ to the fermion sector

We assign the quark $\mathrm{U}(1)_\mathrm{X} \times \mathrm{U}(1)_\mathrm{Z}$ charges such that the neutral component of H_3 couples to only up- and down-type quarks of the third generation while the neutral components of H_1 and H_2 couple to the first and second generation down-type and up-type quarks respectively, i.e.

$$\mathcal{L}^\mathrm{q}_\mathrm{Yukawa} = \sum_{i,j=1}^{2} \left\{ y^\mathrm{d}_{ij} \bar{d}^i_\mathrm{R} H_1^\dagger Q^j_\mathrm{L} - y^\mathrm{u}_{ij} \bar{u}^i_\mathrm{R} \tilde{H}_2^\dagger Q^j_\mathrm{L} \right\} + y_\mathrm{b} \bar{b}_\mathrm{R} H_3^\dagger Q^3_\mathrm{L} - y_\mathrm{t} \bar{t}_\mathrm{R} \tilde{H}_3^\dagger Q^3_\mathrm{L} + \mathrm{c.c.} \tag{IV.8}$$

In this way we forbid scalar-mediated tree-level FCNCs and simultaneously enforce a Cabibbo-like quark mixing, where the gauge eigenstates of the third quark family are aligned with the corresponding flavour eigenstates. This also means that a hierarchy in the VEVs of the Higgs doublets, where $v_3 \gg v_{1,2}$, leads to a third quark family that is much heavier than the first two without a strong hierarchy in the Yukawa couplings. In Table IV.1, we show the most general quark charge assignments allowing the terms in Eq. (IV.8) once the $\mathrm{U}(1)_\mathrm{X} \times \mathrm{U}(1)_\mathrm{Z}$ charges of $H_{1,2,3}$ are fixed. As long as the parameters α, β, γ and δ in Table IV.1 satisfy

$$(\beta - \gamma, \alpha - \delta) \notin \{(-1,-1), (-1,0), (0,0), (1,0), (1,1), (2,1)\}\,, \tag{IV.9}$$

the terms in Eq. (IV.8) are also the *only* allowed quark Yukawa interactions. It is worth noting that in the mass basis, the free parameters in the quark sector are simply the quark masses and the Cabibbo angle. The reader might note that at higher orders, the Yukawa interactions only allow for a mixing between the first and second quark generations, thus opening the question of how to reproduce the observed full CKM

	$\mathrm{U(1)_Y}$	$\mathrm{U(1)_X}$	$\mathrm{U(1)_Z}$
H_1	$\frac{1}{2}$	-1	$-\frac{2}{3}$
H_2	$\frac{1}{2}$	1	$\frac{1}{3}$
H_3	$\frac{1}{2}$	0	$\frac{1}{3}$
$Q_{\mathrm{L}}^{1,2}$	$\frac{1}{6}$	γ	δ
Q_{L}^{3}	$\frac{1}{6}$	β	α
$u_{\mathrm{R}}^{1,2}$	$\frac{2}{3}$	$1+\gamma$	$\frac{1}{3}+\delta$
t_{R}	$\frac{2}{3}$	β	$\frac{1}{3}+\alpha$
$d_{\mathrm{R}}^{1,2}$	$-\frac{1}{3}$	$1+\gamma$	$\frac{2}{3}+\delta$
b_{R}	$-\frac{1}{3}$	β	$-\frac{1}{3}+\alpha$

Table IV.1: Charges of the global $\mathrm{U(1)_X}$, $\mathrm{U(1)_Z}$ and gauge (hypercharge) $\mathrm{U(1)_Y}$ symmetries in the considering class of 3HDMs. The fermion charges together with the constraints in Eq. (IV.9) are chosen so that the only allowed Yukawa terms are those in Eq. (IV.8).

mixing in the quark sector. As this model is thought as an effective theory, one can write the following dimension-6 operators consistent with the imposed symmetries

$$\begin{aligned} &\bar{d}_{\mathrm{R}}^{1,2}\left(H_i^\dagger Q_{\mathrm{L}}^3\right)\left(H_j^\dagger H_k\right), \quad \bar{u}_{\mathrm{R}}^{1,2}\left(\tilde{H}_i^\dagger Q_{\mathrm{L}}^3\right)\left(H_j^\dagger H_k\right), \\ &\bar{b}_{\mathrm{R}}\left(H_i^\dagger Q_{\mathrm{L}}^{1,2}\right)\left(H_j^\dagger H_k\right), \quad \bar{t}_{\mathrm{R}}\left(\tilde{H}_i^\dagger Q_{\mathrm{L}}^{1,2}\right)\left(H_j^\dagger H_k\right). \end{aligned} \tag{IV.10}$$

Such terms will induce naturally small (suppressed by a scale of new physics) mixing terms with the third quark family once Higgs VEVs appear. The operators can in principle be generated à la Frogatt-Nielsen mechanism [30] by integrating out the heavy fields of a high-energy theory. A deeper analysis of this is beyond the scope of this paper.

Finally, we note that the lepton Yukawa sector can be made very SM-like by assigning the lepton $\mathrm{U(1)_X} \times \mathrm{U(1)_Z}$ charges such that they only couple to H_3. We will assume that this is the case throughout this work, and will not discuss the implications on lepton phenomenology any further. However, we want to point out that there are also other interesting scenarios, e.g. where the leptons couple to $H_{1,2,3}$ such that the lepton mass hierarchies are also related to $v_{1,2} \ll v_3$.

2.3 The spectrum, mixing matrices and interactions of the scalar sector

After spontaneous symmetry breaking, the mass terms in the scalar potential V in Eq. (IV.3),

$$\sum_{i,j=1}^{3}\left[\frac{1}{2}A_i(M_{\mathrm{P}}^2)_{ij}A_j + \frac{1}{2}h_i(M_{\mathrm{S}}^2)_{ij}h_j + H_i^-(M_{\mathrm{C}}^2)_{ij}H_j^+\right], \tag{IV.11}$$

can be neatly expressed using

$$
\begin{aligned}
(M_{\rm P}^2)_{ij} &= m_{ij}^2 - \delta_{ij}\sum_{k=1}^{3} m_{ik}^2 \frac{v_k}{v_i}\,, \\
(M_{\rm S}^2)_{ij} &= \tilde{\lambda}_{ij} v_i v_j + (M_{\rm P}^2)_{ij}\,, \\
(M_{\rm C}^2)_{ij} &= \lambda'_{ij} v_i v_j - \delta_{ij}\sum_{k=1}^{3} \lambda'_{ik} v_k^2 + (M_{\rm P}^2)_{ij}\,.
\end{aligned}
\tag{IV.12}
$$

We note that both $M_{\rm C,P}^2$ have an eigenvector $\propto v_i$ with vanishing eigenvalue. The corresponding Goldstone states become the longitudinal polarization states of the massive electroweak gauge bosons.

The electrically neutral scalar, pseudo-scalar and charged scalar mass eigenstates,

$$
\bar{h}_i = (h_{\rm a}, h_{\rm b}, h_{125})\,, \quad \bar{A}_i = (A_{\rm a}, A_{\rm b}, A_{\rm G})\,, \quad \bar{H}_i^{\pm} = (H_{\rm a}^{\pm}, H_{\rm b}^{\pm}, H_{\rm G}^{\pm})\,,
\tag{IV.13}
$$

are related to the interaction eigenstates as

$$
h_i = \mathsf{S}_{ij}\bar{h}_j\,, \quad A_i = \mathsf{P}_{ij}\bar{A}_j\,, \quad H_i^{\pm} = \mathsf{C}_{ij}\bar{H}_j^{\pm}\,,
\tag{IV.14}
$$

The states $A_{\rm G}$ and $H_{\rm G}^{\pm}$ in Eq. (IV.13) denote the Goldstone bosons. Working in the $\xi \ll 1$ limit, the mixing matrices S, P and C are identical up to $\mathcal{O}(\xi)$ but differ at $\mathcal{O}(\xi^2)$. It is here convenient to define an angle $\beta \in [0, \frac{\pi}{2}]$ as

$$
\tan\beta = \frac{v_2}{v_1}\,.
\tag{IV.15}
$$

To the second order in ξ, we have

$$
\mathsf{S} = \mathsf{T} + \xi^2\mathsf{S}'\,, \quad \mathsf{P} = \mathsf{T} + \xi^2\mathsf{P}'\,, \quad \mathsf{C} = \mathsf{T} + \xi^2\mathsf{C}'
\tag{IV.16}
$$

with

$$
\mathsf{T} = \begin{pmatrix} 1 & X\xi & c_\beta\xi \\ -X\xi & 1 & s_\beta\xi \\ -c_\beta\xi & -s_\beta\xi & 1 \end{pmatrix}, \quad X \equiv \frac{m_{12}^2 s_\beta c_\beta}{m_{13}^2 s_\beta - m_{23}^2 c_\beta}\,.
\tag{IV.17}
$$

For the $\mathcal{O}(\xi^2)$ pieces, we have

$$
\mathsf{P}' = \begin{pmatrix} -\frac{1}{2}(X^2+c_\beta^2) & -\frac{1}{2}(1-Y)s_\beta c_\beta & 0 \\ -\frac{1}{2}(1+Y)s_\beta c_\beta & -\frac{1}{2}(X^2+s_\beta^2) & 0 \\ X s_\beta & -X c_\beta & 0 \end{pmatrix}, \mathsf{C}' = \mathsf{P}' + \begin{pmatrix} 0 & Z_1 & 0 \\ -Z_1 & 0 & 0 \\ 0 & 0 & 0 \end{pmatrix}, \mathsf{S}' = \mathsf{P}' + \begin{pmatrix} 0 & 0 & Z_2 \\ 0 & 0 & Z_3 \\ -Z_2 & -Z_3 & 0 \end{pmatrix},
\tag{IV.18}
$$

where

$$
\begin{aligned}
Y &= \frac{(2m_{12}^4 + m_{23}^4)c_\beta^2 - (2m_{12}^4 + m_{13}^4)s_\beta^2}{(m_{13}^2 s_\beta - m_{23}^2 c_b^2)^2} \quad , \quad Z_1 = \frac{(\lambda'_{23} - \lambda'_{13})s_\beta^2 c_\beta^2 m_{12}^2 v_3^2}{(m_{13}^2 s_\beta - m_{23}^2 c_\beta)^2}\,, \\
Z_2 &= (\tilde{\lambda}_{13} - \lambda_{33})c_\beta^2 \frac{v_3^2}{m_{13}^2} \quad , \quad Z_3 = (\tilde{\lambda}_{23} - \lambda_{33})s_\beta^2 \frac{v_3^2}{m_{23}^2}\,.
\end{aligned}
\tag{IV.19}
$$

Here, $Z_{1,2,3}$ parametrize the leading order difference between the mixing matrices, which will be important as these parameters determine the off-diagonal scalar-scalar interactions with the electroweak gauge bosons. We also note that as X, Y, Z_1, Z_2, Z_3 get larger, the expansion in ξ becomes less reliable.

The state h_{125} contains mostly h_3, meaning that it couples substantially to the third quark family. It also receives a mass of the order of $v_3 \sim v$,

$$m^2_{h_{125}} = \lambda_{33} v_3^2 + \mathcal{O}(\xi^2)\,, \tag{IV.20}$$

making this state our candidate for the observed SM Higgs-like 125 GeV state. The exotic scalars $h_{\mathrm{a,b}}$, $A_{\mathrm{a,b}}$ and $H^\pm_{\mathrm{a,b}}$ can all be made heavy as the leading order contribution to their masses is inversely proportional to ξ. To this leading order, $\{h_{\mathrm{a}}, A_{\mathrm{a}}, H^\pm_{\mathrm{a}}\}$ are degenerate in mass. This is also the case for $\{h_{\mathrm{b}}, A_{\mathrm{b}}, H^\pm_{\mathrm{b}}\}$. More accurately, the masses are given by

$$\begin{aligned} m^2_{A_{\mathrm{a}}} = m^2_{h_{\mathrm{a}}} &= -\frac{m^2_{13}}{c_\beta \xi} - m^2_{12} t_\beta - (m^2_{13} c_\beta + X m^2_{12})\xi\,, \quad m^2_{H^\pm_{\mathrm{a}}} = m^2_{A_{\mathrm{a}}} - \lambda'_{13} v_3^2\,, \\ m^2_{A_{\mathrm{b}}} = m^2_{h_{\mathrm{b}}} &= -\frac{m^2_{23}}{s_\beta \xi} - \frac{m^2_{12}}{t_\beta} - (m^2_{23} s_\beta + X m^2_{12})\xi\,, \quad m^2_{H^\pm_{\mathrm{b}}} = m^2_{A_{\mathrm{b}}} - \lambda'_{23} v_3^2\,, \end{aligned} \tag{IV.21}$$

to $\mathcal{O}(\xi)$. This means that the exotic scalars and pseudo-scalars are typically very close in mass when $\xi \ll 1$, i.e. $m^2_{A_{\mathrm{a,b}}} - m^2_{h_{\mathrm{a,b}}} = \mathcal{O}(\xi^2)$. Note also that the couplings λ'_{ij} can either be positive or negative, such that the charged scalars $H^+_{\mathrm{a,b}}$ can both be heavier and lighter than the neutral scalars in the respective family.

We conclude this section by listing the trilinear interactions between the physical scalars and the electroweak gauge bosons, as they are relevant for the collider phenomenology of the charged Higgs boson discussed in section 3. The interactions between the neutral scalars, charged scalars and the W boson are given by

$$\begin{aligned} \mathcal{L} &\supset \mathrm{i}\frac{g_2}{2} W^-_\mu \sum_{i=1}^{3} \left[(\partial^\mu H^+_i) h_i - H^+_i (\partial^\mu h_i)\right] + \mathrm{c.c} \\ &= \mathrm{i}\frac{g_2}{2} W^-_\mu \sum_{i,j=1}^{3} (\mathsf{C}^{\mathrm{T}}\mathsf{S})_{ij} \left[(\partial^\mu \bar{H}^+_i) \bar{h}_j - \bar{H}^+_i (\partial^\mu \bar{h}_j)\right] + \mathrm{c.c}\,, \end{aligned} \tag{IV.22}$$

with

$$\mathsf{C}^{\mathrm{T}}\mathsf{S} = \begin{pmatrix} 1 & -Z_1\xi^2 & Z_2\xi^2 \\ Z_1\xi^2 & 1 & Z_3\xi^2 \\ -Z_2\xi^2 & -Z_3\xi^2 & 1 \end{pmatrix} + \mathcal{O}(\xi^3)\,. \tag{IV.23}$$

The top line in Eq. (IV.22) is written in the interaction eigenbasis of the scalars, while the bottom line is the same expression in terms of the mass eigenstates. The W boson also couples to pairs of charged scalars and pseudo-scalars as

$$\begin{aligned} \mathcal{L} &\supset \frac{g_2}{2} W^-_\mu \sum_{i=1}^{3} \left[(\partial^\mu H^+_i) A_i - H^+_i (\partial^\mu A_i)\right] + \mathrm{c.c} \\ &= \frac{g_2}{2} W^-_\mu \sum_{i,j=1}^{3} (\mathsf{C}^{\mathrm{T}}\mathsf{P})_{ij} \left[(\partial^\mu \bar{H}^+_i) \bar{A}_j - \bar{H}^+_i (\partial^\mu \bar{A}_j)\right] + \mathrm{c.c}\,, \end{aligned} \tag{IV.24}$$

with

$$\mathsf{C}^{\mathrm{T}}\mathsf{P} = \begin{pmatrix} 1 & -Z_1\xi^2 & 0 \\ Z_1\xi^2 & 1 & 0 \\ 0 & 0 & 1 \end{pmatrix} + \mathcal{O}(\xi^3)\,. \tag{IV.25}$$

Similarly, for the trilinear interactions with the Z boson, we have

$$\begin{aligned} \mathcal{L} &\supset \frac{g_2}{2c_{\mathrm{W}}} Z_\mu \sum_{i=1}^{3} \left[(\partial^\mu A_i)h_i - A_i(\partial^\mu h_i)\right] \\ &= \frac{g_2}{2c_{\mathrm{W}}} Z_\mu \sum_{i,j=1}^{3} (\mathsf{P}^{\mathrm{T}}\mathsf{S})_{ij} \left[(\partial^\mu \bar{A}_i)\bar{h}_j - \bar{A}_i(\partial^\mu \bar{h}_j)\right], \end{aligned} \tag{IV.26}$$

where c_{W} is the cosine of the Weinberg angle and

$$\mathsf{P}^{\mathrm{T}}\mathsf{S} = \begin{pmatrix} 1 & 0 & Z_2\xi^2 \\ 0 & 1 & Z_3\xi^2 \\ -Z_2\xi^2 & -Z_3\xi^2 & 1 \end{pmatrix} + \mathcal{O}(\xi^3)\,. \tag{IV.27}$$

2.4 Scalar-fermion couplings

Knowing the mixing matrices S, P and C for the neutral scalars, pseudo-scalars and charged scalars, respectively, to the first orders in ξ, it is straightforward to obtain the Yukawa interactions between the physical scalars and the quarks. Using Eq. (IV.14) we find that h_{125} couples to quarks in a way similar to the SM,

$$\mathcal{L} \supset \sum_q \frac{m_q}{v_3}\, \bar{q}q\, h_{125} + \mathcal{O}(\xi)\,. \tag{IV.28}$$

For the third quark family, this is an obvious consequence of the model's symmetries, as t and b quarks receive their masses from H_3 with $v_3 \lesssim v$, and h_{125} is mostly made of h_3. On the other hand, the first and second family get their masses from $H_{1,2}$ with $v_{1,2} \ll v_3$, so the corresponding Yukawa couplings with the gauge eigenstates $H_{1,2}$ are quite large as $\mathcal{O}(m_q/v_{1,2}) \sim \mathcal{O}(m_q/\xi v_3)$. When shifting to the mass eigenbasis, $h_{1,2}$ contribute to h_{125} only at $\mathcal{O}(\xi)$ thus giving an overall coupling of $\mathcal{O}(m_q/v_3)$.

In the same process, we also find the interaction terms between the quarks and the exotic scalar states $h_{\mathrm{a,b}}$, $A_{\mathrm{a,b}}$ and $H^{\pm}_{\mathrm{a,b}}$. Couplings to the third quark family are generally quite small $\sim m_{\mathrm{t,b}}\xi/v_3$. In our model, phenomenologically the most relevant couplings are with the second quark family instead, which to the leading order in ξ read

$$\begin{aligned} \mathcal{L} \supset{}& \cos\theta_{\mathrm{C}} \frac{\sqrt{2}m_{\mathrm{s}}}{v_1} \bar{s}_{\mathrm{R}} c_{\mathrm{L}} H^-_{\mathrm{a}} - \cos\theta_{\mathrm{C}} \frac{\sqrt{2}m_{\mathrm{c}}}{v_2} \bar{c}_{\mathrm{R}} s_{\mathrm{L}} H^+_{\mathrm{b}} + \mathrm{c.c.} + \mathcal{O}(\xi) \\ &+ \frac{m_{\mathrm{s}}}{v_1}\bar{s}sh_{\mathrm{a}} - \frac{m_{\mathrm{c}}}{v_2}\bar{c}ch_{\mathrm{b}} + \mathrm{i}\frac{m_{\mathrm{s}}}{v_1}\bar{s}\gamma^5 sA_{\mathrm{a}} - \mathrm{i}\frac{m_{\mathrm{c}}}{v_2}\bar{c}\gamma^5 cA_{\mathrm{b}} + \mathcal{O}(\xi)\,, \end{aligned} \tag{IV.29}$$

where θ_{C} is the Cabbibo angle. When the masses of the scalars are in the appropriate range, we can expect that the charged scalars $H^+_{\mathrm{a,b}}$ would be produced in collider experiments through $c\bar{s}$ fusion while h_{a} and A_{a} (h_{b} and A_{b}) would mainly be produced by the $s\bar{s}$ ($c\bar{c}$) fusion.

3 A model independent approach

One of the interesting features of our model is the existence of heavy charged scalars H^+ (H^-) that mostly couple to a $c\bar{s}$ ($\bar{c}s$) pair as their interactions with $t\bar{b}$ ($\bar{t}b$) are small due to the model symmetries. Furthermore, we find that $H^\pm$ can decay to a $W^\pm h_{125}$ pair with a sizable branching ratio (BR) which is still allowed by the current experimental data. It turns out that this unconventional channel, while not explored in the literature before for $m_{H^\pm} > 200$ GeV, can be a rather clean way to search for charged scalars at the LHC.

In the following, we adopt a model independent approach in searching for charged scalars exhibiting those features. In section 5, we will show how the analysis can be used to find discovery regions in the parameter space of the 3HDM we have proposed above. We take a model independent approach to not only test the predictions of our model, but also to offer a guideline for our experimental colleagues to implement this new search channel in the experimental analyses.

We start with the following model independent Lagrangian for $H^\pm$ including its kinetic ($\mathcal{L}_{kin}$) and interaction ($\mathcal{L}_{int}$) terms

$$\mathcal{L}_{kin} \supset D_\mu H^+ D^\mu H^- - m^2_{H^\pm}\ H^+ H^- \,, \tag{IV.30}$$

$$\mathcal{L}_{int} \supset \kappa^p_{cs}\ \bar{c}_{\rm R} s_{\rm L} H^+ + \kappa^m_{cs}\ \bar{s}_{\rm R} c_{\rm L} H^- + i\kappa_{Wh_{125}}\ \left(h_{125}\partial^\mu H^+ - H^+\partial^\mu h_{125}\right) W^-_\mu + \text{c.c.}\,. \tag{IV.31}$$

There are four free parameters in the above Lagrangian *viz.* the charged Higgs mass $m_{H^\pm}$, and the three couplings κ^p_{cs}, κ^m_{cs} and $\kappa_{Wh_{125}}$. In general, κ^p_{cs} and κ^m_{cs} both could be non-zero. In that case, the production cross section, $\sigma(pp \to H^\pm)$ is proportional to the combination $\left[\left(\kappa^p_{cs}\right)^2 + \left(\kappa^m_{cs}\right)^2\right]$. Therefore, instead of two free couplings, we introduce a single free parameter κ_{cs} which is, $\kappa^2_{cs} = \left(\kappa^p_{cs}\right)^2 + \left(\kappa^m_{cs}\right)^2$. From the above model independent Lagrangian, we see that H^+ has only two decay modes: $W^+ h_{125}$ and $c\bar{s}$. The corresponding tree-level partial widths are given by

$$\begin{aligned}\Gamma\left(H^\pm \to W^\pm h_{125}\right) = \frac{\kappa^2_{Wh_{125}} m^3_{H^\pm}}{64\pi m^2_W}\left[1 - \frac{\left(m_{h_{125}} - m_W\right)^2}{m^2_{H^\pm}}\right]\left[1 - \frac{\left(m_{h_{125}} + m_W\right)^2}{m^2_{H^\pm}}\right] \\ \times \left[1 - \frac{2\left(m^2_{h_{125}} + m^2_W\right)}{m^2_{H^\pm}} + \frac{\left(m^2_{h_{125}} - m^2_W\right)^2}{m^4_{H^\pm}}\right]^{1/2}\,,\end{aligned} \tag{IV.32}$$

$$\Gamma\left(H^+ \to c\bar{s}\right) = \frac{3\left[\left(\kappa^p_{cs}\right)^2 + \left(\kappa^m_{cs}\right)^2\right] m_{H^\pm}}{16\pi} = \frac{3\kappa^2_{cs} m_{H^\pm}}{16\pi}\,. \tag{IV.33}$$

where $m_{h_{125}} = 125$ GeV. The expression $\Gamma(H^+ \to c\bar{s})$ is given in the limit of massless c and s quarks. In general, $H^\pm$ can have other decay modes too. We, therefore, take the BR of the decay mode $H^\pm \to W^\pm h_{125}$ denoted by $\text{BR}_{Wh_{125}}$ as a free parameter

instead of $\kappa_{Wh_{125}}$. So, one can write the following in the narrow-width approximation,

$$\sigma(pp \to H^\pm \to W^\pm h_{125}) = \sigma(pp \to H^\pm) \times \mathrm{BR}_{Wh_{125}} = \kappa_{cs}^2 \times \sigma_0(m_{H^\pm}) \times \mathrm{BR}_{Wh_{125}}\,, \tag{IV.34}$$

where $\sigma_0(m_{H^\pm})$ is the cross section of $pp \to H^\pm$ for $\kappa_{cs} = 1$. We show $\sigma_0(m_{H^\pm})$ at the LHC ($\sqrt{s} = 13$ TeV) as a function of $m_{H^\pm}$ in Fig. IV.1.

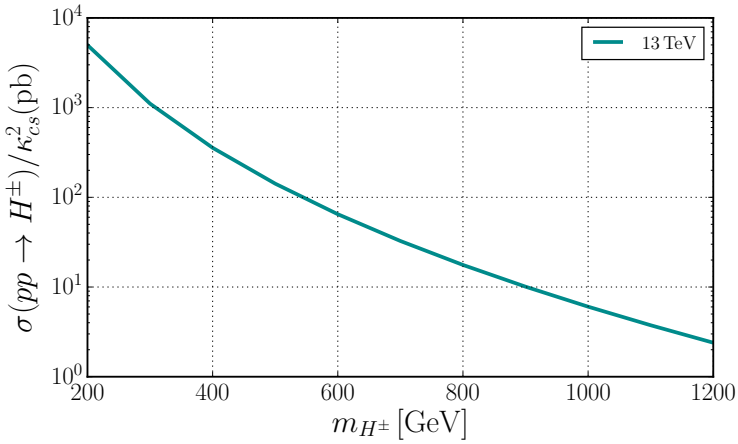

Figure IV.1: $\sigma(pp \to H^\pm)/\kappa_{cs}^2 = \sigma_0(m_{H^\pm})$ as a function of $m_{H^\pm}$ at the LHC ($\sqrt{s} = 13$ TeV).

4 Search for charged scalars produced by $c\bar{s}$ fusion

We implement the model independent Lagrangian of $H^\pm$ as shown in Eqs. (IV.30) and (IV.31) in FeynRules [31] from which we get the Universal FeynRules Output [32] model files for the MadGraph [33] event generator. We use the NNPDF [34] parton distribution functions (PDFs) for the signal and background event generation. For the signal, we use fixed factorization μ_F and renormalization μ_R scales at $\mu_F = \mu_R = m_{H^\pm}$ while for the background these scales are chosen at the appropriate scale of the process. We use Pythia6 [35] for subsequent showering and hadronization of the generated events. Detector simulation is performed using Delphes [36] which employs the FastJet [37] package for jet clustering. Jets are clustered using the anti-kT algorithm [38] with the clustering parameter $R = 0.4$. For the multivariate analysis (MVA), we use the Boosted Decision Tree (BDT) algorithm in the TMVA [39] framework. In this analysis, all calculations are done at the leading order, for simplicity.

4.1 Signal

We focus the H^+ (H^-) production from the $c\bar{s}$ ($\bar{c}s$) initial state followed by the decay $H^\pm \to W^\pm h_{125}$. We consider a semileptonic final state where $W^\pm$ decays leptonically and h_{125} decays to $b\bar{b}$. Therefore, the chain of the signal process in our case is

$$pp \to H^\pm \to W^\pm h_{125} \to \ell^\pm + \not{E}_T + b\bar{b} \; . \tag{IV.35}$$

Here, $\ell = \{e, \mu\}$. We then have one charged lepton, two b-jets and missing transverse energy in the final state and our event selection criteria is exactly one charged lepton (either an electron or a muon including their anti-particles), at least two jets and missing transverse energy that pass the following basic selection cuts:

- Lepton: $p_T(\ell) > 25$ GeV, $|\eta(\ell)| < 2.5$
- Jet: $p_T(J) > 25$ GeV, $|\eta(J)| < 4.5$
- Missing transverse energy: $\not{E}_T > 25$ GeV
- ΔR separation: $\Delta R(J_1, J_2) > 0.4$, $\Delta R(\ell, J) > 0.4$

Here, J_1 and J_2 denote the first and the second highest p_T jets. After selecting the events, we further demand b-tagging on the two leading-p_T jets. The b-tagging on jets can reduce the background very effectively but it can also somewhat reduce the signal. Therefore, to enhance the signal cut efficiency we do not always demand two b's tagging although there are two b-jets present in the signal. Depending on the number of b-tagged jets we demand, we define the following two signal categories

- $1b$-tag: In this category, we demand at least one b-tagged jet among the two leading p_T jets.
- $2b$-tag: In this category, we demand that both the two leading p_T jets are b-tagged. This category is a subset of the $1b$-tag category.

To reconstruct the Higgs boson, we apply an invariant mass cut $|m_{H^\pm} - m_{h_{125}}| < 20$ GeV around the Higgs boson mass $m_{h_{125}} = 125$ GeV. However, the full event is not totally reconstructible due to the presence of the missing transverse energy.

4.2 Background

The main background for the signal with one lepton, at least one or two b-tagged jets and missing energy can come from the following SM processes:

1. $W^\pm + \text{jets}$: The definition of our inclusive $W^\pm + \text{jets}$ background includes up to two jets and we include the b parton in the jet definition i.e. $j = \{g, u, d, c, s, b\}$. We

Process	$W+n\,j$	Wbj	Wbb	$t\bar{t}+n\,j$	tj	tb	tW	WW	WZ	Wh_{125}
x-sec (pb)	1.53×10^5	308.9	41.7	431.3	174.6	2.6	54.0	67.8	25.4	1.1

Table IV.2: Parton-level cross sections of various background processes (without any cut) at the LHC ($\sqrt{s}$ = 13 TeV). Here, n is the number of jets.

generate these background events in two separate parts. In one sample, we only consider light jets i.e.$j = \{g, u, d, c, s\}$ and combine $pp \to W^\pm + (0, 1, 2)\, j$ processes where we set the matching scale $Q_{cut} = 25$ GeV. This background is the largest (the cross section is about 1.53×10^5 pb at the LHC, with $\sqrt{s} = 13$ TeV, without any cut) among all the dominant SM backgrounds we have considered. Although the bare cross section is large, it will reduce drastically after b-tagging due to a small mistagging (light jet is tagged as b-jet) rate. We find that its contribution in the $1b$-tag category is substantial but in the $2b$-tag category is very small. In the other sample, we consider at least one b parton in the final state where we combine $pp \to W^\pm bj$ and $pp \to W^\pm b\bar{b}$ processes (no SM $pp \to W^\pm b$ process exists). This background will contribute significantly in both the categories. We include $pp \to W^\pm h_{125} \to W^\pm b\bar{b}$ and $pp \to W^\pm Z \to W^\pm b\bar{b}$ processes in the $pp \to W^\pm b\bar{b}$ channel.

2. $t\bar{t}+$jets: The definition of our inclusive $t\bar{t}+$jets background includes up to two jets containing also b partons. We generate this background by combining $pp \to t\bar{t} + (0, 1, 2)\, j$ processes using the matching scale $Q_{cut} = 25$ GeV. The matched cross section is about 431 pb before the top decay and without any selection cut applied. We find that this background is the dominant one after the strong basic selection cuts (applied before passing the events to the MVA).

3. Single top: This background includes three types of single top processes – s-channel single top (such $pp \to t\bar{b}$), t-channel single top (i.e. $pp \to tj$) and single-top associated with W (such as $pp \to tW^\pm$) processes. Note that for the $pp \to tW^\pm$ process, the selected lepton can come from two possible ways, either from the decay of the associated $W^\pm$ or from the $W^\pm$ coming from the top decay. These two possibilities are properly included in our event sample. The single top background also contributes significantly to the total background.

4. Diboson: This background includes $pp \to W^\pm W^\mp \to W^\pm + jj$ and $pp \to W^\pm Z \to W^\pm + jj$ processes where two light jets come from the decay of W or Z bosons. In this background, we have also included $pp \to W^\pm Z \to W^\pm \nu\bar{\nu}$ processes where two selected jets come from the parton showers. This background reduces drastically due to the small mistagging efficiency of light jets that are misidentified as b-jets. Finally, in the MVA this background contributes negligibly to the total background. Note that two diboson production processes *viz.* $pp \to W^\pm h_{125} \to W^\pm b\bar{b}$ and $pp \to W^\pm Z \to W^\pm b\bar{b}$ are already considered in the $W+$jets background.

5. QCD multijets: The multijet background arises due to QCD interactions at the LHC and has a very large production cross section, especially in the soft region. The QCD-induced multijet production processes can potentially contribute to the total background for our signal by faking the lepton, $\not{E}_T$ and b-tagged jets. It is

impractical to study this part of the background using a Monte-Carlo simulation since it is computationally challenging to generate enough events due to very low fake rates. In experimental analyses, this contribution is usually estimated from the data. In our analysis, we do not consider this background since it will be largely diminished after strong preselection cuts and will be further reduced due to small fake rates of the considered final states.

The SM background, especially the $W+$jets component, is large and therefore one has to design a clever set of cuts which would notably reduce such a background but would not notably affect the signal. This implies that the cut efficiency for the background is very small and hence, a large number of background events has to be generated. In order to avoid the generation of a large event sample, we apply a strong cut on the partonic center-of-mass energy, $\sqrt{\hat{s}} > 200$ GeV at the generation level of all background processes. This cut can reduce the $W+$jets background by two orders of magnitude. However, this cut has no or very little effect on the other backgrounds *viz.* $t\bar{t}+$jets, single top and diboson ones since the threshold energy for them is either above or slightly below 200 GeV. In the case of a signal, $\sqrt{\hat{s}}$ is always above 200 GeV since we are interested in the parameter space regions where $m_{H^\pm} > m_W + m_{h_{125}} \gtrsim 205$ GeV.

One should note that, in reality, the full reconstruction of $\sqrt{\hat{s}}$ of an event is not possible if there is missing energy present in that event. In this case, one can construct an inclusive global variable $\sqrt{\hat{s}_{min}}$ defined in Ref. [40] which is closest to the actual $\sqrt{\hat{s}}$ of the event. One can roughly approximate $\sqrt{\hat{s}} \approx \sqrt{\hat{s}_{min}}$ if there is only one missing neutrino in the event but this approximation gets poorer with the increase of the number of neutrinos in the final state. For simplicity, we have used the cut $\sqrt{\hat{s}} > 200$ GeV at the generation level. But in reality, one can use a cut on $\sqrt{\hat{s}_{min}}$ to trim the background before passing it for further analysis.

4.3 Multivariate analysis

A Wh_{125} resonance, similar to our case, can also appear from the decay of a heavy charged gauge boson, W'. The search for W' in the $\ell^\pm + \not{E}_T + b\bar{b}$ channel (same final state that we are interested in) has been carried out at the LHC [41, 42]. In these searches, they mainly focus in the TeV-scale W' mass and the analyses are done using the cut-based techniques. A cut-based analysis may not perform well in our case, especially for low $m_{H^\pm}$ region due to the presence of a large SM background [43, 44]. Therefore, we choose to use a MVA to obtain a better signal-to-background discrimination which usually leads to a better significance than a cut-based analysis. See Ref. [45] for a brief review on various multivariate methods and their use in collider searches. In this paper, we only use multivariate techniques and do not compare our achieved sensitivity with the cut-based techniques.

We choose the following twelve simple kinematic variables that are also listed in Table IV.3 for our MVA.

- Transverse momenta of lepton, $p_T(\ell)$ and two leading-p_T jets, $p_T(J_1)$ and $p_T(J_2)$.
- Missing transverse energy $\not{E}_T$ and pseudorapidity of $\not{E}_T$ vector denoted by $\eta(\not{E}_T)$.
- Scalar sum of transverse momenta of all visible particles denoted by H_T.
- Invariant mass of two leading-p_T jets denoted by $M(J_1, J_2)$.
- ΔR separation of (ℓ, J_1), (ℓ, J_2), $(\not{E}_T, \ell)$, (J_1, J_2) and $(\not{E}_T, J_1)$ combinations.

These variables are chosen by comparing their distributions for the signal generated for $m_{H^\pm} = 300$ GeV with the total background distributions. They are selected from a bigger set of variables based on their discriminating power and less correlation. In Fig. IV.2, we show the normalized distributions of these variables for the signal with $m_{H^\pm} = 300$ GeV and the total background. Similar distributions for $m_{H^\pm} = 500$ GeV are shown in Fig. IV.3. From these figures, one can see that each of these distributions has reasonable discriminating power between the signal and the background. We use these kinematic variables simultaneously in a MVA whose output shows large differences in their shapes for the signal and the background. One should notice that the signal distributions deviate more from the background ones as we increase $m_{H^\pm}$. Therefore, isolation of the signal from the background becomes easier for heavier resonances. We, therefore, tune our MVA for lower masses and use the same optimized analysis for larger masses.

Variable	Importance	Variable	Importance	Variable	Importance	Variable	Importance
$p_T(\ell)$	0.095	$\not{E}_T$	0.072	$M(j_1, j_2)$	0.092	$\Delta R(\not{E}_T, \ell)$	0.065
$p_T(j_1)$	0.092	$\eta(\not{E}_T)$	0.076	$\Delta R(\ell, j_1)$	0.088	$\Delta R(j_1, j_2)$	0.072
$p_T(j_2)$	0.074	H_T	0.153	$\Delta R(\ell, j_2)$	0.077	$\Delta R(\not{E}_T, j_1)$	0.044

Table IV.3: Input variables used for MVA (BDT algorithm) and their relative importance. These numbers are obtained for $m_{H^\pm} = 300$ GeV for the $2b$-tag category. These numbers can vary for other choices of parameters.

In Table IV.3, we show the relative importance of each variable in the BDT response for $m_{H^\pm} = 300$ GeV for the $2b$-tag category. For this particular benchmark, the H_T variable has the highest relative importance of about 15%. The greater relative importance implies that the corresponding variable becomes a better discriminator. Note that the relative importance of such a variable can change for other benchmarks and for different LHC energies that can change the shape of the distributions. It can also change due to different choices of algorithms and their tuning parameters.

One should always be cautious while using the BDT algorithm since it is prone to overtraining. This can happen during the training of the signal and background test samples due to improper choices of the tuning parameters of the BDT algorithm. One can decide whether a test sample is overtrained or not by checking the corresponding Kolmogorov-Smirnov (KS) probability. If it lies within the range 0.1 to 0.9, we say the sample is not overtrained. We use two statistically independent samples in our MVA for each benchmark mass, one for training the BDT and another for testing purposes. In our analysis, we ensure that we do not encounter overtraining while using the BDT by checking the corresponding KS probability.

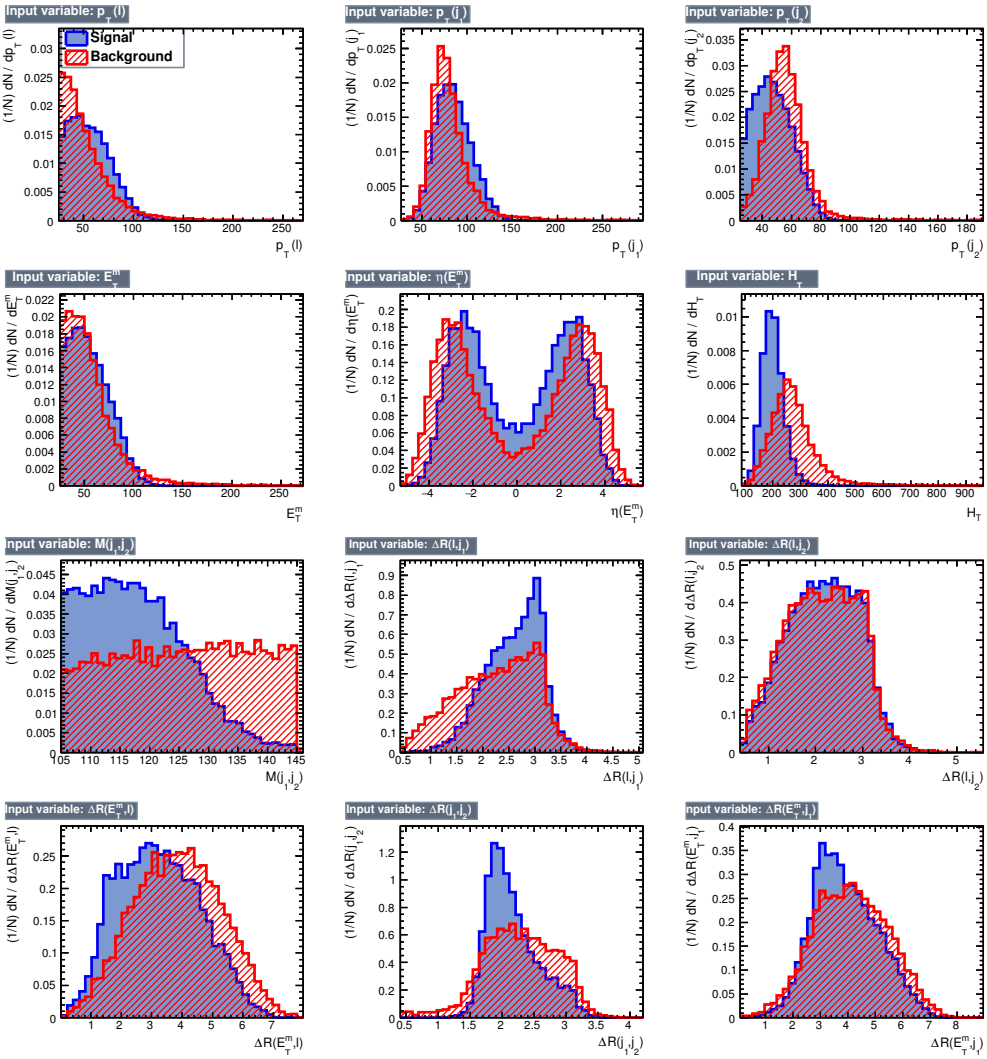

Figure IV.2: Normalized distributions of the input variables at the LHC ($\sqrt{s}$ = 13 TeV) used in the MVA for the signal (blue) and the background (red). Signal distributions are obtained for $m_{H^\pm}$ = 300 GeV, and the background includes all the dominant backgrounds discussed in subsection 4.2. These distributions are drawn by selecting events after the cuts defined in subsection 4.1.

In Figs. IV.4a and IV.4c, we display a normalized BDT output of the signal and the background for $m_{H^\pm}$ = 300 GeV and $m_{H^\pm}$ = 500 GeV, respectively, for the 2b-tag category at the LHC ($\sqrt{s} = 13$ TeV). One can see that the BDT outputs for the signal and the background are well-separated, and this can improve as we go to higher $m_{H^\pm}$ values. One then applies a BDT cut i.e. BDT$_{res} > \mathcal{C}$, where $\mathcal{C} \in [-1, 1]$ on the signal and background samples. The corresponding cut efficiencies are shown as functions of $\mathcal{C}$ in Fig. IV.4b (Fig. IV.4d) for $m_{H^\pm} = 300$ GeV ($m_{H^\pm} = 500$ GeV). The optimal BDT cut (BDT$_{opt}$) is defined for which the significance $\mathcal{N}_S/\sqrt{\mathcal{N}_S + \mathcal{N}_B}$ is maximized (where

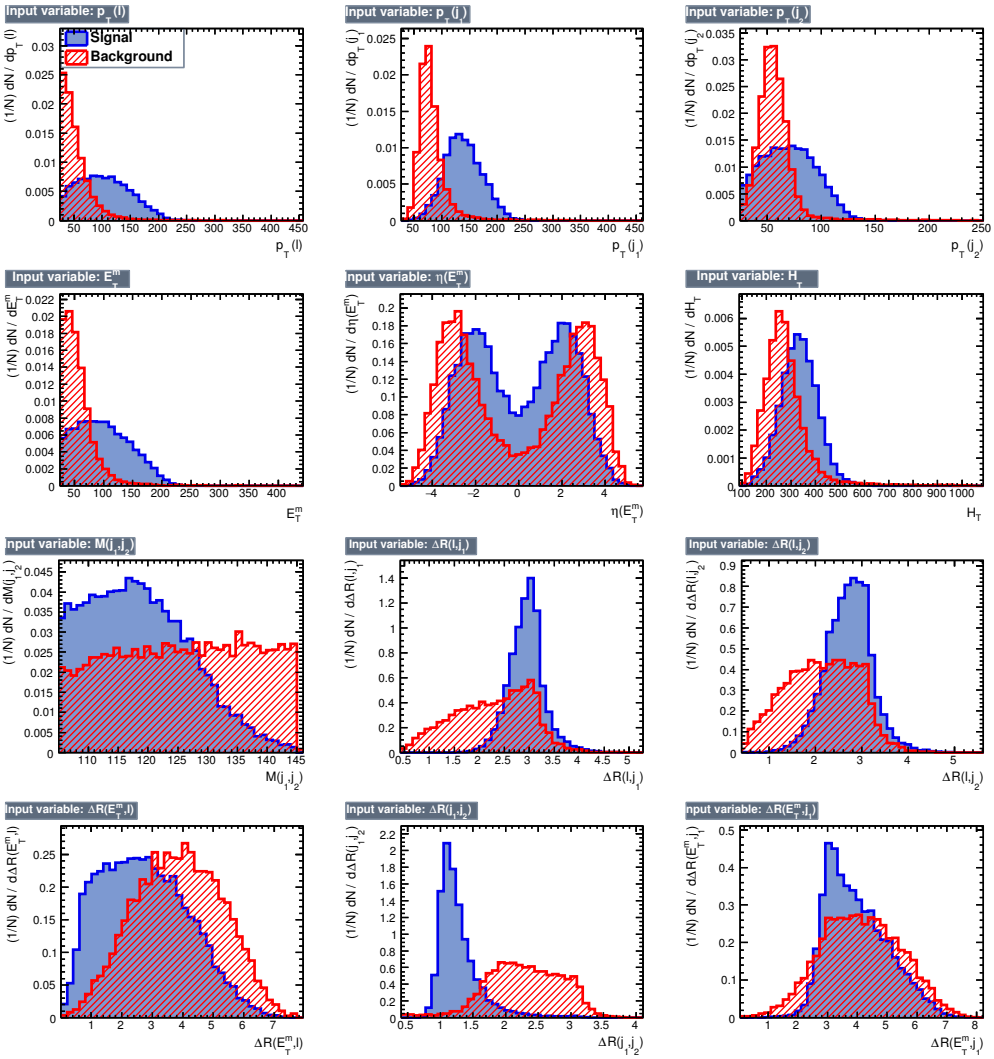

Figure IV.3: The same as Fig. IV.2 but for $m_{H^\pm} = 500$ GeV.

$\mathcal{N}_S$ and $\mathcal{N}_B$ are the number of signal and background events, respectively, for a given luminosity that are survived after the BDT cut). We see in Fig. IV.4b that if we have, at least, 222 signal events (for $\mathcal{L} = 50$ fb^{-1}) before the BDT analysis, it is possible to achieve a maximum 5σ significance for BDT$_{opt} \gtrsim 0.26$. After this cut, the number of signal events is reduced to 118 from 222 but the background events are drastically reduced to 436 from 33031. In Table IV.4, we show $\mathcal{N}_S$ and $\mathcal{N}_B$ along with $\mathcal{N}_S^{bc}$, the minimum number of signal events before the BDT cut that is required to achieve 5σ significance, for different $m_{H^\pm}$ values and for the two selection categories.

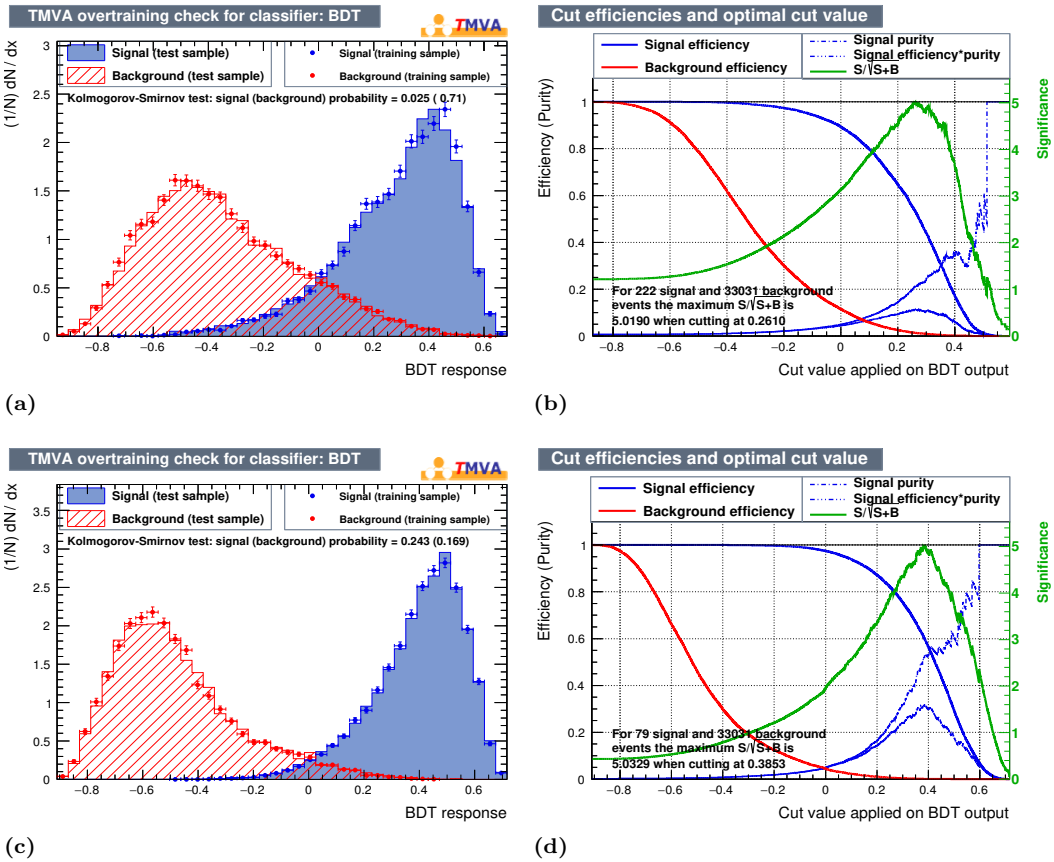

Figure IV.4: (a) The BDT response for the signal and the background for $m_{H^\pm} = 300$ GeV at the LHC ($\sqrt{s} = 13$ TeV) for the 2b-tag category. (b) The corresponding signal and background cut efficiencies and significance as functions of the BDT cut. Discovery significance of 5σ is achieved for the optimal BDT cut, $\text{BDT}_{opt} \gtrsim 0.26$. Similar figures for $m_{H^\pm} = 500$ GeV are shown in (c) and (d) where a maximum 5σ significance is achieved for $\text{BDT}_{opt} \gtrsim 0.39$.

$m_{H^\pm}$	1b-tag category				2b-tag category			
(GeV)	$\mathcal{N}_S^{bc}$	BDT_{opt}	$\mathcal{N}_S$	$\mathcal{N}_B$	$\mathcal{N}_S^{bc}$	BDT_{opt}	$\mathcal{N}_S$	$\mathcal{N}_B$
250	1227	0.31	579	12796	260	0.23	151	758
300	983	0.42	341	4303	222	0.26	118	436
350	680	0.44	262	2485	176	0.29	99	295
500	229	0.48	49	47	79	0.39	47	41
800	149	0.43	55	66	60	0.44	37	17
$\mathcal{N}_{\text{SM}}$	344173	-	-	-	33031	-	-	-

Table IV.4: The number of the SM background events ($\mathcal{N}_{\text{SM}}$) for the 1b-tag category at the LHC ($\sqrt{s} = 13$ TeV) with $\mathcal{L} = 50$ fb^{-1} that enters in the MVA. The minimum number of signal events that can be discovered with 5σ significance using our MVA is denoted by $\mathcal{N}_S^{bc}$ (this is before the optimal BDT cut as shown in the third column). The signal and background events that survived after the optimal BDT cut are denoted by $\mathcal{N}_S$ and $\mathcal{N}_B$, respectively, and they lead to 5σ significance.

5 Discovery regions of the 3HDM parameter space

The question still remains: Can the model we proposed in section 2 predict signals that would be visible using the presented analysis? In this section we find regions of the parameter space where that is the case, which shows that if limits are set by the experimental collaborations, the theory can be further constrained using the current experimental data.

The first task is to match our model to the Lagrangian in Eqs. (IV.30) and (IV.31). For each parameter space point, we choose the lightest charged scalar for the analysis. Although we concentrated our search in the parameter space region with $v_{1,2} \ll v_3$, as to exploit the SM-like h_{125} state in that limit, we do not rely on the validity of the expansion in small ξ in this analysis. The couplings κ_{cs} and $\kappa_{Wh_{125}}$ are found in Eq. (IV.22) after a numerical calculation of the spectrum and mixing matrices. To find the discovery reach of our parameter space, we translate $\mathcal{N}_S^{bc}$ in terms of the model parameters by using the following relation

$$\mathcal{N}_S^{bc} = \sigma(pp \to H^\pm \to W^\pm h_{125} \to \ell^\pm + \not{E}_T + b\bar{b}) \times \epsilon_S \times \mathcal{L}\,, \tag{IV.36}$$

where σ is the cross section after showering and hadronization, ϵ_S is the signal cut efficiency and $\mathcal{L}$ is the integrated luminosity.

For the calculation of $\mathrm{BR}_{Wh_{125}}$, it is important to note that although in general $H^\pm$ can decay to $W^\pm h_{\mathrm{a,b},125}$, we are interested only in the decay mode involving h_{125}, as in our model this is the state that couples the strongest to $b\bar{b}$ (see Eqs. (IV.28) and (IV.29)).

In addition, our model must be able to pass several consistency tests in order to be phenomenologically viable, such as reproducing the electroweak precision measurements. The original formulation [46] for BSM contributions to the electroweak precision observables in terms of the S, T and U parameters assumes that the scale of new physics is $\gtrsim 1$ TeV. As our model allows for new exotic scalars to have masses around the electroweak scale, we must employ the more general formalism introduced in Refs. [47, 48] with an extended set of oblique parameters S, T, U, V, W and X. These can then be used to calculate S', T' and U' for which the standard Z-pole constraints on S, T and U apply. To compute S', T' and U', we have applied the results in Ref. [49], in which S, T, U, V, W and X are computed for a general N-Higgs Doublet Model with the inclusion of arbitrary numbers of electrically charged and neutral $\mathrm{SU(2)_L}$ singlets. To summarize, when scanning the model parameter space for phenomenologically interesting regions, we look for points for which the following constraints are satisfied:

- There are no tachyonic scalar masses and the scalar potential is bounded from below (the corresponding constraints on the quartic couplings can be found in Ref. [12] taking into account that our λ_{ii} differ by a factor two from theirs).
- The tree-level scalar four-point amplitudes satisfy $|\mathcal{M}| < 4\pi$.

- The SM Higgs-like scalar has a mass no more than 5 GeV away from the observed 125 GeV value, and has a Yukawa coupling to the top quark satisfying $|y_{t\bar{t}h_{125}}| \in [0.9, 1.1]$.
- The exotic decays $Z \to h_{\mathrm{a,b}} A_{\mathrm{a,b}}$ are kinematically forbidden, as to not be in conflict with the precision measurements of the Z width.
- The lightest charged Higgs has a mass in the range $[m_{H^\pm}^{(\mathrm{min})}, 1000\,\mathrm{GeV}]$, with a different $m_{H^\pm}^{(\mathrm{min})}$ for each run (taking values 250, 300, 400 or 450 GeV).
- The computed values of S', T' and U' fall within the error bars on S, T and U as reported in Ref. [50].
- The value of $\kappa_{cs}^2 \times \mathrm{BR}_{Wh_{125}}$ is at least 0.5 above the 100 fb^{-1} discovery threshold for the 1b-tag category set by the MVA.

5.1 Scanning the parameter space

A random scan over the parameter space of the theory is both computationally expensive and not efficient. A good alternative, without the need for sophisticated statistical methods but still very powerful is the use of Genetic Algorithms (GA).

Following the guidelines set in Ref. [51], we wrote a GA in `Mathematica` for finding the parameter points in the discovery region, with a fitness function taking into account all the constraints listed above and including the so-called biodiversity enhancement to explore the parameter space more thoroughly.

GAs start from a randomly generated initial population, with each full cycle resulting in a new generation of candidates. The fittest parameter points are selected for every generation and their parameters are modified (by crossover and/or mutations) leading to a new generation. The new candidate points are then used in the next iteration of the GA. The GA finishes when either a maximum number of generations or a satisfactory fitness level is reached. We decided to build the GA relying on mutations only as it usually performs comparably to GAs including a crossover but it is simpler to implement, and it was stopped once a given number of valid parameter points was reached.

5.2 Results of the GA parameter scan

We performed five independent scans with different initial population sizes ranging from 50 to 1000, with varying mutation rates and different lower limits on $m_{H^\pm}$. We found 2116 parameter space points of the proposed model satisfying all the constraints within the discovery region of our analysis. In Figs. IV.5a and IV.5b, we show the 5σ discovery contours of $\kappa_{cs}^2 \times \mathrm{BR}_{Wh_{125}}$ corresponding to 1b- and 2b-tag categories, respectively, as functions of $m_{H^\pm}$ for $\mathcal{L} = 50, 100$ fb^{-1} at the LHC ($\sqrt{s} = 13$ TeV). Here, these functions are overlayed with the corresponding values for the parameter points found by the GA

scanning procedure. We find that both selection categories are almost equally sensitive in probing the parameter space of our model. However, the $2b$-tag category is slightly more sensitive than the $1b$-tag category since the background reduction is better for the former. The irregularities in the charged Higgs mass dependence seen in Figs. IV.5a and IV.5b are due to a combination of points from scans with different lower limits on $m_{H^\pm}$.

As discussed before, since a W' can also produce a Wh_{125} resonance, we compare our reach with the Wh_{125} resonance search data. In Fig. IV.5b, the shaded region is excluded by the ATLAS Wh_{125} resonance search data [41] in the $\ell + \not{E}_T + b\bar{b}$ channel. To obtain this, we translate the 95% confidence level (CL) upper limit (UL) on the cross section set by ATLAS in terms of our model parameters by using the following relation,

$$(\sigma \times \mathrm{BR})_{UL} \times \epsilon_{W'} = \sigma(pp \to H^\pm) \times \mathrm{BR}(H^\pm \to W^\pm h_{125}) \times \epsilon_{H^\pm} \tag{IV.37}$$

where $\epsilon_{W'}$ and $\epsilon_{H^\pm}$ are the cut-efficiencies for the W' and $H^\pm$ respectively and they are different, in general. For simplicity, we assume $\epsilon_{W'} = \epsilon_{H^\pm}$ while obtaining the exclusion region on our model parameters. For instance, for $m_{H^\pm} = 800$ GeV, $\kappa^2 \times \mathrm{BR}_{Wh_{125}} \gtrsim 2 \times 10^{-3}$ is excluded with 2σ CL using $\mathcal{L} \approx 36$ fb^{-1} data but $\kappa^2 \times \mathrm{BR}_{Wh_{125}} \lesssim 2 \times 10^{-3}$ region can be discovered with 5σ significance if we go to a higher luminosity. The exclusion region starts from $m_{H^\pm} = 500$ GeV since the latest data used here are available for W' masses above 500 GeV.

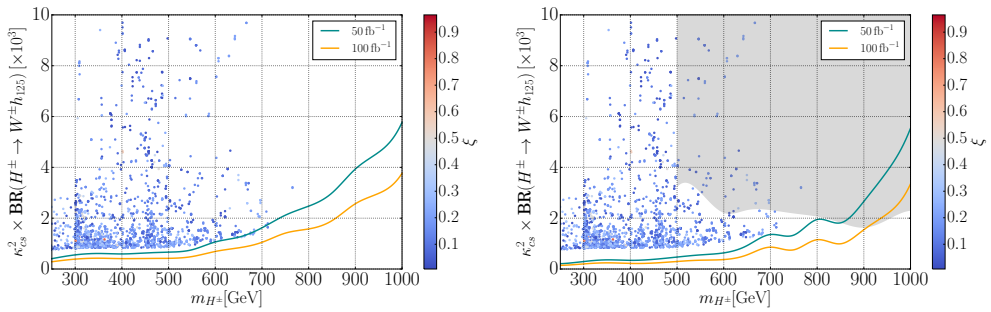

Figure IV.5: The 5σ discovery contours of $\kappa^2_{cs} \times \mathrm{BR}_{Wh_{125}}$ (scaled by 10^3) as functions of $m_{H^\pm}$ for $\mathcal{L} = 50, 100$ fb^{-1} at the LHC ($\sqrt{s} = 13$ TeV) for (a) $1b$-tag category and (b) $2b$-tag category. The dots represent the parameter points resulting form the GA scan with the corresponding values of ξ encoded in their color.

Although the lightest charged scalar (identified as $H^\pm$ for the analysis) does not primarily decay into Wh_{125}, it can still reach the discovery regions due to being mainly produced through $c\bar{s}$ fusion and having BR(Wh_{125}) comparable to the BR of the other decay channels. In Fig. IV.6a we show the BR($H^\pm \to W^\pm h_{125}$) vs BR($H^+ \to$ light quarks) for the lightest charged scalar, where light scalars refers to first and second generations and the dashed line represents the case when both decay modes dominate. For the parameter points not close to this line, the remaining decay width is mostly

due to the $H^\pm \to W^\pm h_{\mathrm{a,b}}$ decay. For a few outlier points, the $H^+ \to t\bar{b}$ mode is also relevant.

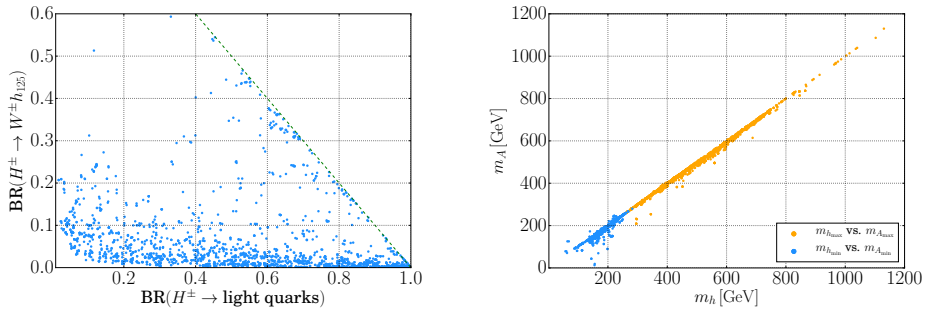

Figure IV.6: (a) BR($H^+ \to W^+ h_{125}$) vs. BR($H^+ \to$ light quarks). Here, 'light quarks' refers to 1st and 2nd generation quarks. The dashed line represents when BR($H^+ \to W^+ h_{125}$) + BR($H^+ \to$ light quarks) = 1, i.e. when these two channels dominate the total decay width. For almost all points far away from this line, the lightest charged Higgs often decays to $W^\pm h_{\mathrm{a,b}}$. (b) Scalar vs. pseudo-scalar masses for the lightest (blue) and heaviest (orange) states. The alignment of these masses is consistent with the $\xi \ll 1$ expansion.

It is worth noting that although the GA did not rely on the validity of the $\xi \ll 1$ expansion, it often found points where that is the case. Although the initial populations had a hierarchy in the VEVs of the scalar fields ($v_{1,2} \ll v_3$), the GA had no inherent constraints stopping it from exploring the regions without it. Notably, the majority of the found points did show that feature and therefore a diminished hierarchy in the Yukawa couplings of the quark sector together with all the features described in section 2. That can also be seen in Figs. IV.5a–IV.5b where we have indicated the specific values of ξ for the valid parameter points. We have checked the difference between the $\mathcal{O}(\xi)$ expressions for masses and the full numerical calculation, and find that for a vast majority of the valid parameter points the $\xi \ll 1$ expansion is reliable.

In Fig. IV.7, we show distributions of quartic couplings, values of ξ and mass parameters in the scalar potential, as well as the Higgs VEVs, for points in the discovery region found by the GA. Indeed, the typical values of $v_{1,2}$ are likely to be below 100 GeV, with v_2 extending over a larger domain than v_1, while v_3 values are mostly concentrated close to the maximal 246 GeV limit. There is still a small number of valid points incompatible with the ξ-expansion due to the smallness of one of m_{ij}^2. Such points would still be in the discovery region, although without the features that assume $\xi \ll 1$. As can be seen from Fig. IV.6b, the masses of the exotic scalars and pseudo-scalars tend to align as predicted by the $\xi \ll 1$ expansion (see Eq. (IV.21)).

6 Summary and conclusions

We have, in this article, introduced a class of 3HDMs with a global $\mathrm{U(1)_X} \times \mathrm{U(1)_Z}$ family symmetry that is softly broken by bi-linear terms in the scalar potential. We

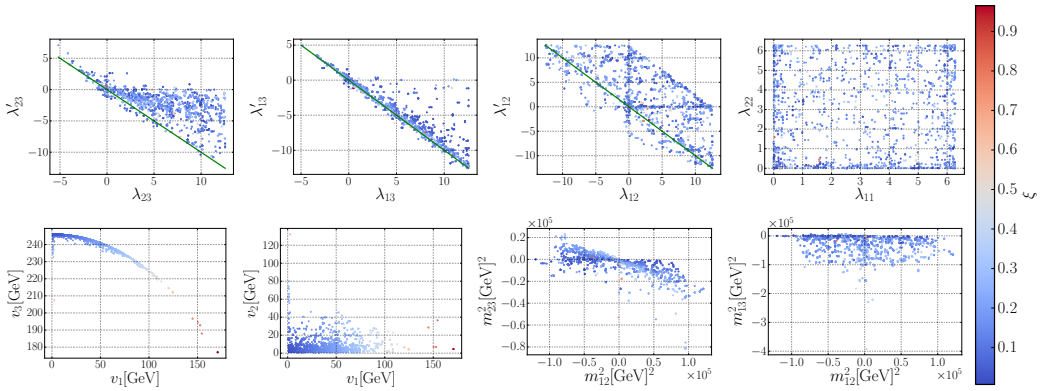

Figure IV.7: Distribution of different parameters and ξ values for points in the discovery region found by the Genetic Algorithm. The green solid line in the first three plots indicates when $\lambda_{ij} = -\lambda'_{ij}$.

have shown how to assign the X and Z charges of the quarks such that no tree-level FCNCs are present, while enforcing the Cabibbo-like structure of V_{CKM}. We described how a mixing with the third quark family can be induced from dim-6 operators, which would explain the smallness of the corresponding entries in V_{CKM}. Moreover, we showed that a hierarchy in the VEVs of the three Higgs doublets, $v_{1,2} \ll v_3$, leads to a heavy third quark family without the need for a strong hierarchy in the Yukawa couplings (contrary to what happens in the SM where e.g. $y_{\text{up}}/y_{\text{top}} \sim 10^{-5}$). The same hierarchy has been exploited to derive simple closed expressions for the scalar masses and mixing matrices by expansions in the small parameter $\xi \equiv \sqrt{v_1^2 + v_2^2}/v_3 \ll 1$.

A generic prediction of the model is that the new scalars $h_{\text{a,b}}$, $A_{\text{a,b}}$ and $H^{\pm}_{\text{a,b}}$ are likely to couple strongly to the s and c quarks, yielding different signatures in colliders at variance with the standard searches focusing on the third quark family. As an example, we studied collider phenomenology of the lightest charged Higgs when its mass is in the 250 – 1000 GeV range, under the assumption that the other charged Higgs is sufficiently heavy to be dropped out of the analysis. In that case, the lighter charged Higgs would be resonantly produced through a $c\bar{s}$ fusion, and, for certain regions of the parameter space, subsequently decay to Wh_{125}. All other decay channels are assumed to only contribute to its total width.

We particularly focused on one of the possible channels – the $c\bar{s} \to H^+ \to W^+ h_{125}$ channel, which has not been explored before in the context of heavier charged Higgs searches. This channel is specific to our class of 3HDMs and is particularly sensitive to the sub-TeV charged Higgs mass and small-ξ regions. We showed that this unconventional channel, when combined with the power of a multivariate analysis, leads to good signal-to-background ratios even for masses below 500 GeV and thus can be used to probe models with that particular feature at the LHC. We employed a model independent formulation so that our approach can be applied to any model which predicts a sufficiently large cross section for the $c\bar{s} \to H^+ \to W^+ h_{125}$ process to be observed in

the future LHC runs. Our analysis can also be applied to improve sensitivity for W' searches especially for the sub-TeV masses.

We then used a genetic algorithm to find parameter space points in our 3HDM which would yield signals with $> 5\sigma$ significance, while still satisfying the standard phenomenological constraints. Although the scan did not rely on $\xi \ll 1$, a vast majority of the points were consistent with that limit and thus showed all the features mentioned above and described in section 2. This shows that the described unconventional search strategy can effectively probe realistic multi-Higgs theories with the current LHC data, and so we think it should be seriously considered by our experimental colleagues.

Acknowledgments

The authors would like to thank Johan Rathsman for fruitful discussions. The work of T.M. is supported by the Swedish Research Council under contract 621-2011-5107 and 2015-04814 and the Carl Trygger Foundation under contract CTS-14:206. J. E. C.-M. was partially supported by Lund University. R.P. and J.W. were partially supported by the Swedish Research Council, contract numbers 621-2013-428 and 2016-05996. R.P. was also partially supported by CONICYT grant PIA ACT1406.

References

[1] G. C. Branco, P. M. Ferreira, L. Lavoura, M. N. Rebelo, M. Sher, and J. P. Silva, "Theory and phenomenology of two-Higgs-doublet models," *Phys. Rept.* **516** (2012) 1–102, arXiv:1106.0034 [hep-ph].

[2] S. Weinberg, "Gauge theory of CP nonconservation," *Phys. Rev. Lett.* **37** (Sep, 1976) 657–661. https://link.aps.org/doi/10.1103/PhysRevLett.37.657.

[3] G. Branco, A. Buras, and J.-M. Gérard, "Cp violation in models with two- and three-scalar doublets," *Nuclear Physics B* **259** no. 2, (1985) 306 – 330. http://www.sciencedirect.com/science/article/pii/0550321385906388.

[4] F. Botella, G. Branco, and M. Rebelo, "Minimal flavour violation and multi-higgs models," *Physics Letters B* **687** no. 2, (2010) 194 – 200. http://www.sciencedirect.com/science/article/pii/S0370269310003072.

[5] I. P. Ivanov and C. C. Nishi, "Symmetry breaking patterns in 3HDM," *JHEP* **01** (2015) 021, arXiv:1410.6139 [hep-ph].

[6] A. G. Akeroyd, S. Moretti, K. Yagyu, and E. Yildirim, "Light charged Higgs boson scenario in 3-Higgs doublet models," *Int. J. Mod. Phys.* **A32** no. 23n24, (2017) 1750145, arXiv:1605.05881 [hep-ph].

[7] J. E. Camargo-Molina, R. Pasechnik, and J. Wessén, "Charged scalars from $SU(3)^3$ theories," in *6th International Workshop on Prospects for Charged Higgs Discovery at Colliders (CHARGED 2016) Uppsala, Sweden, October 3-6, 2016.* 2017. arXiv:1701.02757 [hep-ph]. https://inspirehep.net/record/1508618/files/arXiv:1701.02757.pdf.

[8] M. Merchand and M. Sher, "Three doublet lepton-specific model," *Phys. Rev.* **D95** no. 5, (2017) 055004, arXiv:1611.06887 [hep-ph].

[9] S. Moretti and K. Yagyu, "Constraints on Parameter Space from Perturbative Unitarity in Models with Three Scalar Doublets," *Phys. Rev.* **D91** (2015) 055022, arXiv:1501.06544 [hep-ph].

[10] D. Das and U. K. Dey, "Analysis of an extended scalar sector with S_3 symmetry," *Phys. Rev.* **D89** no. 9, (2014) 095025, arXiv:1404.2491 [hep-ph]. [Erratum: Phys. Rev.D91,no.3,039905(2015)].

[11] D. Emmanuel-Costa, O. M. Ogreid, P. Osland, and M. N. Rebelo, "Spontaneous symmetry breaking in the S_3-symmetric scalar sector," *JHEP* **02** (2016) 154, arXiv:1601.04654 [hep-ph]. [Erratum: JHEP08,169(2016)].

[12] V. Keus, S. F. King, and S. Moretti, "Three-Higgs-doublet models: symmetries, potentials and Higgs boson masses," *JHEP* **01** (2014) 052, arXiv:1310.8253 [hep-ph].

[13] I. P. Ivanov, V. Keus, and E. Vdovin, "Abelian symmetries in multi-Higgs-doublet models," *J. Phys.* **A45** (2012) 215201, arXiv:1112.1660 [math-ph].

[14] **ATLAS Collaboration** Collaboration, "Search for charged Higgs bosons in the $H^{\pm} \to tb$ decay channel in pp collisions at $\sqrt{s} = 13$ TeV using the ATLAS detector," Tech. Rep. ATLAS-CONF-2016-089, CERN, Geneva, Aug, 2016. https://cds.cern.ch/record/2206809.

[15] **CMS** Collaboration, V. Khachatryan *et al.*, "Search for a charged Higgs boson in pp collisions at $\sqrt{s} = 8$ TeV," *JHEP* **11** (2015) 018, arXiv:1508.07774 [hep-ex].

[16] H. Georgi and M. Machacek, "Doubly Charged Higgs Bosons," *Nucl. Phys.* **B262** (1985) 463–477.

[17] **ATLAS** Collaboration, G. Aad *et al.*, "Search for a Charged Higgs Boson Produced in the Vector-Boson Fusion Mode with Decay $H^{\pm} \to W^{\pm}Z$ using pp Collisions at $\sqrt{s} = 8$ TeV with the ATLAS Experiment," *Phys. Rev. Lett.* **114** no. 23, (2015) 231801, arXiv:1503.04233 [hep-ex].

[18] **CMS** Collaboration, A. M. Sirunyan *et al.*, "Search for Charged Higgs Bosons Produced via Vector Boson Fusion and Decaying into a Pair of W and Z Bosons Using pp Collisions at $\sqrt{s} = 13$ TeV," *Phys. Rev. Lett.* **119** no. 14, (2017) 141802, arXiv:1705.02942 [hep-ex].

[19] **ATLAS** Collaboration, G. Aad *et al.*, "Search for charged Higgs bosons decaying via $H^{\pm} \to \tau^{\pm}\nu$ in fully hadronic final states using pp collision data at $\sqrt{s} = 8$ TeV with the ATLAS detector," *JHEP* **03** (2015) 088, arXiv:1412.6663 [hep-ex].

[20] **ATLAS** Collaboration, G. Aad *et al.*, "Search for a light charged Higgs boson in the decay channel $H^+ \to c\bar{s}$ in $t\bar{t}$ events using pp collisions at $\sqrt{s} = 7$ TeV with the ATLAS detector," *Eur. Phys. J.* **C73** no. 6, (2013) 2465, arXiv:1302.3694 [hep-ex].

[21] **CMS** Collaboration, V. Khachatryan *et al.*, "Search for a light charged Higgs boson decaying to c$\bar{\text{s}}$ in pp collisions at $\sqrt{s} = 8$ TeV," *JHEP* **12** (2015) 178, arXiv:1510.04252 [hep-ex].

[22] **CMS Collaboration** Collaboration, "Search for Charged Higgs boson to $c\bar{b}$ in lepton+jets channel using top quark pair events," Tech. Rep. CMS-PAS-HIG-16-030, CERN, Geneva, 2016. https://cds.cern.ch/record/2209237.

[23] **DELPHI** Collaboration, J. Abdallah *et al.*, "Search for charged Higgs bosons at LEP in general two Higgs doublet models," *Eur. Phys. J.* **C34** (2004) 399–418, arXiv:hep-ex/0404012 [hep-ex].

[24] **OPAL** Collaboration, G. Abbiendi *et al.*, "Search for Charged Higgs Bosons in e^+e^- Collisions at $\sqrt{s} = 189 - 209$ GeV," *Eur. Phys. J.* **C72** (2012) 2076, arXiv:0812.0267 [hep-ex].

[25] S. Moretti, "The $W^\pm$ h decay channel as a probe of charged Higgs boson production at the large hadron collider," *Phys. Lett.* **B481** (2000) 49–56, arXiv:hep-ph/0003178 [hep-ph].

[26] R. Enberg, W. Klemm, S. Moretti, S. Munir, and G. Wouda, "Charged Higgs boson in the $W^\pm$ Higgs channel at the Large Hadron Collider," *Nucl. Phys.* **B893** (2015) 420–442, arXiv:1412.5814 [hep-ph].

[27] S. Moretti, R. Santos, and P. Sharma, "Optimising Charged Higgs Boson Searches at the Large Hadron Collider Across $b\bar{b}W^\pm$ Final States," *Phys. Lett.* **B760** (2016) 697–705, arXiv:1604.04965 [hep-ph].

[28] S. Dittmaier, G. Hiller, T. Plehn, and M. Spannowsky, "Charged-Higgs Collider Signals with or without Flavor," *Phys. Rev.* **D77** (2008) 115001, arXiv:0708.0940 [hep-ph].

[29] W. Altmannshofer, J. Eby, S. Gori, M. Lotito, M. Martone, and D. Tuckler, "Collider Signatures of Flavorful Higgs Bosons," *Phys. Rev.* **D94** no. 11, (2016) 115032, arXiv:1610.02398 [hep-ph].

[30] C. Froggatt and H. Nielsen, "Hierarchy of quark masses, cabibbo angles and cp violation," *Nuclear Physics B* **147** no. 3, (1979) 277 – 298. http://www.sciencedirect.com/science/article/pii/055032137990316X.

[31] A. Alloul, N. D. Christensen, C. Degrande, C. Duhr, and B. Fuks, "FeynRules 2.0 - A complete toolbox for tree-level phenomenology," *Comput. Phys. Commun.* **185** (2014) 2250–2300, arXiv:1310.1921 [hep-ph].

[32] C. Degrande, C. Duhr, B. Fuks, D. Grellscheid, O. Mattelaer, and T. Reiter, "UFO - The Universal FeynRules Output," *Comput. Phys. Commun.* **183** (2012) 1201–1214, arXiv:1108.2040 [hep-ph].

[33] J. Alwall, R. Frederix, S. Frixione, V. Hirschi, F. Maltoni, O. Mattelaer, H. S. Shao, T. Stelzer, P. Torrielli, and M. Zaro, "The automated computation of tree-level and next-to-leading order differential cross sections, and their matching to parton shower simulations," *JHEP* **07** (2014) 079, arXiv:1405.0301 [hep-ph].

[34] R. D. Ball *et al.*, "Parton distributions with LHC data," *Nucl. Phys.* **B867** (2013) 244–289, arXiv:1207.1303 [hep-ph].

[35] T. Sjostrand, S. Mrenna, and P. Z. Skands, "PYTHIA 6.4 Physics and Manual," *JHEP* **05** (2006) 026, arXiv:hep-ph/0603175 [hep-ph].

[36] **DELPHES 3** Collaboration, J. de Favereau, C. Delaere, P. Demin, A. Giammanco, V. Lemaître, A. Mertens, and M. Selvaggi, "DELPHES 3, A modular framework for fast simulation of a generic collider experiment," *JHEP* **02** (2014) 057, arXiv:1307.6346 [hep-ex].

[37] M. Cacciari, G. P. Salam, and G. Soyez, "FastJet User Manual," *Eur. Phys. J.* **C72** (2012) 1896, arXiv:1111.6097 [hep-ph].

[38] M. Cacciari, G. P. Salam, and G. Soyez, "The Anti-k(t) jet clustering algorithm," *JHEP* **04** (2008) 063, arXiv:0802.1189 [hep-ph].

[39] A. Hocker *et al.*, "TMVA - Toolkit for Multivariate Data Analysis," *PoS* **ACAT** (2007) 040, arXiv:physics/0703039 [PHYSICS].

[40] P. Konar, K. Kong, and K. T. Matchev, "$\sqrt{\hat{s}}_{min}$: A Global inclusive variable for determining the mass scale of new physics in events with missing energy at hadron colliders," *JHEP* **03** (2009) 085, arXiv:0812.1042 [hep-ph].

[41] **ATLAS Collaboration** Collaboration, "Search for heavy resonances decaying to a W or Z boson and a Higgs boson in final states with leptons and b-jets in 36.1 fb^{-1} of pp collision data at $\sqrt{s} = 13$ TeV with the ATLAS detector," Tech. Rep. ATLAS-CONF-2017-055, CERN, Geneva, Jul, 2017. https://cds.cern.ch/record/2273871.

[42] **CMS** Collaboration, A. M. Sirunyan *et al.*, "Combination of searches for heavy resonances decaying to WW, WZ, ZZ, WH, and ZH boson pairs in proton-proton collisions at $\sqrt{s} = 8$ and 13 TeV," *Phys. Lett.* **B774** (2017) 533–558, arXiv:1705.09171 [hep-ex].

[43] J. Li, R. Patrick, P. Sharma, and A. G. Williams, "Boosting the charged Higgs search prospects using jet substructure at the LHC," *JHEP* **11** (2016) 164, arXiv:1609.02645 [hep-ph].

[44] R. Patrick, P. Sharma, and A. G. Williams, "Exploring a heavy charged Higgs using jet substructure in a fully hadronic channel," *Nucl. Phys.* **B917** (2017) 19–30, arXiv:1610.05917 [hep-ph].

[45] P. C. Bhat, "Multivariate Analysis Methods in Particle Physics," *Ann. Rev. Nucl. Part. Sci.* **61** (2011) 281–309.

[46] M. E. Peskin and T. Takeuchi, "Estimation of oblique electroweak corrections," *Phys. Rev. D* **46** (Jul, 1992) 381–409. https://link.aps.org/doi/10.1103/PhysRevD.46.381.

[47] I. Maksymyk, C. P. Burgess, and D. London, "Beyond s, t, and u," *Phys. Rev. D* **50** (Jul, 1994) 529–535. https://link.aps.org/doi/10.1103/PhysRevD.50.529.

[48] C. Burgess, S. Godfrey, H. König, D. London, and I. Maksymyk, "A global fit to extended oblique parameters," *Physics Letters B* **326** no. 3, (1994) 276 – 281. http://www.sciencedirect.com/science/article/pii/0370269394913226.

[49] W. Grimus, L. Lavoura, O. Ogreid, and P. Osland, "The oblique parameters in multi-higgs-doublet models," *Nuclear Physics B* **801** no. 1, (2008) 81 – 96. http://www.sciencedirect.com/science/article/pii/S0550321308002289.

[50] **Particle Data Group** Collaboration, C. Patrignani *et al.*, "Review of Particle Physics," *Chin. Phys.* **C40** no. 10, (2016) 100001.

[51] J. E. Camargo-Molina and J. Wessén, "(in preparation),".

Printed by Media-Tryck, Lund 2018 NORDIC SWAN ECOLABEL 3041 0903

Lund University
Faculty of Science
Department of Astronomy and Theoretical Physics
ISBN 978-91-7753-671-0 (print)
ISBN 978-91-7753-671-7 (pdf)